## Contents

# DUCTILITY OF CONCRETE BEAMS REINFORCED WITH HYPRID FRP REBARS

**Mounir M. kamal\*, Mohamed A. Safaan\*, Mohamed A. Al-Gazzar\*\***
*\* Civil Engineering Department, Faculty of Engineering, Menoufyia University, Egypt*
*\*\* Ministry of Public Works and Water Resources, Menoufyia, Egypt*

## ABSTRACT

Aiming to improve the ductility of FRP reinforced concrete members, the flexural behavior of concrete beams reinforced with innovative hybrid FRP rebars was investigated. Four simply supported beams (127x200x1730 mm) were cast using normal and high strength concrete mixes and different reinforcement ratios. Similar beams were reinforced using GFRP bars and steel. The in-house manufactured FRP bars were 9.5 mm in diameter with a sand-coated surface. The hybrid rebars were manufactured by replacing 10 percent of the glass fiber volume with 0.35 mm-diameter nylon threads. The nylon thread is more ductile than the glass fibers with improved mechanical properties. The beams were tested in flexure under four-point loading till failure. The structural behavior was compared in terms of ultimate loads, deformations and modes of failure. The results demonstrated the efficiency of the hybridization in improving the ductility of test beams. Design equations based on the strain compatibility and equilibrium of forces were derived to predict the load capacity of the beams reinforced with the hybrid rebars and were found to be adequate based on the available experimental results.

**Keywords:** Ductility, hybrid, GFRP bars, RC beams, deflection, design*.*

## INTRODUCTION

With regard to the inherent corrosion nature of conventional steel, FRP rebars seems to be a promising alternative as internal reinforcement for concrete. FRP rebars are ideally suited to reinforce concrete elements in aggressive environments and for use in applications that require electromagnetic transparency. A wide range of applications of these advanced composites as internal concrete reinforcement is still rather limited. This is basically attributed to major engineering drawbacks of the FRP materials in terms of low modulus of elasticity, as in GFRP rebars, and lack of ductility of most commercially available FRP products.

Ductility describes the ability to sustain inelastic deformation prior to failure without significant loss in the load carrying capacity [1]. Properly designed steel reinforced concrete members are highly ductile due to steel yielding and consequently its ability to consume a substantial amount of energy while allowing the full compressive strain capacity of concrete to develop. On the other hand, mono-fiber FRP composites are brittle exhibiting a perfectly linear elastic tensile stress-strain relationship up to failure. This behavior suggests that the main source of inelastic energy dissipation would be due to cracking and crushing of concrete. For this reason, design criteria based on concrete crushing rather than rebar rupture was accepted to slightly improve the performance of flexural members [2-4]. Also, the brittle nature of FRP reinforced concrete elements restricts their use in seismic zones and no redistributions of bending moments in statically intermediate elements is allowed [5]. According to the current design provisions, the suggested margin of safety against failure is higher than that used in traditional steel reinforced concrete beams so that the FRP reinforced member would have a higher reserve of strength compensating the lack of ductility [4]. Based on the mentioned shortcomings, restrictions of application and the requirements of current design codes, it can be concluded that improving the ductility of FRP rebars and/or concrete is required to improve the structural performance of FRP reinforced concrete elements and achieve economic utilization of materials.

## METHODS OF IMPROVING THE DUCTILITY OF FRP RC BEAMS

With regard to the high tensile strength of FRP rebars, using high strength concrete and effective confinement of the compression zone provided by intensive stirrups was recommended by Clarke and O'Regan [6] in order to develop the full strain capacity of the FRP reinforcement and gain plastic deformability. The confining stirrups should be carefully designed so as not to increase the concrete compressive strength and alter the mode of failure. In 1995, Naaman proposed the use of slurry infiltrated fiber concrete, a kind of steel fiber-reinforced concrete with a high fiber volume fraction, in order to improve the ductility of FRP prestressed beams. Substantial ductility was achieved due to the formation of a plastic hinge at the compression zone [7]. Alsayed and Alhozaimy [8] investigated the influence of adding steel fibers to the concrete mix on the ductility of concrete beams reinforced with FRP rebars. The results indicated that the ductility of the FRP reinforced beams cast with ordinary concrete was 50% less than that of similar steel RC beams. The results showed that inclusion of 1% of hooked steel fibers doubled the ductility index of the FRP beams and that the ductility improvement was directly related to the fiber content. To avoid using expensive non-corrosive steel fibers in the concrete mix, Safaan and Afify [9] investigated the use of 0.4 mm diameter and 20 mm long polypropylene fibers added to the concrete mix with a content of 0.25% of cement weight. It was found that the ultimate concrete strain was effectively increased in the beams cast with fibrous concrete resulting in higher tensile stress in the FRP reinforcement and higher ultimate loads. Also, a favorable nonlinear load-deformation response was developed and the ductility index was 20% higher when the fibrous concrete was used compared to ordinary and high strength concrete. Similar results were obtained by Belarbi and Wang [10] by applying 55 mm long polypropylene fiber mesh. Their extended work showed that the fibers provided enhanced ductile bond behavior of the GFRP reinforced concrete beams. Also, the flexural behavior was improved in terms of ultimate loads and the ductility index that was increased by 36%. Accelerated durability tests addressing bond and flexural behavior of RC beams showed that the durability of the system was improved due to the use of fibers.

Li and Wang [11] investigated the flexural behavior of GFRP reinforced beams cast with HSC and engineered cementitious composite (ECC) matrix. ECC is a newly developed material intended to replace conventional concrete in certain applications that require sufficient ductility. The material contains water, cement, sand, fiber and some common chemical additives; while coarse aggregates are not used as they tend to adversely affect the ductile behavior of the composite [12]. A typical composition employs water/cement and sand/cement ratio of 0.50 and a fiber content less than 2 percent by volume of the mix. The material is characterized by developing a strain hardening response in tension, high strain capacity up to 6%, crack width control and high compressive strength. The test results revealed that ECC beams exhibited significant improvement in the flexural performance in terms of ductility, load carrying capacity, shear resistance and damage tolerance in terms of crack width and spalling compared with similar steel reinforced beams. Also, it was suggested that the elimination of shear reinforcement in RC beams is possible when ECC replaces concrete. This conclusion was based on the test results showing that the ECC beams without shear reinforcement demonstrated better performance than HSC beams with dense steel stirrups. Despite these interesting results, studying the cost effectiveness of the proposed material and volumetric changes is rather important knowing that the cement content in the proposed mix is 1250 kg/m$^3$, which is about 3.5 times the amount used in ordinary mixes and 2.5 times the usual amount in HSC mixes.

The second approach to improve the ductility is to tailor the reinforcing fibers and/or their geometric architecture to produce hybrid, braided and hybrid braided FRP rebars. Hybrid rebars are manufactured by mixing different types of fibers. The ductile behavior is obtained through multiple breaking of the low elongation fibers before total failure of the rebar [13]. Bakis et al. [14] discussed how to manufacture ductile FRP rebars using different combinations of E-glass, carbon, aramid and PVA fibers in a polyester matrix. The best result concerning ductility improvement was obtained by replacing 25% of glass fibers with carbon fibers, provided that the carbon fibers are uniformly distributed in the cross section rather than gathered in the core. Braided rebars are manufactured from two or more yarns that are intertwined in the bias

direction to form an integrated structure. Harris et al. [15] adopted the braiding method to manufacture ductile hybrid FRP rebars simulating the behavior of steel with a high initial modulus, a definite yield point, and a high level of ultimate strain. Carbon fibers were used for core yarns and aramid fibers for braided sleeve yarns. The test results showed that increasing the braiding angle increases the ultimate strain and decreases the initial stiffness that can be in return increased by increasing the core to sleeve volume fraction. Although this technique was successful in the research phase, its implementation in practical applications was limited because of the complicated and costly manufacturing process.

The attempts to manufacture E-glass braided rebars by Sadek [16] and hybrid rebars by Safaan [17] utilizing the raw materials available in the Egyptian market showed that the braiding process was much more complicated, while the hybrid rebars had higher ultimate loads and ultimate strain capacity. A simple hand-operating equipment was used by Safaan to produce twisted hybrid rebars in which nylon threads were used to replace different volume fractions of E-glass fibers.  The test results showed that replacing 10% of glass fibers achieved a favorable nonlinear response before failure and increased the strain capacity to 4% instead of 2% in mono-fiber rebars. This ductility improvement was associated with acceptable losses in the tensile strength and modulus of elasticity.

An important aspect related to ductility improvement in FRP reinforced beams is the necessity of imposing a unified parameter for measuring ductility. The ductility in steel reinforced beams is the ratio of the deformation at failure to that at yielding. Obviously, such a definition is not applicable in case of FRP beams that do not exhibit yielding. Jaeger et al. [18] proposed an index based on deformability to evaluate the ductility of FRP-reinforced concrete beams. This index, known as the J-factor, is defined as the product of the moment factor and the deflection factor. The moment factor and deflection factor are defined as the ratios of moment and deflection at ultimate state to those at a concrete compressive strain of 0.001, respectively. This strain level was selected as the beginning of inelastic deformation of concrete. The research results of Vijay et al. [19] showed that this index was not consistent as the beams that failed by rebar rupture due to low reinforcement ratios had larger J-factor compared to the beams that failed in compression, even though the compression failure was more ductile and gradual than tensile rupture. Another ductility index was defined by Naaman and Jeong [7] as the ratio of the inelastic energy to the total energy. The research conducted by Belarbi and Wang [10] showed that this index was incapable of capturing the ductility improvement when fibrous concrete was used instead of ordinary concrete, while the J-factor provided acceptable ductility measure. Until a unified and more consistent ductility index is found, the ductility index in the current work was simply taken as the ratio of the deflection measured at the ultimate load and the deflection measured at 80 percent of the ultimate load.

## AIM OF THE EXPERIMENTAL WORK AND RESEARCH SIGNIGICANCE

The aim of the experimental work in this research was to study the flexural behavior of simple concrete beams reinforced with hybrid FRP rebars in comparison with similar beams reinforced with GFRP and steel reinforcement. FRP reinforced beams were designed to fail due to concrete crushing and rupture of the FRP rebars, so that the ductility performance can be evaluated for the two modes of failure adopted by the current design codes. For this purpose, normal and high strength concrete mixes and different reinforcement ratios were considered.

The mono-fiber and hybrid rebars were produced in the laboratory using glass fibers, nylon threads and polyester. The production process was convenient with regard to the satisfactory mechanical properties of the rebars, simplicity of the production technique and the availability of the raw materials at reasonable prices in the local market. The significance of the current work lies in the application of hybrid rebars that developed an appealing nonlinear behavior before rupture without series losses in tensile strength and stiffness. Also, the produced hybrid rebar is cheaper than the GFRP rebar as lower cost nylon threads are used to replace a fraction of the glass fibers. Another important aspect is the easy implementation of the nylon thread in a pultrusion production line as the threads are required to be thoroughly distributed in the cross

section of the rebar. New design equations were derived based on strain compatibility and equilibrium of forces using the ACI equivalent stress block to account for the bilinear stress-strain relationship of the produced hybrid rebars.

## TESTING OF BEAMS REINFORCED WITH FRP BARS & STEEL

**Materials**

**Concrete:** two concrete mixes were used to provide normal and high compressive strength at 28 days. The materials used were ordinary Portland cement, crushed dolomite as coarse aggregate with a maximum nominal size of 14 mm, natural sand with a fineness modulus of 2.55. A high range water reducer meeting the requirements of ASTM C-33, (type A, F), was used with a dose of 1% of cement weight to improve the workability in the high strength concrete mix. Cement: Dolomite: Sand: water proportions for ordinary concrete were 1: 3.3: 1.8: 0.54 and for high strength concrete these ratios were 1: 3: 1.78: 0.42. Six cylinders 150x300 mm and three prisms 100x100x500 mm were cast and tested at 28-days age to determine the compressive strength, modulus of elasticity and modulus of rupture for each mix. The test results are listed in Table (1).

**Table 1: Mechanical Properties of Concrete Mixes**

| Mix | Mechanical Properties (MPa) | | |
|-----|------|------|--------|
| | $f'_c$ | $f_r$ | $E_c$ |
| 1 | 30 | 3.1 | 25 900 |
| 2 | 50 | 4.6 | 33 770 |

**Steel:** Deformed high tensile steel bars with a diameter of 9.5 mm were used as longitudinal reinforcement with a yield stress of 530 MPa. The transverse reinforcement consisted of 6-mm mild steel stirrups with a yield stress of 300 MPa.

**GFRP rebars:** Sand coated 9.5 mm GFRP rebars were manufactured in the laboratory adopting the production technique described by Safaan [17]. The manufactured rebar had about 60 percent by volume E-glass fibers in a polyester matrix. The fibers were twisted at an off-axis angle of 30 degrees. The bras were produced with a length of 2.0 m and cut to the desired length using a saw.

**Hybrid FRP rebars:** these rebars were manufactured by replacing 10 percent by volume of the E-glass fibers with 0.35 mm-diameter nylon threads. The low modulus, yet highly ductile nylon thread was obtained from the workshops of the Suez Canal Authority, Egypt. Twisted strands of this thread are used in manufacturing durable tying ropes. To suit this application, 30 percent by weight fiberglass is added to the polymer to increase the tensile strength and stiffness of the thread.

**Table 2: Mechanical Properties FRP Rebars**

| rebar | Mechanical Properties (MPa) | | | |
|-------|-----|--------|-------|--------|
| | $f_u$ | $f^*_u$ | $E_f$ | $e_{fu}$ |
| GFRP | 745 | 700 | 41800 | 0.02 |
| Hybrid | 625 | 590 | 38000 | 0.042 |

Table (2) gives the mechanical properties of the produced rebars in terms of the average tensile strength $f_u$, the guaranteed tensile strength $f^*_u$, the initial modulus of elasticity $E_f$ and the ultimate strain $e_{fu}$. Figure (1) shows the tensile stress-strain relationship for the manufactured GFRP and hybrid rebars. Each data point represents the average of three results obtained from the flexure test described in reference [17]. Figure (1) shows that the GFRP rebars developed a linear elastic response till failure, while the hybrid rebars developed a bilinear response with strain hardening at a load $f_{fy}$ = 385 MPa. The strain hardening modulus $E_y$ was 7.8 GPa, which is 21 percent of the initial elastic modulus, Figure (2).
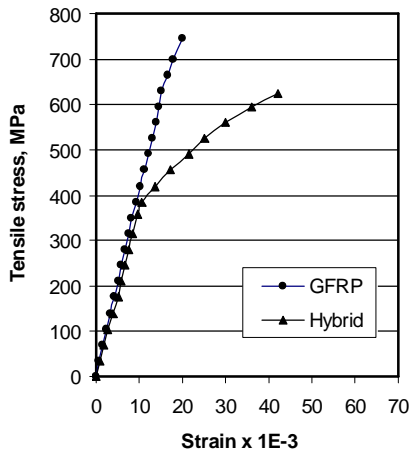
**Fig. 1: Tensile Stress-Strain Relationship for GFRP and Hybrid Rebars**
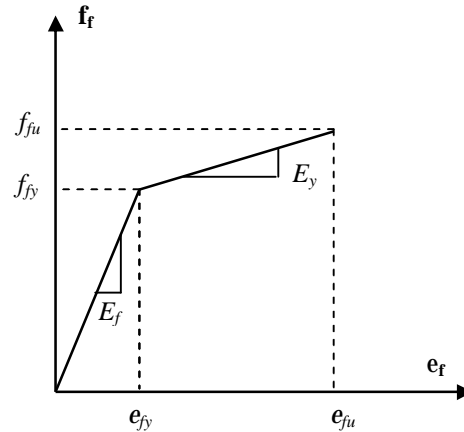
**Fig. 2: Idealized Stress-Strain Relationship for Hybrid FRP Rebars**

## Beam Specimens: Design & Testing

A total of 12 beams (127x200x1730 mm) were cast. The beams were divided into three series S, M and H reinforced with steel, mono GFRP and hybrid rebars, respectively. The web reinforcement in all beams consisted of closed steel stirrups along the shear span at 90-mm center-to-center spacing. The beams were singly reinforced as the hanging bars ran only along the shear span. Figure (3) shows the geometry and reinforcement details.
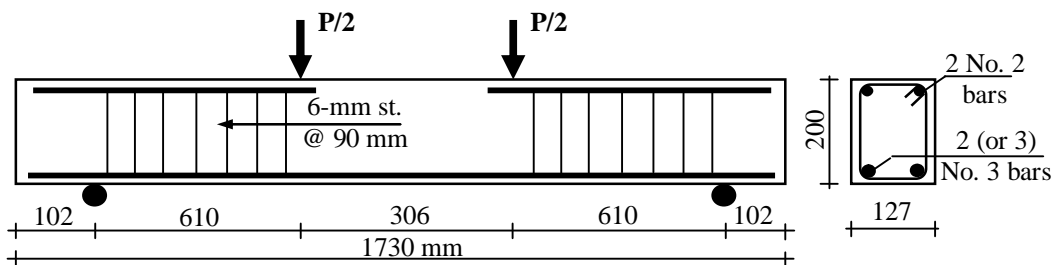


**Fig. 3: Dimensions and Reinforcement Details of Test Specimen**

### Design

the design criteria for conventional beams reinforced with steel were based on the provisions of the ACI 318-95 code [19] for ultimate strength design. The reinforcement ratio ranged from 0.23 to 0.48 of the balanced ratio to ensure a flexural failure. Nominal flexural and shear capacities were computed based on the actual material properties without using the reduction factors specified by the code. Similarly, the flexural design of the GFRP reinforced beams was based on the provisions of the ACI440.1R-03 design guide [4]. While the ACI 440.1R-03 design equations were directly applied for the design of test beams in series M, these equations needed some extension to account for the bilinear response of the hybrid rebars in series H when the failure is governed by concrete crushing. In this case the tensile stress in the rebar is smaller than the tensile strength $f_{fu}$ and can not be calculated directly as in the case with GFRP rebars characterized by a linear stress-strain response.

The following equations based on equilibrium of forces and strain compatibility were derived to compute the balanced reinforcement ratio $\rho_b$ and nominal moment $M_n$ when failure is initiated due to concrete crushing (the reinforcement ratio $\rho_f$ is higher than the balanced ratio $\rho_b$).

$$\rho_b = 0.85\beta_1 \frac{f_c'}{f_{fu}} \frac{\varepsilon_{cu}}{e_{cu} + e_{fu}} \qquad (1)$$

$$M_n = A_f f_f \left(d - \frac{a}{2}\right) \qquad (2)$$

$$a = \frac{A_f f_f}{0.85 f_c' b} \qquad (3)$$

$$f_f = 0.85\beta_1 \frac{f_c'}{r_f} \frac{\varepsilon_{cu}}{e_{cu} + e_f} \qquad (4)$$

In the above equations $\varepsilon_{cu}$ is the ultimate concrete strain and taken 0.003, $A_f$ is the tension reinforcement area and $f_f$ is the tensile stress in the FRP bar. Depending on the stress level in the FRP rebar, the following constitutive relationships are applied:

$$f_f \leq f_{fy}: \; e_f = f_f / E_f \qquad (5)$$

$$f_{fy} < f_f \leq f_{fu}: \; e_f = e_{fy} + (f_f - f_{fy})/E_y \qquad (6)$$

Substituting $e_f$ from Equation (5) into Equation (4) and solving for $f_f$ gives:

$$f_f = \left( \sqrt{\frac{(E_f e_{cu})^2}{4} + \frac{0.85\beta_1 f_c'}{r_f}} - 0.5 E_f e_{cu} \right) \leq f_{fy} \qquad (7)$$

Substituting $e_f$ from Equation (6) into Equation (4) gives the following relation from which the tensile stress $f_f$ can be computed by a trial and error procedure:

$$f_f = 0.85\beta_1 \frac{f_c'}{r_f} \frac{e_{cu}\Delta E_f}{e_{cu}\Delta E_f + f_f - f_{fy}(1-\Delta)} \qquad (8)$$

where $\Delta$ is the ratio of the hardening modulus to the initial modulus ($E_y / E_f$).
When the reinforcement ratio is less than the reinforcement ratio, failure is initiated by rebar rupture. The following equations adopted by ACI 440.1R-03 were used to compute the nominal moment:

$$M_n = 0.8 A_f f_{fu} \left(d - \frac{\beta_1 c_b}{2}\right) \qquad (9)$$

$$c_b = \left(\frac{e_{cu}}{e_{cu} + e_{fu}}\right) d \qquad (10)$$

Table (3) gives the design details of the test beams in terms of the nominal load $P_n$, FRP rebar stress $f_f$, the shear strength component $V_c$ provided by concrete, the nominal shear strength $V_n = V_c + V_s$ provided by concrete and web steel reinforcement, and the factor of safety against shear failure ($2V_n/P_n$). The beams were identified by their series followed by two numbers; the first is the number of tension rebars and the second is the concrete grade.

**Table 3: Design Details of the Concrete Beams**

| Beam | $\rho / \rho_b$ | $P_n$ (kN) | $f_f$ (MPa) | $V_c$ (kN) | $\dfrac{2V_n}{P_n}$ |
|------|------|------|------|------|------|
| S2/30 | 0.32 | 45.6 | -- | 21.0 | 2.41 |
| S3/30 | 0.48 | 65.7 | -- | 21.0 | 1.67 |
| S2/50 | 0.23 | 47.0 | -- | 27.1 | 2.59 |
| S3/50 | 0.35 | 68.9 | -- | 27.1 | 1.77 |
| M2/30 | 1.34 | 46.3 | 597 | 2.41 | 1.57 |
| M3/30 | 2.01 | 54.6 | 477 | 3.61 | 1.37 |
| M2/50 | 0.97 | 44.4 | 700 | 2.25 | 1.63 |
| M3/50 | 1.45 | 67.2 | 571 | 3.37 | 1.11 |
| H2/30 | 2.58 | 36.2 | 458 | 2.19 | 2.00 |
| H3/30 | 3.86 | 47.9 | 413 | 3.28 | 1.56 |
| H2/50 | 1.86 | 40.6 | 504 | 2.04 | 1.77 |
| H3/50 | 2.79 | 53.5 | 448 | 3.06 | 1.38 |

**Testing**

All beams were tested to ultimate load under four-point bending over a simple span of 1.53 m and a shear span of 0.61 m providing a shear span-to-depth ratio of 3.39. Both ends of the beam were free to rotate and translate under load.  The load was applied by means of a 100 kN capacity flexural machine. The machine is equipped with a digital control console. The load was applied in increments of 2.5 kN in case of series S beams and increments of 1.0 mm displacement in case of M and H series beams. Mid-span deflection was recorded at each load step using a dial gage. Strains were measured using a demountable mechanical strain gage. The strains were measured using punched steel disks affixed at a gage length of 200 mm about the beam center. The disks were affixed to both sides of the beam at the level of the tension reinforcement and also 5 mm below the extreme compression concrete fiber.

## TEST RESULTS AND DISCUSSIONS

The structural behavior of the tested beams was studied in terms of ultimate loads, load-deflection response, and ductility. Also, the accuracy of the derived design equations was verified. A summary of the results is given in Table (4). The results are given in terms of the ultimate loads, stress in the GFRP reinforcement, measured concrete compressive strain at failure, the mode of failure and ductility index (the ratio of the deflection measured at the ultimate load and the deflection measured at 80 percent of the ultimate load).

**Table 4: Summary of the Experimental Test Results**

| Beam | $P_n$ (kN) | $f_f$ (MPa) | $\varepsilon_{cu} \times 10^{-5}$ | Failure mode | Ductility index |
|------|------|------|------|------|------|
| S2/30 | 45.9 (1.01)* | -- | 200 | steel yielding | 2.00 |
| S3/30 | 67.0 (1.02) | -- | 210 | steel yielding | 2.50 |
| S2/50 | 46.8 (0.99) | -- | 225 | steel yielding | 1.94 |
| S3/50 | 68.0 (0.99) | -- | 240 | steel yielding | 2.40 |
| M2/30 | 47.0 (1.02) | 588 (0.98)* | 450 | concrete crushing | 1.45 |
| M3/30 | 47.0 (0.86) | 430 (0.90) | 150 | shear-compression | 1.54 |
| M2/50 | 53.7 (1.21) | 675 (0.96) | 325 | rebar rupture | 1.50 |
| M3/50 | 60.8 (0.90) | 495 (0.87) | 340 | shear-compression | 1.87 |
| H2/30 | 41.2 (1.14) | 500 (1.09) | 240 | shear-compression | 1.60 |
| H3/30 | 47.7 (0.99) | 413 (1.00) | 260 | shear-compression | 1.64 |
| H2/50 | 39.0 (0.96) | 490 (0.97) | 300 | concrete crushing | 1.60 |
| H3/50 | 55.5 (1.04) | 460 (1.03) | 330 | concrete crushing | 2.32 |

 * ( ):  experimental / theoretical
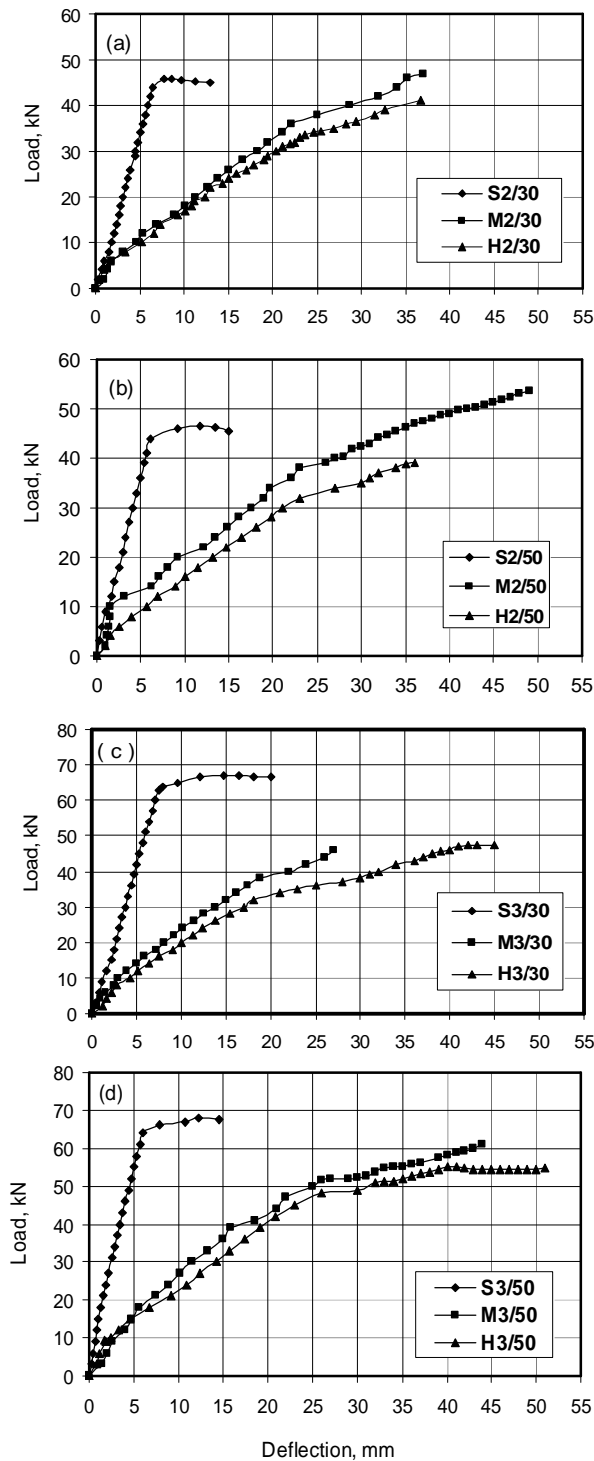
**Fig. 4.a-d: Load-Midspan Deflection for Test Beams in Series S, M and H**

**Ultimate loads:** the results reported in Table (4) shows that the GFRP reinforced beams in series M that failed as designed due to concrete crushing or rebar rupture achieved higher ultimate loads compared to similar steel beams with the same reinforcement area. Because of the different failure modes, it was not convenient to compare the ultimate loads of series M and H beams to evaluate the influence of hybridization. Theoretically, the beams were assumed to

lose 10-20 percent of their loading capacity due to hybridization. However, the average loss in the load capacity based on the experimental results was only 12 percent.

The tensile stresses in the FRP rebars reported on Table (4) were computed based on the measured tensile strains and the material constitutive laws. The measured stresses were in good agreement was the theoretical values computed by the proposed equations. It can be seen that the ultimate load in series M and H beams did not exceed the ultimate load in the corresponding beams in series S as long as the stress level in the GFRP bars at ultimate was less than the yield stress of steel (530 MPa). It can also be seen that in case of series M beams, the stress level at failure increased as the compressive strength increased, which made it possible to take advantage of the high strength of the GFRP bar. However, that was not the case in series H beams in which the stress level was not significantly influenced by the concrete strength. This result demonstrated less sensitivity of the ultimate load to the increase in the concrete compressive strength similar to the steel reinforced beams. This trend is attributed to the large strains developed in the reinforcement associated with a smaller depth of the compression zone. This result is also related to the fact that increasing the ultimate strain in the FRP reinforcement increases the tendency to fail in compression as the balanced ratio decreases for the same concrete compressive strength and rebar tensile strength. This would actually increase the safety against probable change in the mode of failure from concrete crushing to rebar rupture due to the use of concrete with a higher grade than specified in the design.

**Load-deformation response:** The load-deflection curves for the tested beams are shown in Figure (4.a-d). it can be seen that the deflection in series H beams was always higher than the deflection in the corresponding series M beams during the whole course of loading. The figures shows a typical three-stage behavior for the under-reinforced steel reinforced beams that correspond to uncracked section, cracked section linear elastic to yield and post-yield of reinforcement. On the other hand, all FRP reinforced beams somehow exhibited a non-linear response near failure independent of the reinforcement type and ratio and the mode of failure. Except for beam M3/30 that failed in explicit shear-compression failure, the beams in series M developed a significant nonlinear response before failure. This can be attributed to the crushing of concrete all along the maximum bending moment region as in beam M2/30 or in more than one location as in beams M2/50 and M3/50.

**Ductility:** the ductility index values reported in Table (4) shows that the steel reinforced beams always had a higher ductility index compared to the corresponding FRP reinforced beams. Also, it can be seen that the use of hybrid rebars improved the ductility compared to mono-fiber rebars. The best result was obtained in beam H3/50 that achieved a ductility index that was very close to that of the corresponding steel reinforced beam. The reported values for the rebar tensile stress in Table (4) shows that the tensile stress at failure was limited to 70-85 percent of the design strength. For this reason better ductility measures might be achieved by lowering the reinforcement ratio to increase the tensile stress in the rebars as long as the strain capacity of concrete is not exhausted.

The adequacy of the proposed design equations was evaluated based on the accuracy of predicting the ultimate loads, mode of failure and safety against shear failure. With regard to predicting the ultimate loads, Table (4) shows that the ratio of the experimental to theoretical ultimate loads was in the range 0.96 to 1.21 for the beams that failed as designed due to flexure, concrete crushing or rebar rupture. The rest of the beams that failed prematurely in shear compression achieved 0.86-0.99 of their theoretical ultimate loads. The only exception was in beam H2/30 that achieved an ultimate load that was 13 percent higher than the theoretical load. It was noticed that this beam was experiencing a compression failure when the outermost flexure crack extended rapidly towards the load, and the beam failed due to concrete crushing under the load. Considering the ability of predicting the mode of failure, all beams failed as designed except for beams M3/30, M3/50, H2/30 and H3/30. Except for beam M3/30 that developed a standard shear-compression failure, the other three beams failed in a similar sequence by developing a high compressive strain in the maximum moment region and instead of developing a standard compression failure, these beams failed suddenly due to concrete
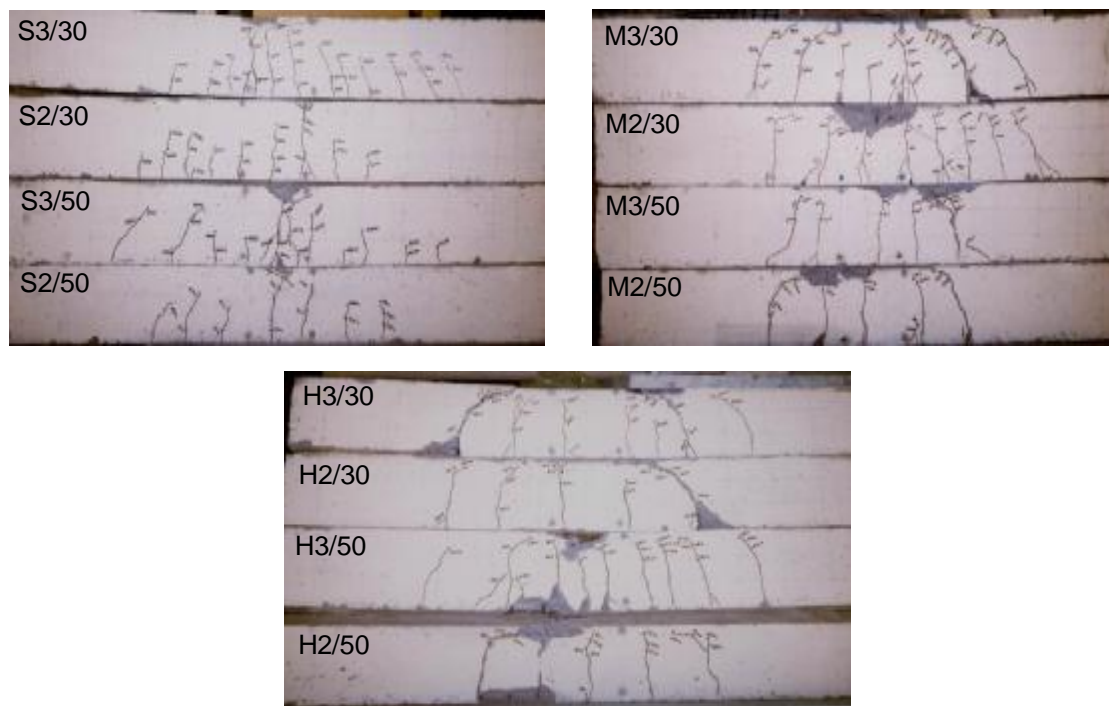
**Fig. 5: Cracking Patterns of Test Beams**

crushing under the load, followed by concrete crushing in the maximum moment region as can be clearly seen in beam M3/50, Figure (5).  The obtained experimental results demonstrated the capability of the derived design equations to predict the ultimate loads and modes of failure. However, it seems that the shear capacity has been overestimated for the FRP reinforced beams that failed prematurely as the computed safety margin against shear failure was not consistent was the obtained results.

## CONCLUSIONS

The experimental work conducted in this research demonstrated the advantages of developing a new hybrid FRP rebar for concrete reinforcement. The produced rebar has appealing features in terms of a bilinear stress-strain relationship, lower cost and the easy implementation in pultrusion production lines. Based on the results obtained from the current research, the following main conclusions can be summarized:

1. The in-house manufactured GFRP bars and hybrid FRP rebars with a diameter of 9.5 mm provided a satisfactory performance as tension reinforcement in simple concrete beams.
2. limited loss of stiffness was observed in the post-cracking stage due to the use of the hybrid rebars instead of GFRP rebars. Both types of FRP reinforcement showed a high deformation capacity at failure.
3. Compared to similar GRRP reinforced beams, the average loss in the load capacity based on the experimental results was only 12 percent when hybrid rebars were used.
4. Using hybrid FRP rebars improved the ductility compared to GFRP rebars. The best result of ductility improvement was achieved when higher strength concrete and higher reinforcement ratio were applied resulting in a ductility index that was very close to that of similar steel beam.
5. The benefits of hybridization can be realized in over-reinforced beams as long as the tensile stress in the rebar is greater than the hardening stress.
6. Better utilization of the GFRP reinforcement was achieved by using high strength concrete to increase the stress level in the rebars.

7. The hybrid FRP reinforced beams demonstrated less sensitivity of the ultimate load to the increase in the concrete compressive strength in a trend similar to that of the steel reinforced beams.

8. The previous conclusion reflected the fact that increasing the ultimate strain in the FRP reinforcement increases the tendency of failure due to concrete crushing as the balanced ratio decreases for the same concrete compressive strength and rebar tensile strength. This would increase the safety margin against probable change in the mode of failure from concrete crushing to rebar rupture due to the use of concrete with a higher grade than specified in the design.

9. The ultimate loads and modes of failure were well predicted utilizing the derived design equations to account for the bilinear stress-strain relationship of the hybrid rebars.

## REFERENCES

1. Naaman, A. E., and Harajli, M. H. and Wight, J. K. (1986), "Analysis of ductility in partially prestressed concrete flexural members" PCI Journal, V. 31, No. 3, pp. 64-87.

2. Sonobe, Y., et al. (1997), "Design guidelines of FRP reinforced concrete building structures" Journal of Composites for Construction, V. 1, No. 3, pp. 90-113.

3. Theriault, M. and Bemokrane, B. (1998), "Effect of FRP reinforcement ratio and concrete strength on flexural behavior of concrete beams" Journal of Composites for Construction, V. 2, No. 1, pp. 7-16.

4. ACI 440.1R-03 (2003), "Guide for the Design and Construction of Concrete Reinforced with FRP Bars" ACI Committee 440, 42 pp.

5. Fukuyama, H. , Masuda, Y., Sonobe, Y. and Tanigaki, M. (1995), "Structural performance of concrete frame reinforced with FRP reinforcement" Non-metallic (FRP) Reinforcement of Concrete Structures, editor: Taerwe L. , E&FN, London, pp. 275-286.

6. Clarke, J. L. and O'Regan D. P. (1995), "Design of Concrete Structures Reinforced with Fiber Composite Rods" Proceedings of the Second International RILEM Symposium on Non-Metallic (FRP) Reinforcement for Concrete Structures (FRPRCS-2), Ghent, Belgium, pp. 646–653.

7. Naaman, A. E. and Jeong, S. M. (1995), "Structural ductility of concrete beams prestressed with FRP tendons" Non-metallic(FRP) Reinforcement of Concrete Structures, editor: Taerwe L. , E&FN, London, pp. 379-386.

8. Alsayed S. H. and Alhozaimy, A. M. (1999), "Ductility of concrete beams reinforced with FRP bars and steel fibers" Journal of Composite Materials, Vol. 33, No. 19, pp. 1792-1806.

9. Safaan, M. A. and Afify, M. R. (2005), "Behavior o concrete beams reinforced with in-house manufactured GFRP bars" Proceedings of the 4th Middle East Symposium on Structural Composites for Infrastructure Applications: Sustainability of Knowledge, editor: Hosny, A., Alexandria, Egypt.

10. Belarbi, A. and Wang, H. (2004), "Steel-free hybrid reinforcement system for concrete bridge decks" Technical Report No. UTC R52, Center for Infrastructure Engineering Studies, University of Missouri, Rolla, USA, pp. 205.

11. Li, V. C. and Wang, S. (2002), "Flexural behavior of glass-fiber reinforced polymer (GFRP) reinforced engineered cementitious composite beams" ACI Materials Journal, V. 99, No. 1, pp. 1-21.

12. Li, V. C. and Kanda, T. (1998), "Engineered cementitious composites for structural applications" ASCE Journal Materials in Civil Engineering, Vol. 10, No. 2, pp. 66-69.

13. Tamuzs, V., Tepfers, R., Apinis, R., Vilks, U. and Modniks, J. (1996), "Ductility of hybrid fiber composite reinforcement for concrete" Proceedings of the 1st International Conference on Composites in Infrastructures, Editor: Saadatmanesh, H. and Ehsani, M. R., Tucson, Arizona, pp. 110-122.

14. Bakis, C. E., Nanni. A. and Terosky, J. A. (1996), "Smart pseudo-ductile reinforcing rods for concrete: manufacture and test" Proceedings of the 1st International Conference on Composites in Infrastructures, Editor: Saadatmanesh, H. and Ehsani, M. R., Tucson, Arizona, pp. 95-108.

15. Harris, H. G., Somboonsong, W. anf Ko, F. K. (1998), "New ductile hybrid FRP reinforcing bar for concrete structures" Journal of Composites of Construction, Vol. 2, No. 1, pp. 28-37.

16. Sadek, E. F. (2004), "Stydying the use of fiber reinforced plastics in producing reinforcing bars for concrete" M. Sc. Thesis, Faculty of Engineering, Ain Shams University, Cairo, Egypt, pp. 216.

17. Safaan, M. A. (2004), "Mechanical properties of locally produced hybrid FRP bars as concrete reinforcement" International Conference on Future Vision and Challenges for Urban Development, Housing & Building Research Center (HBRC), Cairo, Egypt, 20-22 December 2004. HBRC Journal, Vol. 1, No. 1, December 2004, ISSN 12479/2004, 1-13.

18. Jaeger, L. G., Mufti, A. and Tadros, G. (1997), "The concept of the overall performance factor in rectangular section reinforced concrete beams" Proceedings of the 3rd International Symposium on Non-Metallic (FRP) Reinforced Concrete Structures, Japan Concrete Institute, Sapporo, Japan, V. 2, pp. 551-558.

19. Vijay, P. V., Kumar, S. V. and GangRao, H. V. S (1997), "Shear and ductility behavior of concrete beams reinforced by GFRP rebars" Proceedings of the 2nd Conference on Advanced Composite Materials in Bridges and Structures, editor: M. El-Badry, Canadian Society for Civil Engineering, Montreal, Canada, pp. 217-226.

20. ACI Committee 318 (1995), "Building Code Requirements for Reinforced Concrete, ACI-95 and commentary ACI 318R-95" ACI, pp. 369.

# CURING DURATION
# OF HIGH PERFORMANCE CONCRETE

**Nadia M. Nofal**

*Associate Professor, Housing and Building National Research Center, Cairo, Egypt*
*Email: n.nofal@hbrc.edu.eg*

## ABSTRACT

The objective of this experimental work is to evaluate the minimum curing duration of high performance concrete which has a direct impact on construction rate and economy. The exploratory study summarized the influence of the duration of moist curing on the variation of strength with distance from the drying surface. The strength at an age of 28 days was used as the basis for comparison.

Six concrete mixtures with water / cementitious materials ratios 0.35 and 0.47 and two different cementitious materials (silica fume and fly ash) were used. The former water / cementitious materials ratio is intended to be representative of the hydration and drying behavior of a high – performance concrete with a low water / cementitious materials ratio .

Four moist curing periods were adopted. At the end of the moist – curing period, the specimens were sealed and allowed to dry at 25 °C and 60 % relative humidity .Tensile strength was measured at 28 days as a function of distance from the drying surface using cylindrical test specimens with circular notches cast at various depths (15, 25 & 55 mm). The notches created reduced cross sections that forced failures to occur at predetermined distances from the drying surface. Relationships between tensile strength and depth from drying surface were compared with those of specimens continuously moist cured.

The experimental results showed interesting results with respect to the duration of curing which may be sufficient to ensure adequate strength development.

**Keywords:** Curing, high performance concrete – tensile strength, mortar, hydration.

## INTRODUCTION

A review of the predecessors to ACI 318 -95 [1] revealed that the general requirements for curing of concrete have changed very little since the first standard regulations were proposed in 1909 (Meeks and Carino) [2]. The basic requirement has been to cure concrete made with normal Portland cement for a period of at least 7 days and to cure high – early strength concrete for at least 3 days.

The ACI code provides validation of the 7 - day criterion, and since high – early strength concrete will gain strength more rapidly, the code permits a 3 - day curing period. In 1971 code, a requirement was added to maintain the concrete temperature above 10°C during curing. Also, the ACI code does not address curing requirements for concrete made with other cementitious materials, since the nature of the cementitious system affects early – age strength development characteristics, this omission may be a major deficiency in the current code. Therefore, existing curing practices may not be optimal for high – performance concrete.

A better understanding is needed for the external supply of moisture and of the adequacy of membrane – forming compounds when a low water / cementitious ratio is involved.

The effects of self–desiccation are also important considerations in high- performance concrete with low w/c ratio. "Self–desiccation refers to the process by which concrete dries itself from the inside", moisture in the paste is consumed by the hydration reactions, and the internal relative humidity may decrease to the point where there is not enough remaining free water to sustain hydration. Consequently, hydration will terminate at an early age if additional moisture is not

provided. To prevent early- age self – desiccation, water that is consumed by hydration needs to be replaced by the ingress of external moisture. However, for how long is moist curing effective? As hydration proceeds, capillary pores in the paste become discontinuous, thereby hindering the ingress of additional water into the concrete. When this state is reached, additional moist curing may be of little or no benefit, because the water may not be able to penetrate to the interior quickly enough to maintain saturation of the capillaries and sustain hydration. Current curing requirements, based on research on conventional concrete, do not consider these factors.

Hilsdorf and co-workers [3] have presented a rational approach to establish the curing duration. A key factor affecting this duration is the controlling criterion for adequate long-term performance. Hilsdorf's studies showed that, in most cases, the critical curing duration was controlled by compressive strength. This is an important finding because it tends to affirm that strength – based criteria may be the most practical approach to evaluate the adequacy of curing, possibly even when durability is a primary concern. Hilsdorf summarized the four factors that must be considered in establishing minimum curing durations:

§   Curing sensitivity of the concrete as influenced primarily by the cementitious system.
§   Concrete temperature as it affects the rate of hydration (and therefore, rate of strength development and reduction in porosity).
§   Ambient conditions during and after curing as these affect the rate of strength development and severity of drying of the surface layer.
§   Exposure conditions of the structure in service as these affect the required (skin) properties of adequate service life.

Current curing practices and standards are based on studies related primarily to strength development characteristics of conventional concretes. Most high performance concretes however are fundamentally different from conventional concrete because they typically have a low water – cementitious materials ratio and one or more admixtures, in addition to supplementary cementitious materials as silica fume or fly ash which are commonly used in practicable mixtures to achieve high strength. Since the composition of high performance concrete differs from conventional mixtures, early age characteristics of the hydrating paste will also differ, therefore existing curing practices may not be optimal for high performance concrete. This experimental research examines the influence of the duration of moist curing on the variation of strength with distance from the drying surface. The question that has to be answered: is what fraction of the standard – cured strength has to be attained at the end of the curing period to ensure that the design strength is attained in the interior of the member (at the depth of the first layer of reinforcement)?

## EXPERIMENTAL PROGRAM

### Scope

Six concrete mixtures were used in this experimental research with water / cementitious materials ratios 0.35 and 0.47. For all the tested concrete mixtures, four moist curing periods were used (1, 3, 7 and 28 days). At the end of the moist curing periods, the specimens were sealed and allowed to dry at 25 °C and 60 % relative humidity. Reference specimens were continuously moist and cured by storing them in a water bath for 28 days.

Tensile strength was measured at 28 days as a function of the distance from the drying surface using cylindrical test specimens with circular notches made at various depths. The notches created reduced cross sections that forced failures to occur at predetermined distances from the drying surface. The estimated average tensile strength at a depth of 25 mm was used as the basis for evaluating the influence of the different curing procedures.

The objective was to determine the minimum curing duration which enables the development of a satisfactory level of strength at the reinforcement level (depth).

Three notch depths for each treatment (15, 25 and 50 mm) and three replicate specimens were tested for each notch depth.

**Procedure**

Six main test series of concrete mixes were included in this study, details of each mix are shown in table 1. Egyptian ordinary Portland cement was used; its physical and chemical properties were in compliance with the limits of the Egyptian standard specification (E.S.S) 373-1991. The specific surface area was 3750cm$^2$/gm, and compressive strength was 27 and 33 N/mm$^2$ at 3 and 7 days respectively.

**Table 1: Investigated Concrete Mixtures**

| Ingredients (kg/m$^3$) | w/c 0.47 | | | w/c 0.35 | | |
|---|---|---|---|---|---|---|
| | Mix I | Mix II | Mix III | Mix IV | Mix V | Mix VI |
| **Cement** | 350 | 308 | 297.5 | 350 | 308 | 297.5 |
| **Dolomite** | 1183.3 | 1183.3 | 1183.3 | 1134 | 1134 | 1134 |
| **Sand** | 583.3 | 583.3 | 583.3 | 756 | 756 | 756 |
| **Water** | 165 | 165 | 165 | 122.5 | 122.5 | 122.5 |
| **Silica** | - | 42 | - | - | 42 | - |
| **Fly ash** | - | - | 52.5 | - | - | 52.5 |
| **HRWR (liter/m$^3$)** | 3.5 | 3.5 | 3.5 | 8.75 | 8.75 | 8.75 |

The used coarse aggregate was dolomite with a nominal maximum size of 20mm. Uniform standard fine sand with a fineness modulus of 2.6 was used. The aggregate properties are in complete compliance with the limits of the (E.S.S) 1109 -2002.

Silica fume, which is a by product of Ferro silicon industry, and, it contains more than 97% silica was used with a percentage of 12 % replacement of cement weight.
Another, ultra fine, highly pozzolanic cement enhancer which is used in high performance concrete, with commercial name  "Super- Pozz Fly Ash " was used with a dosage of 15 % cement replacement. The chemical and physical properties are shown in table 2. It is a highly reactive alumina silicate pozzolan which adds strength and durability to cementitious mixes, whilst its fineness and spherical particle shape improves workability.

A high range water reducer (HRWR) admixture of dosage 1% and 2.5 % of cementitious materials weight was used  for water/cementitious ratios 0.47 and 0.35 respectively.
The concrete was mixed according to ACI 211.1.

**Table 2:  Chemical and Physical Properties of Super-Pozz Fly Ash**

| Typical Chemical Analysis (%) | | Physical Properties | |
|---|---|---|---|
| **Silica, SiO$_2$** | 53.5 | **Relative density** | 2.2 |
| **Alumina, Al$_2$O$_3$** | 34.3 | **Theoretical surface Area ( cm$^2$/g )** | 13000 |
| **Iron, Fe$_2$O$_3$** | 3.6 | | |
| **Calcium, CaO** | 4.4 | **pH, in water** | 11-12 |
| **Potassium,K$_2$O** | 0.8 | **Moisture content %** | < 0.2 |
| **Titanium, TiO$_2$** | 1.7 | **Colour** | Light grey |
| **Loss in ignition @ 950 °C** | 0.4 | **Particle shape** | spherical |

Cylinder molds with a nominal inside diameter of 100mm and a height of 200mm were used. Each mold included a 10mm thick plastic ring with an inside diameter of a bout 90mm. The rings were positioned at depths of (15, 25, 50) mm from the top surface. The rings were held in place by friction. Care was taken when filling the molds to avoid disturbing their positions. Figure 1 shows the cross section of the mold filled with concrete and a set of molds prepared for casting showing the rings in place.
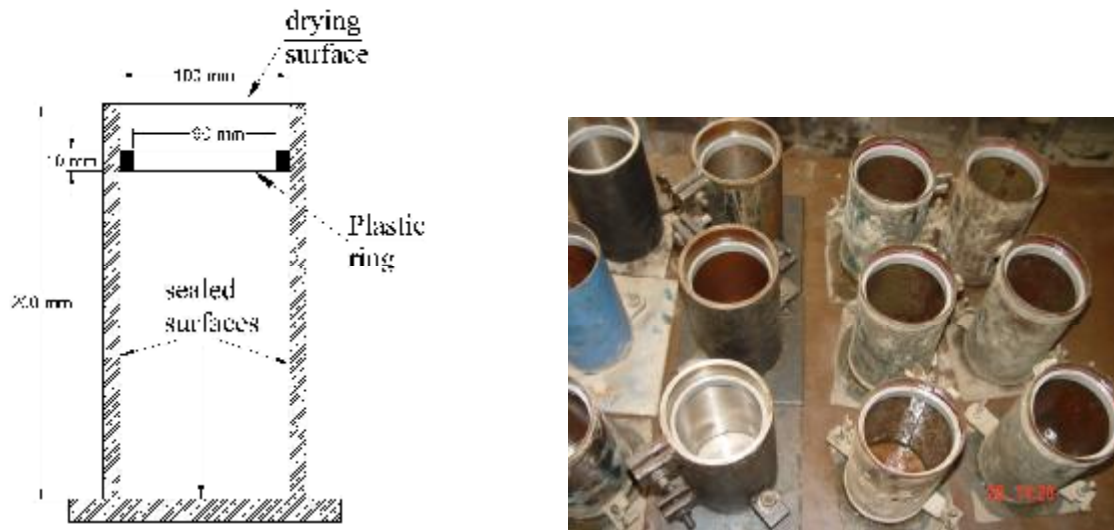
**Fig. 1: Cross Section of the Mold and Set of Molds Prepared for Casting**

Each mold was filled in three layers, and consolidated with a tamper plus a vibrating table to reduce the occurrence of large voids. The top surface was smoothed with a trowel. At the end of the designated period of moist curing, the molds were removed, and the bottoms and sides of the cylinders were covered with plastic tape so that subsequent drying would occur only from the top surface. At an age of 27 days, the cylinders were prepared for tensile testing. For the continuously moist-cured cylinders, the specimens were removed from the water bath. Steel disks of 25mm thickness and with a central threaded hole, were bonded to the ends of the cylinders using a high-strength structural grade epoxy.

Short rods were screwed into the disks before bonding to keep the holes free of epoxy. Figure 2 shows some of the specimens prepared for testing.



**Fig. 2: Some of the Specimens Prepared for Testing**

The epoxy was allowed to cure overnight. On the 28th day, the specimens were tested in uniaxial tension. A hydraulic, servo-controlled testing machine, applied the tensile load, which was transferred to the disks through a "hook and eye" linkage to reduce bending effects. Figure 3 shows this linkage system and the overall view of the tensile test. Load was applied by constant movement of the machine cross head so that the applied stress rate was kept constant.
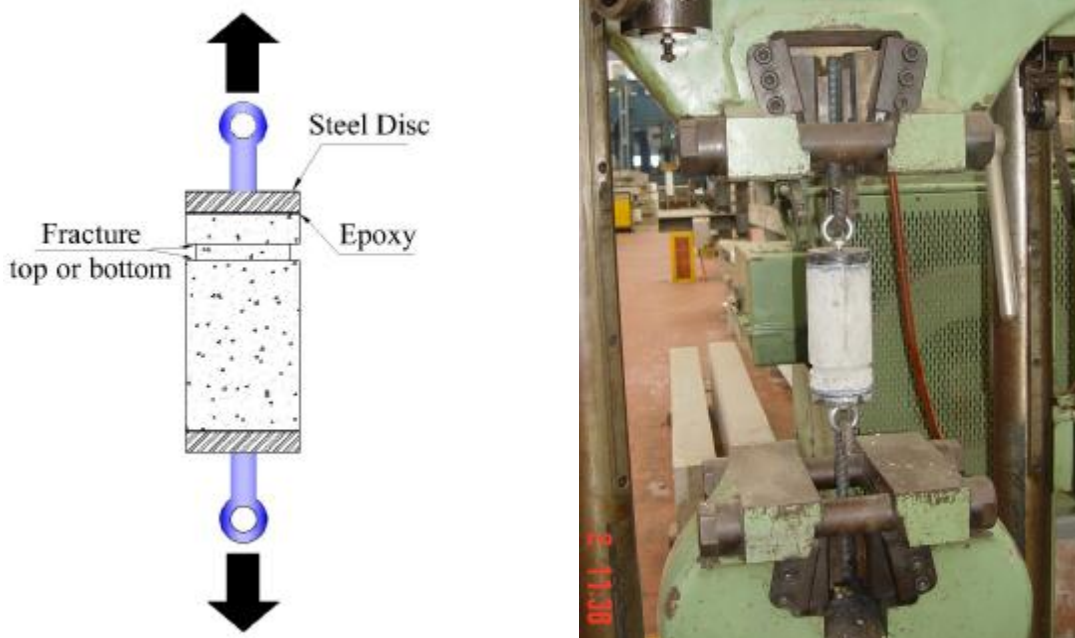
**Fig. 3:  Linkage System and Overall View of the Tensile Test**

After testing was completed, the disks were removed carefully with a hammer and chisel, and the top portion of the cylinders was split in half using the splitting-tension loading method. The exposed surfaces were examined visually to estimate the depths of the drying fronts (indicated by the lighter shade). The drying front was more difficult to observe in the (w/c = 0.47) specimens because of their generally shade compared with the (w/c = 0.35) specimens.

## RESULTS & DISCUSSION

Hereinafter, the effect of different curing regimes or curing durations on the strength development at 28 days age of high performance concrete mixtures incorporating different kinds and dosages of pozzolanic material as well as mixtures without pozzolana is investigated.

### Tensile Strength Development

Figure 4 shows the strength development at 15 mm from the drying surface as a function of the curing period. Two levels of tensile strength could be seen. The higher strengths correspond to the group of mixes with the lower water content (w/c = 0.35), and of course the lower strengths for the mixes with the higher water content (w/c = 0.47). The figure shows that within the surface layer of the concrete (15 mm depth), the maximum strength is almost attained at 7 days of curing. These results are helpful when the quality of the concrete cover is a concern.

It was stated before, that curing durations for concrete made with supplementary cementitious materials besides Portland cement did not receive attention in different Codes of Practice. Therefore, it was aimed during this preliminary investigation to investigate the minimum curing period for high performance concrete. The minimum curing period is that required for the cementitious materials to attain some degree of hydration or maturity. ACI Committee 308(1998) [4] specifies that the strength at the end of the curing period should be at least 0.7 of the design strength. As this limiting strength ratio is for compressive strength, another limiting tensile strength ratio of 0.9 is suggested here as the criterion for accepting the minimum curing period. Through the present work, the requirement for curing duration is evaluated at the depth

of the first layer of reinforcement. The rationale for this requirement is to ensure that the bond strength of the reinforcing steel will attain the value assumed in the structural design.

Figure 5 shows the tensile strength of all the investigated mixes at 25mm depth from the drying surface at different curing durations starting from one day till 28 days. As could be seen, more than 90% of the 28 day strength is reached after only 3 days of curing. It is interesting to note that for the two groups of mixes having relatively low (w/c) ratio, there was no appreciable difference between them regarding the curing duration. This suggests that the (w/c) ratio is more influencing than the effect of pozzolana on the minimum curing duration.

Comparing the two groups of mixes show that for the first group with 0.47 (w/c) ratio, the curves of the three mixes were parallel and showed almost identical trend. On the other hand, the second group of mixes with 0.35 (w/c) ratio exhibited two distinct patterns; one for the mixes incorporating pozzolana and the other one for the ordinary mix. These results imply that the effect of pozzolana on the curing period and also the maturity becomes more apparent with lower (w/c) ratio.

The tensile strength results at 50 mm depth from the drying surface are shown in Figure 6. The 50 mm depth can be considered as the level of the second layer of reinforcement. Most of the mixes attained more than 90% of their 28 day strength at 3 day curing. Two mixes only did not follow this trend, namely the fly ash mix with 0.47 (w/c) ratio and the silica fume mix with 0.35 (w/c) ratio.  However, the 90% ratio is found by interpolation between the results at 3 and 7 days to be achieved after 5 days of curing.
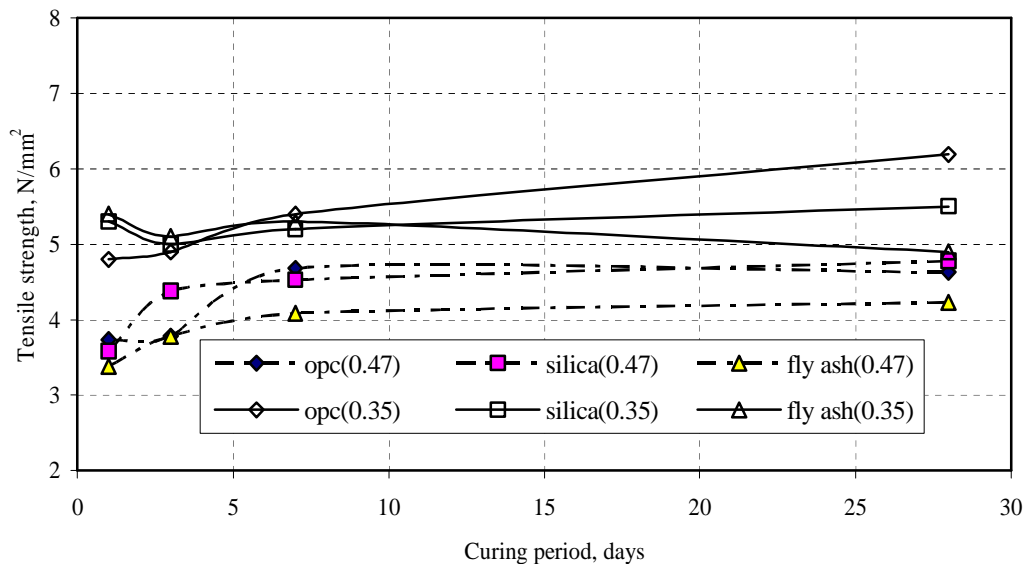


**Fig. 4: Time-Tensile Strength Development at 15 mm Depth from Drying Surface**
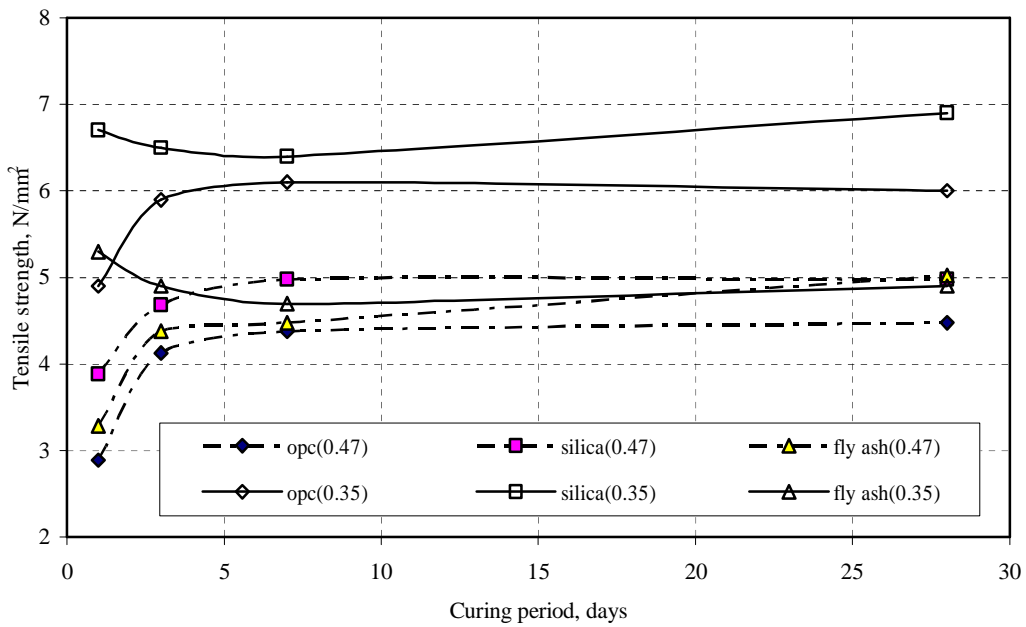
**Fig. 5: Time-Tensile Strength Development at 25 mm Depth from Drying Surface**
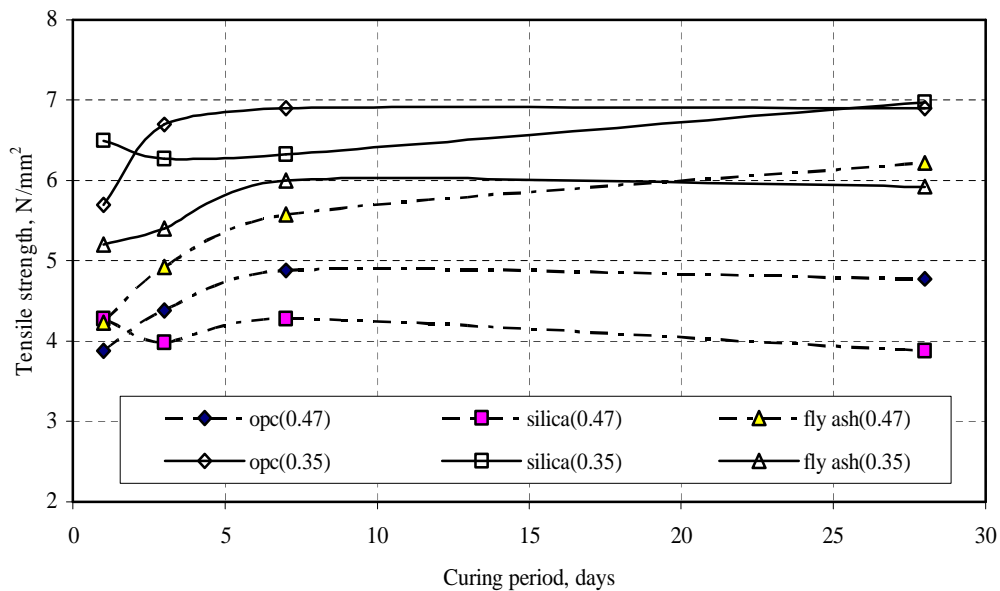


**Fig. 6: Time-Tensile Strength Development at 50 mm Depth from Drying Surface**

Reviewing the results cited for the preceding three figures clearly show that with relatively low (w/c) ratio the curing period can be shortened to 3 days only if the reinforcement lies within 25 mm from the exposed surface. The curing period should be extended to 5 days if the strength at 50 mm from the exposed surface is of concern.

**Variation of Tensile Strength with Depth**

The variation of tensile strength with depth, or the strength profile, at the different adopted curing periods has a prime importance in judging the efficient curing period in relation to the reinforcement depth. Thus ensuring a good reinforcement bond to the surrounding concrete at the reinforcement level, which affects the composite behavior of the structural elements.

Figures 7 through 9 present the mixes with 0.47 (w/c) ratio. The figures disclose the following main remarks:

§   At all depths, the strength after 7 days curing duration are almost identical to those continuously cured till the age of testing.
§   Starting from 25 mm depth from the drying surface, the strengths after 3 days of curing achieved more than 90% of the corresponding values after 28 days curing.
§   The surface layer of the specimens, less than 15 mm depth, is more sensitive to curing duration than at higher depths. The reason of that is the relatively higher drying rate at the surface layer as compared to the deeper layers.
§   The 3 day curing period is not sufficient for the surface layer to attain a satisfactory level of strength. Meanwhile, the silica fume mix at 3 days curing duration achieved about 91% of the corresponding 28 day strength. This result is attributed to the chemical as well as the physical roles of the ultra fine silica fume in refining the pore structure of  the paste, and thereby increasing the ability of the concrete to maintain its internal moisture from evaporation. Another possible explanation of this finding: the capillary pores in the paste become discontinuous, thereby hindering the ingress of additional water into the concrete. When this state is reached, additional moist curing may be of little, or no, benefit.
§   Fly ash mixture at 3 and 7 days curing period developed 90% from its 28 days strength at 15 mm and 25 mm depth, and 80%, 90% at 50 mm respectively. Note that the mixture with fly ash requires a significantly longer curing period to achieve 90% of the 28 days strength. This is probably related to the slower rate of the pozzolanic reaction of fly ash compared with that of silica fume.



**Fig. 7: Strength Profile of the Ordinary Mix (w/c= 0.47)**

**Fig. 8: Strength Profile of the Silica Fume Mix (w/c= 0.47)**



**Fig. 9: Strength Profile of the Fly Ash Mix (w/c= 0.47)**

Reducing the water content of the investigated mixes to 0.35 (w/c) ratio slightly affected the strength profile as shown in Figures 10 through 12, from which the following observations are drawn:

§   The ordinary mix, except for the surface layer (about 15 mm depth), developed its 28 day strength after only 3 days of moist curing.

§   A great enhancement regarding curing duration can be achieved by incorporating the silica fume pozzolana within the mixture constituents. Fig. 11 shows that more than 90% of the 28 day strength is achieved after only one day of moist curing. The properties of this mix are superior to all other mixes regarding the strength achievement rate. The superior quality of this mix is attributed to the relatively low water content and the incorporation of the ultra fine silica fume pozzolana. The resulting mixture is thought to have rather small closed pores (discontinuous) that enable good water retention properties and eventually could hinder water ingress from outside.

§   The fly ash mixture behaved like the ordinary mixture regarding the minimum curing duration, but the surface layer is much better as its accepted level of strength is achieved after3 and 7 days of moist curing.
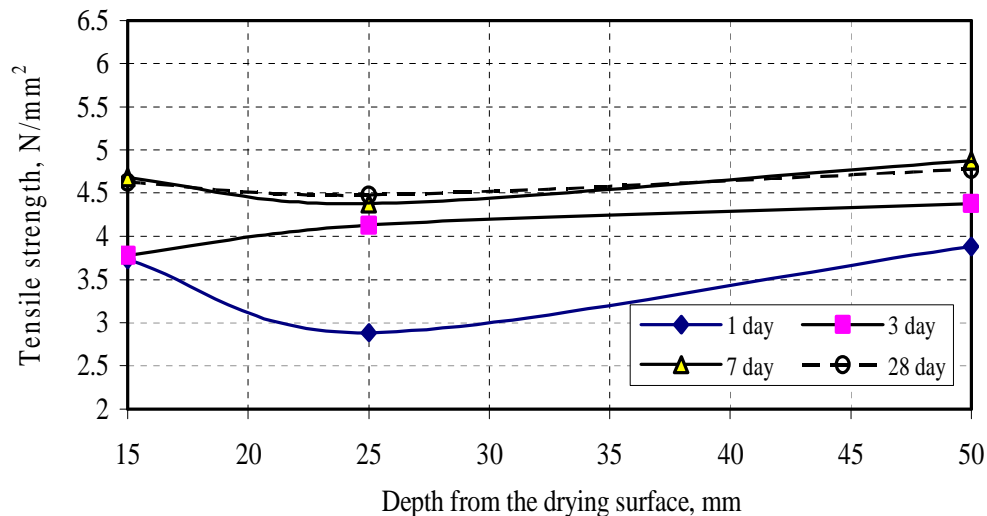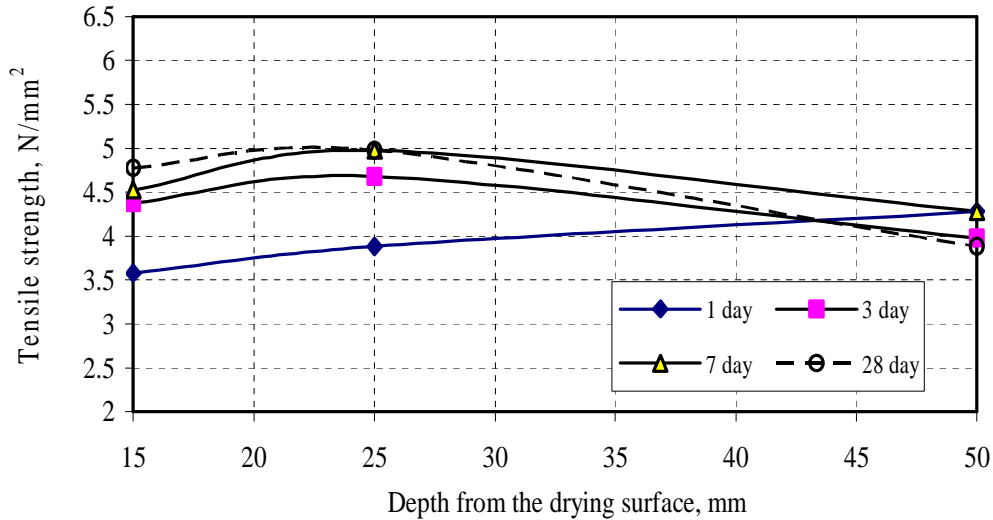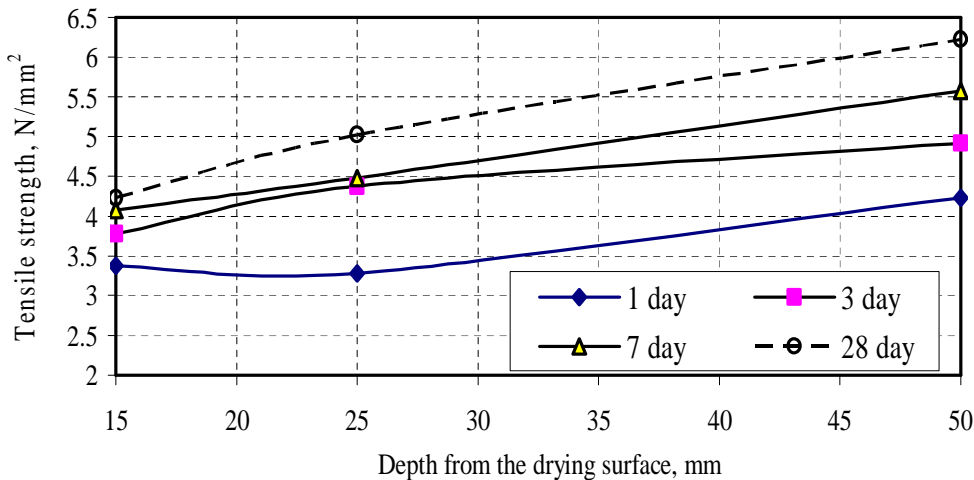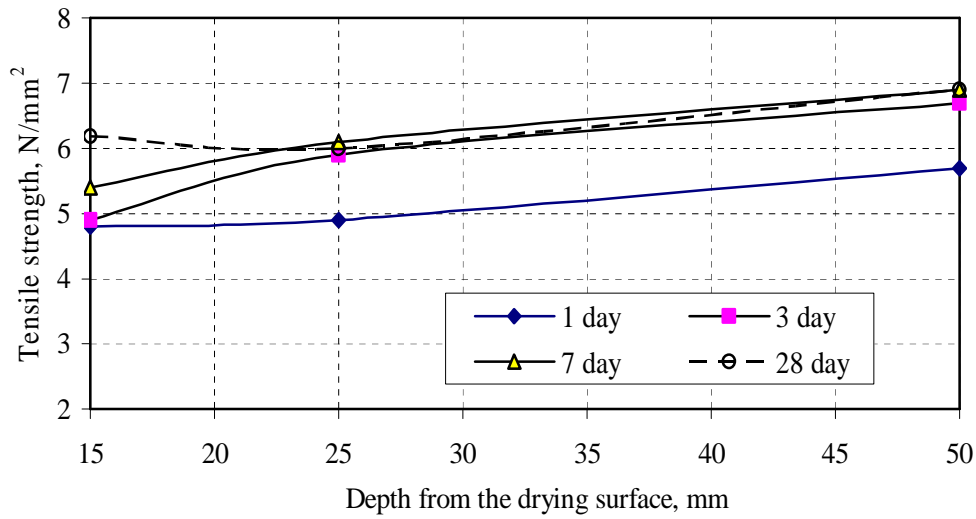
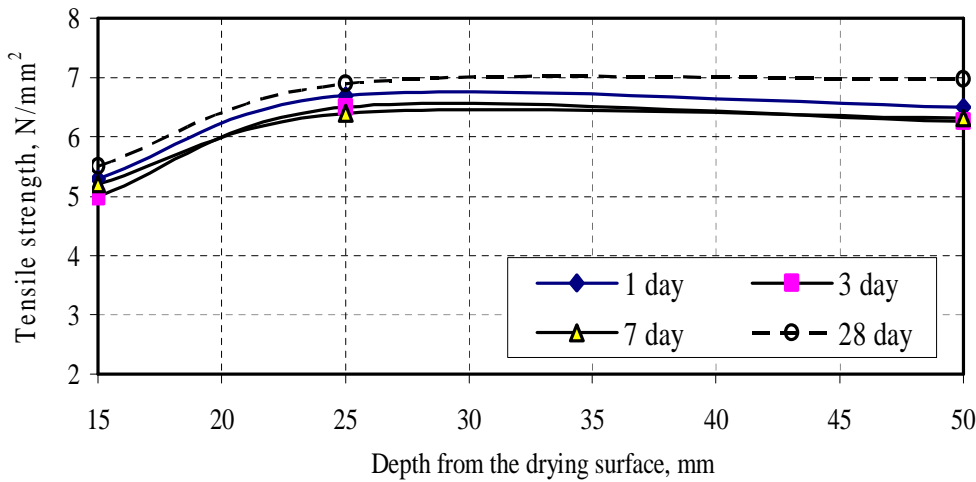**Fig. 10: Strength Profile of the Ordinary Mix (w/c= 0.35)**



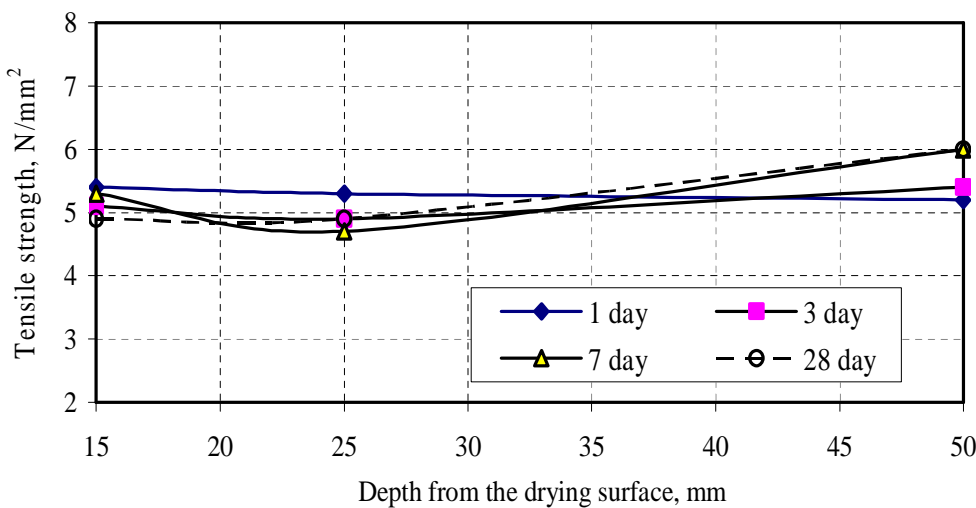**Fig. 11: Strength Profile of the Silica Fume Mix (w/c= 0.35)**



**Fig. 12: Strength Profile of the Fly Ash Mix (w/c= 0.35)**

**Compressive Strength as a Basis for Evaluating Curing Duration**

As outlined before, the ACI Committee 308(1998) [4] specifies that the strength at the end of the curing period should be at least 0.7 of the design strength. One main disadvantage of this criterion is that it does not consider the variation of strength along the concrete depth, i.e. with the distance from the drying surface. Of course, this is not possible using cubes compressive testing.

Figure 13 shows that for the investigated mixes with relatively low (w/c) ratio and with the incorporation of pozzolana, the criterion of 0.7 strength ratio is justified after one day of curing, which is a misleading result. In spit of the simplicity of the compression test, it is not suitable for evaluating the minimum curing duration of high performance concrete. These results confirm the validity of the adopted approach of evaluating the minimum curing duration of high performance concrete via direct tension test at the predetermined failure planes.
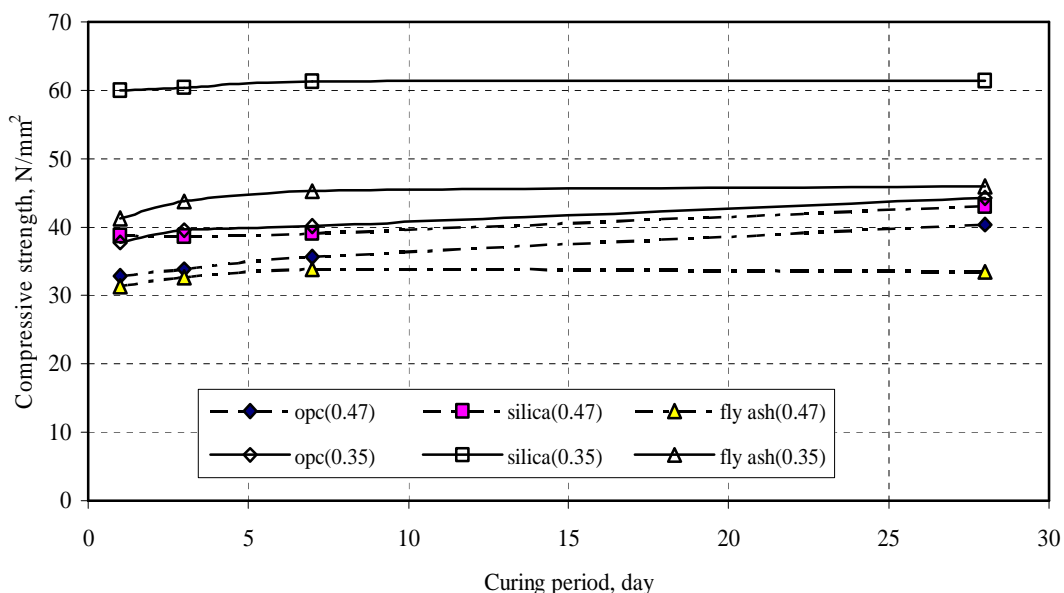


**Fig. 13: Curing Duration-Compressive Strength Development**

## CONCLUSIONS

The current Codes of Practice specify a minimum curing duration depending on a justification of a certain ratio of the design strength or the 28 day compressive strength. The adoption of this approach is based on experience and investigations regarding traditional concrete. While these specifications could be appropriate for traditional concrete, it is not so for high performance concrete. That is because high performance concrete has less and discontinuous voids in the cementitious matrix, which improves its ability to hold the internal moisture and also hinder the ingress of external water at a certain maturity time. The current investigation revealed that:

- The compression test is not suitable for evaluating the minimum curing duration of high performance concrete.
- The strengths developed along the element depths are not the same. Therefore, it is suggested to evaluate the specified strength at the reinforcement level.
- The effect of pozzolana on the curing duration is more recognized with further reductions in the water content.
- It is possible with for high performance concrete, except for the surface layer, to terminate water curing after 3 days as the measured strengths after 3 days of curing at different depths starting from 25 mm achieved more than 90% of the corresponding values after 28 days of curing.

- In the mixes containing silica fume, a satisfactory level of the surface layer (15 mm) strength is achieved after 3 days of curing. In the other mixes, the criterion of 90% of the 28 day strength is justified after 7 days of curing.
- With relatively low water content (w/c = 0.35) and the incorporation of silica fume in a sufficient quantity, the curing duration can be shortened dramatically to 1 day only for the range considered in this study. The test results for this mix proved that the strength criterion is achieved at all depths including the surface layer.

## REFRENCES

1.  ACI 318, 1995, "Building Code Requirements for Structural Concrete (ACI 318-95) and commentary (ACI 318R-95)" , American Concrete Institute, Farmington Hills, MI.
2.  Meeks, K.W. and Carino, N.J., 1999, "Curing of High-Performance Concrete: Report of the state of the Art", NISTIR6295, Nat. Inst. of stds and Tech., Gaithersburg,MD.
3.  Hilsdorf, H.K., 1995, "Criteria For the Duration of Curing", Proceeding of the Adam Neville Symposium on Concrete Technology, Las Vegas, June 12, 1995 V.M. Malhotra, Ed., pp. 129-146.
4.  ACI 308, 1998, "Standard Specification for Curing Concrete (ACI 308.1-98) ", American Concrete Institute, Farmington Hills, MI.
5.  Carino, N.J., and Meeks, K.W., 2001, " Curing of High Performance Concrete: Phase 1 Study", NISTIR 6505. , Nat. Inst. of stds and Tech., Gaithersburg,MD.
6.  Torii, K. and Kawamura, M., 1994 "Mechanical and Durability-Related Properties of High-strength Concrete Containing Silica Fume", High-Performance Concrete, Proceedings, ACI International Conference, sp-149, V.M Malhotra, Ed., American Concrete Institute, Farmington Hills, MI, pp.461-474.
7.  Good speed, C.H., Vanikar, S., and Cook, R.A., 1996, "High-Performance Concrete Defined for High Way Structures", Concrete International, Vol. 18, No.2, February, pp. 62-67.
8.  Carino, N.J., Lew, H.S. and Volz, C.K., 1983, "Early Age Temperature Effects on Concrete Strength Prediction by Maturity Method", Journal of the American Concrete Institute, Vol. 8-0, No.2, March-April pp. 93-101.
9.  Bartlett, F.M., and Mac Gregor, J.G., 1999, "Variation of In-place Concrete Strength in Structures", ACI Materials Journal, Vol. 96, No.2, March- April, pp. 261-270.

# INFLUENCE OF AGGRESSIVE ENVIRONMENTAL CONDITIONS ON MECHANICAL PROPERTIES OF GRP COMPOSITES

**Mahmoud K. Mahmoud and Aly A. Emam**
*Materials Properties & Quality Control Research Institute*
*Housing &Building National Research Center, Dokki, Giza, Egypt*

## ABSTRACT

Today, with the increasing needs for performance-oriented materials and structural systems, the development and introduction of advanced composite materials represents a milestone in materials technology. Some of the intriguing characteristics of such materials are the high stiffness to weight ratio and the ability to be tailored to fit certain design or loading conditions. The combination of diverse material components produces performance far exceeding that of the individual elements. This synergism makes composite materials both enabling and pervasive in civil and industrial applications.  However, hygrothermal and aggressive environmental conditions may have a severe impact on polymer composites mechanical properties, and hence their durability. This study investigates the influence of some aggressive environmental conditions on the basic mechanical properties of glass fiber reinforced polymer composites. The test samples were fabricated in the laboratory by hand lay-up method and cured at room temperature and atmospheric pressure. By using 20% glass fiber volume fraction in polyester matrix, three fiber orientations had been considered; unidirectional, bidirectional, and chopped. The samples were immersed for up to 90 days in chemicals having concentrations of 5, 10, and 20%, tap water, sewage water, and hydraulic oil. The influence of variations in these parameters on the mechanical behavior of GRP composites was investigated by measuring the corresponding changes in the tensile strength, fracture toughness, and modulus of elasticity. The general trend of the results indicates that mechanical properties decrease with the increase of concentration and/or immersion period. The study also show that subjecting GRP composites to aggressive environmental conditions for extended period of time, 90 days in this investigation, reduces the tensile strength and fracture toughness by 50% and 27%, respectively. Moreover, the major drop in tensile strength and fracture toughness occurs in the first 30 days of immersion in all used chemicals and solutions.

**Keywords:**    GRP composite, tensile strength, fracture toughness, compact tension, and environmental condition.

## INTRODUCTION

The fiber reinforced plastic composite (FRP) is a system that is created by the synthetic combination of two or more materials; namely: a selected reinforcing element and a compatible polymeric resin. The present world wide development programs in plastic composites are leading to materials with extremely high structural strength to weight ratios. This is a factor of great importance in all forms of transport facilities, where reduction in weight results in greater efficiency and energy saving. This is one of the outstanding advantages of FRP since it allows the possibility of introducing stiffness and strength into a product where it is really required.  In FRP composites, the strengthening mechanism depends mainly on the geometry of the reinforcement. This may be single layer or multilayer, continuous or discontinuous, unidirectional, bidirectional or chopped.

Composite materials are progressively gaining acceptance for use in offshore applications, where their perceived virtues of low weight and good corrosion resistance is much sought after by designers and operators.  Glass fiber reinforced plastics (GRP) in particular have won widespread acceptance in nonstructural applications, including fire water piping, decking and cable trays and sewage.  However, there is considerable interest in the use of GRP of various types in more demanding applications.  Such new applications involve using the material in contact with aggressive environmental conditions such as chemicals, sewage water, and elevated temperatures.  Although the temperatures involved in many applications are too high to permit the use of organic matrix composites, there is a range of applications, where the temperatures are reasonable for the use of GRP composites.

Most of the work in the field of fracture mechanics has been focused on the study of fracture under mode I (i.e., tensile mode) loading conditions.  However, many structures are loaded in complex conditions, hence, the cracking patterns are generally combinations of the three typical modes; I: tension, II: shear, and III: transverse shear.

There has been a limited amount of experimental work done on mixed mode fracture, the observations on compound mode-I and mode-III fracture have been very scarce and there is no general agreement among authors on the effect of the addition of mode-III component to pure mode-I loading.  Although the general conclusion is that the addition of mode III lowers the mode-I contributions [1,2]. Pook [3] found out that mode I toughness is relatively insensitive to transverse shear.

The tensile strength and the fracture toughness behavior of composite materials have been studied in many previous investigations [2,3]. However, the use of composites as load bearing structural components depends to a large extent on their ability to withstand, in addition to regular loading, sever environmental conditions and time dependent loads [4].  The fracture behavior of composites under service loads is also of vital importance. The majority of pervious investigations [5-9] focused on studying the effects of thermal, hygrothermal, and offshore environmental conditions on the mechanical characteristics of polymer composites.

The focus of the current investigation is to measure the tensile strength and the fracture toughness of GRP composites when immersed in various chemicals such as sulfuric acid ($H_2SO_4$), hydrochloric acid (HCl), sodium hydroxide (NaOH), water ($H_2O$), sewage water and hydraulic oil. In order to achieve this objective, several mechanical tests are carried out on composite. The fracture toughness (compact-tension) test is performed to study the influence of fiber volume fraction and fiber geometry on the fracture toughness ($K_Q$).  One of the objectives of this research is to relate the fracture toughness ($K_Q$) and static strength of composite materials subjected to some aggressive environments.

In particular, some static tests are first carried out on polyester and GRP composites to obtain the mechanical properties using various percentages of fiber content (%$V_f$). Then, an attempt to correlate the experimental tensile strength, modulus of elasticity and fracture toughness ($K_Q$) for unidirectional, bidirectional, and chopped GRP composites has been discussed.


## MATERIALS AND METHODS

The tested composite materials consist of E-glass fiber laid in a thermoset polyester resin (SIROPOL 7440). The tensile specimens were prepared according to ASTM  D5083-02 [10]. The plain coupon tensile specimen has a rectangular cross section 25mm width, 215mm length and thickness 16.1mm. Specimens were stored at room temperature ($23^o$ C) and ambient humidity (50 %) according to ASTM D 618-05 [11].  Tension test was carried out on the 100 KN computerized AG-SHIMADZU-AUTOGRAPH Universal Testing Machine loading at a speed of 5 mm/min.

Fracture toughness tests were carried out according to the ASTM D5045-99 and ASTM E399-90 [12,13] standard specifications, using compact tension notched pre-cracked test specimens as shown in Fig.1. An optical microscope, as a magnified visual The available technique, used to measure the pre-crack length, is the aid, is used to observe and measure of the pre-crack length.

The conditional fracture toughness ($K_Q$) for compact tension is calculated as:

$$K_Q = \left\{ P_Q / bw^{1/2} \right\} f(a/w) \tag{1}$$

where,

$P_Q$   applied force corresponding to the 5% secant line;
b     specimen thickness;
w    specimen width;
a     crack length; and
 $f(a/w)$ is a geometry function which is given by :

$$f(a/w) = (2 + a/w)\{ 0.886 + 4.64(a/w) - 13.32(a/w)^2$$
$$+ 14.72(a/w)^3 - 5.6(a/w)^4 \}/(1 - a/w)^{1.5} \tag{2}$$

The thickness of the specimen was then checked for plane strain conditions, i.e. if the thickness is large with respect to the size of plastic zone, which is proportional to $(K_Q/\sigma_t)^2$. The criterion adopted for the ASTM standard specimens is as follow:

$$b \geq 2.5(K_Q/s_t)^2 \tag{3}$$

where $\sigma_t$ is the tensile strength.
If $K_Q$ satisfies the condition expressed by Eq. (1), $K_Q$ can be considered as the fracture toughness ($K_{IC}$). Five specimens were tested at each condition as indicated in Table 1. Before testing, specimens were immersed in (5,10 or 20%) concentrations of $H_2SO_4$, HCl, NaOH solution acid and sewage water and hydraulic oil for periods of 30, 60 and 90 days.

**Table 1:  Experimental Testing Program.**

| Materials | Environmental Conditions | | | Test |
|---|---|---|---|---|
| | Chemical | Concentration (%) | Immersion period (days) | |
| Polyester GRP Composites: § Unidirectional § Bidirectional § Chopped | $H_2SO_4$ HCl NaOH Sewage water Hydraulic oil | 5 10 20 | 30 60 90 | Tensile Strength Fracture Toughness |
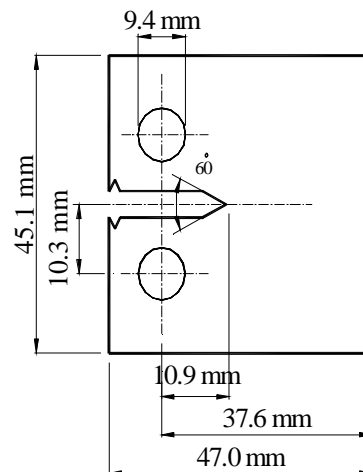
**Fig. 1: Compact Tension Test Specimen.**

## RESULTS AND DISCUSSIONS

In this section the mechanical behavior tensile and fracture toughness of GRP composites are discussed. The results of the tests are depicted in Tables (2) to (9). The effects of fiber volume fraction and composite lay-up scheme are also presented.

### (a)    Effects of fiber orientation and volume fraction

#### 1-Tensile strength

Experimental tensile strength results are obtained in the form of stress- strain ($\sigma$- $\varepsilon$) relations for polyester and GRP composite. The elastic modulus of elasticity is calculated from the slope the $\sigma$- $\varepsilon$ curves.    Table (2) shows that the ultimate tensile strength and modulus of elasticity increase with the increase in the fiber volume fraction. This is due to the fact that the load is transmitted through the fiber and by increasing the fiber volume fraction, the load carrying capacity of the material improves. The effect of fiber orientation; unidirectional, bidirectional, and chopped on the ultimate tensile strength and modulus elasticity is shown in Tables (3)-(6) and depicted graphically in Figs.(2)-(5).

#### 2-Fracture Toughness

The variation of fracture toughness with fiber volume fraction $V_f$ are tabulated in Table (2).  The fracture toughness increases for bidirectional and chopped glass/polyester with added fiber in the matrix.
Regardless of the $V_f$ value, it is noted that the fracture toughness of bidirectional material is higher than that of polyester and chopped composite material as illustrated in Figs. (6)-(8).

### (b)    Effects of environmental conditions

The effects of some aggressive environments, presented by chemicals with various concentration and other solutions, on the ultimate tensile strength and fracture toughness values of the GRP specimens after exposure up to 90 days are shown in Tables (3)-(9) and Figs. (2) through (8). A discussion of these results is presented hereinafter.

### 1- Tensile strength

The ultimate tensile strength after immersion of GRP composites in various chemical solutions (Hydrochloric acids (HCl), Sulfuric acids ($H_2SO_4$), and Sodium hydroxide ($N_aOH$), hydraulic oil and water) of different acid concentrations (5,10 and 20%) and for a variety of periods 30, 60 and 90 days are recorded in  Tables (3)-(6) and shown in Figs. (2)-(5).

In general the ultimate tensile strength of all GRP tested samples decreases as the period of immersion and/or concentration of chemicals is increased. These results also show that the first 30 days of immersion is the most influential time period on the tensile strength, particularly for bidirectional composite samples, after which the pace of reduction slows down.

The change in ultimate tensile strength of GRP composites depends upon the type of chemical/ solution and its concentration.  The regular tap water has no significant influence on the tensile strength. Moreover, hydraulic oil and sewage water cause a negligibly small reduction in the tensile strength. The specimens immersed in Sulfuric acid ($H_2SO_4$), with 20% concentration, showed a drop of almost 50% in the tensile strength after 90 days. For the same immersion period and concentration percentage, Hydrochloric acid (HCl) and Sodium hydroxide ($N_aOH$) reduce the tensile strength by 15% and 12%, respectively.

This global reduction in tensile strength of the tested composite samples may be due to the absorption and/or penetration followed by a reaction between the acids used in these tests and the matrix creating micro-cracks. As these cracks propagate, fiber-matrix debonding may occur which results in degraded structural component.

**Table 2: Experimental Static Properties of Polyester and GRP Composites.**

| Group | Material | Fiber volume fraction $V_f$ (%) | Modulus of elasticity E (MPa) | Stress intensity Factor $K_Q$ ($MPa\, m^{0.5}$) | Tensile strength (MPa) |
|---|---|---|---|---|---|
| I | Polyester | - | 2450 | 2.8 | 55 |
| II | Unidirectional GRP Composite | 20 | 6400 | - | 270 |
|  |  | 25 | 7500 | - | 310 |
|  |  | 30 | 8700 | - | 390 |
| III | Bidirectional GRP Composite | 20 | 7100 | 15.2 | 155 |
| IV | Chopped GRP Composite | 20 | 6000 | 12.1 | 82 |

### 2- Fracture toughness

The changes in fracture toughness of all tested GRP composites depend on type of chemical, its concentration, and duration of immersion. In general, the fracture toughness decreases with the increase of concentration and/or immersion period as shown in Tables ()-() and as depicted graphically in Figs. (6)-(8). The influence of Sulfuric acid ($H_2SO_4$) with 20% concentration is very significant since it reduces the fracture toughness by 27% after 90 days of immersion. This is

followed by Sodium hydroxide ($N_aOH$) and then Hydrochloric acid (HCl) solutions causing reductions of 25% and 20%, respectively.

The influence of tap water, hydraulic oil, and sewage water on the fracture toughness of GRP composites is negligibly small. On the other hand, their influence on polyester specimens is very significant. For instance, fracture toughness of polyester samples placed in sewage water for 90 days is reduced by almost one third. This result is very revealing since it sheds some light on the fact that some aggressive environments may have devastating effects on the matrix that incubates the fibers, which is the main load-carrying component of polymer fiber composites. Consequently, matrix deterioration may become an initiator for material failure, and hence, a life-limiting factor of the structural element.

Figs. (7) and (8) indicate that chopped GRP composites have a better fracture toughness performance as compared to bidirectional composites. This may be due to changes in fracture modes of the two material lay-ups. In general, uni- and bi-directional composites develop fiber-matrix interface failure modes after matrix crack propagation, while as such interfaces are naturally eliminated for chopped fiber composites. Hence, it is worthy noting that the global reduction in the fracture toughness may be attributed to the penetration and reaction of chemicals and the matrix that lead to micro-cracks and then to fiber-matrix debonding. It should also be mentioned that the major drop in the fracture toughness occurs in the first 30 days of immersion in all used chemicals and solutions. This may be due to GRP composite specimens reach saturation limit thereinafter the reaction pace slows down and hence the whole rate of the composite deterioration process.

**Table 3: Effect of Chemicals on the Tensile Strength of Polyester.**

| Chemical | Concent-ration (%) | Tensile Strength (MPa) | | |
|---|---|---|---|---|
| | | Immersion period (days) | | |
| | | 30 | 60 | 90 |
| $H_2SO_4$ | 5 | 48 | 43 | 25 |
| | 10 | 45 | 40 | 21 |
| | 20 | 35 | 25 | 15 |
| HCL | 5 | 50 | 48 | 47 |
| | 10 | 48 | 47 | 46 |
| | 20 | 47 | 46 | 45 |
| NaOH | 5 | 51 | 50 | 49 |
| | 10 | 50 | 48 | 45 |
| | 20 | 49 | 45 | 40 |
| $H_2O$ | - | 53 | 52 | 51 |
| Oil | - | 52 | 51 | 50 |
| Sewage water | | 48 | 45 | 43 |

**Table 4: Effect of Chemicals on the Tensile Strength of GRP Unidirectional Composite ($V_f$=20%).**

| Chemical | Concent-ration (%) | Tensile Strength (MPa) | | |
|---|---|---|---|---|
| | | Immersion period (days) | | |
| | | 30 | 60 | 90 |
| $H_2SO_4$ | 5 | 250 | 200 | 180 |
| | 10 | 230 | 181 | 160 |
| | 20 | 170 | 165 | 140 |
| HCL | 5 | 260 | 250 | 240 |
| | 10 | 255 | 245 | 235 |
| | 20 | 250 | 240 | 230 |
| NaOH | 5 | 265 | 260 | 255 |
| | 10 | 260 | 250 | 245 |
| | 20 | 255 | 240 | 235 |
| $H_2O$ | - | 265 | 263 | 260 |
| Oil | - | 260 | 258 | 250 |
| Sewage water | | 255 | 240 | 230 |

**Table 5: Effect of Chemicals on the Tensile Strength of GRP Bidirectional Composite ($V_f$=20%).**

| Chemical | Concent-ration (%) | Tensile Strength (MPa) | | |
|---|---|---|---|---|
| | | Immersion period (days) | | |
| | | 30 | 60 | 90 |
| $H_2SO_4$ | 5 | 135 | 130 | 125 |
| | 10 | 130 | 121 | 110 |
| | 20 | 125 | 112 | 90 |
| HCL | 5 | 145 | 143 | 140 |
| | 10 | 140 | 138 | 135 |
| | 20 | 138 | 135 | 130 |
| NaOH | 5 | 146 | 143 | 135 |
| | 10 | 141 | 138 | 130 |
| | 20 | 138 | 135 | 125 |
| $H_2O$ | - | 148 | 147 | 146 |
| Oil | - | 147 | 146 | 146 |
| Sewage water | | 135 | 133 | 130 |

**Table 6: Effect of Chemicals on the Tensile Strength of GRP Chopped Composite ($V_f$=20%).**

| Chemical | Concent-ration (%) | Tensile Strength (MPa) | | |
|---|---|---|---|---|
| | | Immersion period (days) | | |
| | | 30 | 60 | 90 |
| $H_2SO_4$ | 5 | 75 | 70 | 60 |
| | 10 | 72 | 65 | 50 |
| | 20 | 65 | 50 | 40 |
| HCL | 5 | 80 | 79 | 73 |
| | 10 | 78 | 75 | 71 |
| | 20 | 75 | 73 | 70.5 |
| NaOH | 5 | 81 | 79 | 77 |
| | 10 | 79 | 74 | 73 |
| | 20 | 78 | 72 | 70 |
| $H_2O$ | - | 82 | 81 | 80 |
| Oil | - | 81 | 80 | 79.5 |
| Sewage water | | 79 | 75 | 73 |

**Table 7: Effect of Chemicals on the Fracture Toughness of Polyester.**

| Chemical | Concent-ration (%) | Tensile Strength (MPa $m^{1/2}$) | | |
|---|---|---|---|---|
| | | Immersion period (days) | | |
| | | 30 | 60 | 90 |
| $H_2SO_4$ | 5 | 2.0 | 1.95 | 1.8 |
| | 10 | 1.9 | 1.8 | 1.6 |
| | 20 | 1.8 | 1.7 | 1.5 |
| HCL | 5 | 2.2 | 2.1 | 2.0 |
| | 10 | 2.15 | 2.0 | 1.9 |
| | 20 | 2.1 | 1.95 | 1.8 |
| NaOH | 5 | 2.3 | 2.25 | 2.2 |
| | 10 | 2.2 | 2.0 | 1.95 |
| | 20 | 2.1 | 1.95 | 1.85 |
| $H_2O$ | - | 2.4 | 2.4 | 2.3 |
| Oil | - | 2.3 | 2.35 | 2.3 |
| Sewage water | | 2.1 | 2 | 1.9 |

**Table 8: Effect of Chemicals on the Fracture Toughness of GRP Bidirectional Composite**
**($V_f$=20%).**

| Chemical | Concent-ration (%) | Tensile Strength (MPa $m^{1/2}$) | | |
|---|---|---|---|---|
| | | Immersion period (days) | | |
| | | 30 | 60 | 90 |
| $H_2SO_4$ | 5 | 13.0 | 12.8 | 12.0 |
| | 10 | 12.5 | 12.1 | 11.5 |
| | 20 | 12.0 | 11.7 | 11.0 |
| HCL | 5 | 14.1 | 14.0 | 13.7 |
| | 10 | 13.7 | 13.5 | 13.0 |
| | 20 | 13 | 12.5 | 12.0 |
| NaOH | 5 | 14.2 | 14.1 | 13.8 |
| | 10 | 14.15 | 14.0 | 13.6 |
| | 20 | 14.0 | 13.4 | 13.1 |
| $H_2O$ | - | 15.0 | 14.8 | 14.8 |
| Oil | - | 15.0 | 14.8 | 14.7 |
| Sewage water | | 14.5 | 14.3 | 14.1 |

**Table 9: Effect of Chemicals on the Fracture Toughness of GRP Chopped Composite**
**($V_f$=20%).**

| Chemical | Concent-ration (%) | Tensile Strength (MPa $m^{1/2}$) | | |
|---|---|---|---|---|
| | | Immersion period (days) | | |
| | | 30 | 60 | 90 |
| $H_2SO_4$ | 5 | 11.5 | 11.0 | 10.3 |
| | 10 | 11.1 | 10.8 | 10.1 |
| | 20 | 10.3 | 10.0 | 9.5 |
| HCL | 5 | 11.8 | 11.3 | 11.0 |
| | 10 | 11.5 | 11.1 | 10.5 |
| | 20 | 11.0 | 10.3 | 10 |
| NaOH | 5 | 11.9 | 10.5 | 10.5 |
| | 10 | 11.5 | 11.1 | 10.0 |
| | 20 | 11.1 | 10.5 | 9.5 |
| $H_2O$ | - | 12.0 | 11.8 | 11.7 |
| Oil | - | 11.9 | 11.8 | 11.8 |
| Sewage water | | 11.5 | 11.4 | 11.2 |
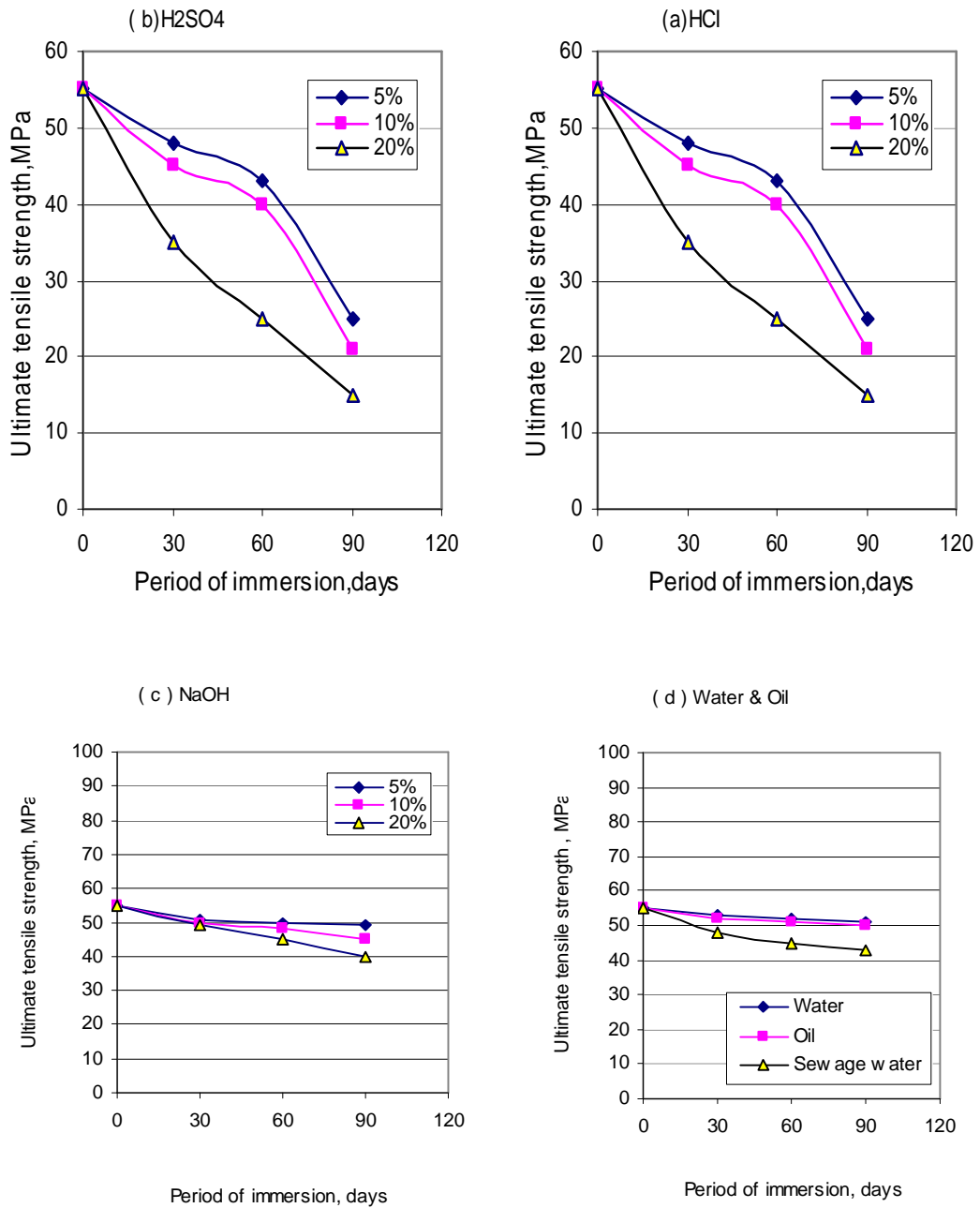
Fig. 2: Tensile Strength versus Period of Immersion in Various Solutions, Polyester.
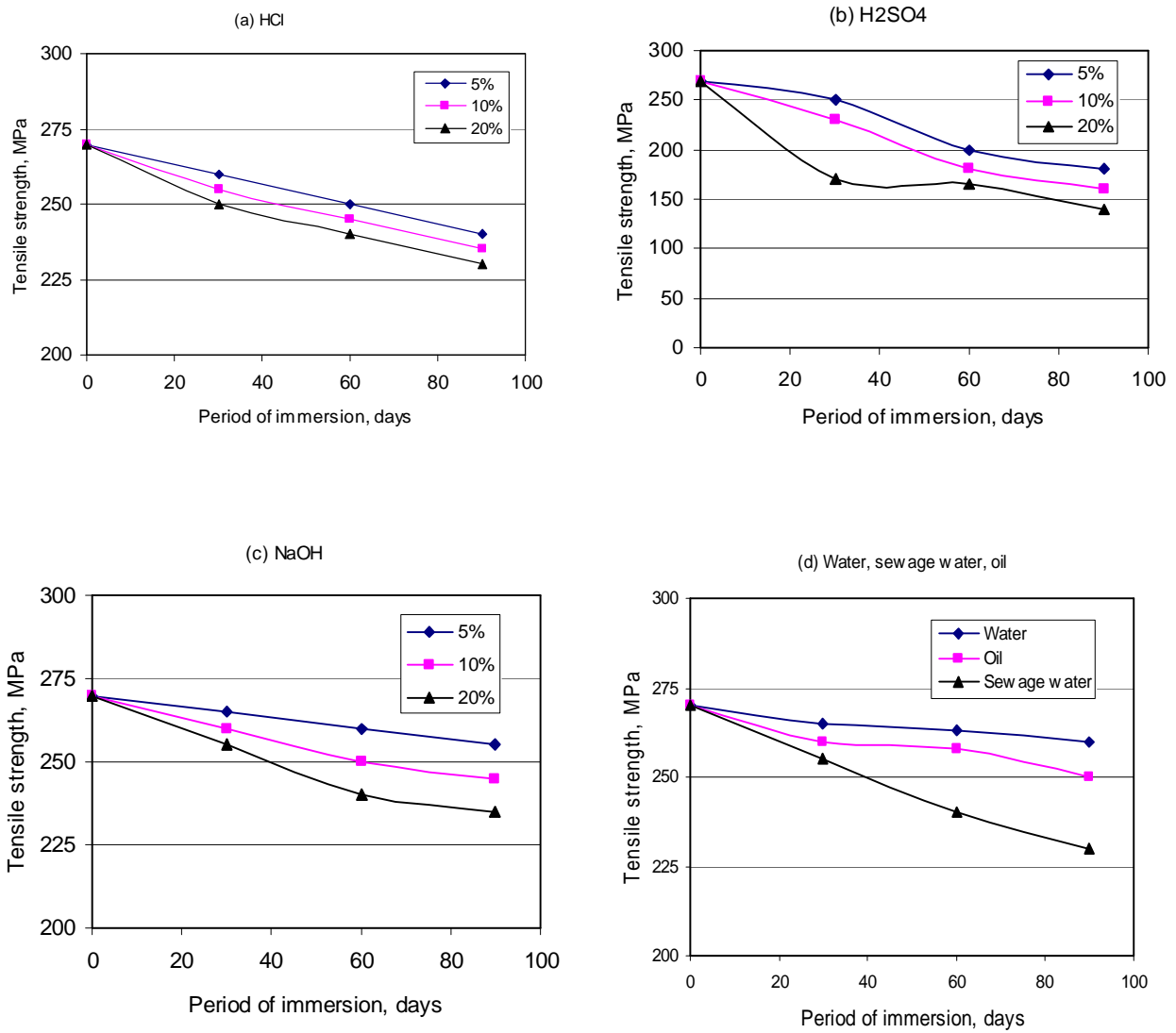
Fig. 3: Tensile Strength versus Immersion Period for Various Solutions, Unidirectional Composite.
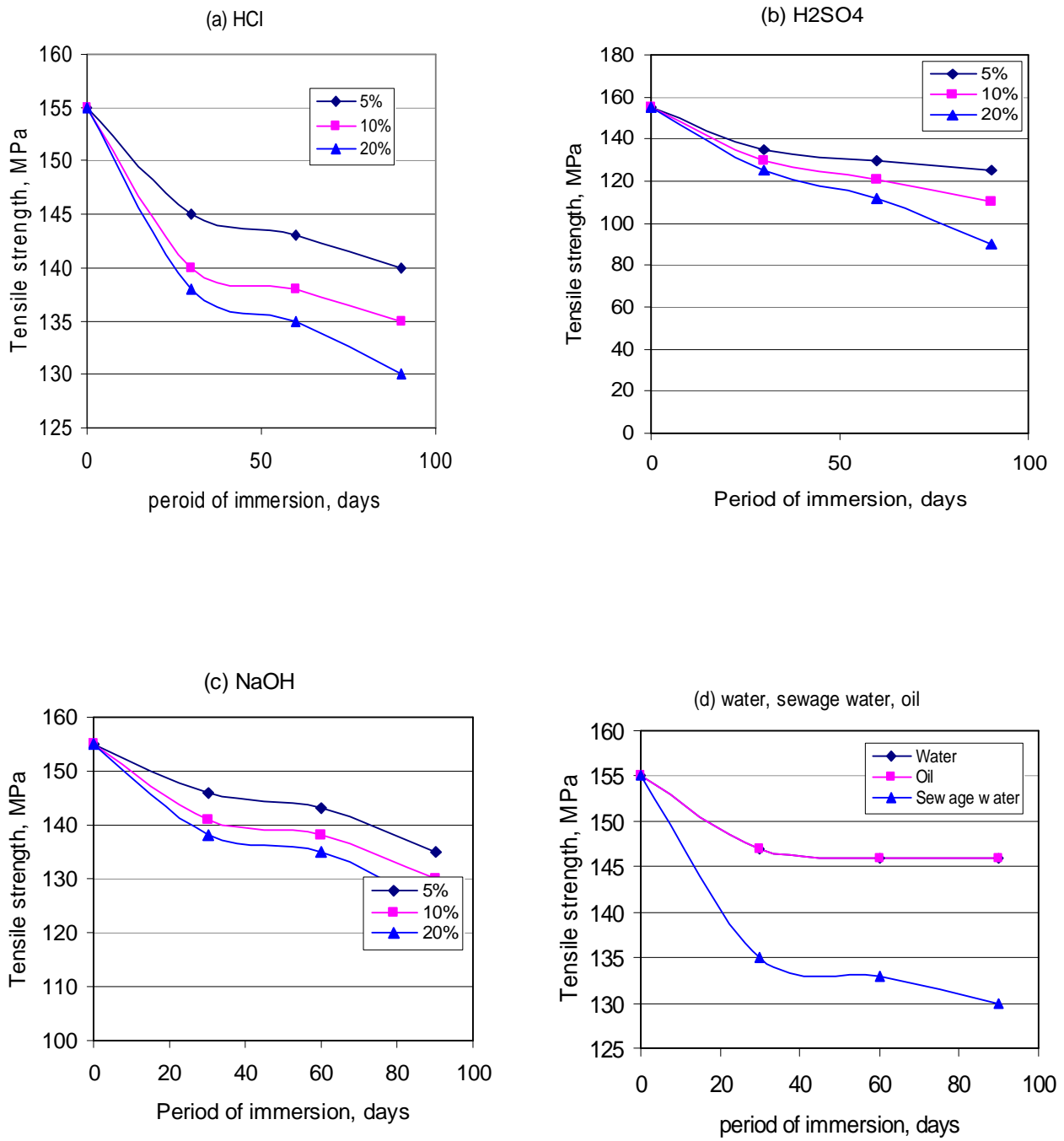
**Fig. 4: Tensile Strength versus Immersion Period for Various Solutions, Bidirectional Composite.**

**Fig. 5: Tensile Strength versus Immersion Period for Various Solutions, Chopped Composite.**

**Fig. 6: Fracture Toughness versus Immersion Period for Various Solutions, Polyester.**

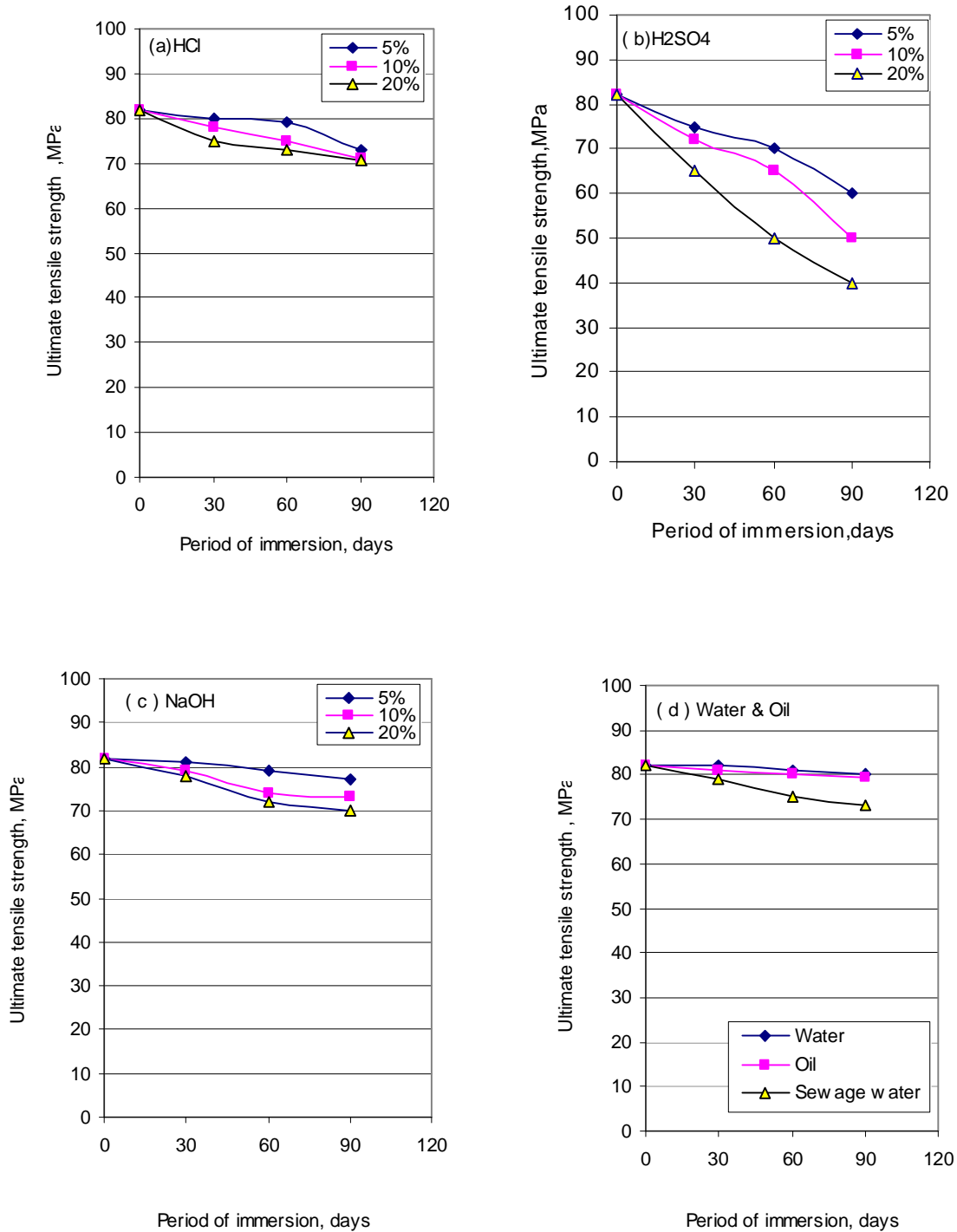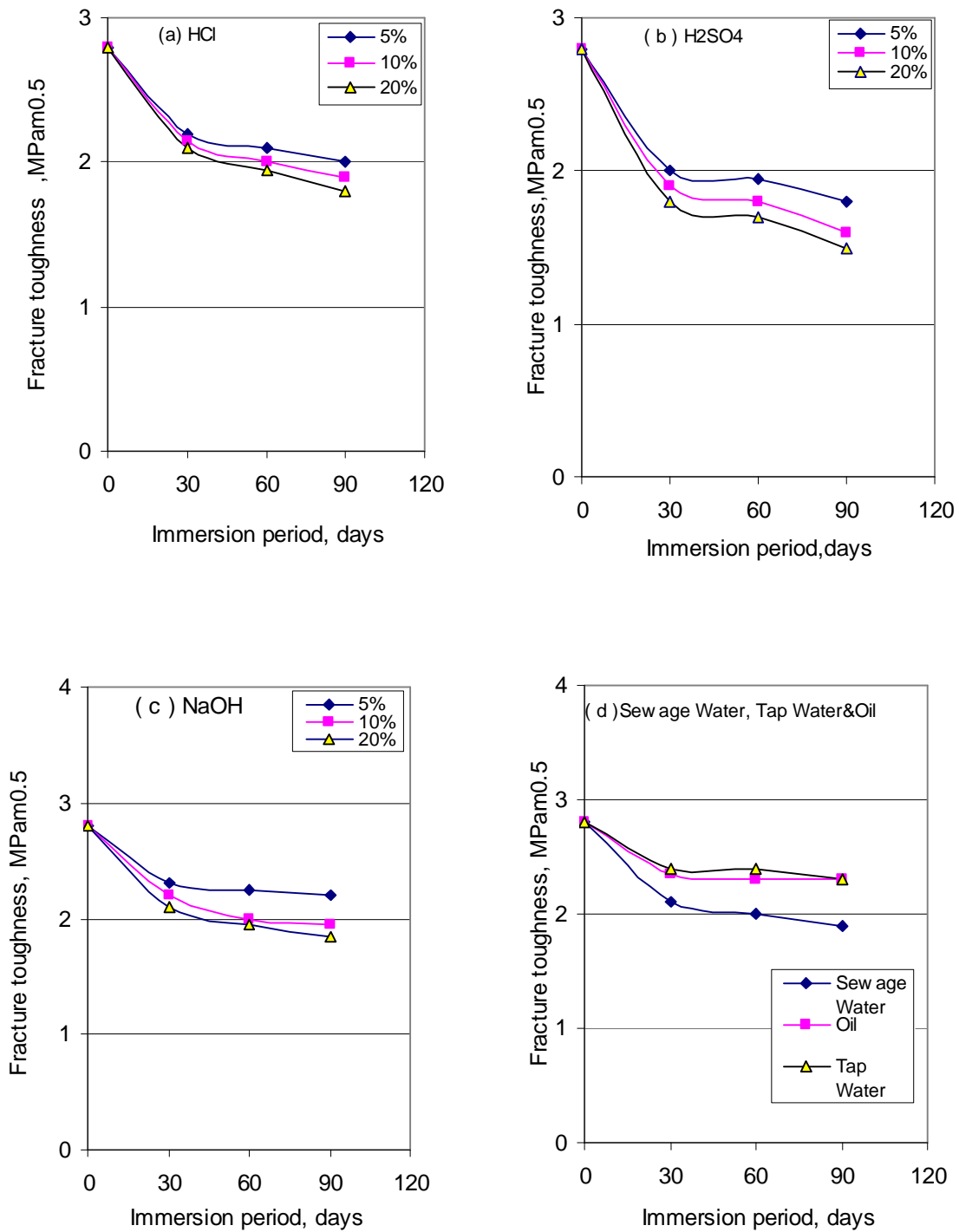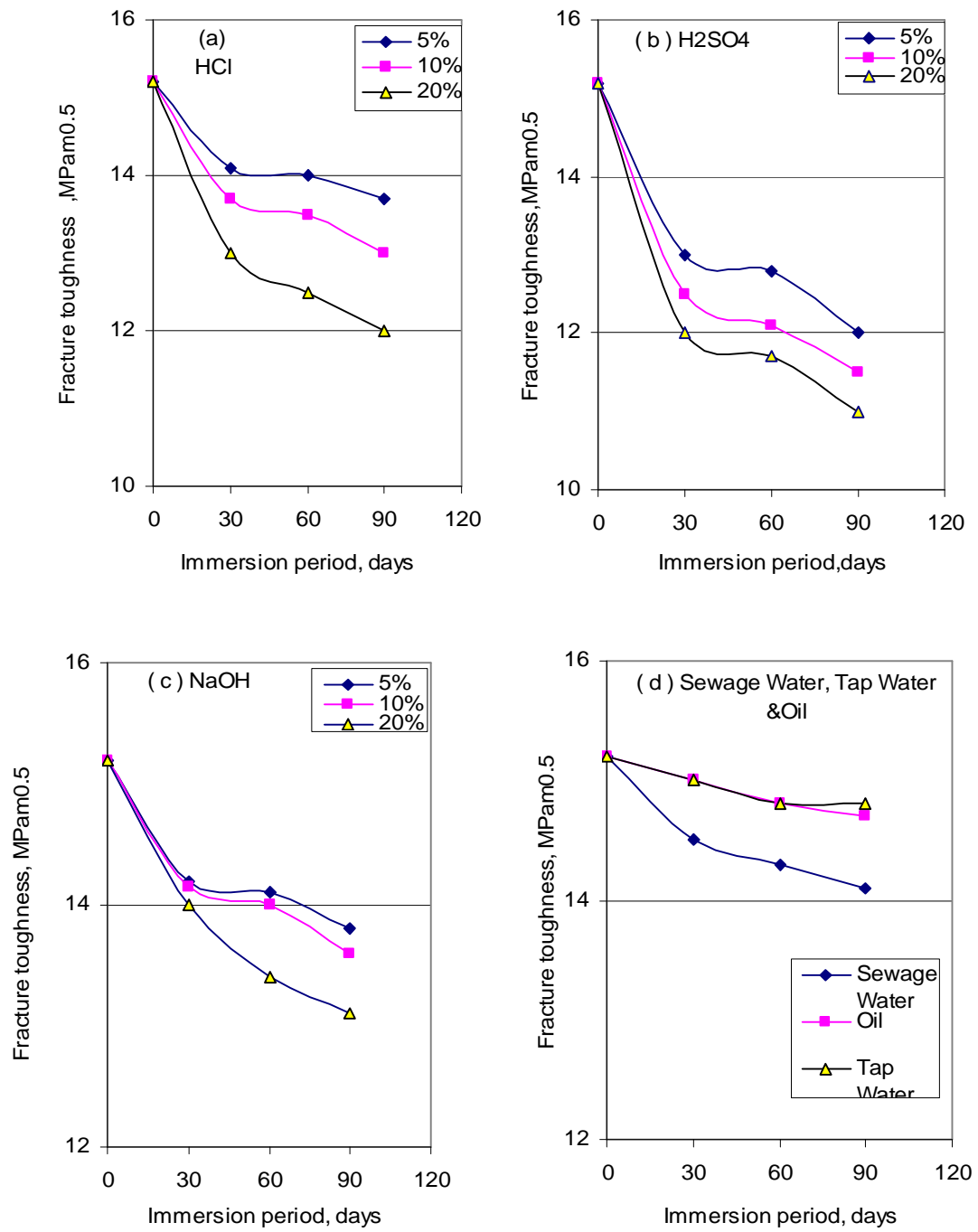**Fig. 7: Fracture Toughness versus Immersion Period for Various Solutions, Bidirectional Composite.**
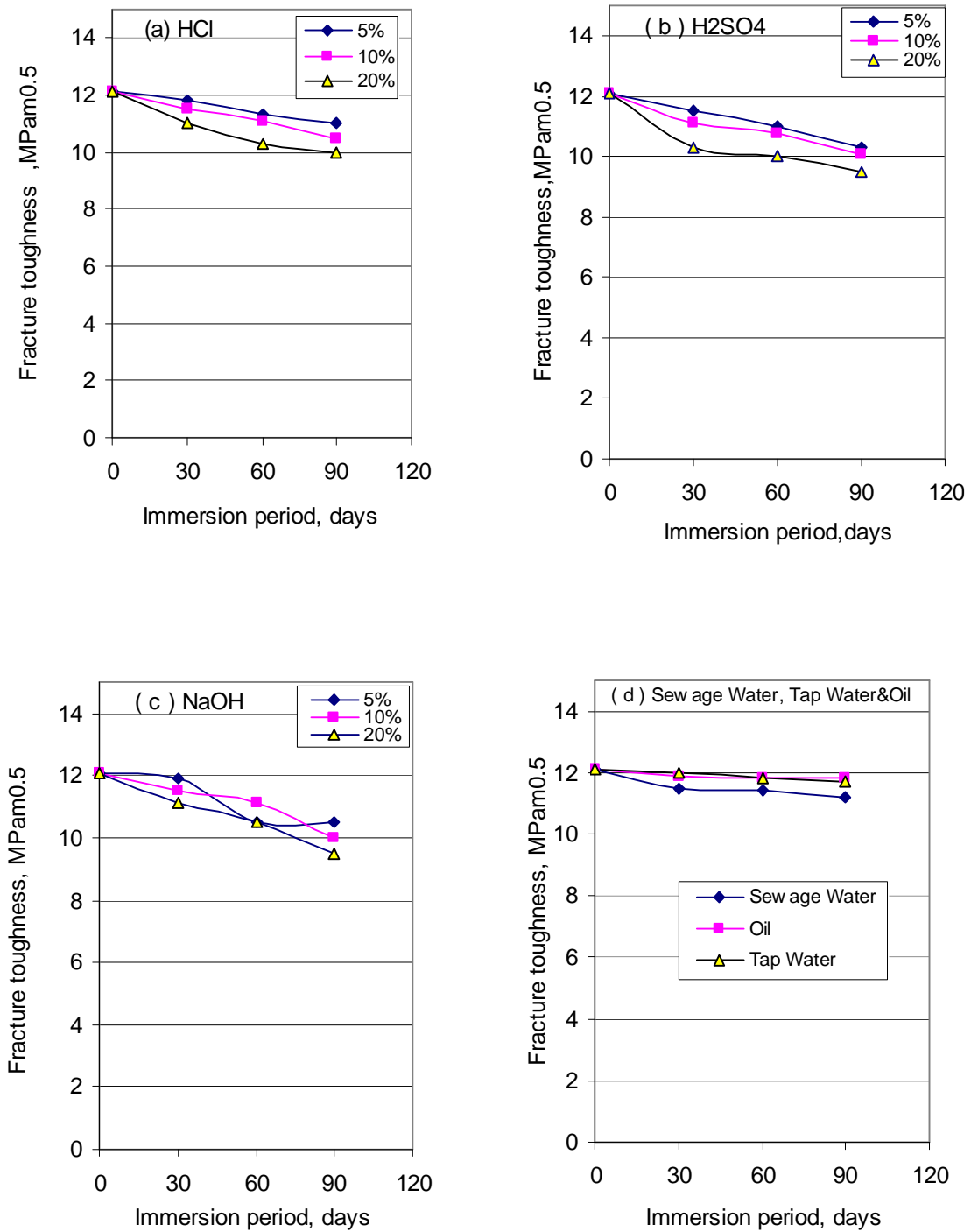
**Fig. 8: Fracture Toughness versus Immersion Period for Various Solutions, Chopped Composite.**

## CONCLUSIONS

The present investigation yields the following conclusions:
1.  The experimental tensile strength, modulus of elasticity and fracture toughness increase with the increase of the fiber volume fraction.
2.  The changes in the mechanical properties of GRP composites follow a similar depreciation trend either as the concentration of chemical or the immersion period is increased.
3.  The immersion of GRP composite samples for up to 90 days in sewage water causes 13% reduction in tensile strength and 6% in fracture toughness.
4.  The most aggressive environmental condition represented in the use of 20% concentration sulfuric acid for 90 days results in 50% loss in GRP composite tensile strength and 26% reduction in the fracture toughness. Such result is very significant and revealing at least from the industrial point of view. It limits the use of GRP composites, within the scope of the current experimental investigation, as containers or pipelines for such aggressive chemicals.
5.  The effect of immersing of samples for up to 90 days in tab water or hydraulic oil on GRP composites tested properties is insignificant.
6.  Continuous bidirectional fiber lay-up tends to slightly improve resistance to aggressive environmental conditions compared to unidirectional or chopped GRP composites.


## REFERENCES

1.  Agarwal, B.D and Broutman, L.J., "Analysis and Performance of Fiber Composite", A Willey-Inter Science Publication, 1980.
2.  Chamis, C.C., " Simplified Composite Micromechanics Equations for Strength, Fracture Toughness and Environmental Effects" Annual Conf. of the Society of the Plastic Industry (39), Reinforced Plastics/ Composite Institute, New York, 1984.
3.  Strait , L . H . , Karasek M . L . , and Amateau, M .F. "   Effects of Seawater Immersion on the Impact Resistance of Glass fiber Reinforced   Epoxy Composite" Journal of Composite Materials, Vol. 26, No.14, pp 2118 –33, 1992.
4.  Sierakowski, R. L., and Chaturvedi, S.K. "Dynamic Loading and Characterization of Fiber-Reinforced Composites" John Wiley & Sons, New York, 1997.
5.  Voluntary Product Standard, "Custom Contact-Molded Reinforced–    Polyester Chemical Resistant Process Equipment", Japan, pp15-69, June 1970.
6.  Daniel M., Yaniv G., and Peimanidis G., "Hygrothermal and Strain    Rate Effects on Properties of Graphite/Epoxy Composite", Journal of Engineering Materials and Technology, Vol.  110, pp 169-173, 1988.
7.  Alfred R. E., "The Effect of Temperature and Moisture Content on the Flexural Response of Kevlar/Epoxy Laminates: Part-I [0/90] Filament    Orientation", Journal of Composite Materials, Vol. 15, pp100-115, 1981.
8.  Hale J.M., Gibson A.G. and Speake S.D., "Tensile Strength Testing   of Pipes at Elevated Temperatures in Aggressive Offshore    Environments", Journal of Composite Materials, Vol. 32, pp 969-86, 1998.
9.  Shen CHI. and Springer G.S., "Effect of Moisture and Temperature on the Tensile Strength of composite Materials", Journal of Composite Materials, Vol.  11, pp 2-16, 1977.
10. ASTM D5083-02 "Standard Test Method for Tensile Properties of Reinforced Thermosetting Plastics Using Straight-Sided Specimens" American Society of Testing and Materials, 2002.
11. ASTM D618-05 "Standard Practice for Conditioning Plastics for Testing", American Society of Testing and Materials, 2005.
12. ASTM D5045-99 "Standard Test Methods for Plane-Strain Fracture Toughness and Strain Energy Release Rate of Plastic Materials" American Society of Testing and Materials, 1999.
13. ASTM E399-90 "Standard Test Method for Plane Strain Fracture Toughness of Metallic Materials", American Society of Testing and Materials, 1990.

# INVESTIGATIONS ON THE PERFORMANCE OF CONCRETE MADE WITH BLENDED FINELY MILLED WASTE GLASS

**I. M. Metwally**

*Researcher, Department of Reinforced Concrete, Housing & Building National Research Centre*
*87 El- Tahrir St., Dokki, Giza, Egypt.*
*Email: im2aa@yahoo.com*

## ABSTRACT

Non-recyclable waste glass, which is produced from fluorescent lamps factories, constitutes a problem for solid waste disposal in various countries worldwide. Thereby, the accumulation of waste glass in the plants without being used represents not only a significant loss of money and energy by occupying a big area from plants but also a negative impact to the environment. This study is considered a significant interest in the development of environmentally friendly concrete with waste glass.

Using waste glass as a construction material is a good way to help the environment through grinding and using it as a partial replacement of cement by weight in concrete. Five different concrete mixes with various percentages of finely milled waste glass (FMWG) were prepared. The test results showed that the FMWG has a pozzolanic characteristics and using it as a mineral admixture in concrete, had a bad effect on workability, but improved considerably mechanical properties of concrete at later ages and the optimum percentage of FMWG that gives the maximum values of compressive, splitting tensile and bond strengths is 10%. Results also showed that expansion due to alkali-silica reaction was minimized obviously by increase the FMWG content.

**Keywords**: Finely Milled Waste Glass; Pozzolanic Material

## INTRODUCTION

Non-recyclable waste glass constitutes a problem for solid waste disposal in many countries. Since the glass is not biodegradable, landfills do not provide an environment-friendly solution. Consequently, there is a strong need to utilize waste glasses. Several tones of waste fluorescent lamps glass accumulate in their factories without any use.

Efforts have been made in the concrete industry to use waste glass as a partial replacement of the coarse or fine aggregates. Due to the strong reaction between the alkali in cement and the reactive silica in glass, the use of glass in concrete as part of the coarse aggregate was not satisfactory because of the marked strength regression and excessive expansion[1]. The strength loss due to the sand substitution by the crushed glass was reported to be between 5 to 10% [2] .

 A typical pozzolanic material features two characteristics: it should contain high silica content, and have a large surface area. The glass might satisfy the basic requirements for a pozzolan if it could be milled to a size fine enough to passify the alkali-silica reaction and to activate the pozzolanic behavior.[3,4]

This paper presents a preliminary study on the assessment of the pozzolanic activity of finely milled waste glass as well as its potential use in concrete as a partial replacement of cement.

## MATERIALS

The fine aggregate is sand with a fineness modulus of 2.6, and the coarse aggregate is gravel, its nominal maximum size equal 20 mm.

All concrete mixes containing one type of cement was type I ordinary Portland cement (OPC). The used waste glass was obtained from fluorescent lamps industry. It was ground by electrical mill to pass form 45 μm sieve to satisfy the physical requirements of ASTM C 618.[5] Its specific surface area equal 6500 $cm^2$/gm was measured by the nitrogen adsorption method (BET).

Table (1) shows that finely milled waste glass (FMWG) is considered as a pozzolanic material because it satisfies the chemical and physical requirements of ASTM C 618. [5]

One type of chemical admixture was used with a dosage of 1% by weight of cementitious materials content (OPC+FMWG) in all concrete mixes, it is sulphonoated melamine based in solid form (powder), which is classified as a superplasticizer meeting the requirements of ASTM C 494 [6].

**Table 1: Chemical Analysis and Physical Properties of FMWG and OPC**

| Chemical analysis | | | |
|---|---|---|---|
| Element | FMWG | ASTM C 618[5] requirements for pozzolanic material | OPC |
| $SiO_2$ | 73.0% | - | 20.3% |
| $AL_2O_3$ | 1.52% | - | 4.88% |
| $Fe_2O_3$ | - | - | 2.86% |
| $SiO_2+AL_2O_3+Fe_2O_3$ | 74.52% | Min. 70.0% | - |
| CaO | 5.10% | - | 63.02% |
| MgO | 3.22% | - | 2.13% |
| $Na_2O$ | 15.88% | - | 0.42% |
| $K_2O$ | 0.35% | - | 0.17% |
| $SO_3$ | - | Max. 4.0% | 2.26% |
| Chlorides | - | - | - |
| L.O.I. | 1.03% | Max. 10.0% | 2.85% |
| Physical properties | | | |
| Property | FMWG | ASTM C 618[5] requirements for pozzolanic material | OPC |
| Specific gravity | 2.50 | - | 3.15 |
| Specific surface area | 6500 $cm^2$/gm,BET | - | 2800 $cm^2$/gm,Blaine |
| % Passing from 45 μm | 100% | Min. 66% | - |
| Color | white | - | Grey |

## EXPERIMENTAL WORK

Five concrete mixes were prepared to determine the effect of changing FMWG percentages on different properties of concrete. The details of concrete mixes are indicated in Table (2).

**Table 2: Mix Proportions for Different Concrete Mixes, kg/m³**

| Mix code | Description | OPC | FMWG | Sand | Gravel |
|---|---|---|---|---|---|
| M0 | 100% OPC | 350 | - | 649 | 1293 |
| M1 | 95% OPC+5%FMWG | 333 | 17 | 648 | 1292 |
| M2 | 90%OPC+10%FMWG | 315 | 35 | 647 | 1288 |
| M3 | 85%OPC+15%FMWG | 297 | 53 | 645 | 1284 |
| M4 | 80%OPC+20%FMWG | 280 | 70 | 643 | 1281 |
| OPC+FMWG | 350 kg/m³ | | | | |
| Superplasticizer | 3.5 kg/m³ | | | | |
| w/c | 0.40 | | | | |

Lime-FMWG strength development test was conducted according to ASTM C 593 [7] to confirm the activity of FMWG with lime. The hydrated lime, FMWG and graded sand were mixed by 9, 18 and 73% by weight respectively and water was adjusted to achieve a flow of 65 to 75% consistency through a flow table test. The mixture was cast in 50 mm cube molds, wrapped by wet burlap, sealed by plastic bag, and cured at 54C$^o$ in an oven. Compressive strength test of cubes was carried out after 7 days curing at 54C$^o$, and after an additional 21 days curing at 23 C$^o$ in water to indicate the long-term strength gain.  Three specimens were tested and averaged for each age. As recommended by ASTM C 593[7], a satisfactory pozzolanic material should have a minimum compressive strength equal 4.1 MPa (41.8 kg/cm$^2$) when mixed with lime after 7 days curing at 54 C$^o$,  and after an additional 21 days curing at 23 C$^o$ in water.

Slump test was carried out to determine the slump of fresh concrete (consistency of fresh concrete) for each mix.

15 X 15 X 15 cm cubical concrete specimens were made for measuring the compressive strength and 15 X 30 cm cylindrical specimens were used for finding the splitting tensile strength and bond strength.

Study of the expansion due to the possible reaction between the alkalis in the cement and the silica in the glass was carried out in accordance with ASTM C 1260.[8]  The 25 X 25 X 100 mm mortar bars were made by graded natural sand, OPC, and FMWG. The W/C ratio was 0.47 and the cementitious/ sand ratio was 1/2.25. For the five batches containing FMWG as a partial replacement of OPC (0, 5, 10, 15, and 20%).

After 24 h. of curing, the bars were placed in water at 80C$^o$ for another 24h. to gain reference length. They were then transferred to a solution of NaOH at 80C$^o$.

Changes in the length of the mortar bars were checked for 14 days after their surface was dried by using a comparator, a length comparison measuring device with sensitivity of 0.002 mm. The mortar bars without FMWG were also tested as control specimen. The comparison with the control is an indication of whether or not the silica in glass is reactive with the alkalis in cement and from the solution. It also manifests the ability of FMWG in suppression of the expansion by consuming more lime in concrete.

## RESULTS AND DISCUSSION

### Activity of FMWG with Lime

The compressive strength of the lime-FMWG mixtures are shown in Fig. (1). The FMWG satisfied the minimum strength requirement  (41.8 kg/cm$^2$) at 7 days test, and attained an increase in strength after additional 21 days of curing in water. From Fig. (1) and as recommended by ASTM C 593 [7] is evident that FMWG has a satisfactory activity with lime and it has been considered as a pozzolanic material.
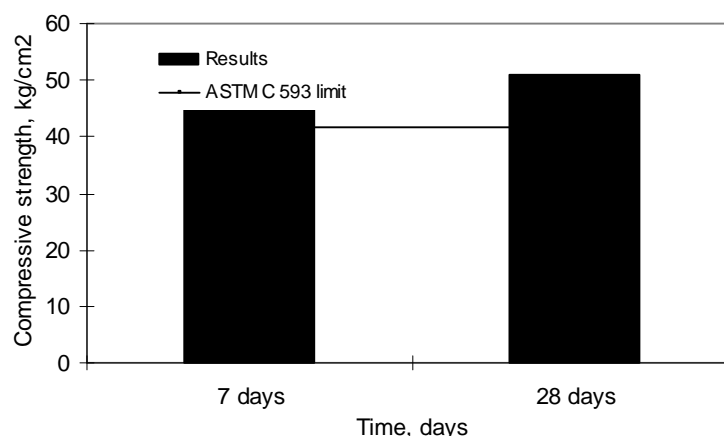


**Fig. 1: Compressive Strength of Lime-FMWG Mixture**

**Workability**

Fig. (2) demonstrates the effect of increasing FMWG percentage on the slump results. From this, it is obtained that there is a great reduction in slump (loss in workability) with increasing the amount of FMWG from 0% to 20%. For instance, M1 (5% FMWG) has a slump loss equals-4% and M4 (20% FMWG) its rate equals-45% compared to control mix M0 (100% OPC) without FMWG. The reduction in slump is due to very fine particles and high specific surface area of FMWG (6500 cm$^2$/gm, BET).
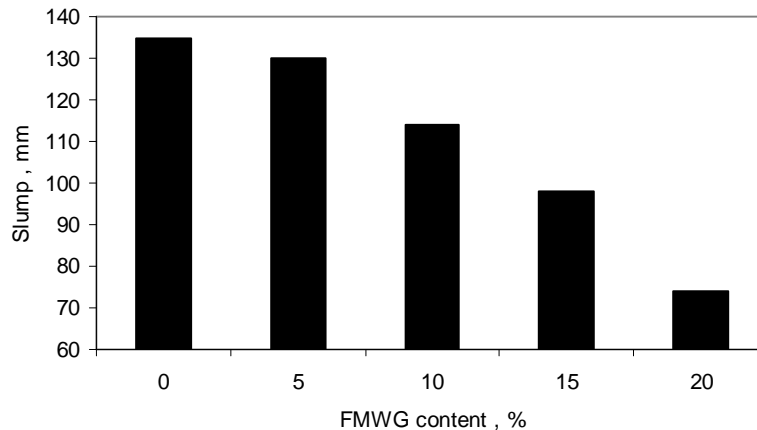


**Fig. 2: Effect of FMWG on Concrete Slump**

**Compressive Strength Development**

The compressive strength at 7, 28 and 91 days are shown in Fig. (3). The test results indicate that the particular content of FMWG, which may be referred to as the optimum content is 10% after this limit, the strength decreased. At the optimum content, FMWG is sufficient to react with all liberated lime [Ca(OH)$_2$] produced from the hydration process of cement to form the stable and very dense cementitious compound; calcium silicate hydrate (CSH), which it is responsible for improving  all concrete strengths. Any excess of FMWG beyond the optimum content works only as a filler material and hence, lower strengths may be observed due to decreasing the amount of clinker.

It is seemed from Fig. (3), after age of 7 days (at 28 and 91 days), when the pozzolanic effect became significant, the degrees of strength enhancement were high. The 91 days compressive strength of concrete mixes containing 5 and 10% FMWG were about 1.12 and 1.17 nearly times respectively the strength of the control mix that contained 100% OPC. The effect of FMWG in improving concrete strength seems to be maximum at age of 91 days.
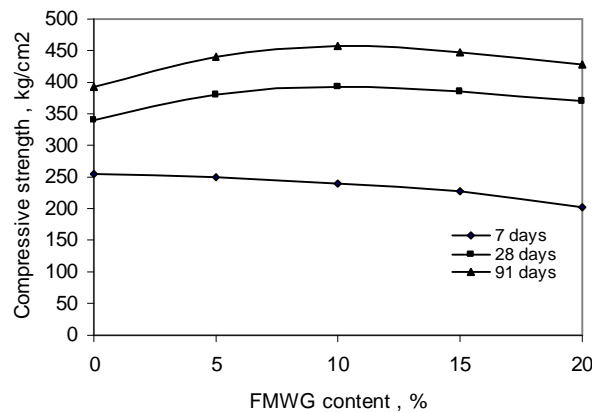
**Fig. 3: Effect of FMWG on Concrete Compressive Strength**

## Strength Activity Index

The strength activity indexes of all concretes containing various replacements of FMWG are presented in Fig. (4). ASTM C 618 [5] recommends that a pozzolan have a minimum strength activity index of 75% for it to benefit concrete. As a consequence, the activity indexes of all concretes satisfy the crite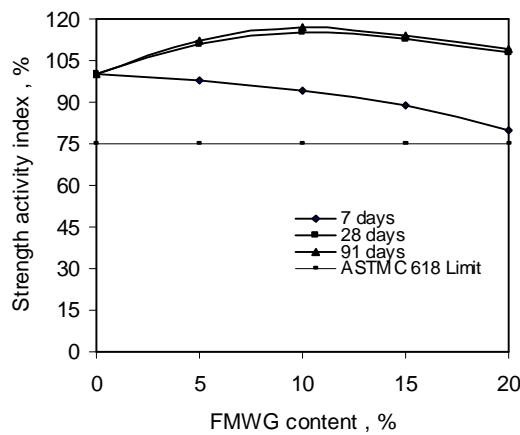ria. The relatively higher strength indexes at later age (91 days) could be attributed to the completion of the hydration process of FMWG and OPC with time. It is known that the pozzolanic reaction at ordinary room temperature is slow and therefore a long curing period is needed to observe the positive benefits of FMWG.



**Fig.4: Strength Activity Index of Concretes Containing FMWG**

## Splitting Tensile and Bond Strength

The behavior of concrete mixes containing various percentages of FMWG in splitting tensile and bond tests are approximately similar to that in compression test, as indicated in Fig. (5) and (6), because the relationship between compressive strength and both splitting tensile and bond strength is directly proportional and fairly strong.
From Fig. (5) and (6), it is found that the optimum percentage of FMWG that gives the highest value of splitting tensile and bond strength is 10% at 28 days, it obtained an increase in strength equal 10% and 12% respectively compared to control mix without FMWG.
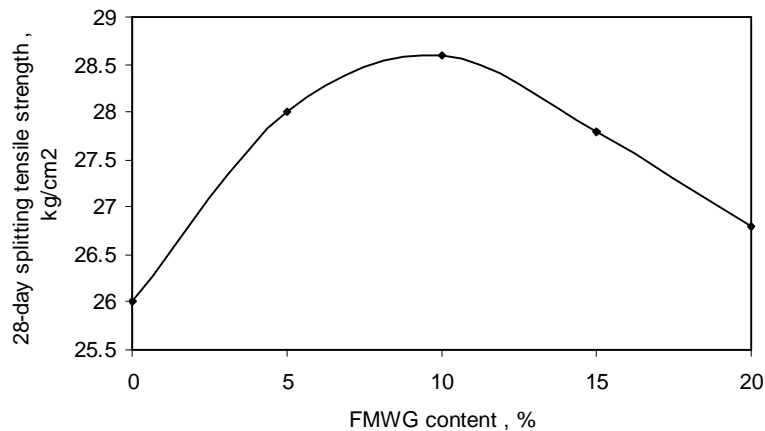
**Fig. 5: Effect of FMWG on Concrete Tensile Strength**
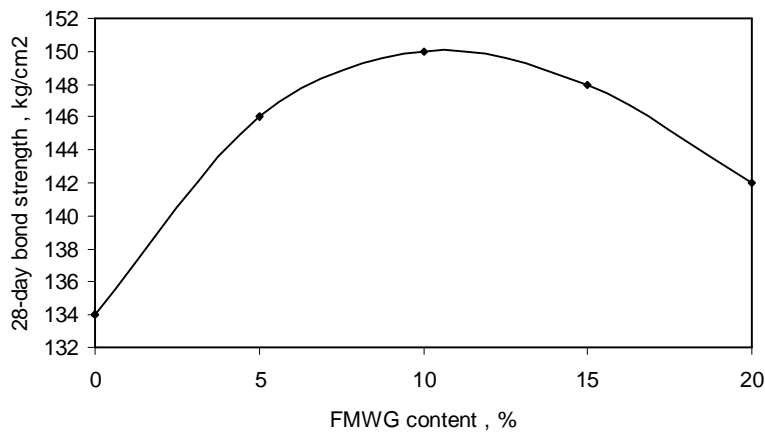


**Fig. 6: Effect of FMWG on Bond Strength of Concrete**

**Expansion Due to Alkali-Silica Reaction**

The percent expansions of the mortar bars with and without FMWG additives are shown in Fig. (7). It was evident that with the increase of FMWG contents from 0% to 20%, there are a clear reduction in mortar expansions comparing to that of control mix. For example, M4 (20% FMWG) attained a big drop in expansion equal 71% at 14 days comparing to control mix without FMWG. All batches had expansions below 0.1% (acceptable limit according to ASTM C 1260 [8]). The expansion tests showed that not only was the FMWG not expansive as was expected due to the possible alkali-silica reaction, but it actually helped hinder the expansion as compared to the control mix. This is referred to the direct reduction of available alkali as $Ca(OH)_2$ in the medium needed to support the reaction because $Ca(OH)_2$ (liberated lime from cement hydration process) consumed by reacting of FMWG with it, hence decrease of alkaline of system will be expected.

**Fig. 7: Expansion of Mortar Bars with and without FMWG**

## CONCLUSIONS

The following conclusions are derived:
1.  Waste glass, if powdered finer than 45µm, it is considered as a pozzolanic material because of these reasons:
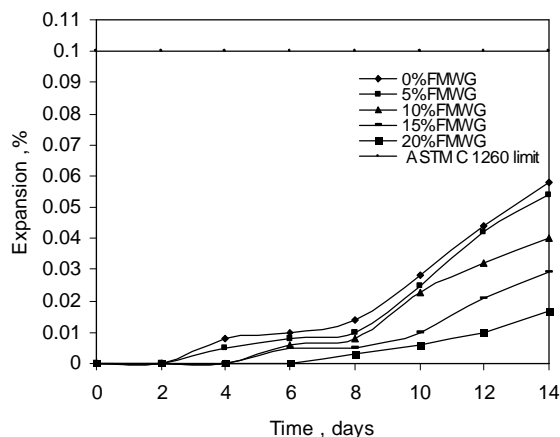    *   It satisfies the requirements for pozzolanic material according to ASTM C 618 [5], concerning the chemical compositions and physical properties.
    *   It has a satisfactory activity with lime, the compressive strength of the lime-FMWG mixture was higher than the minimum strength limit (4.1MPa) according to ASTM C 593[7].
    *   The strength activity indexes of all FMWG-concrete mixes are higher than the threshold limit of 75% as recommended by ASTM C 618[5].
2.  When FMWG is used as a partial replacement of cement, there is a clear loss in concrete workability with increasing the amount of FMWG from 0% to 20%.
3.  The pozzolanic effect of FMWG in concrete is more obvious at later ages (28 and 91 days). The optimum percentage of FMWG that gives the maximum values of compressive, splitting tensile and bond strength is 10%.
4.  The expansions of the mortar bars decrease with increase the FMWG content, the percentage that recorded the minimum value is 20%.
5.  As OPC-FMWG concrete is a new technique, it is a very inviting and promising fields for research works. The following points may be considered:
    *   Long - Term concrete properties together with its durability should be studied for longer terms of time, i.e., 1,2, and 3 years.
    *   Behavior of structural elements as reinforced concrete beams and columns.

## REFERENCES

1.  Johnson, C.D., "Waste Glass as Coarse Aggregate for Concrete", Journal of Testing and Evaluation, 2(5), 1974, pp. 344-350.
2.  Panchakarla, V.S. and Hall, M.W., "Glascrete-Disposing of Non-Recyclable Glass", Materials for a New Millennium, Proceeding of ASCE Materials Engineering Conference, Washington, D.C., 1996, pp. 509-518.
3.  Shao, Y.; Lefort, T.; Moras, S.; and Rodriguez, D., "Studies on Concrete Containing Ground Waste Glass", Cement and Concrete Research, 30(3),2000, pp. 91-100.
4.  Shehab, H.; Ismail, G.; Abd El-Megied, S.; and Metwally, I.M., "Improvement of Properties of Concrete Containing Slag Cement by Adding Silica Fume", Construction Materials and

Economic Challenges in Arab World Conference, Building Research Centre, Cairo,2000, pp.653-668.

5. ASTM Standards, "Coal Fly Ash and Raw or Calcined Natural Pozzolan for Use as a Mineral Admixture in Concrete", ASTM C 618-01, 2001,pp.318-321.

6. ASTM Standards, "Standard Specification for Chemical Admixtures for Concrete", ASTM C 494-92, 1992, pp.1251-1259.

7. ASTM Standards, "Fly Ash and Other Pozzolans for Use with Lime", ASTM C 593-95, 1995, pp.318-321.

8. ASTM Standards, "Potential Alkali Reactivity of Aggregates", ASTM C 1260-01, 2001, pp.684-688.

# FLEXURAL BEHAVIOUR OF POLYPROPYLENE FIBRES REINFORCED CONCRETE BEAMS

**Ahmed H. Ghallab**

*Assistant professor, Structural Department, Faculty of Engineering, Ain Shams* University.
*E-mail: ahghallab@yahoo.co.uk*

**Atef Badr**

*Lecturer of Structural Engineering, Mansoura University.*
*e-mail: atefbadr@hotmail.com*

## Abstract

The flexural behaviour of polypropylene fibre reinforced concrete I-beams- with and without stirrups- was evaluated in this study. The main studied factors were the volume ratio of polypropylene fibre, the stirrups ratio and the surface type of polypropylene fibre. All beams had the same dimensions and longitudinal reinforcement and tested under two third point loads. The results showed that polypropylene fibres were effective in reducing the cracks' width and crack propagation. Also, the increase in fibre volume ratio, however, after a certain limit, did not necessarily improve the flexural behaviour of polypropylene fibre reinforced concrete beams. The results also showed that while polypropylene fibres had only slight effect on the beam stiffness, ( cracking moment and ultimate moment), combining polypropylene fibres and stirrups improved the behaviour of reinforced concrete beams and changed its failure mode. In addition, analysis of the results showed that the cracking and ultimate moment of polypropylene fibre reinforced concrete beams can be calculated using the same methods used in conventional reinforced concrete beams.

**Keywords:** Concrete, Fibre, Polypropylene Fibre, Flexural behaviour.

## INTRODUCTION

Fiber reinforced concrete (FRC) is an ordinary concrete with randomly distributed short fibres. The main role of the fibre is to bridge the cracks in the matrix and prevent them from extending. Hence, help to improve the concrete post-cracking behaviour such as ductility, cracking control, and impact resistance [1-3]. In general, the improvement in the matrix behaviour varies according to the fibre type, volume ratio ($V_f$), aspect ratio ($l_f/d_f$), matrix composition and maximum aggregate size [4,5]. Common fibres added to structural concrete are either metallic such as steel or synthetic polymeric such as polypropylene and nylon. The effect of inclusion of fibres such as steel fibre on the behaviour of reinforced concrete beams has been studied by many researchers, and it has been reported that the addition of steel fibres to reinforced concrete beams improved their behaviour in shear and flexure [6-9].
Among the polymeric fibres, polypropylene is the most widely used in concrete due to its good resistance to acids and alkalis in addition to the cheapness of the raw material compared (on the volume basis) with steel fibres and other alternatives[10,11].
The effect of PPF on the properties of concrete was studied by many researchers [2,12-16]. The excellent control of cracking due to improvement in flexural toughness and impact resistance of PPFRC is well known and reported widely [2,3,15,17]. However, the effect of PPF on other properties is not well documented. Some studies reported slight improvements in compressive, tensile and flexural strengths [13-15], while others [2] showed either no effect or slight adverse effect on these properties due to the inclusion of polypropylene fibres. The difference between the results may be related to the difference in PPF parameters and matrix composition.

However, few studies were conducted to study the effect of inclusion of polypropylene fibres on the flexural behaviour of reinforced concrete beams. Furthermore, more research is needed to investigate the possibility of combining polypropylene fibres and stirrups to improve the behaviour of reinforced concrete beams and reduce the congestion of steel reinforcement especially in the irregular shaped sections surfaces  such as T-sec or I-sec. The present study aimed to investigate the effect of polypropylene fibre with variable volume ratio ($V_f$ = 0.25% and 0.5%) on the flexural behaviour of reinforced concrete I-beams with and without stirrups. Also, study the effect of inclusion of polypropylene fibres on the analysis method used to calculate the flexural strength of ordinary reinforced concrete beams.

## EXPERIMENTAL PROGRAM

**Materials**

The concrete was produced using ordinary Portland cement conforming to BS 12: 1996 and natural aggregate. The nominal maximum size of the coarse aggregate was 10-mm. The fine aggregate complied with zone M of BS 882, 1992. Two types of polypropylene fibres were used in this study as shown in Table 1.

**Table 1: Properties of Polypropylene Fibre**

| Properties | Fibre type | |
|---|---|---|
| | Type 1 | Type 2 |
| Nominal Diameter  (μm) | 55 | 18 |
| Fibre surface type | coarse | fine |
| Length   (mm) | 18 | 18 |
| Aspect ratio ($l_f/d_f$) | 330 | 1000 |
| Specific gravity | 0.91 | |
| Melting point | 170    °C | |
| Ignition point | 590    °C | |
| Tensile modulus | 4.1   GPa | |
| Tensile strength | 560  MPa | |

**Mixes**

The concrete mix proportions were chosen based on the results of trial mixes carried out to optimise the mix proportions and fiber content. The optimisation of the of PPFRC basic mix proportions was based on combined properties including workability, compressive strength, flexural strength and flexural toughness. Details of the concrete mix proportions and fibre content of each beam are given in Table 2.
The nominal water to cement ratio was 0.40. However, the actual water content varied according to the fibre content to maintain comparable workability as measured from the slump test according to BS 1881: Part 102, 1983.

**Mixing and preparation of beams**

A conventional rotary concrete mixer was used. The dry coarse aggregate, cement and sand were first mixed for about one minute before adding half of the mixing water. After two minutes of mixing, the remaining mixing water and super-plasticiser were added. The fibres were added slowly to the running mixer, after three minutes, to avoid clumping. Mixing was continued for another two minutes to achieve uniform distribution of the fibre. Workability of the fresh concrete was assessed using the slump test. The slump values are given in Table 2. After casting, the concrete was compacted using a vibrating table. From each mix, a main beam having "I" cross section was cast in addition to three 100-mm cubes and two 100 x 100 x 500 mm prisms.  The results of tested specimens are shown in Table 3.

The beams and the cubes were covered with wet hessian and polyethylene sheets overnight. They were then de-moulded after 24 hours and cured in an environmental chamber maintained at 20±2 °C and 97±3 % relative humidity until testing at 14 days.

**Table 2: Details of the Concrete Mix Proportions**

|  | Cement kg/m$^3$ | Sand kg/m$^3$ | Gravel kg/m$^3$ | W/C Ratio | Super-plasticizer litre/m$^3$ | Fibre type | Fibre ratio V$_f$% | Slump mm |
|---|---|---|---|---|---|---|---|---|
| B1 | 425 | 915 | 915 | 0.40 | 3.4 | ---- | ------ | 120 |
| B2 | 425 | 915 | 915 | 0.43 | 3.4 | Type1 | 0.50 | 110 |
| B3 | 425 | 915 | 915 | 0.40 | 3.4 | ----- | ---- | 105 |
| B4 | 425 | 915 | 915 | 0.43 | 3.4 | Type1 | 0.50 | 100 |
| B5 | 425 | 915 | 915 | 0.41 | 3.4 | Type1 | 0.25 | 120 |
| B6 | 425 | 915 | 915 | 0.42 | 3.4 | Type2 | 0.25 | 105 |

**Test procedure and measurements**

The test beams were geometrically similar having I-cross section, total length of 2800 mm and an effective span length of 2600 mm between supports. The dimensions and the reinforcement details for the test beams are shown in Fig 1, while Table 3 shows the properties of these beams. All beams were loaded by two third point loads up to failure using a 1000 kN hydraulic jack. Seven pairs of demec points were mounted across the beam depth at a distance of 200 mm on one side at the mid-span of the beam for the measurement of concrete strains. Steel strains were measured using electrical strain gauges mounted on main longitudinal steel and stirrups as well. The initiation of the cracks was detected using a magnifying lense. Deflection of the beams during test at the mid-span and under the concentrated loads was measured using LVDTs. Steel strains and deflections were measured at each load step while concrete strain was measured at appropriate interval using the demec gauges.

**Table 3: Properties of Test Beams**

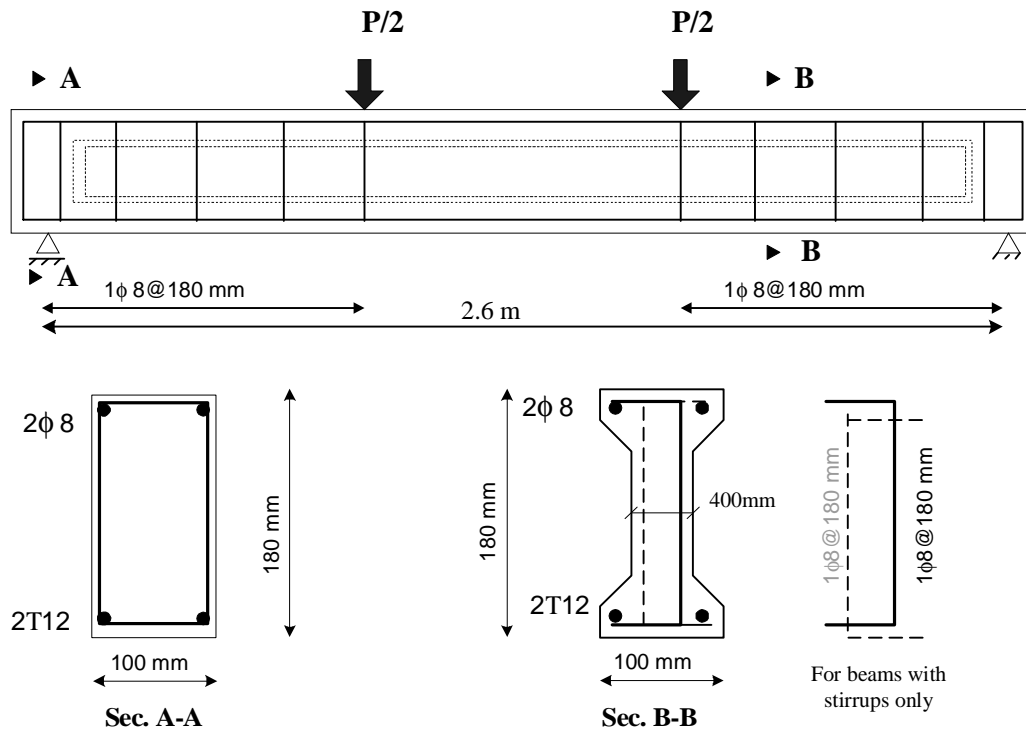| Beam no. | $f_{cu}$ (MPa) | $f_{ctr}$ (MPa) | A$_s$ | $f_y$ (MPa) | A$_{s'}$ | $f_y$ (MPa) | Stirrups | V$_f$% |
|---|---|---|---|---|---|---|---|---|
| B1 | 56.1 | 4.29 | 2T12 |  | 2φ8 |  | ------ | ----- |
| B2 | 50.6 | 3.93 | 2T12 |  | 2φ8 |  | ------ | 0.5 |
| B3 | 59.8 | 4.41 | 2T12 | 497 | 2φ8 | 361 | 1φ8/180mm | ----- |
| B4 | 51.8 | 4.08 | 2T12 |  | 2φ8 |  | 1φ8/180mm | 0.5 |
| B5 | 62.6 | 4.86 | 2T12 |  | 2φ8 |  | 1φ8/180mm | 0.25 |
| B6 | 63.5 | 4.98 | 2T12 |  | 2φ8 |  | 1φ8/180mm | 0.25 |

**Fig. 1: Dimensions and Reinforcement Details of Tested Beams**

## TEST RESULTS

### Cracking patterns:

Fig. 2 shows the cracks patterns at failure for the tested beams. The crack patterns for beams in each group; beams without stirrups or beams with stirrups, were nearly similar. As failure was approached the FRC beams developed new cracks between the primary cracks. The new cracks were the result of increased ductility and sustainable beam curvature.

The extension of the cracks through the beam height was lower in case of FRC beams compared with RC beams due to the action of the fibres that restrained the propagation of cracks. The effect of fibres on the crack height was significant in case of the beam without stirrups and less significant when stirrups were used.

Also, during loading, the primary cracks' height was not inversely proportional with the increase in polypropylene fibre content (beam with $V_f$= 0.25% had less crack height than that with $V_f$= 0.5%). This contradicts with the case of steel fibre, as reported by other researchers [18,19,6]. This might be because the crack extension depends on several factors such as concrete tensile strength, beam stiffness, bond strength between concrete and fibre, and fibre volume ratio. At early age of concrete, the failure of fibre was governed by the bond strength between concrete and fibre rather than fibre strength and as concrete strength increases, the bond strength and concrete tensile strengths increase, hence, beam with higher concrete strength was expected to have lower crack extension (the highest concrete compressive strength and tensile strength obtained in this study were at $V_f$ =0.25% not at $V_f$ = 0.5%).

At ultimate load, beams with fibres and stirrups failed in flexure while the others failed in shear. Also, the presence of fibres in reinforced concrete beams prevented extensive damage of concrete in the compression zone, thus helping the beam to be intact after the maximum load was reached.
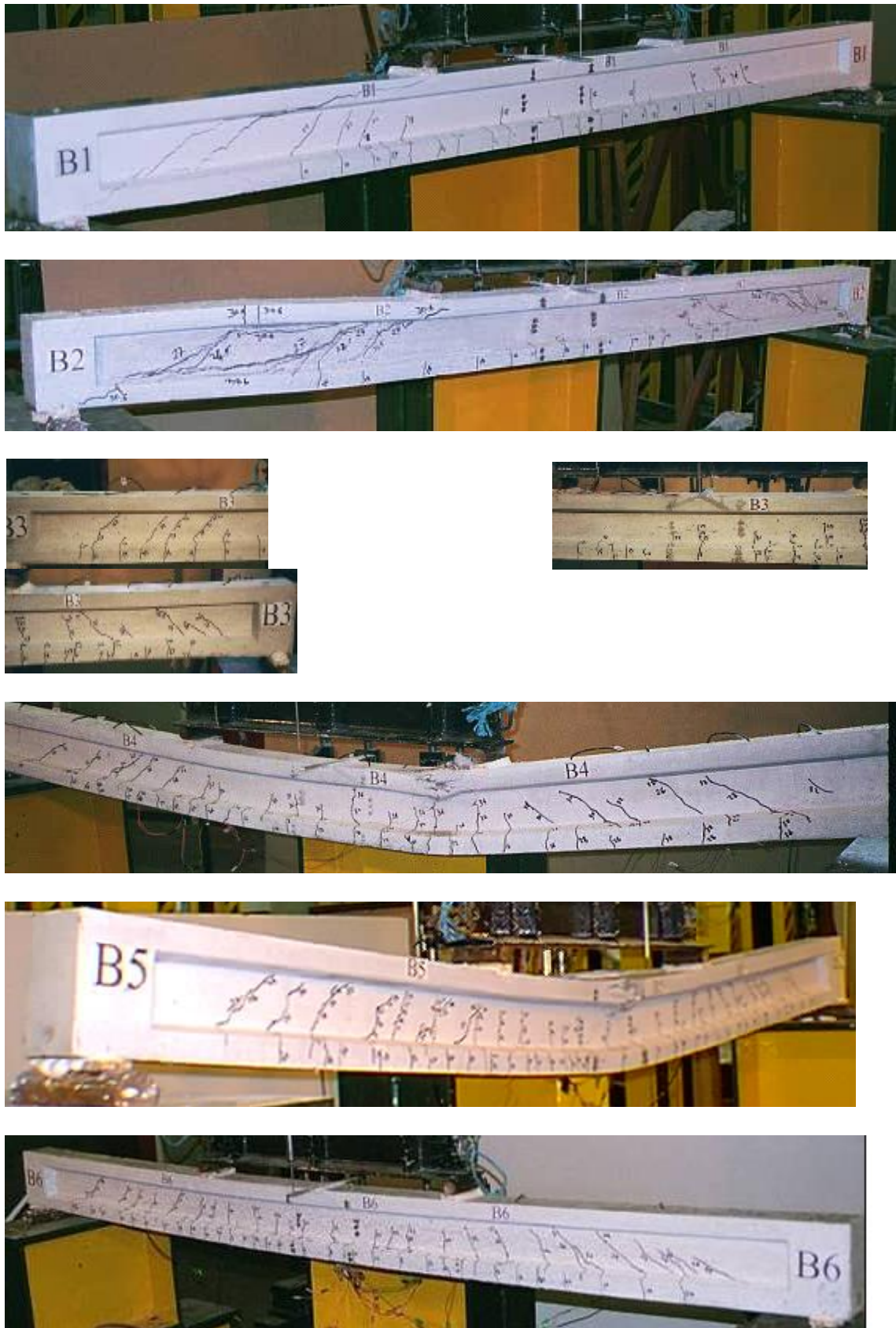
**Fig. 2: Cracks Patterns for Test Beams**

**Cracking strength**

Table 4 shows the actual cracking moment for the tested beams. The presence of the polypropylene fibres with higher volume ratio (0.5%) slightly reduced the flexural cracking resistance, while the inclusion of polypropylene fibres with moderate ratio (0.25%) slightly improved the flexural cracking resistance. This was observed in case of beams with or without stirrups. This is because the high volume ratio of polypropylene fibres reduced the mix workability and a higher (water/ cement) ratio was required to obtain the required workability, which results in lower concrete strength, and hence, lower flexural tensile strength.

**Table 4: Cracking, Yield & Ultimate Moments of Tested Beams**

| Beam no. | $M_{cr}$ (kN.m) | $M_y$ (kN.m) | $M_{ult}$ (kN.m) | Mode of failure |
|----------|-----------------|--------------|------------------|-----------------|
| B1 | 2.18 | 10.88 | 11.05 | Shear |
| B2 | 2.13 | 10.7 | 13.31 | Shear |
| B3 | 2.09 | 14.44 | 16.57 | Shear |
| B4 | 1.87 | 13.09 | 16.83 | Flexural |
| B5 | 2.35 | 13.96 | 17.23 | Flexural |
| B6 | 2.44 | 14.05 | 16.75 | Flexural |

**Load-deflection behaviour**

Table 5 shows the deflection of the tested beams at the mid span at different load stages and the slope of the relation between load and deflection in the uncracked, working and ultimate stages. The slope of the relation between load and deflection can give a good idea about the flexural rigidity (or stiffness) of the beam during loading. Beams without fibres (B1 and B3) show higher flexural rigidity before cracking. After cracking, its rigidity dropped to about 40% relative to that before cracking, due to the rapid progress of cracks through the section height.
For FRC beams, the slope of load-deflection relation in the uncracked stage was less than that of RC beam. However, after cracking the drop was smaller than that of RC beams (relative slope after cracking to that before cracking ranged between 52% and 70% showing the effectiveness of the fibres.

**Table 5: Deflection at Different Load Levels**

| Beam no. | Deflection (mm) | | | Slope of P-Δ curve (KN/mm) | | |
|----------|----------|---------|---------|----------------------|----------------------|----------------------|
| | Cracking | Yielding | Ultimat | $0 \rightarrow P_{cr}$ | $P_{cr} \rightarrow P_y$ | $P_y \rightarrow P_{ult}$ |
| B1 | 0.94 | 12.05 | 12.9 | 6.28 | 2.67 | 1.96 |
| B2 | 1.3 | 12.97 | 20.5 | 3.58 | 2.55 | 1.65 |
| B3 | 1.02 | 18.87 | 44.9 | 5.77 | 2.40 | 1.27 |
| B4 | 0.96 | 16.24 | 90.0 | 4.85 | 2.53 | 1.12 |
| B5 | 1.18 | 15.99 | 97.6 | 4.80 | 2.50 | 1.31 |
| B6 | 1.46 | 17.87 | 93.5 | 3.53 | 2.37 | 1.14 |

As shown in Fig. 3-a, the relation between load and deflection of beams without stirrups (B1, B2) show two stages, and while the failure of both beams was due to shear, the deflection at ultimate of beam B2 was higher than that of B1 (about 60% higher). This gave an adequate warning before failure.
In case of beams with stirrups and with or without fibres, the relation between load and deflection shows three stages (Fig. 3-b). Before cracking the difference between the load-deflection relation was negligible. At yield, beam B5 had the least deflection while at ultimate it had the maximum deflection among the tested beams.
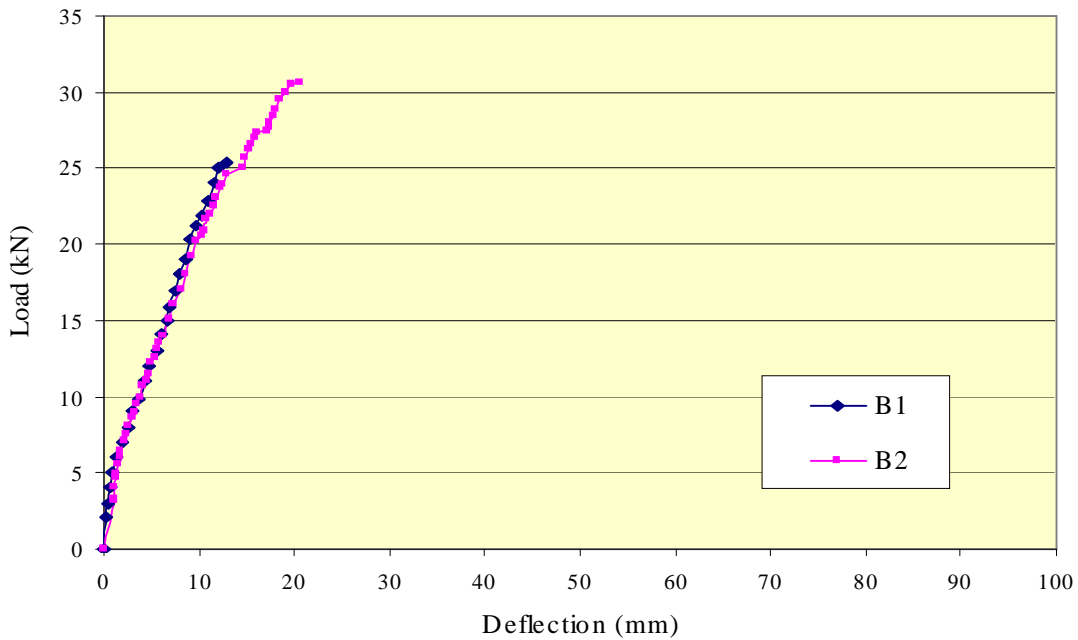
**Fig. 3-a: Relation between Load and Deflection of Beams without Stirrups.**
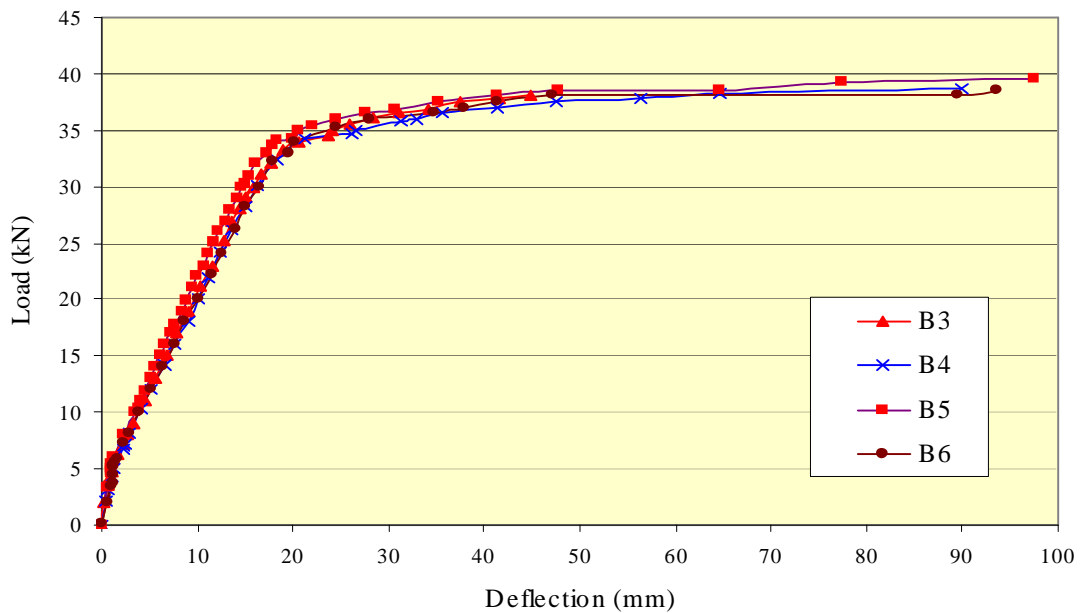


**Fig. 3-b: Relation between Load and Deflection of Beams with Stirrups**

**Ultimate flexural strength**

In this study, all beams without fibres failed in shear, while those with both fibres and stirrups failed in flexure. In case of the beams without stirrups, there was an improvement in the ultimate load by about 20% due to the inclusion of fibres. While in the case of beams with stirrups, the addition of fibre slightly increased its ultimate flexural strength, (the increase in the flexural strength ranged between 1 and 4%). Although the results for ultimate bending are not conclusive since flexural strength was not exhausted in the beam without fibres, it can be stated that the effect of fibres on the ultimate flexural strength was negligible. However, the inclusion of fibre increased the shear strength and changed the failure mode of beam with stirrups from shear failure to flexure failure.

The comparison between beams B4 and B5 (different fibre volume ratio) shows that beams B4 and B5 had almost the same ultimate moment and the same type of failure, although they had a different fibre volume ratio. The difference in ultimate load can be related to the difference in concrete strength; and it can be concluded that in case of flexural failure, the increase in fibre ratio- above a certain limit- has no effect on the ultimate strength.

Also, the higher ultimate strength of beam B5 than that of beam B6 can be attributed to the coarse surface of fibre used in B5 that resulted in higher bond strength between concrete and fibre that enabled the fibre to resist higher load before failure.

**Concrete strain**

Fig. 4-a and Fig. 4-b show the distribution of concrete strain along the beam height at the mid span at different load levels. As can be seen, in the absence of stirrups, the addition of fibre to concrete reduced the tensile concrete strain, increased the neutral axis depth and the compressive strain. The improvement in the concrete strain, however, was not proportional with the increase in fibre ratio as the improvement in concrete strain was higher for beam with lower fibre ratio (B4 and B5). Also, the concrete strain distribution of beam B6 was almost similar to that of beam B3. This can be attributed to the lower bond strength between fibre and concrete in beam B6 due to the fine surface of the fibres.
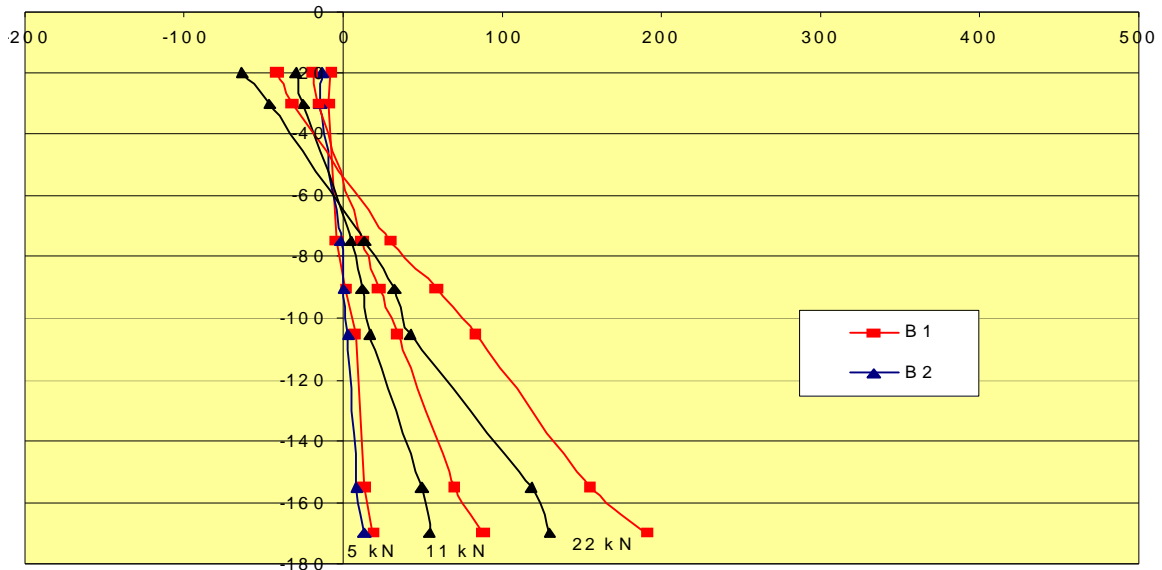


**Fig. 4-a: Distribution of Concrete Strain for Beams without Stirrups at the Mid Span Along the Beam Height at Different Load Levels.**
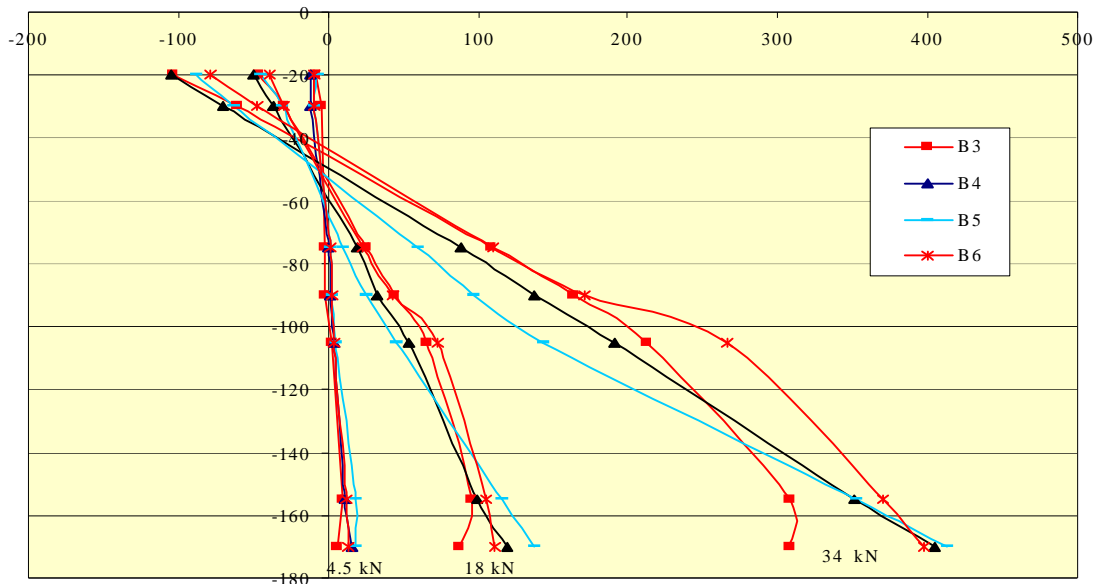
**Fig. 4-b: Distribution of Concrete Strain for Beams with Stirrups at the Mid Span along the Beam Height at Different Load Levels.**

**Steel strain**

During loading, the relation between load and tensile steel strain for beams with stirrups show three stages, as shown in Fig (5). For beams with stirrups, the relation between load and strain was linear and almost typical up to yield. At yield, strain for FRC beams was less than that of RC beam by about 25% resulted in less crack width. After yielding, there was a rapid increase in steel strain for FRC beams and almost double that for RC beam indicating higher ductility

For beams with stirrups, the ultimate steel strain of beam without fibers (B3) was less than those of the beams with fibers as its failure was due to shear with low ductility. After yielding, beams B5 and B6 show sudden increase in the steel strain that due to the failure of fiber and the transfer of its load to the steel bars (failure of fibre in beam B6 was faster than that of fibre in beam B5 due to its lower bond strength).

For compression reinforcement, beam with low concrete strength had a higher compressive steel strain during loading. This can be seen from Fig. (6), as the compressive steel in Beam B4 has the highest strain among all beams while that in beam B5 (had the highest concrete strength) was less than the other beams.
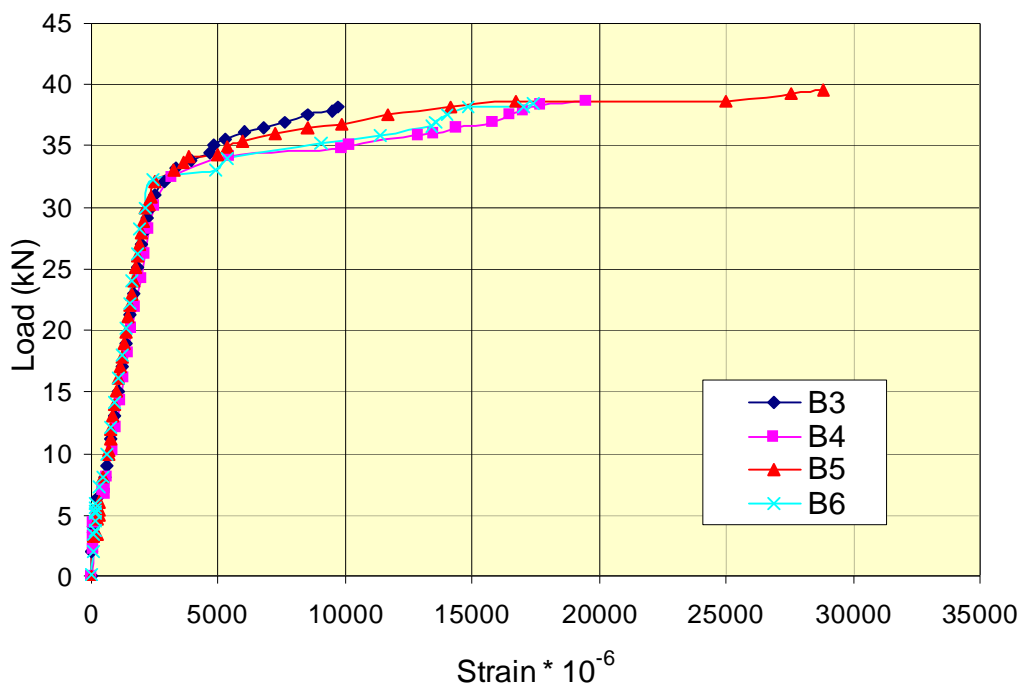
**Fig. 5: Relation between Load and Tensile Steel Strain at the Mid Span for Beams with Stirrups.**
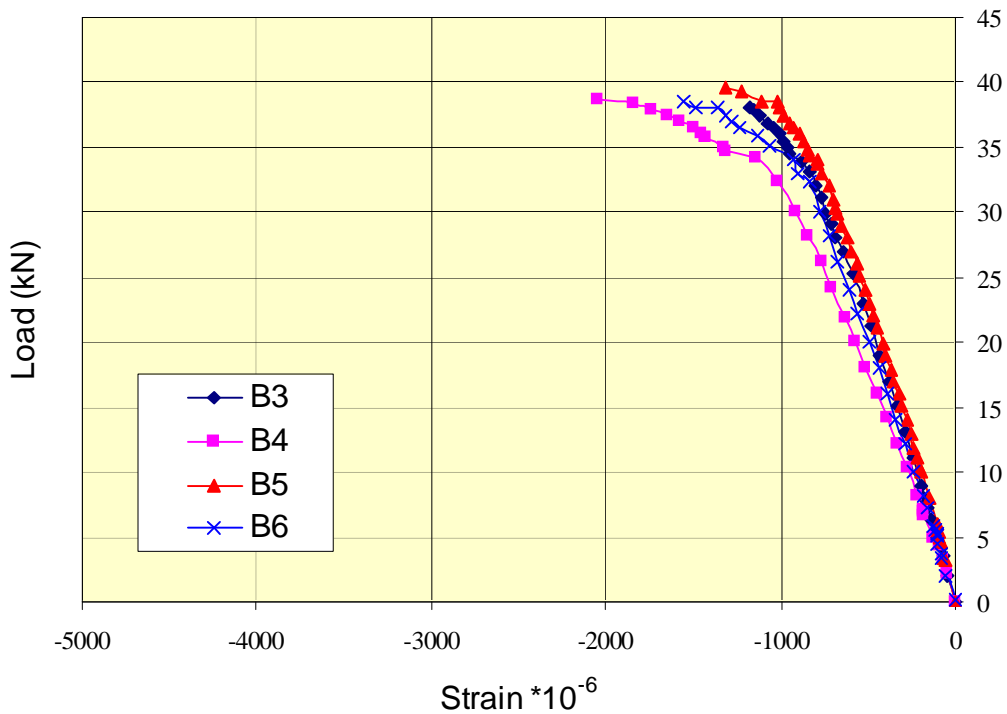


**Fig. 6: Relation between Load and Compressive Steel Strain at the Mid Span for Beams with Stirrups.**

## THEORETICAL ANALYSIS

The experimental results showed that both the cracking moment and the ultimate moment can be calculated using the same equation used for ordinary reinforced concrete. The cracking moment ($M_{cr}$) can be calculated from the following equation:

$$M_{cr} = \frac{f_{ctr}I_g}{y} \tag{1}$$

Where:

$f_{ctr}$= flexural tensile concrete strength ( taken as  $0.6 \sqrt{f_{cu}}$  MPa)   (2)
$f_{cu}$= characteristic concrete strength (MPa)
$I_g$ = gross moment of uncracked section
$y$ = depth from the bottom fibre to the neutral axis.

The ultimate moment for I-section can be calculated as follows (Fig 7):

$$M_{ult} = A_s f_s \left( d_s - \frac{b_1 c}{2} \right) - A'_s\, f'_s \left( d'_s - \frac{b_1 c}{2} \right)$$

*or*    (3)

$$= A'_s\, f'_s \left( d'_s - \frac{b_1 c}{2} \right) + 0.67 f_{cu}(B - b_w)h_f \left( \frac{h_f - b_1 c}{2} \right)$$

Where:

$A_s$ = area of tensile steel
$A_{s'}$ = area of compressive steel
$b_w$ = width of the rectangle section
$B$ = width of the flange
$d_s$ = effective depth of tension steel
$d'_s$ = effective depth of compressive steel
$f'_s$ = yield strength of compressive steel
$f_y$ = yield strength of tensile
$F_f$ = concrete compressive force resisted by flange
$F_w$ = concrete compressive force resisted by web
$F'_s$ = compressive force resisted by compressive steel
$h$ = total height of cross section
$h_f$ = height of the flange.
$b_1$ = *concrete compression block reduction factor*

*And*     $c$ is the neutral axis depth and can be calculated from the following equation

$$c = \frac{A_s f_s - A'_s\, f'_s - 0.67 f_{cu}(B - b_w)h_f}{0.67 f_{cu} b_w * b_1} \tag{4}$$

a) cross section

b) stresses and forces for R-sec.

c) stresses and forces for T-sec.
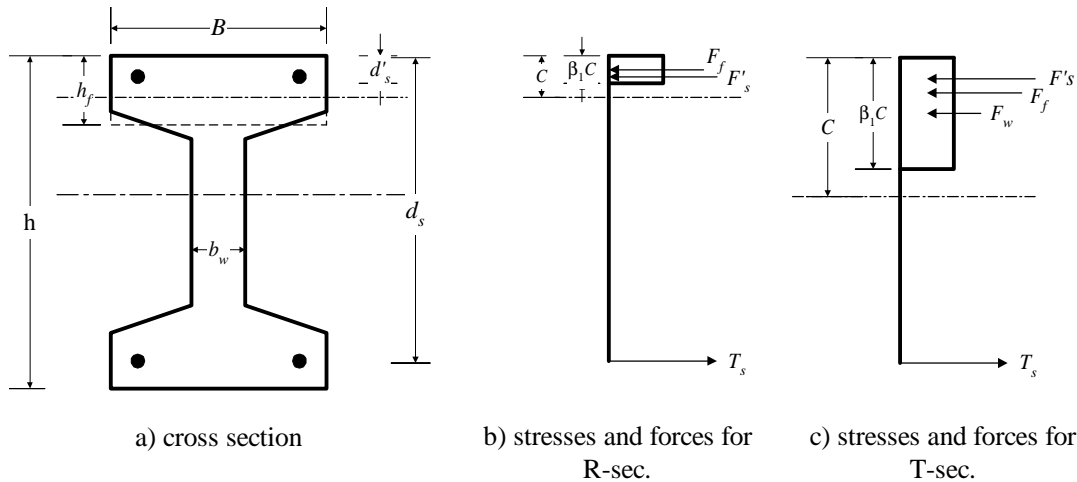
**Fig. 7: Relation between Load and Compressive Steel Strain at the Mid Span for Beams with Stirrups.**

For rectangular section B= $b_w$ in the previous equations; and for beams failed in flexure $f_s$= $f_y$. Fig. 8 shows the relation between the actual cracking moment and the calculated cracking moment using equation 1 for the actual flexural strength and that obtained from equation 2. Fig. 9 shows a relation between the actual and calculated ultimate moments. A good agreement between the results can be seen in both cases (except for beams without stirrups at ultimate).
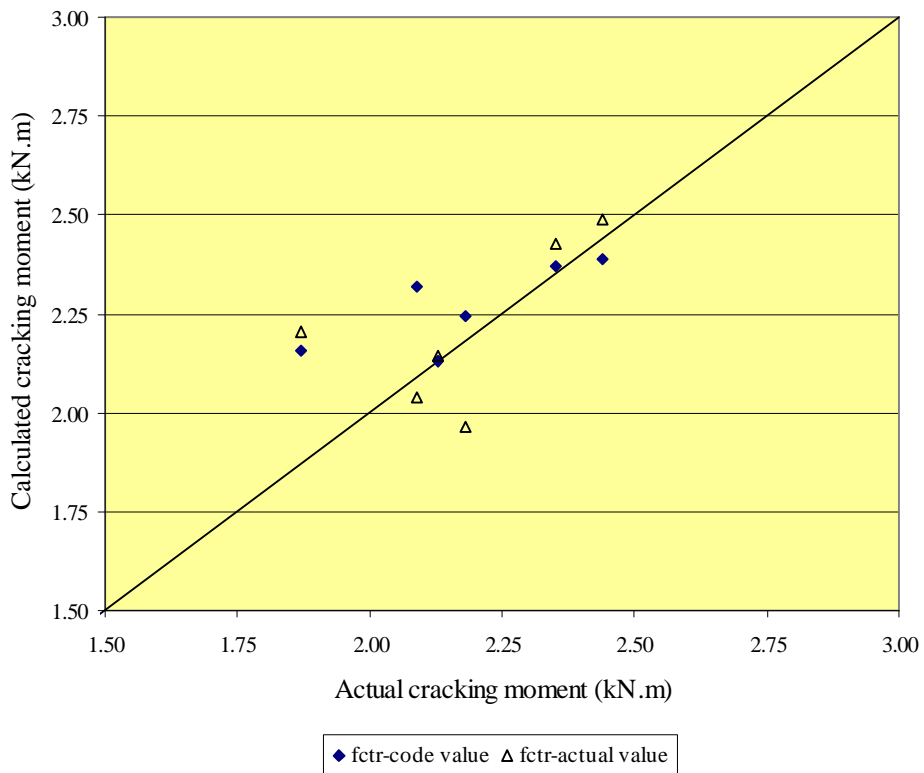


**Fig. 8: Relation between Actual and Calculate Cracking Moments.**
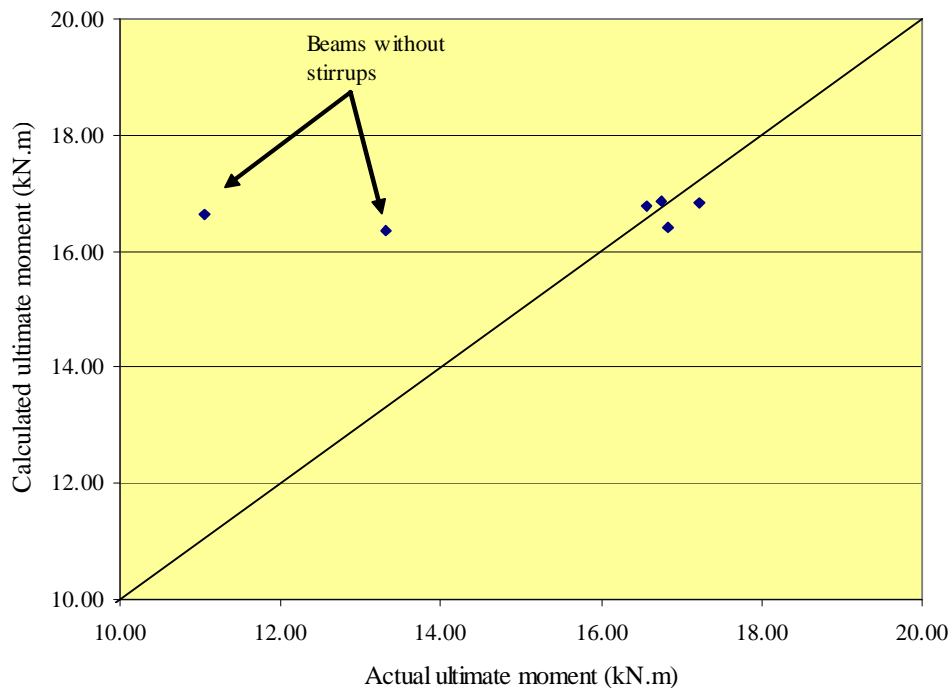
**Fig. 9: Relation between Actual and Calculate Ultimate Moments.**

## CONCLUSIONS

To study the effect of polypropylene fibres (PPF) on the flexural behaviour of reinforced concrete beams with or without stirrups, six full scale I-beams with the same dimensions and longitudinal steel but with different fibre parameters were loaded up to failure. Based on the test results the following conclusions were obtained:

1.  The inclusion of polypropylene fibres into reinforced concrete beams reduced the crack propagation and steel tensile stress, and significantly improved the ductility of the reinforced concrete beams. However, PPF had a negligible effect on the cracking moment and ultimate moment.
2.  There was a remarkable positive interaction between PPF and stirrups in improving the ductility of the beams. PPF increased the shear strength and changed the failure mode of one beam with stirrups from shear failure to flexural failure.
3.  The increase in fiber volume ratio did not necessarily mean further improvement in behaviour of FRC beams. Over a certain value (0.25 % by volume in this study) the increase of fibre volume ratio had a slight effect on the behaviour of FRC beams.
4.  While the inclusion of polypropylene fibres had a minor effect on the beam stiffness before cracking, the rate of stiffness decay of the PPFRC beam after cracking was lower than that of the beams without fibres.
5.  For the same fibre volume ratio, using fibre with coarse texture or rough surface improves the flexural behaviour of the beam than using fibre with fine texture or smooth surface.
6.  Due to the contribution of fibre in shear strength, there is a significant improvement in the flexural strength of beams failed in shear. However, this improvement was negligible in beam failed in flexure.
7.  Both the cracking and ultimate moments of FRC beams can be calculated using the same equations used for conventional reinforced concrete beams.

## REFERENCES

1. Soroushian P., Khan A. and Hsu J.W. (1992), "Mechanical properties of concrete materials reinforced with polypropylene or polyethylene fibres". ACI Materials Journal, 89, No. 6, pp. 535-540.
2. Alhozaimy M., Soroushian P. and Mirza F., (1996), " Mechanical properties of polypropylene fiber reinforced concrete and the effects of pozzolanic materials". Cement & Concrete Composites, 18, No. 2, pp. 85-92.
3. Bindiganavile V. and Banthia N., (2003), "Crack growth resistance of fiber-reinforced concrete under drop-weight impact loading". ACI Special Publication 190, pp. 203-220.
4. Peled A., Akkaya Y. and Shah S.P., (2000), "Effect of fiber length in extruded and cast cement composites". ACI Special Publication 190, pp. 1-16.
5. ACI Committee 544, (2005), "State of the art report on fiber reinforced concrete". American Concrete Institute, USA,
6. Tan K-H., Paramasivam P. and Tan K-C., (1995), "Cracking characteristics of reinforced steel fiber concrete beams under short- and long- term loadings". Advanced Cement Based Materials, No. 2, pp. 127-137.
7. Abdul-Ahad R.B. and Aziz O.O. (1999), "Flexural strength of reinforced concrete T-beams with steel fibers". Cement & Concrete Composites, 21, No. 4, pp. 263-268.
8. Chunxiang Q. and Patnaikuni I., (1999), "Properties of high-strength steel fiber-reinforced concrete beams in bending". Cement and Concrete Composites, 21, Issue 1, pp. 73-81.
9. Cucchiara G., Mendola L. and Papia M., (2004), "Effectiveness of stirrups and steel fibres as shear reinforcement". Cement and Concrete Composites, 26, Issue 7, pp. 777-786.
10. Laresen E.T. and Krenchel H., , (1991), "Fiber-reinforced cementitious materials". Materials Research Society Symposium Proceedings 211, pp. 119-124.
11. Malhotra V.M., Carette G.G. and Bilodeau A., (1994), "Mechanical properties and durability of polypropylene fibre reinforced high-volume fly ash concrete for shotcrete applications". ACI Materials Journal, 91, No. 5, pp. 478-486.
12. Hughes B.P. and Fattuhi N. I., (1977), "Prediction the flexural strength of steel and polypropylene fibre-reinforced cement-based beams". Composites, pp. 57-61.
13. Al-Tayyib A.J., Al-Zahrani M.M, Rasheeduzzafar and Al-Sulaimani G.J., (1988), "Effect of polypropylene fiber reinforcement on the properties of fresh and hardened concrete in the Arabian gulf environment". Cement and Concrete Research, 18, No. 4, pp. 561-570.
14. Allan M.L and. Kukacka  L.E., (1995), "Strength and durability of polypropylene fibre reinforced grouts". Cement and Concrete Research, 25, No. 3, pp. 511-521.
15. Badr A., Richardson I.G., Hassan K.E. and Brooks J.J.,(2001), "Performance of monofilament and fibrillated polypropylene fibre-reinforced concretes". Proceedings of the 2nd International Conference on Engineering Materials, San Jose, CA, USA1, pp. 735-744.
16. Bayasi Z. and McIntyre M., (2002), "Application of fibrillated polypropylene fibers for restraint of plastic shrinkage cracking in silica fume concrete". ACI Materials Journal, 99, Issue 4, pp. 337-344.
17. Feldman D. and Zheng Z., (1993), "Synthetic fibres for fibres concrete composites. materials". Research Society Symposium Proceeding, Pittsburgh, PA, USA, 305, pp. 123-128.
18. Swamy R.N., Al-Ta'an S.A. and Ali S.A.R., (1979), "Steel fibers for controlling cracking and deflection". Concrete International, 1, No.8, pp. 41-49.
19. Swamy R.N. and Al-Ta'an S.A., (1981), "Deformation and ultimate strength in flexure of reinforced concrete beams made with steel fiber concrete". Journal of the American Concrete Institute, 78, pp 395-405.

# Evaluation of the Strength of Structural Walls Poured Using COFFOR Structural Formwork under Lateral Loads

## O. E. El-Salam, S. M. Elzeiny, A. M. Mourad, and T. K. Mohamed
*Assistance Professor, Housing and Building National Research Center, Cairo, Egypt*
*Email: shmelzny@gmail.com*

## ABSTRACT

COFFOR is a new structural formwork system used for construction of reinforced concrete walls.  The structural behavior of walls cast using this system under the effect of lateral loads was studied.  The contribution of the stay in place COFFOR formwork in the lateral ultimate strength of the walls is investigated.  An experimental program included four half scale reinforced concrete walls cast using COFFOR formwork was executed.  A theoretical study based on the ultimate strength design theory was preformed to evaluate the wall strength.  The results showed that the COFFOR formwork improved the shear strength of the walls, however, the ultimate flexural capacity was governed by dowels between the wall and its foundation.

**Keywords:** Walls, Lateral Loads, COFFOR, Shear Capacity

## INTRODUCTION

COFFOR is a light weight patented structural stay in place formwork system used for construction of reinforced concrete structures. The COFFOR system unit is an integrated formwork consists of two parallel faces connected to each other with a zigzag steel bar.  Each face is composed of a steel screen mesh stiffened with cold formed steel channels.  The panels are manufactured and assembled at the factory.  COFFOR system can be used in construction of reinforced concrete slabs and walls with different shapes.  Some researches were executed to evaluate the use of the COFFOR system as a structural formwork[1,2].  In these researches the contribution of the COFFOR in the ultimate strength of the reinforced concrete structural walls was investigated.  The COFFOR formwork is very effective in construction of bearing walls structures with medium height.

## EXPERIMENTAL WORK

### Test Program
The test program included four walls specimens 3B, 3C, 3D and 3E.  The wall 3B was cast using COFFOR formwork without reinforcement while the wall 3C was cast in a wooden formwork and reinforced with steel bars considered as an equivalent to the sections of COFFOR elements.  The walls 3D and 3E were reinforced and cast in a wooden formwork and COFFOR, respectively.    Table 1 shows the details of the test program.

**Table 1: Experimental Program for the Tested Slabs.**

| Specimen | dim.(mm) | RFT | | Notes |
|---|---|---|---|---|
| | | Vert. | Horz. | |
| 3B | 1220x1270x200 | Dowels $\phi$ 6/230 | --- | Without RFT.+ Coffor |
| 3C | 1220x1270x200 | 4 $\phi$ 6 /face + Dowels $\phi$ 6/230 | 4 $\phi$ 6 /face | RFT. equivalent to the channels in Coffor + wooden formwork |
| 3D | 1220x1270x200 | 11 $\Phi$ 10/face | 14 $\phi$ 8 /face | RFT. + wooden Formwork |
| 3E | 1220x1270x200 | 11 $\Phi$ 10/face | 14 $\phi$ 8 /face | RFT. + Coffor |

\* F   High grade steel

**Details of the Tested Walls**

The dimensions of the tested walls were 1220 mm length, 1270 mm height and the thickness was 200 mm.  Each wall has a rigid reinforced concrete base of 2500 mm length and cross section of 400 x 500 mm. The base was reinforced with 4 deformed bars of 18 mm diameter at the both sides. The stirrups were deformed bars of 12 mm diameter each 100 mm. The details of the walls are as follows:

Wall 3B (poured in COFFOR formwork without reinforcement): Additional horizontal U smooth bars of 6 mm diameter each 200 mm were placed at both sides of the wall and dowels of smooth bars of 6 mm diameter each face at diastase equals to 230 mm were impeded in the base as shown in Figure 1.

Wall 3C (poured in waterproof wooden formwork): The reinforcement used was 6 mm diameter of smooth bars each face at diastase equals to 230 mm in vertical direction and 6 mm diameter of smooth bars each face at diastase equals to 400 mm in horizontal direction. Additional horizontal U smooth bars of 6 mm diameter each 400 mm were placed at both sides of the wall and dowels of 6 mm diameter of smooth bars each face at diastase equals to 230 mm were impeded in the base as shown in Figure 2.

Wall 3D (poured with waterproof wooden formwork): The wall was reinforced vertically with deformed bars of 10 mm diameter each face at diastase equals to 115 mm and horizontally with smooth bars of 8 mm diameter each face at diastase equals to 100 mm. Additional horizontal U smooth bars of 8 mm diameter each 100 mm were placed at both sides as shown in Figure 3. The vertical reinforced were extended in the base with sufficient impeded length.

Wall 3E (poured in COFFOR formwork): The wall had the same reinforcement as wall 3D as shown in Figure 4. The mechanical properties of reinforcement used are shown in Table 2.  The compressive strength of concrete was 17.8 MPa.

**Details of COFFOR Formwork**

The COFFOR formwork consists of two parallel faces connected to each other with a zigzag of smooth bars of 6 mm diameter.  Each face was composed of a steel screen mesh stiffened with cold formed steel channels as shown before in Figures 1 to 4.  The channels are arranged at 230 mm spacing and the zigzag bar is spaced 300 mm.
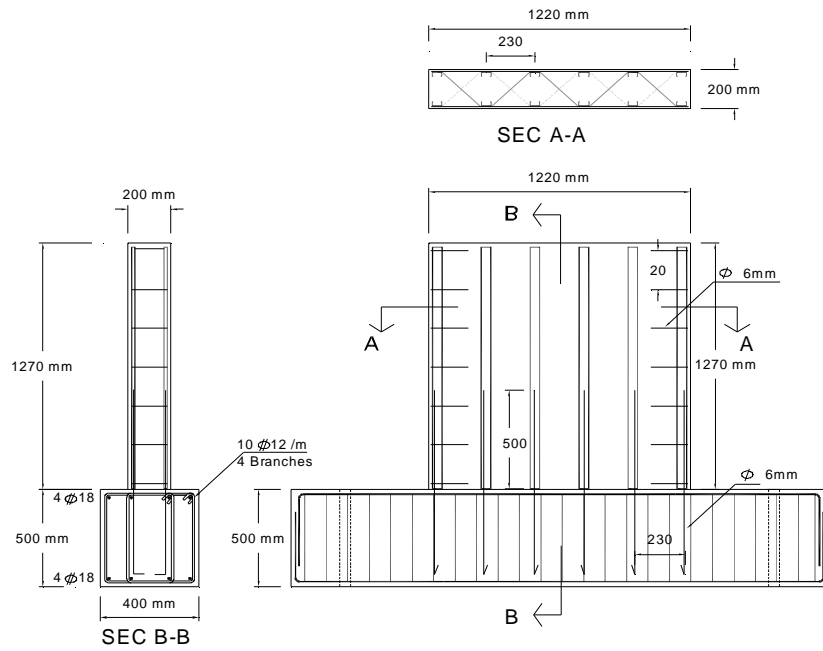
**Fig. 1: Reinforcement and Details of Specimen 3B.**
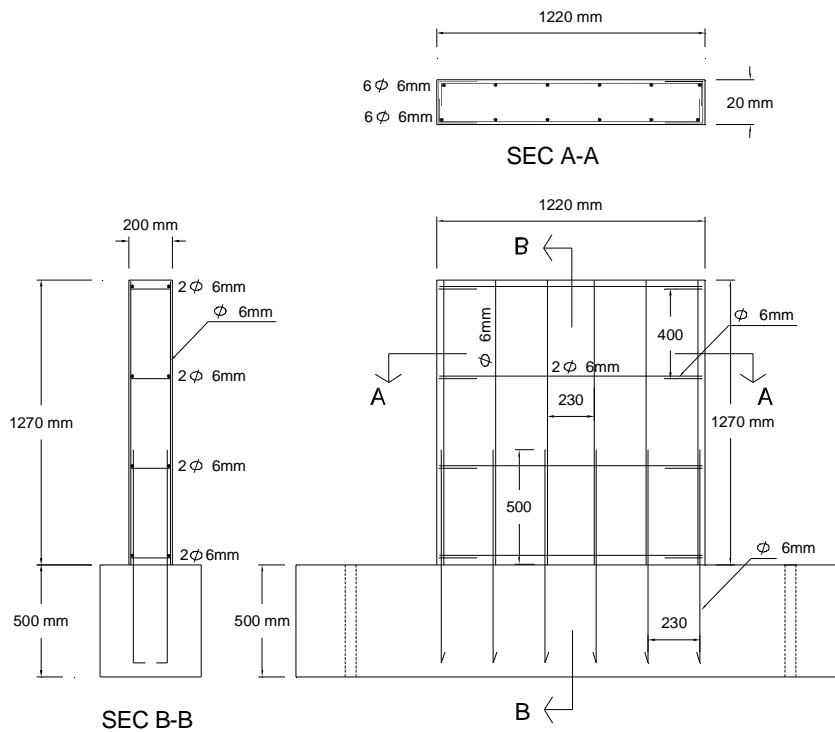


**Fig. 2: Reinforcement and Details of Specimen 3C.**
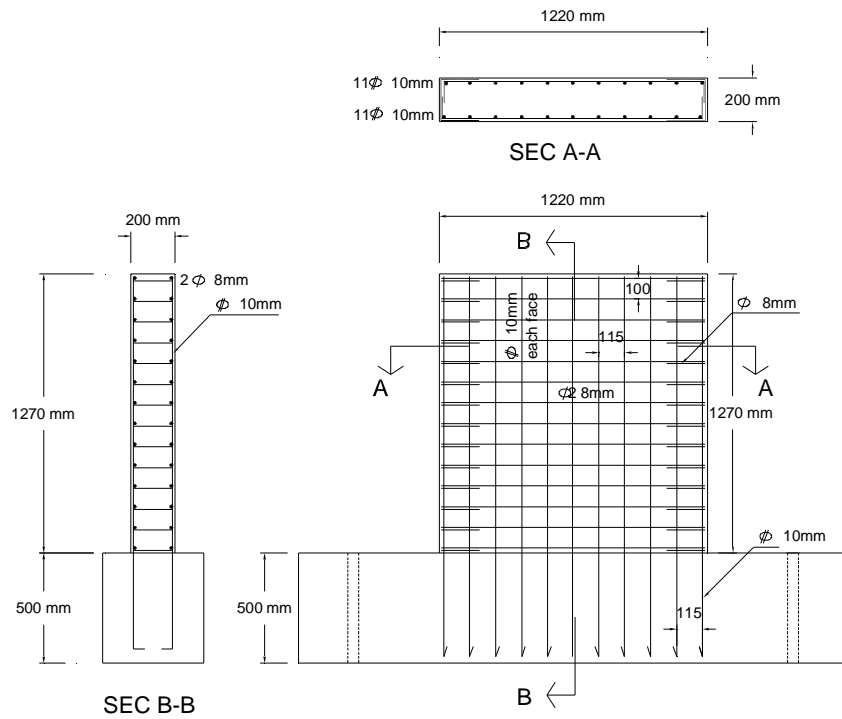
**Fig.  3: Reinforcement and Details of Specimen 3D.**
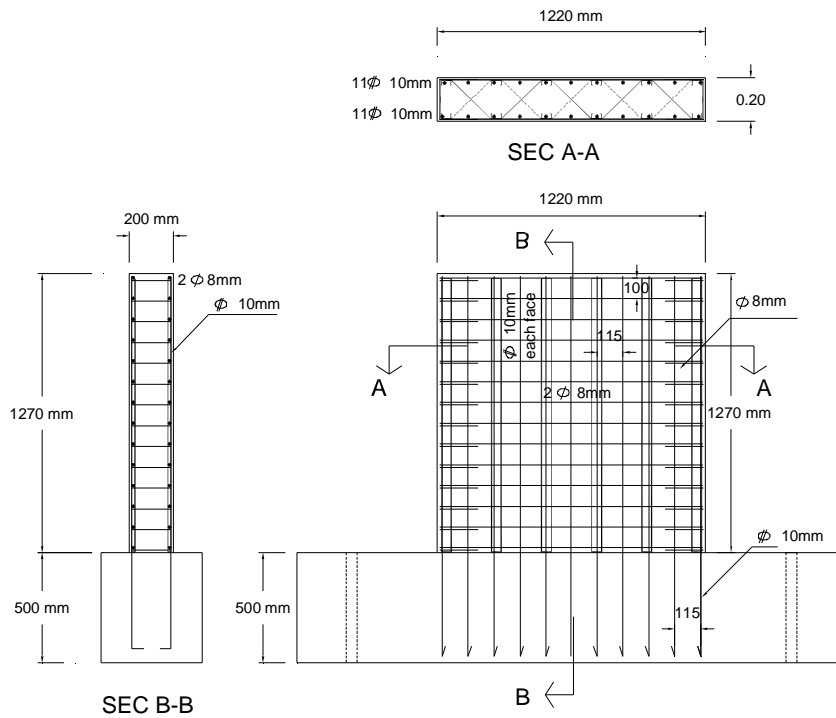


**Fig.  4: Reinforcement and Details of Specimen 3E.**

**Table 2: Mechanical Properties of Reinforcement and COFFOR.**

| Diameter (mm) | $F_y$ (N/mm$^2$) | $F_u$ (N/mm$^2$) | Elongation % |
|---|---|---|---|
| 6 | 258 | 370 | 28.33 |
| 8 | 324 | 471 | 20 |
| 10 | 402 | 607 | 25 |
| 12 | 570 | 778 | 12.5 |
| Load for each Coffor channel | ---- | 20 (KN) | 1 |

**Test Setup Procedure and Measurements**

The test setup was prepared to apply lateral displacement at the top of the walls as shown in Figure 5.  The reinforced concrete base was fixed to the lab rigid floor using two 50 mm anchor bolts spaced by 2000 mm.  The sliding of the base was prevented using anchor shear studs between the base and the lab rigid floor.  The horizontal displacement was applied by a horizontal actuator provided with electronic load cell, and a linear variable transducer. The actuator was hinged to the rigid horizontal reaction girder of the laboratory main double portal 2000 KN test rig. The connection between the actuator and the specimen was designed to allow rotation.  The horizontal displacement at the top of the test specimen was measured by $\pm100$ mm stroke linear variable displacement transducer (LVDT). The total deformations along the wall diagonals were measured using two $\pm50$ mm stroke LVDT's. The horizontal load was measured using $\pm680$ KN electronic tension-compression load cell.  The load and the displacement measuring devices were connected and controlled by Lab View computer software program. The test was executed by on-line measurement and control computerized system. The steel strains and COFFOR channels strains were recorded using electric strain gages (S.G.).
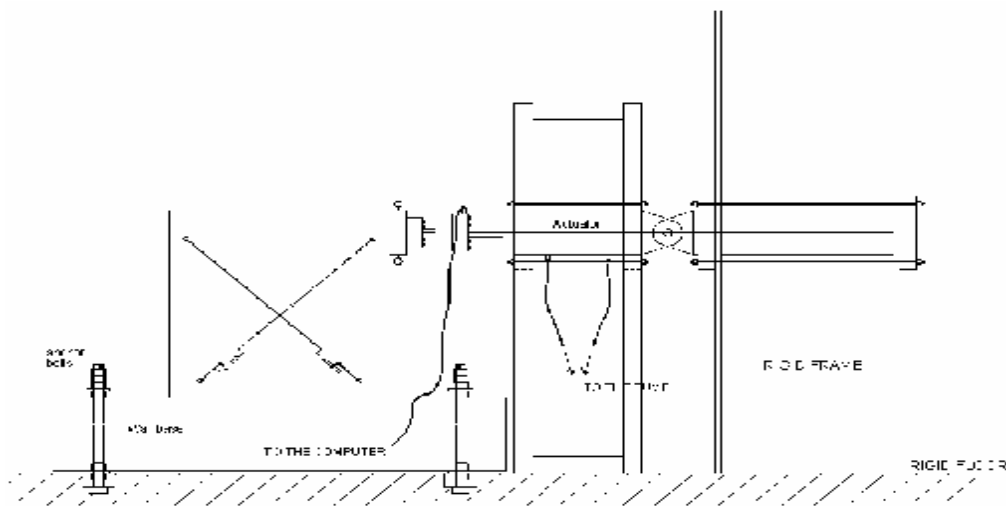


**Fig.  5: Details of Test Setup.**

## RESULTS AND DISCUSSION

**Crack Pattern and Mode of Failure**

The walls 3B and 3C failed in ductile flexural mode of failure due to yielding of dowels. Separation between the wall and the base was observed at the tension side and extended at failure up to about  90 % of the wall length as shown in Figure 6.  The wall 3E failed in the same ductile flexural mode of failure.  In wall 3D, flexural crack appeared at the tension side and separation between wall and its base occurred, then diagonal tension crack occurred suddenly

and governed the failure as shown in Figure 7. The ultimate load dropped progressively after the formation of the diagonal crack.



**Specimen 3B**



**Specimen 3C**

**Fig.  6: Mode of Failure for Walls 3D and 3C**

**Load Displacement Relationship**

The load-displacement relationships of the tested walls are shown in Figure 8 and 9.  For specimen 3B, 3C the ultimate loads were 65, 69.5 KN at a displacement of 24 and 25 mm respectively, and the ultimate load was almost constant up to failure. For specimen 3D the ultimate load was 395 KN at displacement of 20.8 mm then the load dropped progressively due to shear failure. For specimen 3E the Ultimate load was 400 KN at a displacement of 40 mm, and the load was almost constant up to failure.

**Specimen 3D**



**Specimen 3E**

**Fig. 7: Mode of Failure for Specimens 3D and 3E.**
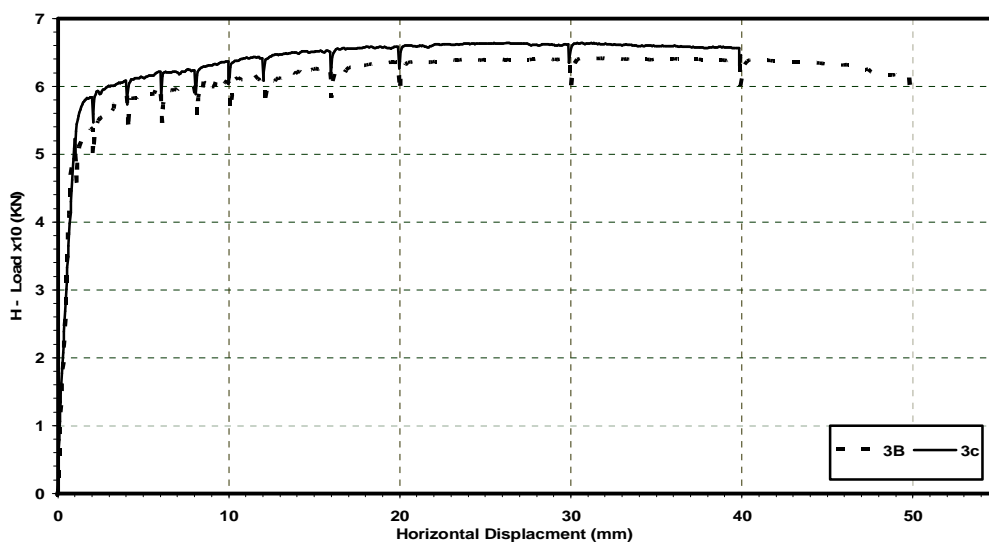


**Fig. 8: Load Displacement Curve for the Walls 3B, 3C.**
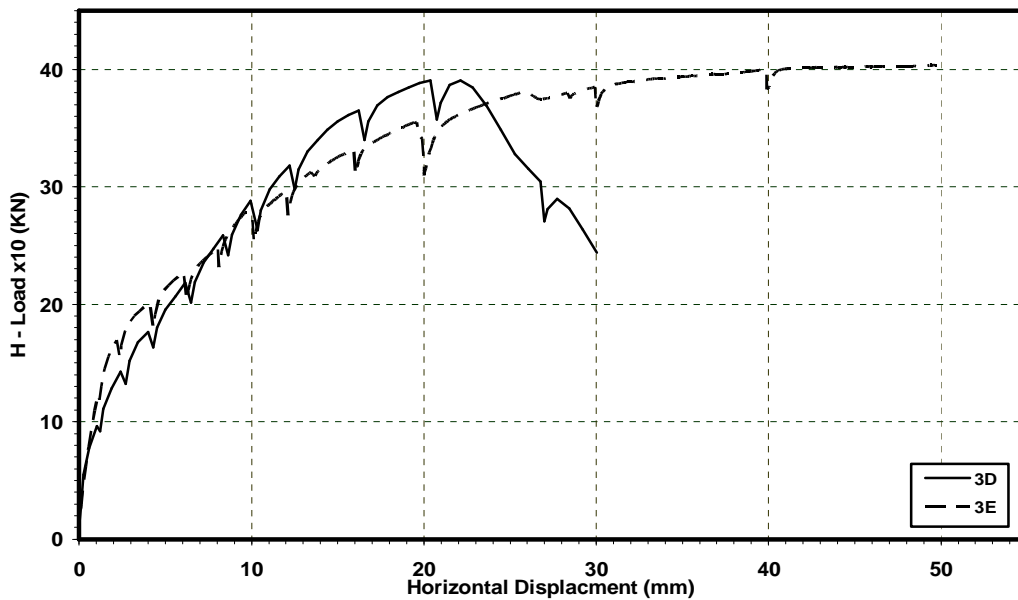
**Fig. 9: Load Displacement Curve for the Walls 3D and 3E.**

**Ultimate Strength**

The ultimate strength and the corresponding displacements for the tested walls are given in Table 3. The ultimate strengths of the walls 3B and 3C were close to each other and the strength was governed by the area of the steel dowels. The ultimate shear strength of the wall 3D was close to the ultimate flexural strength of the wall 3E. However, the shear failure occurred in wall 3D at small value of lateral displacement.

**Table 3: Ultimate Load , Corresponding Displacement and Ductility Factor.**

| Specimen | Ultimate Load (KN) | Horizontal Disp. (mm) | Ductility |
|---|---|---|---|
| 3B | 65 | 24 | 62.5 |
| 3C | 69.5 | 25 | 42.1 |
| 3D | 390 | 20.5 | 14.61 |
| 3E | 400 | 40 | >>15.38 |

**Stiffness**

The lateral stiffness of the walls poured using COFFOR formwork was the same as the walls poured using wooden formwork. The stay in place COFFOR steel formwork did not improve the lateral wall stiffness. The wall lateral stiffness was governed by the steel dowels or vertical reinforcement impeded in the base and extended in the wall.

**Ductility**

The ductility factor was defined as the ratio between the displacement at failure $\Delta_F$ and the displacement at yield $\Delta_Y$ as follows:

$$D = \frac{\Delta_F}{\Delta_Y}$$

( 1 )

where

$\Delta_F$ the displacement corresponding to a reduction of 80 % of the ultimate load.

$\Delta_Y$ the displacement at yield.

Table 3 shows the ductility factors of the tested walls. Walls 3B, 3C and 3E showed ductile behavior and produced high ductility factors. The wall 3D which failed in brittle shear mode produced low ductility factor.

## THEORETICAL ANALYSIS

The ultimate shear and flexural strengths of the tested walls were calculated theoretically based on the strut and tie model[3] and the ultimate strength theory[4,5,6] ,respectively. The following assumptions were considered.

- Full bond between COFFOR channels and concrete up to failure was assumed (as observed in experimental tests).
- The ultimate strength of the COFFOR channels was taken according to the material tests (refer to Table 2).
- The principals of the strut and tie model and the ultimate theory for design of reinforced concrete were applied.
- All materials safety factors were considered equal to one.
- The contribution of the steel screen mesh and the lateral zigzag bars of the COFFOR formwork were not included.
- The ultimate shear strength was calculated based on the actual compression strut formed in experimental tests as shown in Figure (10).
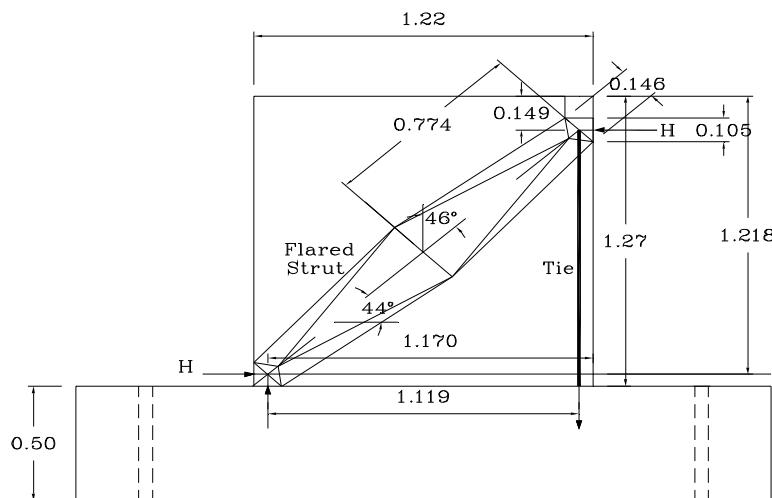


**Fig. 10:  Actual Shape of Compression Strut of Walls Based On Theoretical Approach.**

**Flexural Strength**

The ultimate flexural strengths of the test walls were calculated theoretically based on the ultimate theory taking into account all the material properties. Figure (11) shows the stress distribution of the bottom cross section of the wall at initial loading and at failure.
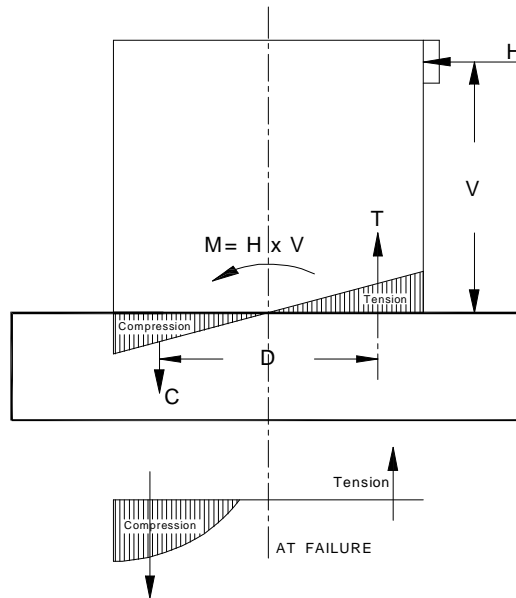
**Fig. 11:  Stress distribution of the Wall Cross Section.**

### Strut and Tie Model

The strut and tie model is a method describe the mechanism of paths of transfer loads. Generally the strut and tie model consist of two parts, ties which transfer shear with diagonal tension and strut which transfer shear with diagonal compression.  Many researchers suggested different shapes for the struts that joining the loading points and supports.   In the next paragraph, proposed strut by Khaled[8] et. al, (1998) was considered in the current research.

### Proposed Flared Stress Field

Khaled[7,8], (1998), modified the flared stress field suggested by Schlaich and Anagnostou, (1990). He improved the bearing stresses to exceed $f_c'$ at the nodal zones by adopting William-Warnke failure surface as mentioned by Chen and Han, (1988). Also he analyzed the stresses in the suggested flared stress field taking into account the lateral confining effect of the reinforcement that intersect the field.

### Failure Criterion

The failure criterion used in The modified flared stress field suggested by Khaled, (1998), is different than the simplified one proposed by Schlaich and Anagnostou, (1990). In this model the William-Warnke failure surface is adopted. This failure surface is given by;

$$s_1 = a_o + a_1 r_t + a_2 r_t^2 \tag{2}$$

$$s_2 = b_o + b_1 r_c + b_2 r_c^2 \tag{3}$$

$$s_m = \frac{s_1 + s_2 + s_3}{3} \tag{4}$$

Where, $s_m$ is the mean stress, $s_1$, $s_2$, $s_3$ are the principal stresses at a point, $r_c$ and $r_t$ are the stress components perpendicular to the hydrostatic axis at angles $\theta = 0$ and $\theta = 60^\circ$,  and $a_0, a_1, a_2, b_0, b_1, b_2$ are material constants. Experimental tests on concrete specimens have indicated that these constants are as follows: $a_0 = b_0 = 0.1025$, $a_1 = -0.8403$, $a_2 = -0.0910$, $b_1 = -0.4507$, and $b_2 = -0.1018$. For plane stress problems, the principal stress $s_3$ is set equal to zero and the 3-D failure surface reduces to the 2-D failure criteria shown in Figure (12), in which the concrete

compressive strength can be as high as $1.24 f'_c$ at a lateral confining pressure of about $0.6 f'_c$, for more details refer to Chen and Han, (1988).

**The Modified Flared Stress Field**

For the stress filed shown on Figure (13-a), the flare angle $f$ is equal to,

$$f = \tan^{-1}\left(\frac{b-a}{2L}\right)$$

(5)

The size of the inclined uni-axial stress field IKL or JKM is equal to L1 and is given by;

$$L_1 = \frac{a}{2}\cos(f) + gL\sin(f)$$

(6)

From the force polygon shown in Figure (13-b), the force in the IKL or JKM stress fields is given by;

$$F_1 = \frac{a\,w\,s_a}{2\cos(f)}$$

Where '$w$' is the stress field thickness, resulting in a uni-axial stress $f_c$ equal to;

$$f_c = \frac{F_1}{w\,L_1} = \frac{a\,s_a}{2\cos(f)\left(\frac{a}{2}\cos(f) + gL\sin(f)\right)}$$

(7)

The horizontal compression and/or tension force acting on stress fields IJK or LKM is also given by;

$$F_2 = \frac{a\,w\,s_a\,\tan(f)}{2}$$

Resulting in tensile stresses in LKM region equal to;

$$f_t = \frac{F_2}{w(1-g)L} = \frac{a\,s_a\,\tan(j)}{2(1-g)L}$$

(8)

Assuming that the ratio between concrete tensile strength $f_t$ to the concrete compressive strength $f_c$ equal to $R$, and for the case where the uni-axial compressive stress $f_c$ reaches $f'_c$ and the maximum tensile stress $f_t$ reaches $f_t$, the ratio $R$ will be equal to;

$$R = \frac{\frac{a}{2}\sin(f)\cos(f) + gL\sin(j)^2}{(1-g)L}$$

(9)

Resulting in;

$$g = \frac{RL - \frac{a}{2}\sin(f)\cos(f)}{RL + L\sin(f)^2}$$

(10)

It can be seen that for given filed dimensions $a, b, w, L$, and a ratio

$R$ between concrete tensile to compressive strengths, the flared stress field can fully be determined once the value of $g$ is known. The length $L_1$ in Figure (13-a) is obtained and the force $F_1$ is calculated using equation (6). The force polygon shown in Figure (13-b) can then be constructed and the bearing stresses at the field narrow end $s_b$ can be determined. The value of $s_b$ should then be checked using the chosen concrete failure criterion Figure (12).

On the other hand, if the angle $f$ is set as a variable, an optimization technique can be used to find its optimum value that maximizes the bearing pressure $s_a$ at the field narrow end. This can be simply done by drawing two curves as shown in Figure (14), with the horizontal axis representing the angle $f$ and the vertical axis representing the bearing stress $s_a$. The first curve represents the bearing stress $s_a$ obtained using equilibrium equations (5) to (10), and the second curve represents the maximum bearing stress corresponding to a lateral confining stress $f_c$ in region IJK, which is equal to

$\dfrac{F_2}{wgL}$ and using the concrete failure criteria shown in Figure (12).

## Effect of Web Reinforcement

if the stress field is crossed by a uniformly distributed reinforcing steel mesh with areas $A_{sh}$ and $A_{Sv}$ at spacing $s_h$ and $s_v$ respectively, and if the nearly horizontal steel reinforcement $A_{sh}$ makes an angle $a$ with the horizontal axis of the field Figure (15), and assuming a rigid-plastic stress-strain curve of steel, the tensile strength of a unity element of such a steel mesh suggested by Siao, (1993-1995) as shown in Figure (16) will be equal ;

$$f_{t,h} = \frac{A_{sh} f_y}{w\, s_h} \cos(a)^2 + \frac{A_{sv} f_y}{w\, s_v} \sin(a)^2 \qquad (11)$$

Where;

$f_{t,h}$    = steel tensile strength in the horizontal direction of the stress field

$A_{sh}$    = horizontal steel area

$A_{sv}$    = vertical steel area

If the tensile stresses in region LKM in the flared stress field shown in Figure (13-a) exceeds the splitting tensile strength of concrete, ft,sp, cracks will appear in this region, and tension must be carried by the existing steel reinforcement, that is ft,h (equation 11).
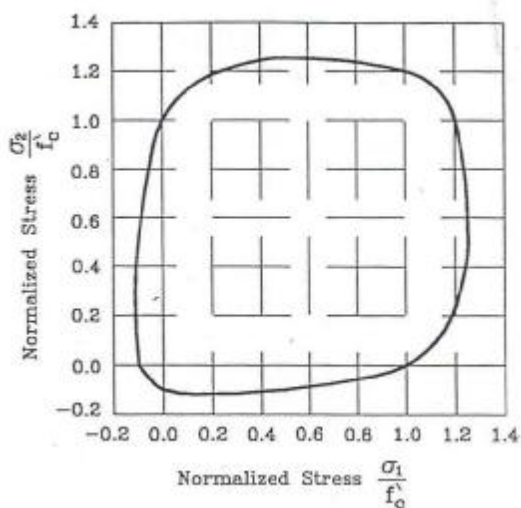
**Fig.  12:  William Wranke 2-Dimesnsional Failure Criteria for Concrete.**
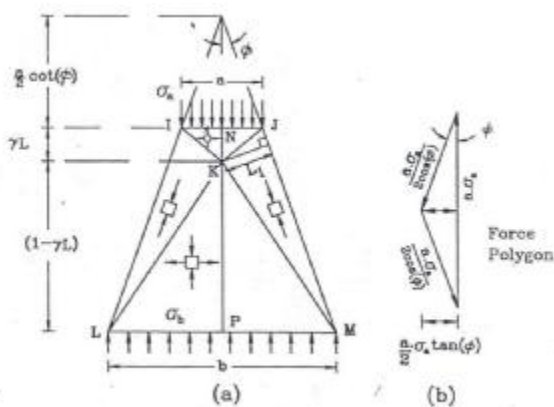


**Fig.  13:  Analysis of Flared Stress Field by Khaled (1998).**
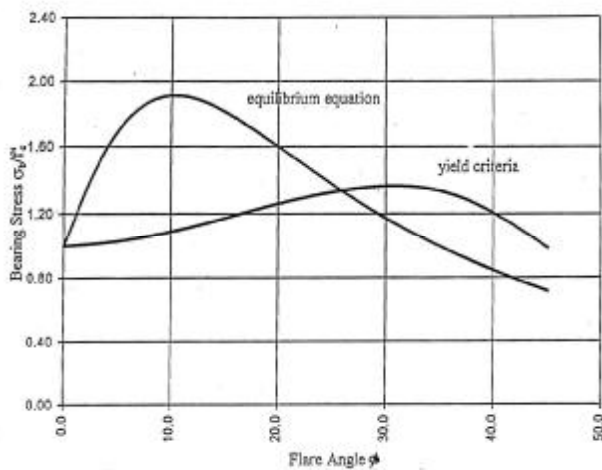


**Fig.  14:  Optimization of Flare Angle $f$ .**
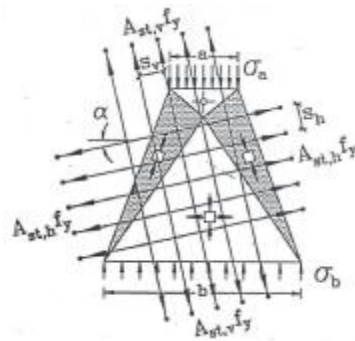
**Fig. 15:  Reinforced Flared Stress Filed by Khaled (1998).**
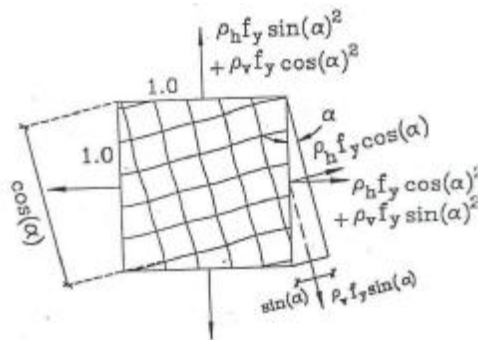


**Fig. 16:  Cracked Prism Tensile Strength by Siao (1993).**

## Discussion

The theoretical analysis of the ultimate strength of walls cast by COFFOR formwork based on the ultimate theory and strut and tie method was conservative.  Also, the increase of the experimental ultimate strength of walls cast by COFFOR compared with theoretical strength refers to the contribution of external fabric mesh. Table 4 shows that for specimen 3B and 3C the theoretical horizontal force $H_{th}$ calculated based on the strut and tie model is bigger than calculated from ultimate flexural capacity, this due to using small cross section area of splice bars and big spacing between each other. For specimen 3D and 3E, the flexural capacity of the wall was increased due to increase the number and cross section area of splice bars.  Also increasing the number of vertical and horizontal bars with increasing the cross section area led to increasing the strut capacity. From the above theoretical analysis it can concluded that specimens 3B, 3C and 3E were fail in flexure and specimen 3D was fail in shear due to forming compression strut.

**Table 4: Comparison between Experimental and Theoretical Analysis.**

| Specimen | $H_{Th , shear failure}$ (KN) | $H_{Th , Flexure failure}$ (KN) | $H_{Exp}$ (KN) | Notes |
|---|---|---|---|---|
| 3B | 324 | | 65 | Coffor only |
| 3C | 322 | 47 | 69.5 | Rft. equivalent to  the channels in Coffor + wooden formwork |
| 3D | 352 | 355 | 390 | RFT + wooden Formwork |
| 3E | 359 | | 400 | Coffor +  RFT |

## CONCLUSION

The goal of this work was to study the use of COFFOR formwork in construction of reinforced concrete walls and based on the experimental test results the following conclusions can be drawn.

- The channel element of the COFFOR formwork can be considered as a vertical reinforcement.
- The wall poured using stay in place COFFOR formwork without reinforcement produced a lateral strength at least equal to the equivalent wall poured using wooden formwork.
- The splice between the 10 mm steel dowels and the steel channels of COFFOR was successful to transmit forces from the dowel to the COFFOR channel if spacing between vertical bars is not less than 120 mm.
- The COFFOR formwork improved the shear strength of the tested walls and prevented the shear failure to occur prior to the flexural failure.
- The theoretical calculation of the ultimate strength of walls cast by COFFOR formwork based on the ultimate theory and strut and tie method was conservative.
- The increase of the experimental ultimate strength of walls cast by COFFOR compared with theoretical strength refers to the contribution of external fabric mesh.

## REFERENCES

1. Technical Approval 16/03-455, Secretariat of the Technical Approval Commission CSTB, Sep. 2003.
2. Architectural Structure Institute of China Academy of Building Research CABR Technology, June, 2003.
3. Examples of The Design of Structural Concrete With Strut and Tie Model, Sp-208, ACI, Nov., 20025
4. ACI 318-2002, Building Code Requirement for Structural Concrete and Commentary, American Concrete Institute, Farmington Hills.
5. ECCS 203-2004, Egyptian Code of Practice for Design and Construction of Reinforced Concrete Structures, Second Edition, 2004.
6. ASCE – ACI 445 (1998), Recent Approaches To Shear Design of Structural Concrete, State of The Art Report by ASCE – ACI, Committee 445, On Shear and Torsion. ASCE, Journal of Structural. Engineering, 124 – 1998, No. 12, PP 1375 - 1417.
7. Mourad, Ahmed. "Behavior of Bottom Loaded Simply Supported Deep Beams" Ph.D. Thesis, Cairo University, 1999.
8. Khaled, S.A.M.H., "A Plasticity Model for 2-Dimensional Reinforced Concrete Compressive Struts", M.Sc. Thesis, Cairo University, 1998.

# IN-PLANE ELASTIC STABILITY OF STEEL ARCHES: APPLICATION TO SOME BRIDGE CASES

**A. H. Salem**

*Ain Shams University, Faculty of Engineering, Abbassia, Cairo, Egypt*

**H. M. Abbas, S.A.Hassanein, S. A. El-Sawaf**

*Al Azhar University, Faculty of Engineering, Nasr City, Cairo, Egypt*

## ABSTRACT

In the present study, the in-plane elastic buckling capacity of three common steel arch bridge cases is studied. The first case is an arch bridge with one, two or three vertical posts. The second case is a bowstring configuration with one, two or three vertical hangers. The third case deals with an open spandrel deck arch bridge with one, two or three posts. Circular, parabolic and inverted catenary arch shapes with prismatic sections are analyzed. The in-plane maximum elastic load carrying capacity is determined for each one of the above cases by using the finite element computer package COSMOS/M[®]. The loading system considered in this study consists of symmetrical uniform distributed loads. For all cases however, the base edge conditions of the structures are assumed hinged except in the case of tied arch or bowstring design in which one base is hinged and the other roller.

## INTRODUCTION

The focus of the present study is the investigation of the in-plane elastic carrying capacities of various steel arched bridges with the variation of the cross sectional areas of their posts or hangers.

It should be mentioned however, that in real bridge designs usually numerous posts or hangers are foreseen. The present study considers up to three posts or hangers only for simplicity's sake. For all these cases of study, the modulus of elasticity $E$ of steel was taken 2100 t/cm$^2$.

## METHOD OF ANALYSIS

An extensive parametric study is conducted for three different geometric arch shapes: circular, parabolic and inverted catenary aimed at the study of their buckling behaviour. A fixed practical value of rise-to-span ratio $h/L$ has been taken 0.2, for the sake of simplicity. The following data and design information were incorporated in a finite element scheme using the computer known package COSMOS/M[®].

The three studied cases of steel arch bridges are:

i. An arch with one, two or three vertical posts with hinged bases as shown in Fig. (1).
ii. A bowstring design whose rib is proportioned so that its moment of inertia $I_{rib}$ is equal to that of the tie $I_{tie}$. The arch rib has been also provided with one, two and three hangers. The base condition consists of one hinged and the other roller as shown in Fig. (2).

iii.  The third case is an open spandrel deck arch bridge with one, two or three posts provided with hinged bases as shown in Fig. (3). The traffic chord lies above the arch and rests on a hinge at one end and a roller at the other. The chord may rest on one, two or three posts.

Three cases of loading shown in figures (1)&(2) were studied to assess the effect of the type of loading on the buckling behaviour of the arch systems.

a.  Circular arch subjected to radial uniformly distributed load of intensity q, known as uniform normal or hydrostatic pressure.
b.  Parabolic arch shape subjected to vertical uniformly distributed load intensity q, on its horizontal projection.
c.  Inverted catenary arch subjected to vertical uniformly distributed load intensity q, along the arch axis to represent the dead weight.

To evaluate the effect of the number of posts or hangers, on the behaviour of the arch systems, the three following arrangements, described below and shown in Figures. (1),(2) and (3), were considered:

§  A single vertical post or hanger located at the crown of the arch.
§  Two vertical posts or hangers, the first one is located at the third point of the arch span while the second at the two third point of the arch.
§  A group of three vertical posts or hangers, the first one being located at the quarter point of the arch span, and the second is immediately located under the crown of the arch while the third lies at the three-quarter point of the arch span.


## REPRESENTATION AND INTERPRETATION OF RESULTS

To cover a wide range of design situations, the parametric study has been conducted to incorporate the three bridge configurations described above, each one will be subjected to an associated load pattern. The in-plane elastic buckling capacity will be investigated with the variation of the cross sectional areas of the hangers in both the simple arch and the bowstring designs or the posts in the open spandrel arch deck shapes. It should be noticed that in the three arch bridge configurations a constant rise-to-span ratio h/L of 0.2 has been taken. This value represents a practical amount adopted in designing such arches that are considered neither deep nor flat. The chosen arches are all provided with hinged bases at their two ends except for the bowstring case where one of the two hinges has been released in the horizontal direction hence substituted by a roller to denote an externally statically determinate simple bridge structure. All posts and hangers are pin-ended at their both extremities to carry only centric normal loads.

The set of curves shown in figures (4) to (12), represent the variation of the in-plane maximum capacity of arches $r_{cr}$ corresponding to different values of $A_P/A_R$ or $A_H/A_R$ taken to vary from 0 to 0.5, where $A_P$, $A_H$ are the cross sectional areas of one post or one tie respectively and $A_R$ is the cross section area of the arch rib.

The ratio $r_{cr}$ that is equal to $\sum \mathbf{Q_{cr}}/(p^2 EI/l^2)$, denotes the elastic critical sum of loading divided by the Euler's load of a simply supported prismatic column with length ($l$) equal to half span of the arch. The critical load $Q_{cr} = 2ql$ or $qL$ or $2qS$, where $2l = L$ which is the projected length of the arch in the horizontal direction and S is half the arch length. The ratio $r_{cr}$ is chosen as a design parameter representative of the loading pattern.

The following three arch bridge configurations are studied:

**A. In-Plane buckling of steel arch bridges with one, two or three posts with the variation of the cross sectional area of the posts**

Fig.(4) gives the results for the case of steel circular arch with one, two or three vertical posts subjected to a radial uniform distributed load. One should note from this figure that a single post does not affect at all the buckling capacity of the structure. For all post cross sectional areas, in this case, the value of $r_{cr}$ remains unchanged as it amounts to 1.38, while for 2 and 3 posts a significant increase of $r_{cr}$ is observed with the increase of the ratio $A_P/A_R$. It is expected that by increasing again the number of posts a further increase in the buckling capacity is very likely to be achieved.

In Fig. (5), the results show another type of arch having a parabolic shape subjected to a uniformly distributed vertical load on horizontal projection. For one post, $r_{cr}$ as before is stabilized at  1.36 that for all values of $A_P/A_R$.

Finally in Fig. (6), $r_{cr}$ is plotted against $A_P/A_R$ for inverted catenary arch case subjected to vertical load uniformly distributed along the arch axis for different number of posts. For one post, $r_{cr}$ is almost a constant value that does not exceed 1.39. For more than one post, $r_{cr}$ is increasing with the increase of the ratio $A_P/A_R$.

From these three figures the value of $r_{cr}$ varied very slightly from 1.36 to 1.39 (2.7%) for the three single post arch geometries and their associated loads.

**B. Variation of the in-plane buckling of steel tied arch bridge having one, two and three hangers with the variation of the cross sectional area of these hangers.**

The figures shown in (7) to (9) represent the bridge cases commonly known as bowstring or tied arch, but with different arch geometry. Fig. (7) gives the results of $r_{cr}$ for the cases of steel circular arched bridges with ties subjected to normal uniformly distributed load along the arch axis for cases of one, two and three hangers. In the case of one central hanger, $r_{cr}$ is almost stabilized at a value of 1.97 for all values of $A_H/A_R$, while it increased further with the addition of one or two more hangers. In Fig. (8), the results of $r_{cr}$ are also shown for a parabolic shape arch subjected to vertical uniformly distributed load on horizontal projection. Finally in Fig. (9), $r_{cr}$ is plotted against $A_H/A_R$ for inverted catenary arch bridge subjected to vertical load uniformly distributed along the arch axis for different number of hangers. The figures showed the same tendency as above, in other words, the value of $r_{cr}$ remains constant for one hanger then increases by the addition of the second one and a further increase is observed with the introduction of a third hanger.

Also, from the above three figures, $r_{cr}$ varied from 1.93 to 2.01 (4.14%) for the three bowstring bridges provided with one hanger.

**C. In-Plane buckling of steel open spandrel deck arch bridges with posts having one, two and three posts with the variation of the cross sectional area of the posts**

Fig. (10) gives the results for the case of steel circular deck arch bridge whose deck is located above the crown of the arch by a vertical distance equals to *h/6*. The arch is subjected to vertical uniformly distributed load on horizontal projection. The results for steel parabolic arch under the same case of loading are shown in Fig. (11), while Fig. (12), shows the results for steel catenary deck arched bridge for the case of one, two and three posts. One should notice that for one post the value of $r_{cr}$ drops suddenly from 1.25 at $A_P/A_R$ equals zero to 0.91 in a relatively limited change of $A_P/A_R$ varying from 0 to 0.05.

As before, the three studied figures indicate clearly a variation of $r_{cr}$ from 0.91 to 0.95 (4.39%) for the three open spandrel deck bridges with one post.



a) Parabolic Arch          b) Catenary Arch          c) Circular Arch
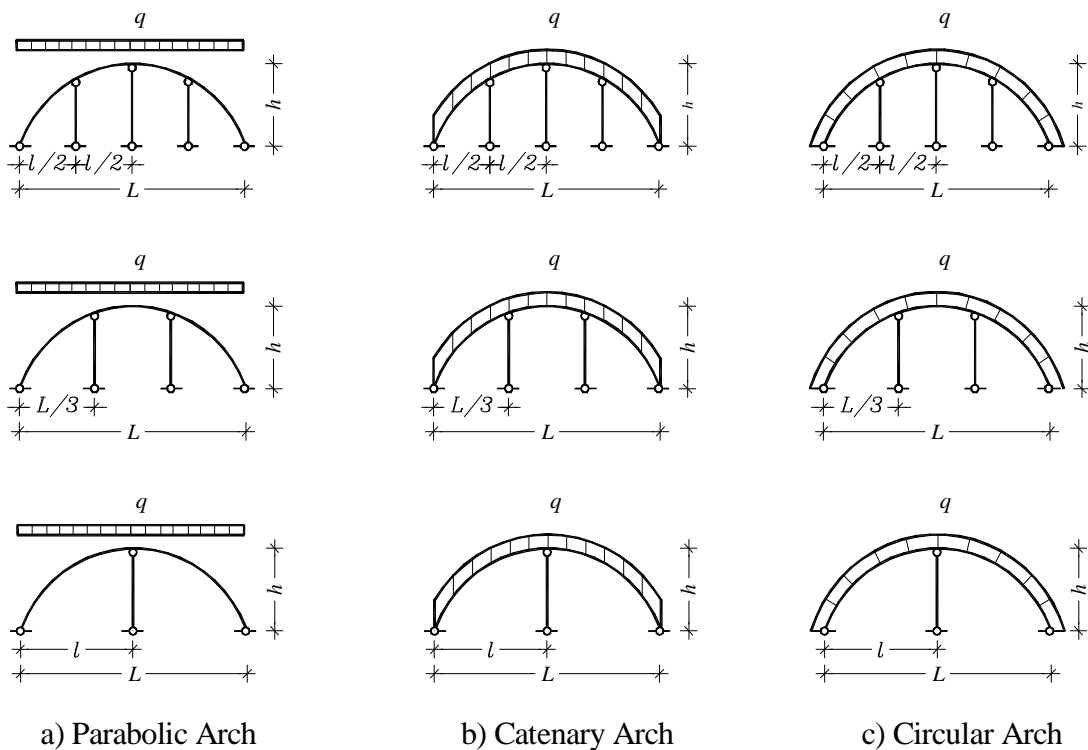
Figure (1) Steel Arched Bridge with One, Two and Three Posts with Hinged Bases

a) Parabolic Arch                b) Catenary Arch                c) Circular Arch
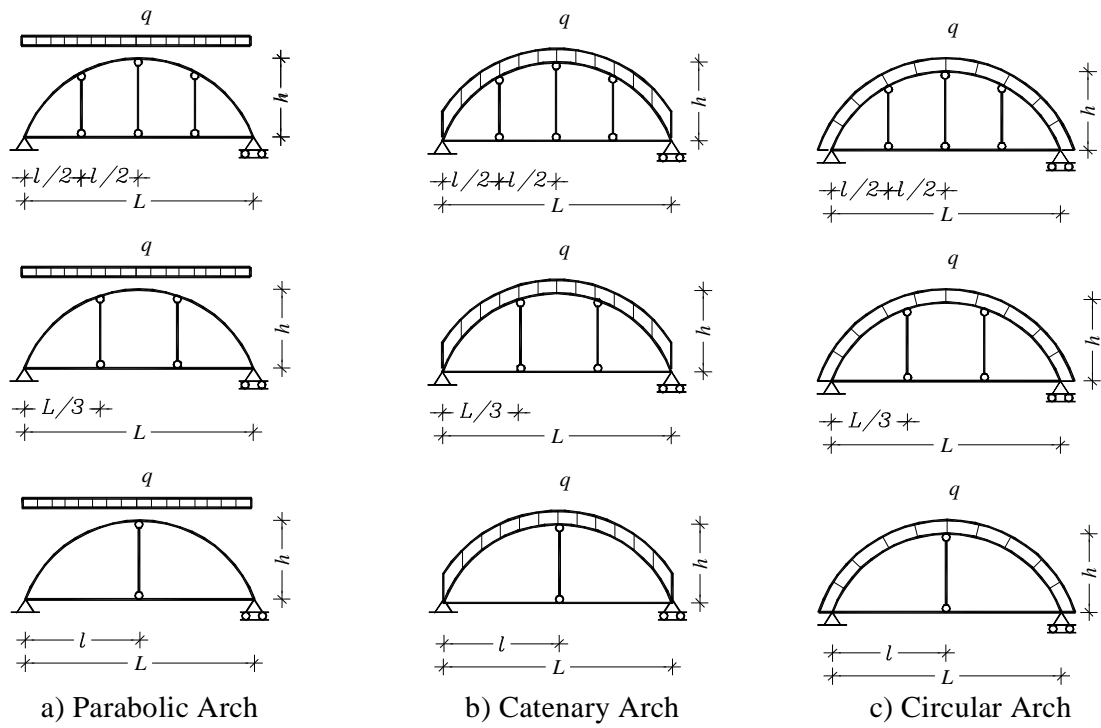
Fig. (2) Steel Arched Bridge with Tie Having One, Two and Three
Hangers with One Base Hinged and the Other Roller
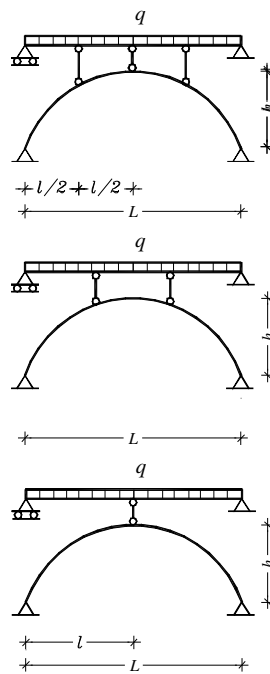


Fig. (3) Deck-Arched Bridge with One, Two and Three Posts
with Hinged Bases
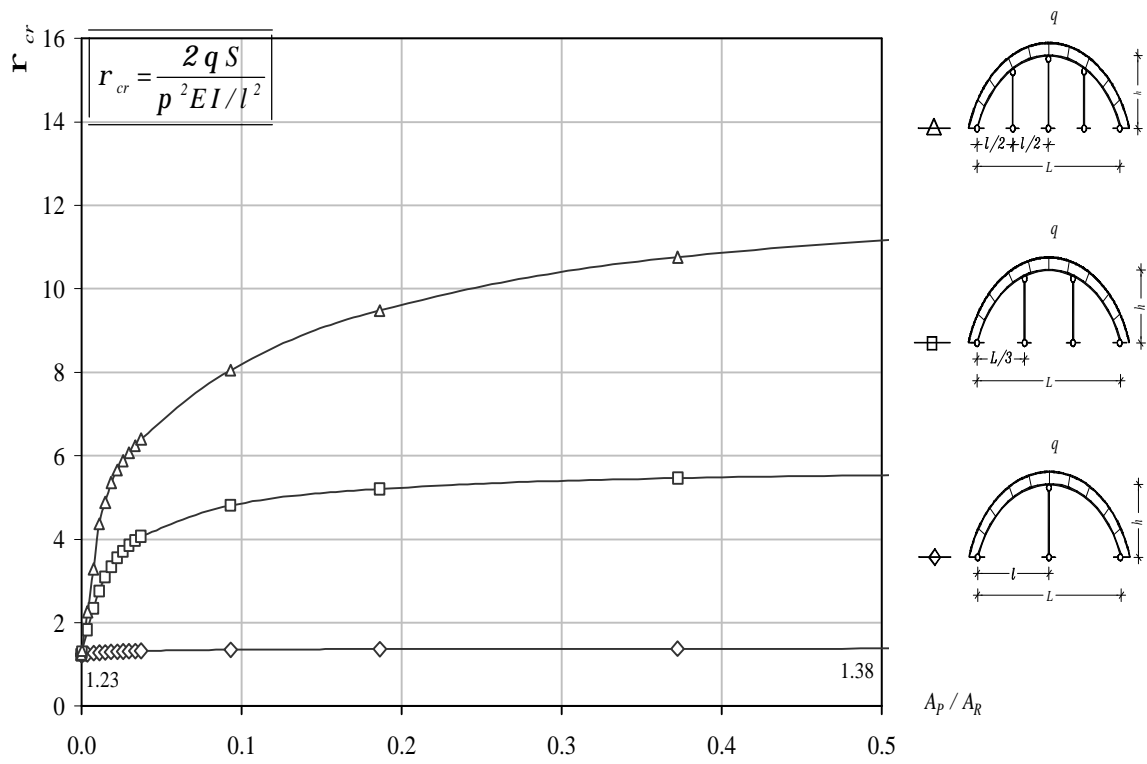
Fig. (4) Effect of Variation of Cross Section Area of posts on ElasticCritical Sum of Loading for Circular Arches Subjected to Radial Loading Uniformly Distributed Along Arch Axis

$$r_{cr} = \frac{2\,q\,l}{p^2\,E\,I\,/\,l^2}$$
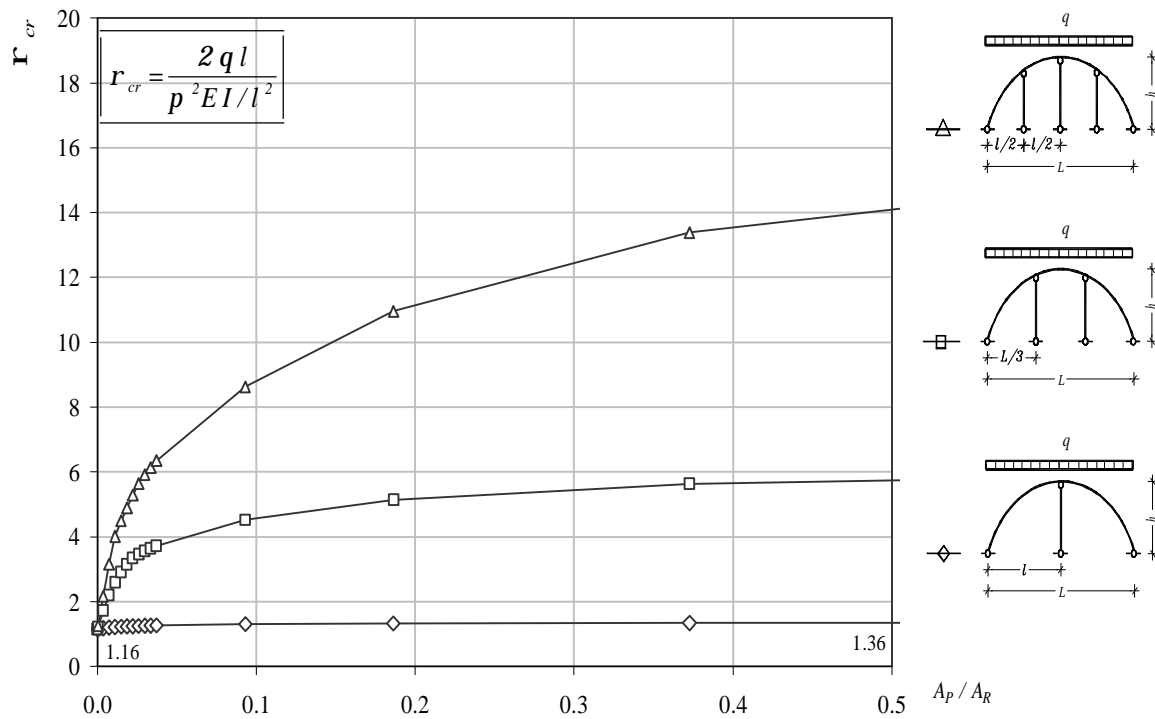
Fig. (5) Effect of Variation of Cross Section Area of  posts on  Elastic Critical Sum of Loading for
Parabolic Arches Subjected to Vertical Load Uniformly Distributed on Horizontal Projection



$$r_{cr} = \frac{2\,q\,S}{p^2\,E\,I\,/\,l^2}$$
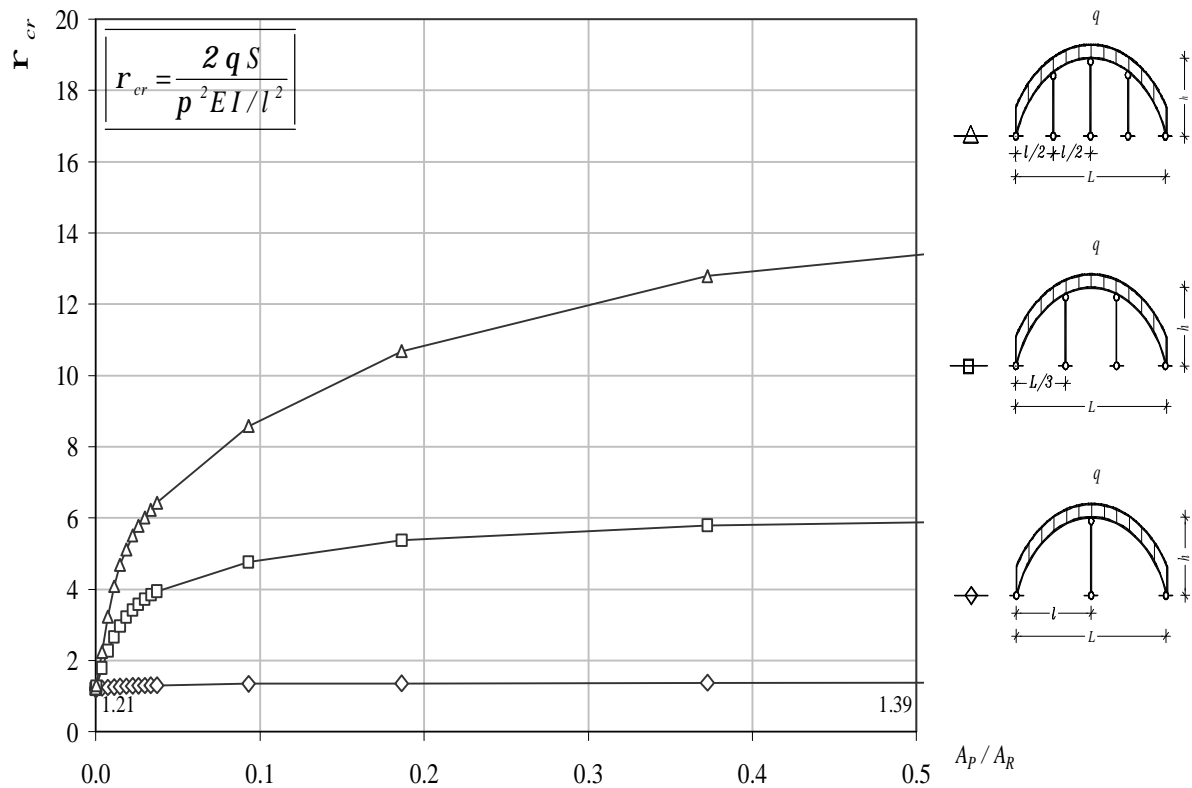
Fig. (6) Effect of Variation of Cross Section Area of  posts on  Elastic Critical Sum of Loading for
Inverted Catenary Arches Subjected to Vertical Load Uniformly Distributed Along Arch Axis

$$r_{cr} = \frac{2qS}{p^2 EI/l^2}$$
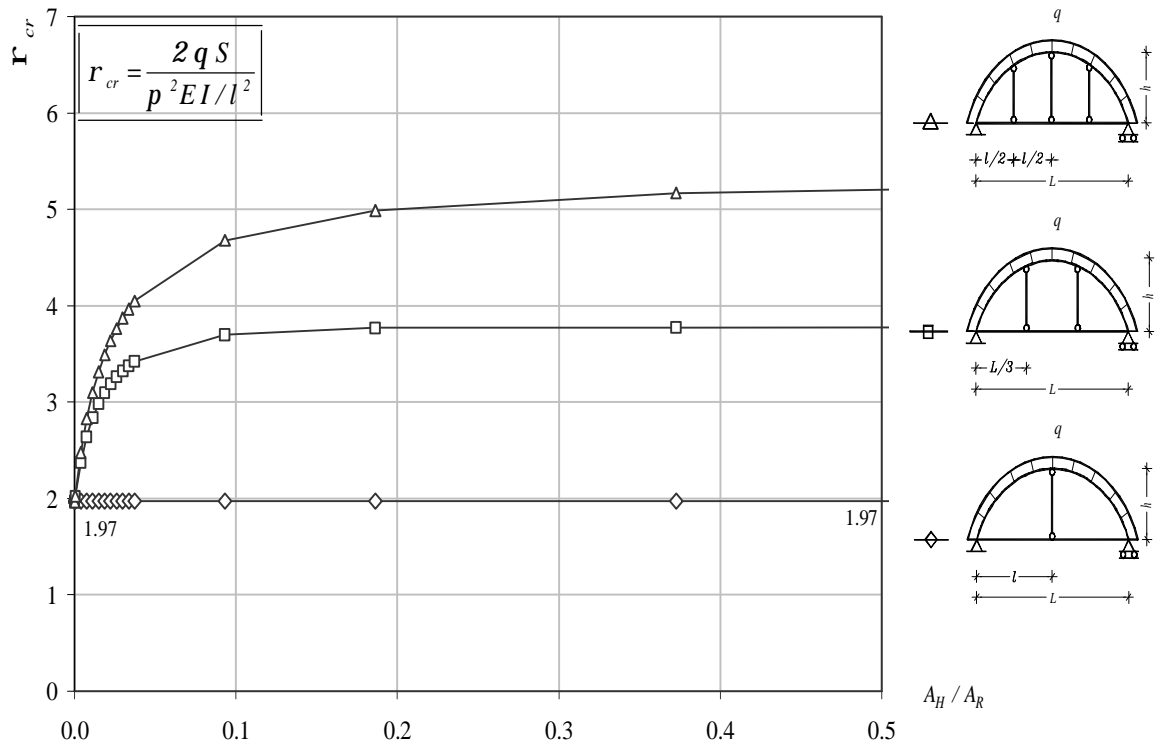
Fig. (7) Effect of Variation of Cross Section Area of Hangers on Elastic Critical Sum of Loading
for Circular Arches with Tie Subjected to Radial Loading Uniformly Distributed Along Arch Axis



$$r_{cr} = \frac{2ql}{p^2 EI/l^2}$$
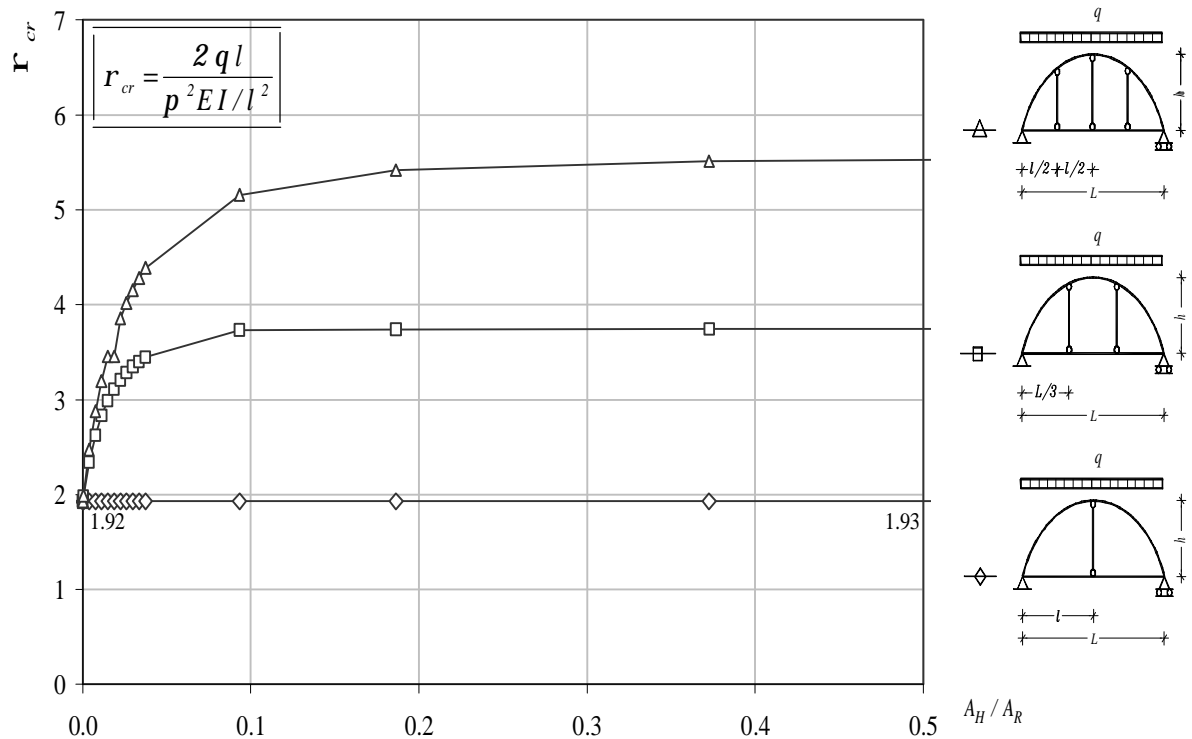
Fig. (8) Effect of Variation of Cross Section Area of Hangers on Elastic Critical Sum of Loading for
Parabolic Arches with Tie Subjected to Vertical Load Uniformly Distributed on Horizontal
Projection
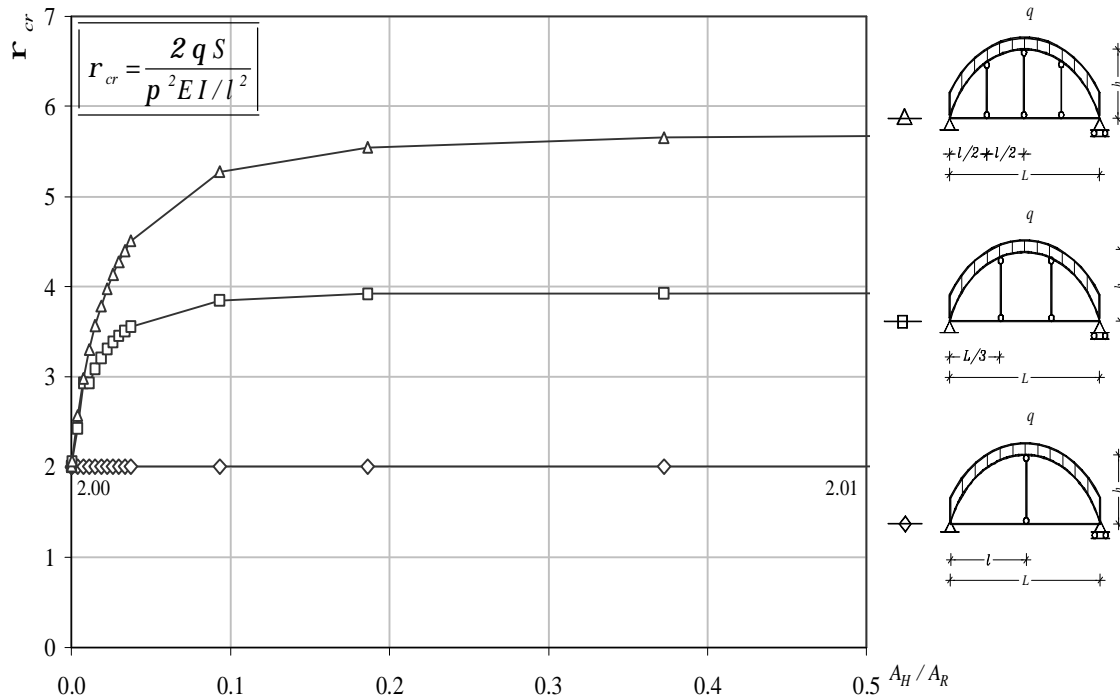
Fig. (9) Effect of Variation of Cross Section Area of  Hangers on  Elastic Critical Sum of
Loading for Inverted Catenary Arches with Tie Subjected to Vertical Load Uniformly Distributed
Along Arch Axis
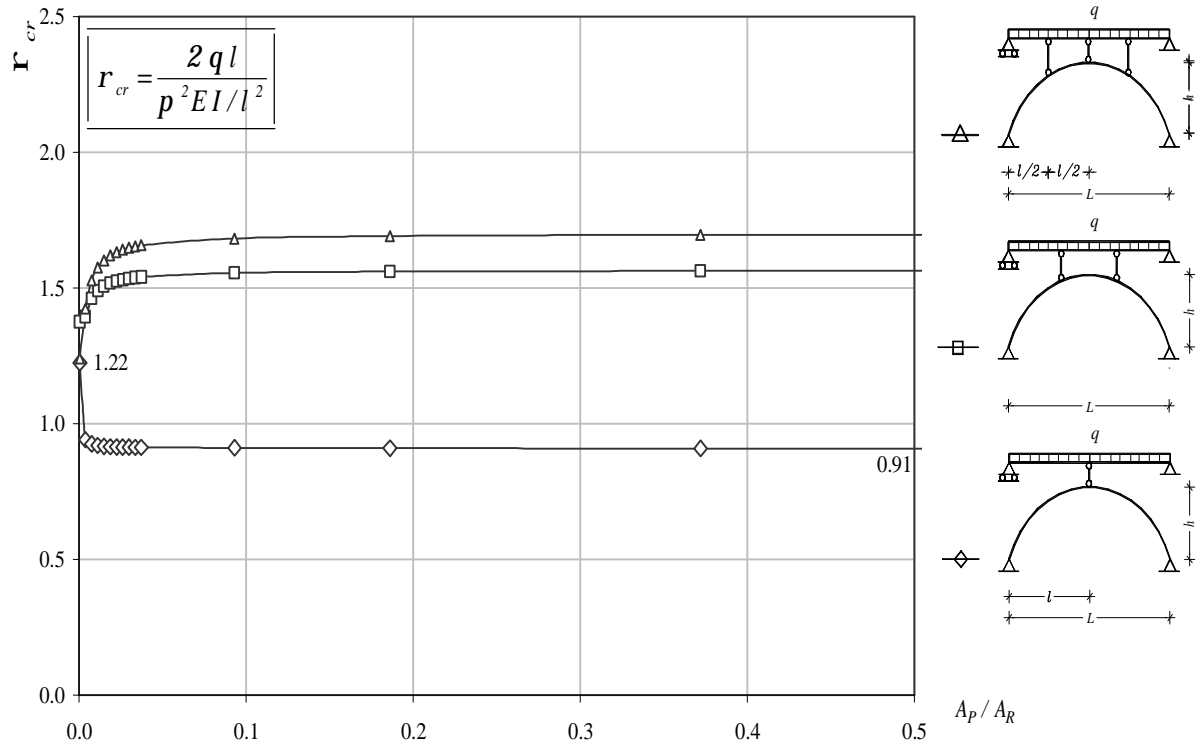


Fig. (10) Effect of Variation of Cross Section Area of  posts on  Elastic Critical Sum of Loading for
Deck Circular Arched Bridge Subjected to Vertical Load Uniformly Distributed on Horizontal
Projection
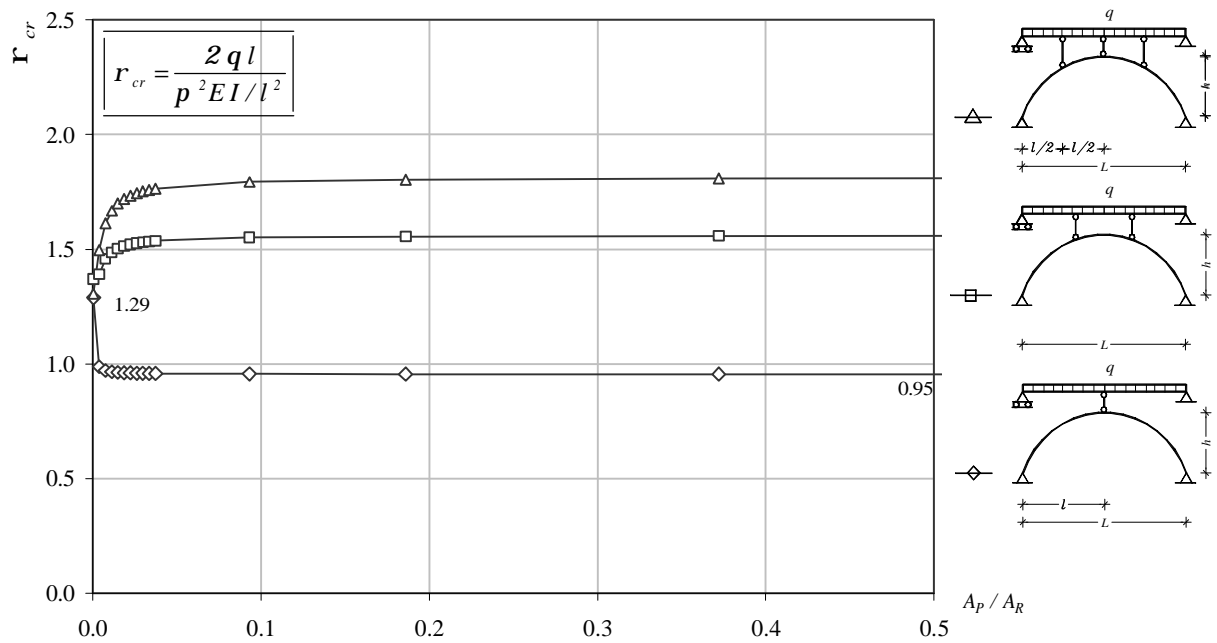
Fig. (11) Effect of Variation of Cross Section Area of  posts on  Elastic Critical Sum of Loading for Deck Parabolic Arched Bridge Subjected to Vertical Load Uniformly Distributed on Horizontal Projection
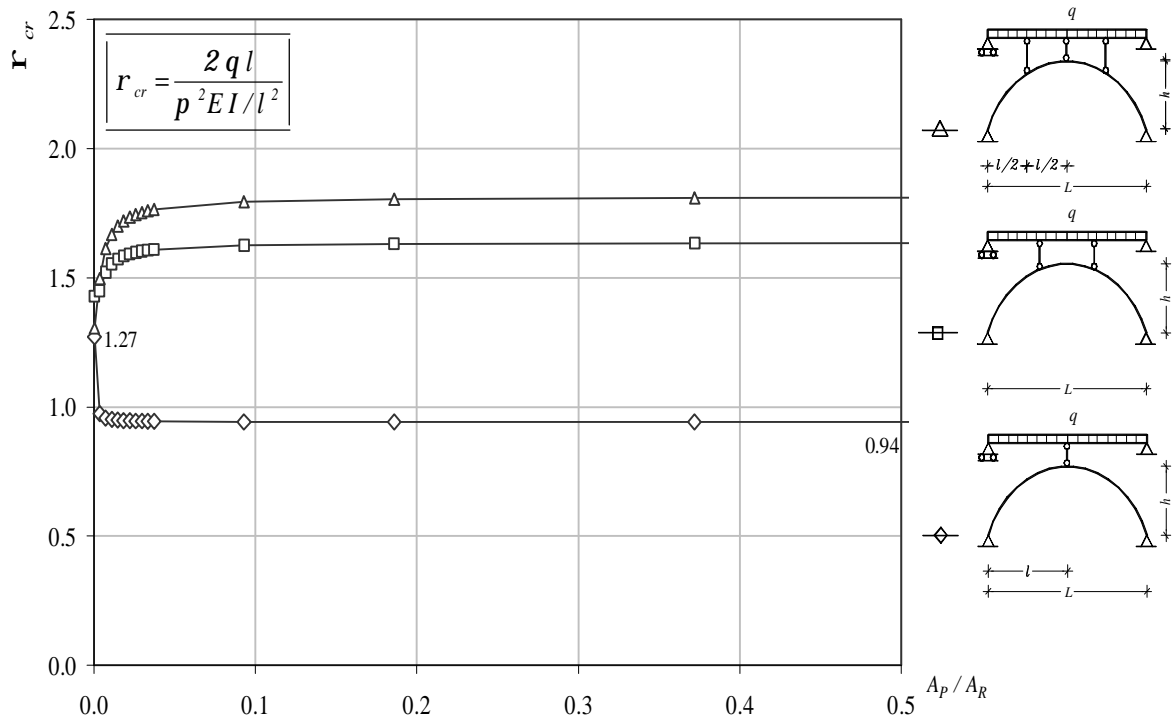


Fig. (12) Effect of Variation of Cross Section Area of  posts on  Elastic Critical Sum of Loading for Deck Catenary Arched Bridge Subjected to Vertical Load Uniformly Distributed on Horizontal Projection

## CONCLUSIONS

The sets of graphs presented in figures (4) to (12), identify clearly the contribution of the posts or hangers, the influence of the arch shapes and the loading pattern on the value of the final buckling load. It is noticed that the in-plane elastic carrying capacity increases by providing the arch with additional posts or extra hangers, but this increase depends on the number of added posts or hangers. From the present study the following are arrived at:

1. The in-plane elastic carrying capacity of the considered arches increases with the increase of $A_P/A_R$ for the case of two and three posts up to $A_P/A_R = 0.5$, while remains nearly constant in case of one post.

2. The in-plane elastic carrying capacity increases with the increase of $A_H/A_R$ in case of two and three hangers up to $A_P/A_R = 0.25$ then increases very slightly after that.

3. From the above mentioned sets of figures, it could be also noticed that the in-plane elastic carrying capacity of arch bridge is larger than the case of arch without tie and no noticeable effect was observed by providing it with a single hanger. However, the in-plane elastic carrying capacity of arch bridge increases by providing the arch with two, three or more hangers.

4. It can be seen also that in case of circular deck arch bridge, the in-plane elastic carrying capacity is nearly constant and is hardly affected by the ratio of $A_P/A_R$. The in-plane elastic carrying capacity of these deck arch bridges increases with the increase of the number of posts and is not sensitive to the initial arch shape.

## REFERENCES

1. El-sawaf S., "Load Carrying Capacity of Steel Arches", (2005), M.Sc. Thesis, Faculty of Eng., Al-Azhar University, Cairo, Egypt.

2. Galambos T. V., (1998), "Guide to Stability Design Criteria for Metal Structures", 5th Edition, John Wiley and Sons, New York.

3. Salem A. H., (1969), "Buckling of Trapezoidal Frames Permitted to Sway", Journal of Structural Division, ASCE, Vol. (95) No. ST12.

4. Salem et al, 2006, "Best Proportions of Arches for In-Plane Maximum Elastic Load Carrying Capacity", Accepted for publication in Ain Shams, Faculty of Engineering Scientific Bulletin.

5. Abbas H., August 2006, "Al Enania Bowstring Bridge - Egypt", Proceedings of the 7th International Conference on Short and Medium Span Bridges, Montreal-Canada.

6. Abbas H., "Arch Bridge Configuration: Does it Fulfill Aesthetic Quality and Economic Consideration?", Proceedings of the 2nd Minia International Conference for Advanced Trends in Engineering MICATE 2002 Minia – Egypt.

# SIMULATION BETWEEN TOOL AND
# AUTOMATIC TOOL CONSTRUCTION OPERATIONS

**Ismail M. Basha, Youssef Mohey El-Din, Mohamed M. Askar and Soad Hosny**
*Construction Engineering Department, Faculty of Engineering, Zagazig University.*

## ABSTRACT:

Construction operations range from manual (tool) to automation (automatic tool) operations, which are difficult to analyze and optimize using standard mathematical methods. Simulation is an alternative method of analysis that offers numerous benefits. Simulation technique proves its capability of assessing productivity of any construction operation that has repetitive nature. To design construction operations it is necessary to make decisions, including determination of crew size, selecting equipment, establishing operating logic, and selecting construction method. This paper presents the effectiveness of applying MicroCYCLONE version 2.7 as a simulation engine in productivity improvements. Different repetitive construction operations are selected as follows:

- Minitunnelling by TBM as automatic tool operation.
- Microtunnelling by pipe jacking and mechanical plastering as power tool operations.
- Manual plastering as tool operation.

The simulation models of these operations were designed and validated according to actual crew design until reaching the best-fit simulation models. Change the simulation model resources to get the optimum one, which produce maximum productivity, minimum cycle time, and minimum cost. Sensitivity analysis was applied to the result of simulation. the productivity improvements result increases in manual operations and decreases by applying automation in the construction operation and these improvements range from 22.75% to 1.68%.

**Keywords:** Simulation, Automation, Minitunnelling, Microtunnelling, MicroCYCLONE and Productivity.

## INTRODUCTION

Productivity is an index that measures outputs (goods and services) related to the inputs (labor, materials, and other resources) which are used to produce them. It is a measurement of the effective use of resources. Numerous factors affect productivity such as: methods, capital, quality, technology, and management. All in all, productivity measurements must be viewed with awareness of related factors, and of a certain amount of distortion. Consequently, it is better to treat productivity as approximate indicators rather than precise measurements [1]. Productivity measurement allows managers to judge performance where the improvements are needed. A number of modeling tools have been specially developed or proposed to measure and improve productivity for the construction management area. Simulation techniques have been applied to various areas in construction.

Halpin and Riggs [2] classified the construction field operations into a hierarchical taxonomy as shown in Figure1. Organization considerations lead a number of hierarchical levels that can be identified in construction. The relative hierarchical of construction management can be identified in four levels, each more detailed or refined than its predecessor (Organizational, Project and activity, operation and process, and work task).

Every construction chore has physical component (muscles action) and information components (brain action). To complete the chore, some combination or human and machine must be able to execute all of the physical and information components. Table 1 presents a system for classifying construction equipment into four categories: tools, power tools, automatic tools, and robots, based on the distribution of physical and information components between man and machine (3). The selected cases in the study cover the first three levels of Everett classification, and the third level of work (operation) according to Halpins hierarchy [4].

In construction the reason for modeling and simulating a production system is to examine the interaction between the flow units, determine the idleness of the productive resources, locate bottlenecks, and estimate the production of the system as it is designed [2]. Simulation technique is a process oriented technique, which is the same to deterministic technique, as both deal with the process activities and their duration. Modeling and simulation of most construction processes have used different simulation engines. There is a large number of simulation languages that are used nowadays in construction. MicroCYCLONE, STROPOSCOPE, DISCO, UM-CYCLONE, and COOPS are some of the simulation engines used in construction operations analysis [5]. In this study, MicroCYCLONE version 2.7 analyzes the selected construction operations and predict production rate as it has a lot of advantages, which can be summarized as follows [6]:

- Simple and small numbers of work tasks are used to describe the repetitive construction operation.
- Limited numbers of resources are defined at each queue node before starting simulation.
- Some work tasks are not repetitive in each cycle so this can be described by using probabilistic arc.
- The work tasks duration's interred in probabilistic distribution format.
- Nonstationary work task duration (Cycle times that increased or decreased with the passing of time) is used in this engine.
- Resource cost inters in the form of fixed cost (Owning, depreciation, etc.) and variable cost (Operating, fuel, etc.).

## REPETITIVNESS OF SELECTED CASES STUDY

Linear construction operations are the operations that involve repetitive units of construction. A tunnelling operation is an example of complex linear construction process, and plastering operation is an example of simple repetitive construction operation. Tunnelling and plastering operations are good examples for the repetitive construction operations. In minitunnelling by tunnel boring machine (TBM) operation the automatic bentonite injection system is fully programmable to allow the operator to inject a pre-determined amount of bentonite at all or specific areas of tunnel without man entry to the tunnel. The TBM is connected to a number of injection stations in the tunnel bentonite line. Each injection station is represented on the computer screen by a box and is illuminated when selected by the operator on the keyboard. The operator can select any station in any order or sequence. The machine is used with a shield (head cutter) as shown in Figure 2(a). It is contacted completely to the soil. This means that the cut is equal to the outer diameter of the tunnel or the pipe, which is to be installed. It operates as slurry or by compressed air to force the ground pressure. The simulation model is developed for estimating the production in number of concrete pipes per hour.

| Hierarchical Level | Basic Focus |
|---|---|
| **Level** { Organizational | Company structure, Head office, Gross project attributes (total cost, duration, profit, cash flow, percent complete, etc.) |
| Focus on What to do<br><br>**Level** { Project | Project definition, Contract, Work breakdown structure (WBS), Cost, Time, Resource, etc. |
| Activity | Time and cost consuming items, Current cost, Time, Resource use, Status, etc. |
| Operation | Construction method, Resource list |
| Focus on How to do<br>**Level** { Process | Technological sequence of work tasks, trade actions. |
| **Level** { Work Task | Field action, Crew members level, Work assignment to labors |

**Fig. 1 : Hierarchical Levels in Construction Management (2)**

**Table 1 : Distribution of Physical and Information Components of Work (3)**

| Hardware | Physical input | Information input | Example |
|---|---|---|---|
| **Tool** | Human | Human | Hammer, shovel, trowel |
| **Power tool** | Machine/human | Human | Jackhammer, vibratory hammer, crane |
| **Automatic tool** | Machine/human | Machine/human | Tunnel Boring Machine (TBM) |
| **Robot** | Machine | Machine | SSR-3 |

(a) Minitunnlling operation by TBM

(b) Microtunnelling operation by hydraulic jack hammer

(c) Manual plastering operation

(d) Mechanical plastering operation

Figure 2 – Cases of study construction operations

In microtunnelling operation by horizontal jack hammer a steel pipe with open front end is driven into the soil as a trenchless construction method as shown in Figure 2(b). The simulation model is developed for estimating the production in number of steel pipes per hour. To construct this

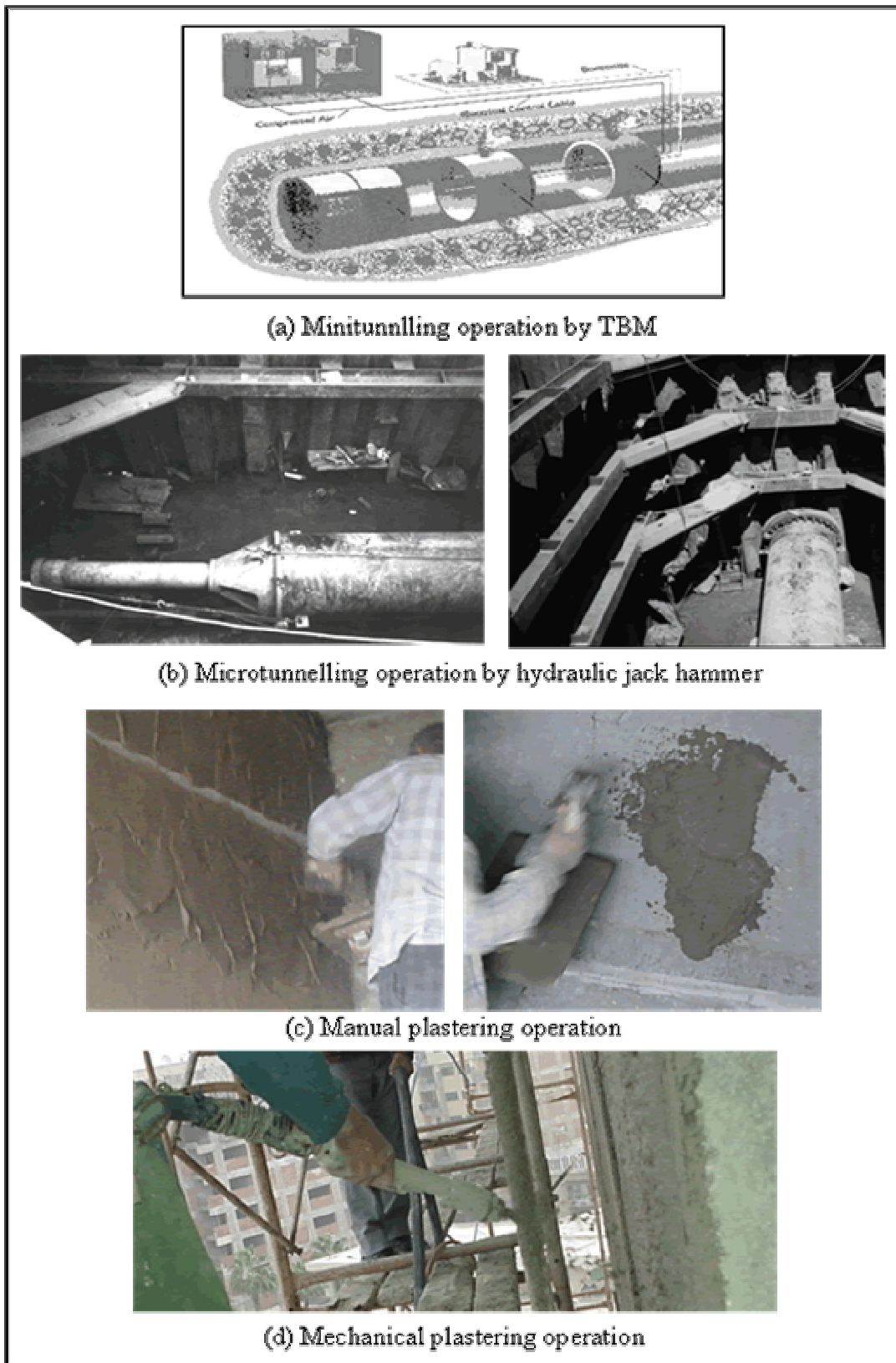operation, the first step is welding the mechanical sealing in sheet piling to prevent water seepage during driving process. After that, lowering and position of steel pipe on a guide girder, then, the welding crew erecting of cylindrical cotter segments to prevent flaring of the pipe. After that, the jack hammer is equipped with a driving steel pipe and driving process start. Welding another pipe section and painting the welding area with epoxy material. Driving process of two welded steel pipes, repeat this process until pipes reach to target pit. After completing driving process, the soil plug formed inside the pipe can be removed by injecting compressed air or pressure water from pushing shaft for small diameter pipes, or by means of a screw conveyor, or by using manual excavating crew (miners).

Plastering operations of walls as shown in Figure 2(c, and d) is a simple example of repetitive construction operations, as the work sequence in each side of wall is semi similar. The plaster finishing surface should at once be flat and fine textured. It is logically, therefore, to spread some fine grained material such as lime or mixed water, over the surface and trowel it smooth and level. A thicker application of material would sag and run down while being spread. Instead, one or two of a  coarser-grained material is first to be spread on the walls to render the surface level and when it becomes dry a thin coat of fine grained material is to be spread over it to provide a level and smooth surface. So, plastering is an example of repetitive construction operation, as each wall side needs the same work to provide a finishing smooth hard level to the walls.

## SIMULATION MODEL

The application of simulation technique requires several steps: select the simulation engine (program) that can be used, design the operation simulation model based on the selected simulation engine, prepare the operations activities duration, simulate the designed model, check simulation results validation, and analyze the simulation results to assess productivity. Simulation model can be constructed through three major phases, model-building, simulation, and sensitivity analysis phases as shown in Figure 3. In the phase I the MicroCYCLONE network model for each case study is built according to the construction method in the Queues, the Combi activities and the Normal activities as shown in Figure 4 for manual plastering operation. The activities' data such as resources, quantities, durations, probabilities of activities, etc. are collected. Data are prepared and analyzed using statistical method for simulation technique. Some of quantitative time data are fed into the simulation model as deterministic duration. Others are fed as probabilistic distribution in the triangle distribution form because of its easy estimation from the reviewers' perspective. Statistical inference is performed to estimate the three values of the triangle distribution to represent each activity (data point): minimum, most probable, and maximum. These values constitute the triangular distribution (lower, mode, and higher values) that will be used in simulation for activities' duration. Although beta distributions are capable of fitfully representing most of the distributional shapes encountered in modeling the activities of construction engineering projects. It needs a large scale of data collected in more than 30 times [7-10]. Nonstationary work task duration is used in microtunnelling operation because the duration of normal work task "Drive 6m of steel pipe" changes continuously in every meter of steel pipe penetrates the soil due to soil weight inside the pipe and friction between soil and pipe [11,12].

## EXECUTION OF SIMULATION MODELS

After preparing and building the simulation model, model resources are defined and simulation process starts. Simulation outputs are compared to the collected data to check the model reality as  in simulation  phase II  shown in Figure 3. Verification is a key process in model design to
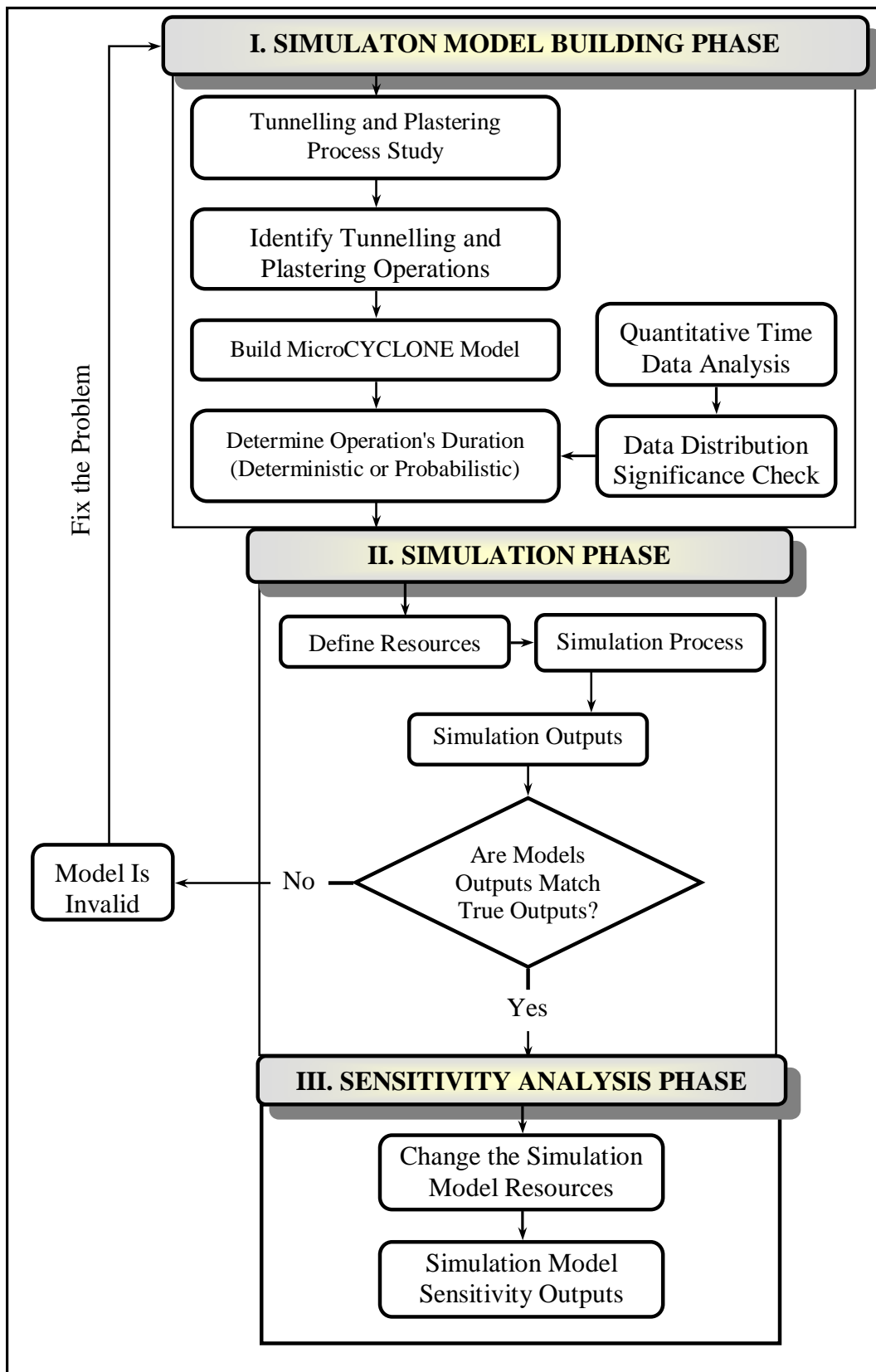
**Fig.3 : Simulation Model Framework**
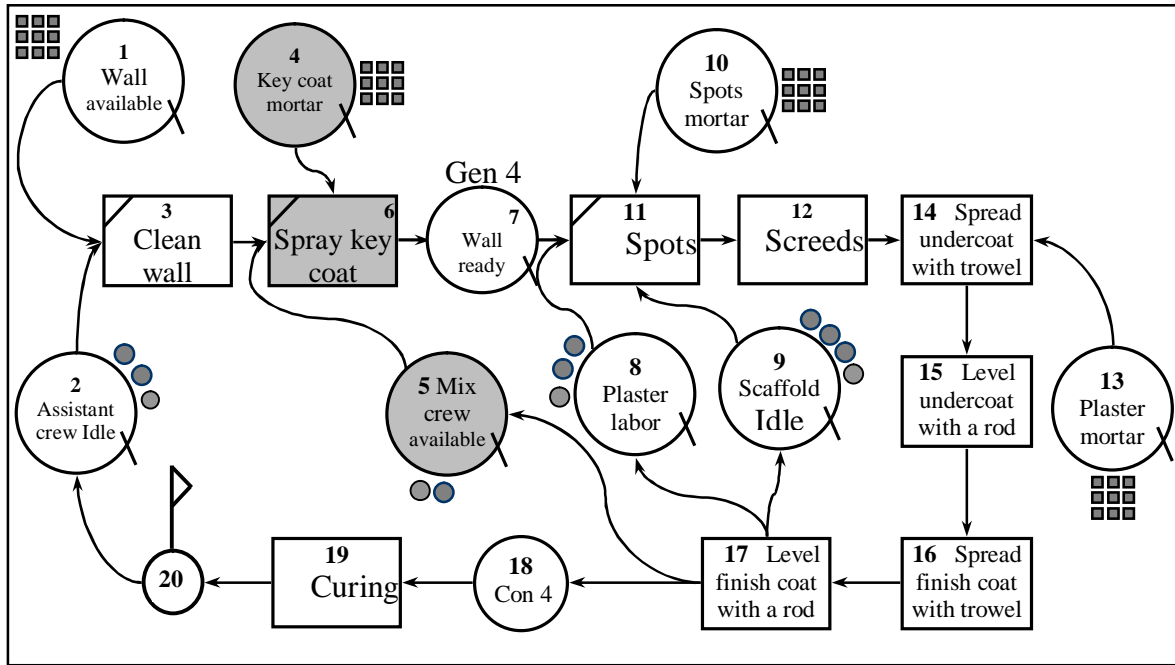
**Fig.4 : MicroCYCLONE Diagram for Manual Plastering Operation**

check the model logic and the work task duration. Productivity model results have to be validated so that they can be used for productivity estimating. After verification, the model will be appropriate to fit the problem and predict productivity of studying process. Therefore, the collected productivity from fields is compared with the estimated productivity from simulation model, which simulates actual crew design. If the model provides close numbers to the collected data; it can be used to present this process in the real world. To determine exactly how far the productivity model predicted results from the collected data, a verification factor has to be calculated for each construction operation. The verification factor is calculated as:

Verification Factor *(VF)*     = ***APMR / CP***
Where;                         ***VF***     = Verification Factor
                              ***APMR*** = Actual Productivity Model Result
                              ***CP***      **=** Collected Productivity from fields

The verification factor (VF) has been calculated for each case study considering its corresponding productivity model result; this has been calculated in Table 2. Based in VF calculation for studying operation, the simulation models are valid where their outputs are acceptable. If these results do not match, the problem must be fixed and the model should be improved to produce close results.

## SENSITIVITY ANALYSIS

After building and verifying the simulation model, Sensitivity analysis phase can start as shown in Figure 3 phase III. The main objective of this research is to optimize the selected construction operations and improve their performance. Some of the common optimization problems often encountered in planning or controlling a construction operation are optimal resources allocation to maximize hourly production, minimize the unit cost, or minimize the processing time of a job.

**Table 2 : Verification Factor (VF) for Studying Operations**

| Construction Operations | | Unit | Actual Productivity Model Result (APMR) | Actual Collected Productivity (CP) | Verification Factor (VF) |
|---|---|---|---|---|---|
| Tunnelling | Minitunnelling | Concrete Pipe/hr | 0.088 | 0.100 | 0.882 |
| Tunnelling | Microtunnelling | Steel Pipe/hr | 0.020 | 0.018 | 1.104 |
| Plastering | Mechanical | m²/hr | 3.129 | 3.670 | 0.853 |
| Plastering | Manual | m²/hr | 1.063 | 1.140 | 0.993 |

Simulation of construction operations involves building a model and experimenting it on a computer in an attempt to study and/or optimize its performance. After devising the model of the operation, the simulation entails, among other things, specifying the configuration of resources that will drive the system. Sensitivity analysis phase is done to check the effect of different resources on the model outputs. Sensitivity analysis is primarily involved studying the responsiveness of a system to the variation of resource configuration. This includes specifying batches of input specifications, keeping track of the system's feedback, and organizing the output. Each resource is changed to check the model limitation and select the optimum number of resources, which produce optimum crew or operation design. For example, the optimum resource configurations for manual plastering operation are shown in Figure 4.

## SIMULATION RESULTS ANALYSIS

MicroCYCLONE production by cycle report shows the production in units per hour per cycle. This report presents the cycle number, the simulation time when that cycle is completed, and the cumulative productivity at that time. The number of cycle can be changed until reaching the steady-state phase. These results of tunnelling operations are formed in Table 3, and the results of plastering operations are shown in Table 4. The last three rows of Table 3 give statistics for the entire set of 100 runs. These statistics give the average, the maximum, and the minimum for the corresponding column. After achieving each cycle the counter add 5 m' of circular concrete pipe length with diameter 2.23 m for minitunnelling operation, and 6 m' of circular steel pipe length with diameter 1.5 m for microtunnelling operation to the total units produced. The last five rows of Table 4 give statistics for the entire set of 1500 cycle. These statistics give the average, the maximum, the minimum, total cost (L.E.), and unit cost (L.E.) for the corresponding column. After achieving each cycle the counter add 53 m$^2$ of plastering (plastering area of interior wall for each room) to the total units produced. If we let $rT$ = (actual cycle duration) – (best cycle duration), then the comparison between models designed depends on $rT$. By observing Figure 5 which presents the saved time at each cycle ($rT$), it is noticed that the area under manual plastering operation curve is the largest one and this area decreases until reaching the area under the minitunnelling by TBM operation curve. By comparing the four curves, the time saved, and productivity improvement after applying simulation are proportional diversely by applying automation in construction operations. Figure 6 shows the productivity improvement percentages as 1.68, 11.51, 14.64, and 22.75 for minitunnelling by TBM, microtunnelling by hydraulic jack hammer, mechanical plastering, and manual plastering operations respectively. In mechanical and microtunnelling operations the percentage of productivity improvement is closely values because these operations are near in the degree of automation.

**Table 3 : Tunnelling Operations Results Analysis**

| Cycle number | Minitunnelling Operation | | | | Microtunnelling Operation | | | |
|---|---|---|---|---|---|---|---|---|
| | Actual model cycle time (Hr.) | Best model cycle time (Hr.) | r T (Hr.) | Average r T (Hr.) | Actual model cycle time (Hr.) | Best model cycle time (Hr.) | r T (Hr.) | Average r T (Hr.) |
| 1 | 7.33 | 6.85 | 0.48 | 0.48 | 9.12 | 8.50 | 0.62 | 0.62 |
| 2 | 8.89 | 8.94 | -0.05 | 0.22 | 9.64 | 10.35 | -0.71 | -0.04 |
| 3 | 9.76 | 10.51 | -0.75 | -0.11 | 15.36 | 10.67 | 4.69 | 1.53 |
| 4 | 12.04 | 11.8 | 0.24 | -0.02 | 17.31 | 11.81 | 5.50 | 2.53 |
| 5 | 7.35 | 6.71 | 0.64 | 0.11 | 18.39 | 12.21 | 6.18 | 3.26 |
| 6 | 11.21 | 11.28 | -0.07 | 0.08 | 19.65 | 14.11 | 5.54 | 3.64 |
| 7 | 9.07 | 8.09 | 0.98 | 0.21 | 20.52 | 14.78 | 5.74 | 3.94 |
| 8 | 12.66 | 11.25 | 1.41 | 0.36 | 20.56 | 16.22 | 4.34 | 3.99 |
| 9 | 6.5 | 7.24 | -0.74 | 0.21 | 21.63 | 16.95 | 4.68 | 4.06 |
| 10 | 10.2 | 11.07 | -0.87 | 0.13 | 22.02 | 18.49 | 3.53 | 4.01 |
| 11 | 13.56 | 12.86 | 0.70 | 0.18 | 24.30 | 18.97 | 5.33 | 4.13 |
| 12 | 7.25 | 6.69 | 0.56 | -0.09 | 24.95 | 19.33 | 5.62 | 4.26 |
| 13 | 10.08 | 9.84 | 0.24 | 0.21 | 26.90 | 21.13 | 5.77 | 4.37 |
| 14 | 10.54 | 8.95 | 1.59 | 0.31 | 27.91 | 23.12 | 4.79 | 4.40 |
| ----- | ----- | ----- | ----- | ----- | ----- | ----- | ----- | ----- |
| 100 | 12.33 | 10.54 | 1.79 | 0.19 | 86.14 | 73.82 | 2.61 | 5.79 |
| **Average** | 11.34 | 11.15 | 0.19 | | 50.32 | 44.53 | 5.79 | |
| **Maximum** | 13.83 | 11.72 | 2.11 | | 86.14 | 73.82 | 12.32 | |
| **Minimum** | 6.23 | 5.33 | 0.90 | | 9.12 | 8.50 | 1.92 | |

| Total units produced = 500 m' | Total units produced = 600 m' |
|---|---|
| **Units produced per cycle = 5 m'** | **Units produced per cycle = 6 m'** |

**Table 4  : Plastering Operations Results Analysis**

| Cycle number | Manual Plastering Operation | | | | Mechanical Plastering Operation | | | |
|---|---|---|---|---|---|---|---|---|
| | Actual model cycle time (Hr.) | Best model cycle time (Hr.) | r T (Hr.) | Average r T (Hr.) | Actual model cycle time (Hr.) | Best model cycle time (Hr.) | r T (Hr.) | Average r T (Hr.) |
| 1 | 44.35 | 38.58 | 5.77 | 5.77 | 17.34 | 13.65 | 3.69 | 3.69 |
| 2 | 50.21 | 46.93 | 3.28 | 4.53 | 16.96 | 15.26 | 1.70 | 2.70 |
| 3 | 57.34 | 45.62 | 11.72 | 6.92 | 18.43 | 12.35 | 6.08 | 3.82 |
| 4 | 59.06 | 44.75 | 14.31 | 8.77 | 15.87 | 17.41 | -1.54 | 2.48 |
| 5 | 49.38 | 50.61 | -1.23 | 6.77 | 18.62 | 16.83 | 1.79 | 2.34 |
| 6 | 49.57 | 39.34 | 10.23 | 7.35 | 19.23 | 14.22 | 5.01 | 2.79 |
| 7 | 43.07 | 31.64 | 11.43 | 7.93 | 15.57 | 12.67 | 2.90 | 2.80 |
| 8 | 53.16 | 45.62 | 7.54 | 7.88 | 17.69 | 11.95 | 5.74 | 3.17 |
| 9 | 50.59 | 52.22 | -1.63 | 6.82 | 17.25 | 14.28 | 2.97 | 3.15 |
| 10 | 56.82 | 49.31 | 7.51 | 6.89 | 18.44 | 13.34 | 5.10 | 3.34 |
| 11 | 50.81 | 47.25 | 3.56 | 6.59 | 16.28 | 12.64 | 3.64 | 3.37 |
| 12 | 42.62 | 40.68 | 1.94 | 6.20 | 19.41 | 16.25 | 3.16 | 3.35 |
| 13 | 53.41 | 47.03 | 6.38 | 6.22 | 18.29 | 15.52 | 2.77 | 3.31 |
| 14 | 46.9 | 42.42 | 4.48 | 6.09 | 17.54 | 11.76 | 5.78 | 3.49 |
| 15 | 55.84 | 56.075 | -0.23 | 5.67 | 19.35 | 13.21 | 6.14 | 3.66 |
| 16 | 58.21 | 48.08 | 10.13 | 5.67 | 17.63 | 14.35 | 3.28 | 3.64 |
| 17 | 46.28 | 39.67 | 6.61 | 5.99 | 15.62 | 18.24 | -2.62 | 3.27 |
| ----- | ----- | ----- | ----- | ----- | ----- | ----- | ----- | ----- |
| 1500 | 52.84 | 50.55 | 2.29 | 11.34 | 17.52 | 16.06 | 1.46 | 2.48 |
| **Average** | 49.85 | 38.51 | 11.34 | | 16.94 | 14.46 | 2.48 | |
| **Maximum** | 59.62 | 57.42 | 2.20 | | 19.65 | 18.33 | 1.32 | |
| **Minimum** | 40.17 | 26.44 | 13.73 | | 15.23 | 11.25 | 3.98 | |
| **Total cost (L.E.)** | **592275** | **542958** | **49290** | | **418965** | **343440** | **75525** | |
| **Unit cost (L.E.)** | **7.45** | **6.83** | **0.62** | | **5.27** | **4.32** | **0.95** | |

**Total units produced = 79500 m$^2$**
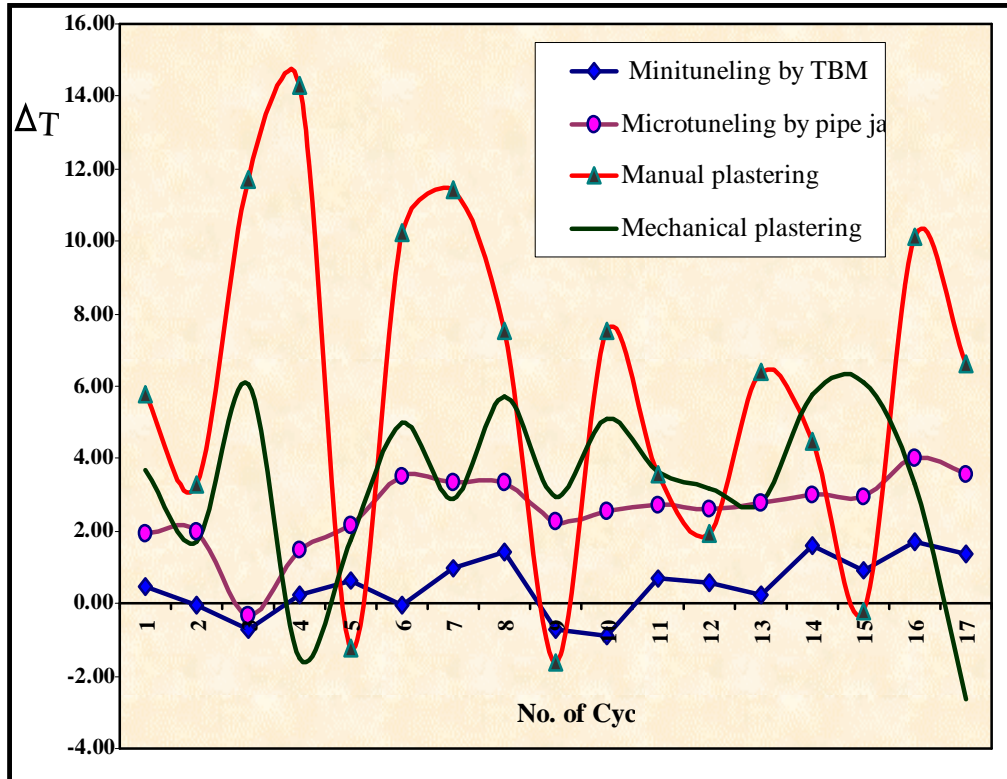
**Units produced per cycle = 53 m$^2$**

**Fig. 5 : Difference in Cycle Time for Cases Study between Actual and Best-Fit Models**
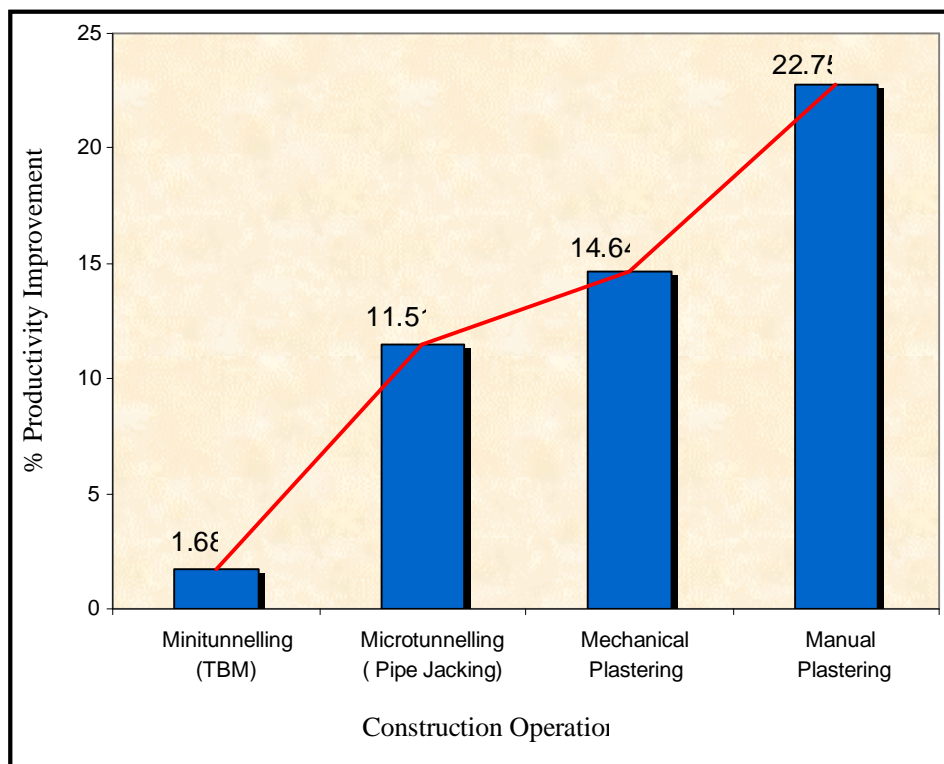


**Fig. 6 : Percentages of Productivity Improvement**

## MODELS VALIDATION

After sensitivity analysis phase, the optimum resource configurations for each construction operation is known. It is important to apply the optimum crew design from the simulation model results to determine the reality and applicability of simulation output. This can be done by calculating the validation factor (DF). For example. The validation factor (DF) for plastering operations in Educational Tanta Hospital project has been calculated by dividing the best estimated productivity using simulation after sensitivity analysis phase by the best collected productivity after applying optimum crew design in actual project. The validation factor (DF) is calculated as:

> Validation Factor *(DF)*    = *BEPS / BCPF*
> Where;                              *DF*      = Validation Factor
>                                           *BEPS* = Best Estimated Productivity from Simulation
>                                           *BCPF =* Best Collected Productivity from Fields

The validation factor (DF) has been calculated for plastering operations in Table 5. Based in DF calculation for studying operation, the simulation model results are valid where their outputs are acceptable.

**Table 5 : Validation Factor (DF) for Plastering Operations**

| Plastering Operations | Optimum Crew Design | Unit | Best Estimated Productivity from Simulation (BEPS) | Best Collected Productivity from Field (BCPF) | Validation Factor (DF) |
|---|---|---|---|---|---|
| Mechanical | • Several walls. <br>• Two assistant labors. <br>• Two plastering labors. <br>• Three scaffolds. <br>• One plastering machine. | $m^2$/hr | 3.665 | 3.850 | 0.953 |
| Manual | • Several walls. <br>• Three assistant labors. <br>• Several $m^3$ of mortars. <br>• Two mixing labors. <br>• Three plastering labors. <br>• Four scaffolds. | $m^2$/hr | 1.376 | 1.120 | 1.229 |

## CONCLUSION

Simulation is a powerful tool which is used to evaluate production rate and compare the different construction methods for repetitive construction operations according to some objectives to select the best one, which fits the required needs. For such comparison to be valid, it is important to compare the alternatives in same conditions so that none is favored more than others.

The productivity improvement is higher in tools operations than by applying machines or automation during the construction operation. The percentages of production rate improvement

for minitunnelling by TBM, microtunnelling by pipe jacking, mechanical plastering, and manual plastering operations are 1.68, 11.51, 14.64, and 22.75 respectively. The productivity improvement percentage is small in automatic operations because the control resource is the equipment as in manufacturing but in manual operations, the tools and human are the main resources and can be easily resized and redesigned with minimum cost increase.

## REFERENCES

1. Stevenson, W. J.. Production/Operation Management, Fifth Edition. McGraw-Hill, NewYork. (1996)
2. Halpin, D. W., and Riggs, L. S.. Planning and Analysis of Construction Operations. John Wiley and Sons, Inc., New York, N.Y. (1992)
3. Everett, J. G., and Slocum, A.H.. "Automation and Robotics Opportunities: Construction versus Manufacturing", Journal of Construction Engineering and Management, ASCE, 120(2), 443-452. (1994)
4. Halpin, D. W.. MicroCYCLONE Users Manual for Construction Operations. Division. of Construction. Engineering, Purdue University, West Lafayette, Ind. (1992)
5. Zayed, T. M.. "Assessment of Productivity for Concrete Bored Pile Construction", Ph.D. Dissertation submitted to the Construction Engineering and Management Division, School of Civil Engineering, West Lafayette, Indiana, USA. (2001)
6. Lutz, J. D., Halpin, D. W., and Wilson, J. R.. "Simulation of Learning Development in Repetitive Construction", Journal of Construction Engineering and Management, ASCE, 120(4), 753-773. (1994)
7. Abourizk, S. M., and Halpin, D. W.. "Probabilistic Simulation Studies for Repetitive Construction Process", Journal of Construction Engineering and Management, ASCE, 116(4), 575-594. (1990)
8. Hijazi, A., Abourizk, S. M., and Halpin, D. W.. "Modeling and Simulating Learning Development in Construction", Journal of Construction Engineering and Management, ASCE, 118(4), 685-700. (1992)
9. Ioannou, P. G., and Martinez, J. C.. "Comparison of Construction Alternatives Using Matched Simulation Experiments", Journal of Construction Engineering and Management, ASCE, 122(3), 231-241. (1996)
10. Law, A. M., and Kelton, W. D.. Simulation Modeling and Analysis. 3rd Edition, The McGraw-Hill, USA. (2000)
11. Mohieldin, Y. A.. "Analysis of Processes with Nonstationary Work Task Duration", Ph.D. Dissertation, University of Maryland, College Park. (1989)
12. Touran, A.. "Modeling Uncertainty in Operations with Nonstationary Cycle Times", Journal of Construction Engineering and Management, ASCE, 117(4), 728-735. (1991)

# THE COST OF QUALITY IN THE EGYPTIAN CONSTRUCTION INDUSTRY

**Adel El-Samadony, Hany El-Sawah**
*Civil Engineering Department, Faculty of Engineering, Helwan University*

**Mohamed Ibrahim Farrag**
*Housing and Building National Research Center*

## ABSTRACT

The effect of non-conformance in quality leads to time and cost overruns in projects. Thus, in order to improve the performance of projects it is necessary to identify the causes and costs of poor quality.

The research presented in this paper quantifies the causes, magnitude and costs of quality experienced in the Egyptian construction industry. The causes and costs of quality in the projects are analyzed and discussed.

The mean expenditure on quality in the Egyptian construction firms is about 26 % of total cost, and the internal failure cost is about 10% from total project cost. The key to continuing success in quality management is the ability to collect poor quality information to improve the performance of the construction process. This information should then be incorporated into the design and management of the new projects. This information can also be used to measure the performance of construction firms so that continuous improvement is based on measurement of performance can be effectively implemented.

## INTRODUCTION

It is widely accepted in the field of management that progress through the application of the principles of quality can, and indeed must, be measured. However, quality measurements vary depending on the application, and as such there exists no universally applicable set of standards. Moreover, progress through the application of quality principles can only be measured by monitoring process improvements and the variation of outcomes and results. Consequently, the evaluation of the degree of success in quality implementation involves the review of the overall organizational success.

It will be impossible to control or mange quality without measure it to determine if the required level of the quality achieved and to provide a sufficient basis for taking action.

Quality cost was presented as one of quality measurement; Juran (Lundvall and Juran, 1974) considered that once quality costs had been identified and were being reduced many associated costs could be reduced as well. Cost Of Quality (COQ) systems are bound to increase in importance because COQ-related activities consume as much as 25 percent or more of the resources used in companies (Ravitz, 1991). The value to a company of conducting a quality cost analysis is to focus on its processes and their measurement and non-value adding activity to highlight waste in terms of a monetary unit of analysis and pinpoint potential improvements. (Roden&Dale2000)

Porter and Rayner (1992) shows that these costs oscillate between 4 and 25 per cent of sales, the average being 18 per cent., while Abed and Dale (1987) show similar data with quality costs as a percentage of sales turnover averaging 9.2 per cent, and ranging from 2 to 25 per cent. Several studies conducted to evaluate the magnitude of quality cost and failure quality cost in

the construction industry. The construction industry institute (CII) introduced in 1990 the QPMS to measure the cost of quality in the construction industry, Ledbetter tracked by QPMS the cost of quality as 11.2 of total labor expenditure (1994), while Barber (2000) determined the cost of failure only in two project as 16 percent of total cost in scheme 1 and 23 percent of total cost in scheme 2, while Willis (1995) stated that the total cost of quality as a percentage of the total labor expenditures (design plus construction) at the time of mechanical completion was 12.0 per cent. This 12.0 per cent was made up of 8.7 per cent prevention and appraisal and 3.3 per cent deviation correction.  The quality cost recognizes as challenge face the construction industry in many countries due to its harmful effect on the cost , time and quality of the construction projects , it is estimated that the cost of producing the required quality constitutes 15 per cent of the total cost of industrial construction  (Ledbetter 1989). While The Construction Industry Development Agency in Australia (CIDA (1995) has estimated the direct cost of rework in construction to be greater than 10 per cent of project cost.

In Norway, Sjoholt (1988) suggestion that total quality cost is about 25 % for Norwegian projects. In Singapore, the Construction Industry Development Board (CIDB) entitled Managing Construction Quality, an average contractor was estimated to spend between 5-10 per cent of the project costs doing things wrong and rectifying them (1989). The pervious studies clearly show the need for a system to identify and measure the quality cost in the construction industry, without a formal systematic quality management system in place, quality deviations may not be identifiable. Consequently, information is lost and activities that need to be improved in order to reduce or eliminate rework cannot be ascertained. (Davis 1989)

The BRE (1982) stated that 15 per cent savings on total construction costs could be achieved through eliminating rework, and by spending more time and money on prevention.  This paper describes the results of a questionnaire survey on the issue of the cost of quality in the Egyptian construction industry.


## PILOT STUDY

A pilot survey was conducted as pre-test sample . The purpose of this pre-test is to discover the shortcoming and the ambiguous of the questionnaire. The pilot survey consists of (6) questionnaire forms and, this pilot study was carried out by interviews with respondents to study their responds, recommendations and suggestions about questionnaire contents and ease to use.

The main purpose of this pre-test sample was to identify how respondents would react to the issue of cost of quality failure in the construction industry. Every respondent agreed that it is important to collect quality failure cost. The results showed that no effort had been made to measure the cost of quality or quality failure in the Egyptian construction industry.


## THE SURVEY

The questionnaire is randomly distributed on the professionals in the construction firms. A total (74) out of (120) distributed questionnaire were returned, (12) of the received were spoiled due to irrelevant or incomplete data. Finally (62) questionnaire was left for analysis (a response rate of 51 %).

The questionnaire was carefully distributed on experts in the Egyptian construction industry, mainly project managers and quality managers. The analysis of respondent body shows that an average of (15) years of the respondents experience in the construction field. This shows the confidence of their answers.

The questionnaire has been divided into four main parts as following:
    A) Quality cost knowledge
    B) Quality cost expenditure in construction firms
    C) Classification of quality cost by causes, responsible, …etc
    D) Application of quality cost information in construction industry

**A-Quality Cost Knowledge**

As a part of analyzing the current situation in a company with respect to quality costing it is necessary to assess the basic understanding of the language of quality costs and the principles underlying the concept across all levels of the organizational hierarchy. (Roden& Dale2000)

**Quality Cost Definitions**

In order to assess respondents' knowledge, The respondents were asked to say their beliefs about the dominated quality cost definitions in their firms, the respondents could choose more than one choice. Fig. 1 shows the frequencies of different respondents opinion about quality cost definitions.
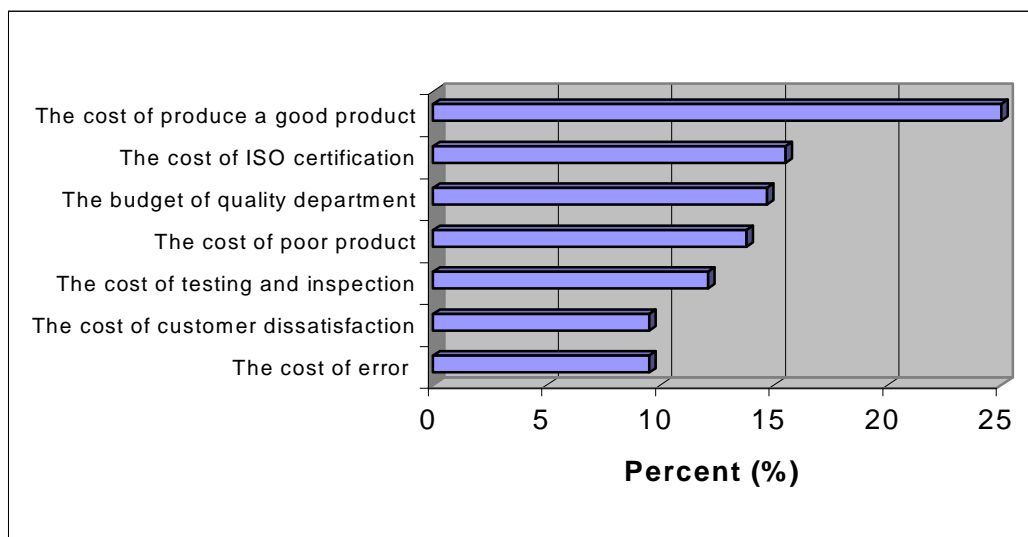


**Fig. 1: Definitions of the Cost of Quality**

From the results it can be noticed that the common quality cost definitions in the Egyptian construction firms is "the cost of producing a good product" because 46.8% of respondents agreed there firm used this definitions.

**The Definitions of Categories of Quality Cost**

Feigenbaum (1951) introduced the prevention, appraisal and failures (PAF) model, He divided the cost of quality into four categories prevention cost, appraisal cost, internal failure cost and external failure cost. Oakland (1993,) describes these costs as follows:

- **Prevention costs:** These costs are associated with the design, implementation and maintenance of the total quality management system. Prevention costs are planned and are incurred before actual operation.
- **Appraisal costs:** These costs are associated with the supplier and customer's evaluation of purchased materials, processes, intermediates, products and services to assure conformance with the specified requirements.
- **Internal failure costs:** These costs occur when the results of work fail to reach designed quality standards and are detected before transfer to customer takes place.
- **External failure costs:** These costs occur when products or services fail to reach design quality standards but are not detected until after transfer to the customer.

To inquire the respondents knowledge about various terms associated with quality cost, each respondents were asked to choose the appropriate definition of the different elements of the

cost of quality (prevention, appraisal, internal and external failure) from four similar definitions, Fig. 2 represents the percent of correct definition for each categories.

Out of (62) respondents, 46.8% agreed to the valid definition of prevention, 33.9 for appraisal, 37.1 % for internal failure and 32.3 for external failure. It can be noticed that less than 50% agreed to the valid definitions . It is clearly that there is lack of awareness and knowledge
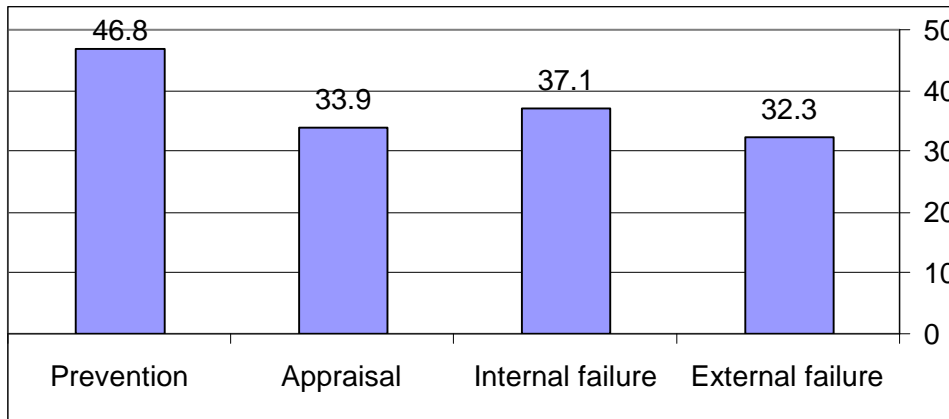


**Fig. 2: The Percent of Correct Definition of Quality Cost Categories**

about the cost of quality terms in the Egyptian construction industry even between the quality experts.

## B- Quality Cost Expenditure in the Construction Industry

The cost of quality as a percentage of construction firms budget is investigated, the respondents were asked to estimate the quality cost in their firms (both conformance and non-conformance cost), The analysis of the results shows that the mean expenditure on quality in the Egyptian construction industry is about **26 %** of the total project cost. This conclusion is compatible with other researches work to estimate the cost of quality like (Barber (2000) who said that the direct costs (of rework) have been found to be as high as 25 percent of contract value, While Hart (1994) claims that more than 25 per cent of the costs can be cut from most constructed facilities through the use of a good, sound quality program. and Sjoholt (1988) who suggested that total quality cost is about 25 % for Norwegian projects.

The quality cost is classified according to PAF model into four Categories (Prevention, Appraisal, Internal failure, and External failure) .The respondents were asked to estimate the cost of each category as a percentage from total quality cost of the firm.

From the results it shown that the most quality cost expenditure on internal failure cost about (39.1 %) from total quality cost, while external failure (22.5%), (19.9%) for prevention cost, and (18.5%) for appraisal cost as shown in Fig. 3.
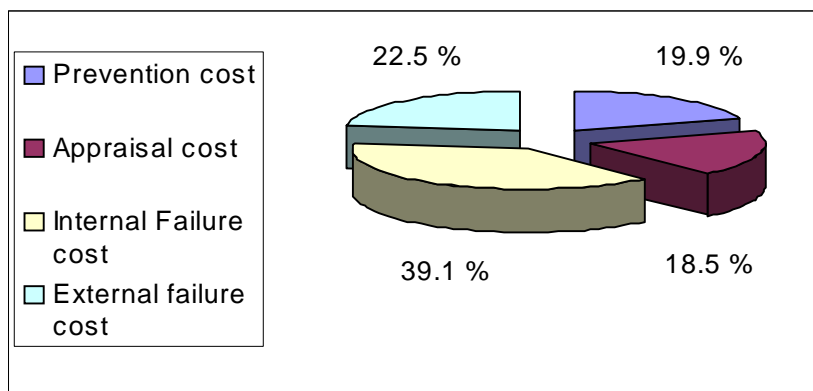


**Fig. 3:  The Quality Cost Categories**

It is obviously clear from the analysis, the internal failure cost consumed the highest percentage of quality expenditure about 40%, while the non-conformance cost is 61% from total quality cost, and the internal failure cost is about 10% ( internal failure percent (39.1 ) * total cost of quality (26) ) from total project cost. This is compatible with other researches work to `estimate the failure cost in the construction project like Nylen (1996) who found that quality failures were to be 10 per cent of the contract value, Cnuddle (1991) who found non-conformance cost to be between 10 per cent and 20 per cent of the total project cost and The Construction Industry Development Agency in Australia (CIDA (1995) has estimated the direct cost of rework in construction to be greater than 10 per cent of project cost.

The saving in the non-conformance cost will significantly effect the cost of construction project and increase the competitive ability of the Egyptian construction firms.

### 3-C-Classification of Quality Cost in the Construction Industry

The cost of quality information should be used to focus on the quality problems and lack of quality system in the construction firms, and to promote an awareness and understanding of the quality process. In order to enhance the understanding of quality cost information in the construction industry the questionnaire investigates some issues like the responsibility of non-conforming quality in the construction firms , the value and occurrence of quality problem in the project phases and the causes of quality failure in the construction  industry

### C.1 The Responsibility of each Stakeholder for Non-Conforming Quality on the Projects:

The respondents were asked to say their beliefs about the responsibility of each of the stakeholders such as the owner, the designer, the consultant, the contractor, the sub-contractor and the supplier on the occurrence of quality failures in the construction industry, they were asked to say their beliefs on five ranked scale from " is not responsible " to " very responsible". The following table shows the percentage of respondent's answers.

**Table 1: The Responsibility of each Stakeholder for Non-Conformance Quality**

|  | Percent | | | | |
|---|---|---|---|---|---|
|  | Do not responsible | Rarely responsible | Sometimes | Responsible | Very responsible |
| The owner | 45.2 | 32.3 | 19.4 | 0.0 | 3.2 |
| The designer | 0.0 | 16.1 | 51.6 | 24.2 | 8.1 |
| The supervisor consultant | 0.0 | 8.1 | 33.9 | 38.7 | 19.4 |
| The contractor | 0.0 | 0.0 | 8.1 | 32.3 | 59.7 |
| The sub-contractor | 0.0 | 6.5 | 16.1 | 22.6 | 54.8 |
| The supplier | 9.7 | 24.2 | 22.6 | 33.9 | 9.7 |

Bar chart in Fig. 4 shows mean values (1-5 where 1 means do not responsible, 2: rarely responsible, 3: responsible, 4: widely responsible, 5: totally responsible.) that indicate the responsibility of quality failure in the construction industry.

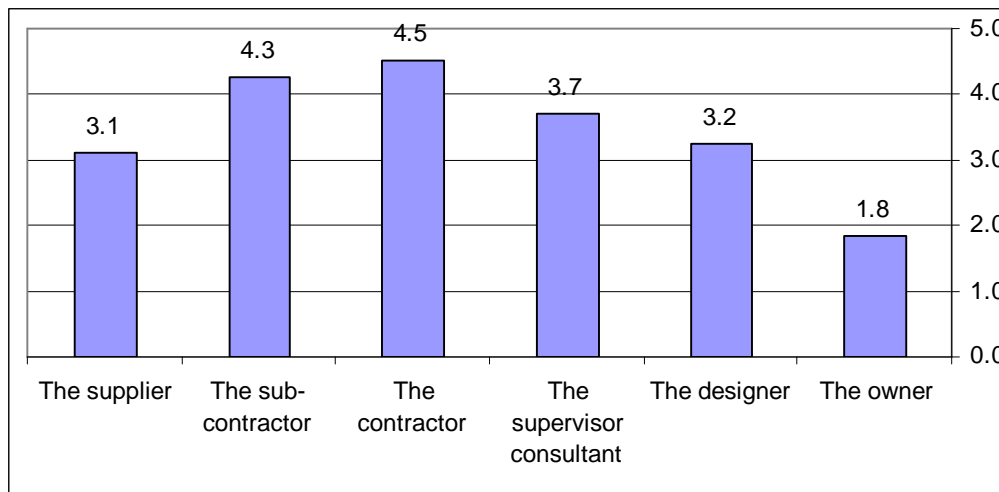**Fig. 4: The Responsibility of each Stakeholder for Non-Conformance Quality**

From the results, the most responsible for quality failure in the construction industry is the contractor with average score (4.5), then the sub contractor with average score (4.3), the consultant with average score (3.7), the designer with average score (3.2), the supplier with average score (3.1), the least responsible is the owner with average score (1.8). This reflect the urgent need for a new supply chain and procurement relationship among construction participations in order to achieve the required performance, and reduce the magnitude and occurrence of poor quality in the construction industry.

### C.2 The Cost and Occurrence of Quality Failure according to Project Phases:

The respondents were asked to state the occurrence of failure during each of the design and construction stages then to estimate the cost of failure because of each phase. Table 2 shows the results of quality failure occurrence in both construction and design stages .

|  | Percent of failure occurrence | | | | |
|---|---|---|---|---|---|
|  | Not | Rarely | Sometimes | Often | Always |
| Design stage | 0 | 2 | 34 | 21 | 5 |
| Construction stage | 0 | 0 | 3 | 23 | 36 |

For mean value (1-5) indicates the design stage with average score (3.5), while the construction stage with average score (4.5), this indicates that the most failure occurrence in the construction stage.

Then the respondents were asked to estimate the cost of quality failure in each stage of the project. Fig. 5 represents the results. The most cost of failure is on construction stage about 67% from total failure cost, while the design stage is responsible for only 33 % of total failure cost in the construction industry. This regards that the failure in the construction process could be more costly because it consumed material, time, equipment and labor.
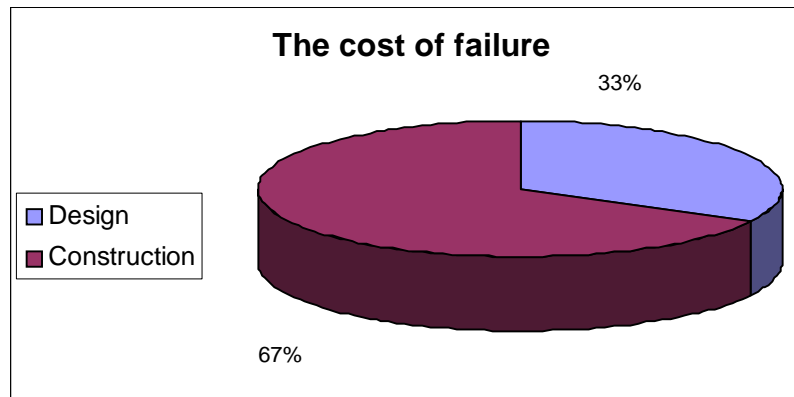
**Fig. 5 The Quality Failure & Construction Phases**

### C.3 The Causes of Non-Conformance Quality in Construction Industry:

The respondents were asked to identify the causes of quality failure in their firms. For mean value (1-5) indicates, the design error with average score 3.5, the execution error with average score 4.2, the planning error with average score 3.1, the communication error with average score 3.1, the equipment with average score 2.4, the defect material with average score 3.1, the supplier with average score 3.3, the personal error with average score 2.1, the geo-technical error with average score 1.8, the theft with average score 1.7, the external factors with average score 2.3 as shown in Fig. 6.
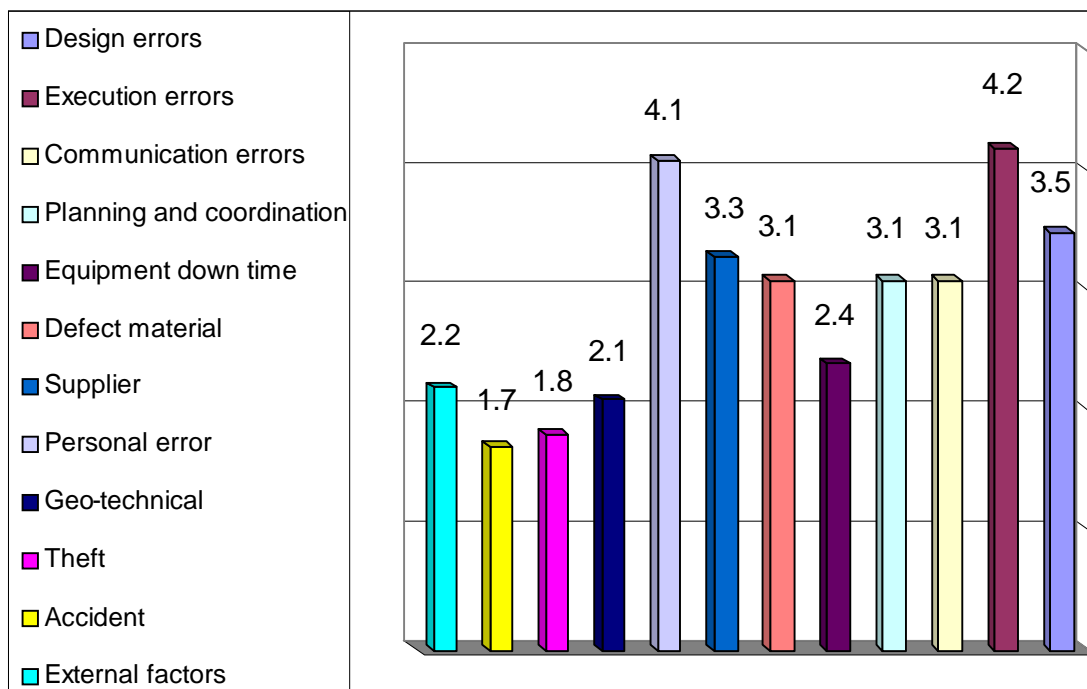


**Fig. 6: The Causes for Quality Failure**

From the results, it can be noticed that the most causes of quality failure in construction industry are execution errors, personal errors and design errors respectively. The result shows that care should be taken in the areas of quality procedure and training to decrease execution and personal errors in the construction industry.

### D-Application of quality cost information in construction industry

Juran described the concept of quality costs as "gold in the mine" because the quality cost system provide the manger with a valuable information about the performance and efficiency of the organization and the opportunity for improvement, in the next part the beliefs of the respondents were investigated about the use of quality cost data in the construction industry.

### D.1 The Cost of Non-Conforming Quality as Performance measurement for the Construction Firms:

The respondents were asked to say their opinion about the ability of using the cost of non-conformance quality as a performance measurement in the construction firms. The answers show that only 6.5 % of the respondents said that the cost of non-conformance can not be used as a performance measure in the construction firms, 8.1 % stated that the cost of non-conformance may be used poorly, 27.4 % stated that it is considered fairly as performance measurement, and 33.9% stated that it is a good performance measurement, while 24.4% agreed completely the ability of cost of non conformance quality as performance measurement. For mean values (1-5) indicates the ability of using cost of non-conformance as performance measurement with average score 3.6, this reflect agree of respondents the ability of quality cost as performance measurement in the construction firms.

### D.2 The Quality Cost Measurement System and the Development of Construction Industry:

The respondents were asked to state their beliefs about that the quality measurement system assists the process of development the construction industry. (32.3 %) of respondents agreed completely that the existence of quality measurement system assists the development of the construction industry, (43.5%) said that it is pretty much assist, (17.7%) of respondents stated that it assists to some extent, (6.5%) stated it rarely assists, and no one of respondents stated that there is any effect of the quality measurement system in the assist of the development of the construction industry, the mean value of respondents is 4 reflecting the agreement of respondents on the role that the quality measurement system could be done in the process of development the construction industry.

### D.3 The Quality Failure Analysis:

The respondents were asked about the ability of using the information from the process of analysis and study the quality failure to prevent the repetition of those failures in the firm's projects and as a tool for development process. Almost two thirds of respondents (64.5%) completely agreed to the ability of using quality failure information to aid in preventing failure in the future projects, while about the third of the respondents (32.3%) faraway agreed to the using of it. These results reflect the agreement of respondents about the importance of quality failure information to aid in preventing the recurrence of the same failure in the reaming part of the project and in the other projects of the firm.

## SUMMARY & CONCLUSION

This paper focuses on investigation the views of the quality experts in the construction industry about quality cost by means of questionnaire. The results of the survey demonstrate that the lack of understanding of quality cost definitions even between the quality and project management experts, there is urgent need to improve the knowledge and awareness of quality cost terms in the construction industry.

The costs of quality in the Egyptian construction industry was evaluated by means of field survey and interview with quality and project management participated in the construction process, the analysis of the results shows that the mean expenditure on quality in the construction industry is about 26% of the total project cost. Also the results show that the most

quality cost expenditure on internal failure cost about (39.1 %) from total quality cost, while external failure (22.5%), (19.9%) for prevention cost, and (18.5%) for appraisal cost.

The most responsible for quality failure in the construction industry is the contractor, and the sub contractor respectively. This reflects the urgent need for a new supply chain relationship among construction participations. Also the results show that the most causes of quality failure in construction industry are execution errors, personal errors and design errors respectively.

The survey highlighted the important of using quality cost information to assists the process of development the construction industry and to prevent the recurrence of the same failure in the reaming part of the project and in the other projects of the firm.

## REFERENCES

1. Ravitz, L. (1991), "The cost of quality: a different approach to no interest expense management", Financial Managers' Statement,.
2. Roden. S, Dale. B.G.(2000), Understanding the language of quality costing ., The TQM magazine Vol. 12, No 3.
3. Abed, M.H. and Dale, B.G. (1987), "An attempt to identify quality-related costs in textile manufacturing", Quality Assurance,.
4. Porter, L.J. and Rayner, P. (1992), "Quality costing for total quality management", International Journal of Production Economics,.
5. CIDB (1989), "Managing construction quality", A CIDB Manual on Quality Management Systems for Construction Operations, Construction Industry Development Board, Singapore.
6. CIDA (1995), Measuring up or Muddling through: Best Practice in the Australian Non-Residential Construction Industry, Construction Industry Development Agency and Masters Builders Australia, Sydney.
7. CII , " Quality performance management System : A blueprint for implementation " (1990) . CII Pub, Construction industry Institute.
8. Barber P. & Tomkins C.(2000)  "Quality failure costs in civil engineering projects "International Journal of Quality & Reliability Management.
9. Willis & Willis A quality performance management system for industrial construction engineering projects international journal of quality & reliability management 1995.
10. Davis, K., Ledbetter, W.B. and Burati, J.L., "Measuring design and construction quality costs", Journal of Construction Engineering and Management, ASCE, 1989.
11. Sjoholt, O. (1988) Quality management system in construction. Norwegian Building Research Institute, Oslo, Norway.
12. BRE (1982), Quality in Traditional Housing "An Investigation into Faults and their Avoidance, Building Research Establishment, Garston.
13. Feigenbaum, A.V. (1951), Total Quality Control, McGraw-Hill, New York, NY.
14. Oakland,J.S.1993 total quality management, Butterworth Heinemann, UK.
15. Hart, R.D. (1994), Quality Handbook for the Architectural, Engineering and Construction Community, Quality Press, Milwaukee, WI.
16. Barber, P., Graves, A., Hall, M., Sheath, D. and Tomkins, C. (2000), ``Quality failure costs in civil engineering projects'', International Journal of Quality and Reliability Management,.
17. Nylen, K.-O. (1996), ``Cost of failure in a major civil engineering project'', Licentiate thesis, Division of Construction Management and Economics, Department of Real Estate and Construction Management, Royal Institute of Technology, Stockholm .
18. Cnuddle, M. (1991), ``Lack of quality in construction & economic losses'', Proceedings of the European Symposium on Management, Quality and Economics in Housing and other Building Sectors, Lisbon.

# PRAGA, THE VESTIGIAL TWIN CITY OF WARSAW: ITS UNIQUE QUALITIES AND FUTURE PROSPECTS

**P.J. MARTYN**

*Institute of Art, Polish Academy (IS PAN), 26/28 Długa Street, 00-950 Warszawa, Poland, tel. 48/22/ 504-82-36, peter.martyn@ispan.pl*

## ABSTRACT

Warsaw is an overwhelmingly modern agglomeration that was 'rebuilt', but to a very much greater extent replanned and thus essentially redefined, following the mass slaughter and physical destruction of the 1939-1945 'world' war. Having been condemned to systematic demolition by the Nazis, the *urbs prima* of Poland was then 'rebuilt' and 'redeveloped' as a major diversion on the 'domestic front' from the 'cold war'. The 'socialist city' – with a functional layout inherited from the modernist movement and a grand-urban architectural profile as reminiscent of Speer's Berlin as Stalin's Moscow – remained largely on paper, but the pre-war city, with, its unique social-cultural *mélange*, was all but completely sacrificed.

Substantial remnants of the 'lost' metropolis predating the 'Great War' of 1914-1918 survived on the opposite, eastern side of the River Vistula, in a cluster of districts and neighbourhoods referred to collectively by the name of Praga. The previously mixed residential quarters under investigation form a microcosmos that links the modern agglomeration with its enigmatic, multicultural and multi-ethnic past. East-bank Praga's strongly pronounced 'otherness' reflects its geographical isolation from West-bank Warsaw. Inadvertently reinforced by the abortive urban planning and social policies of the defunct 'Polish People's Republic', this urban divide is so pronounced that the modern agglomeration should be viewed as two contrasting built and social environments: the greater metropolitan area (Warsaw) and its  vestigial enclave inherited from the past (Praga). The inner East-Bank districts now face complete assimilation within the Main City. Investment in commercial and 'luxury' residential construction, which has altered dramatically the skyline of 'downtown' Warsaw, now threatens to transform beyond recognition the declining social structure and building stock of Praga. While 'regeneration' in this classic case of inner-urban decay is well under way, the implications both for the area and its inhabitants are highly ambiguous, and thus disturbing.

Emphasis must be laid on the historical dimension of Praga's historical separateness and its relevance as such to the urbanity of Warsaw. Endeavours to reinvigorate a localised sense of place and identity among the residents of Praga, known as the *Prażanie*, as well as restore the area's pre-war architecture, are of paramount importance to tempering the volatile, highly competitive urban habitat the more excessive forces released by 'free-market' economics have given rise to since the 1990s. This text expands on themes from papers delivered at the Bibliotheca Alexandrina [9] and Chalmers University, Göteborg [12] in spring and summer 2005. Issues relating to 'revitalisation' in Warsaw's inner East-bank quarters are addressed specifically to readers familiar with the broad question of protecting and actively helping to keep alive areas of the city inherited from the past. The formidable and growing pressures faced by architects, municipal administrators, academics and inhabitants who are able and willing to confront the danger posed by the more destructive realities of modern metropolitan existence would appear to be remarkably similar wherever they are encountered.

## METROPOLIS OF PARADOX: THE POLISH & JEWISH QUESTIONS

The extraordinarily ambiguous history of Poland – for centuries a land regarded by the followers of Judaism as a temporal haven to await the Second Coming – is more readily comprehendible if treated as a great enigma; and one that reached its appalling climax in the 20th century. As a country shaped primarily by geopolitical circumstance, Poland is more readily beheld by its own people as an idealised vision than a tangible geographical entity. An unhappy succession of seasonal states harking back to the original *Respublica*, which was removed from the political map in three successive series of partitions towards the end of the 18th century, has continued to the moment of writing [27i]. 'Resurrected' in 1918 as the Second *Rzeczpospolita* to be again overrun by occupying powers in 1939 before reappearing on the map in 1944 as a 'People's *Respublica*', the next reconstitution of 'Poland', as the Third Republic, coincided with the supposed turning point in world history as symbolised by the fall of the Berlin Wall in 1989. At the initiative of a minority-elected and apparently inept political leadership, a fourth Polish Republic was declared as recently as October 2005.

Marred no less than it was moulded by the same historical processes, emerging as a sizeable and rapidly modernising urban centre during a period when the country it was supposed to serve as capital did not possess its statehood, Poland's principal city is best understood as a metropolis of paradox. Dependent in pre-modern times on the Latin name *Varsovia*, which gave rise to the French *Varsovie* and the Italian *Varsavia*, the modern English variation on the Polish Warszawa (pronounced *Var-shava*; i.e almost identically to the Russian *Варшава*) comes from the German derivation: *Warschau* (compared to the Yiddish *Varshe*). The historically-grounded Arabic name: (which transliterates as Wiiso) is pronounced 'wee-so' [1]. Throughout much of its post-mediaeval history Warsaw has been a political battleground. Questions of an essentially urban character have taken second place to, or been actively subdued by, issues of an overwhelmingly ideological nature – with dire consequences for the well-being of the city's inhabitants, its physical environment, architectural heritage and cultural identity [13].

One hundred years ago, however, not only did Warsaw figure among the largest cities of Europe, its future seemed assured as one of the most dynamic urban centres in the world at large. As third metropolis within the Russian Empire and first city of a country which had long since ceased to function as an independent territorial body, this was a city of tremendous cultural as well as social confrontation. At the height of his wealth and influence the entrepreneur and diplomat Ferdinand de Lesseps expressed his conviction that Warsaw was destined to be one of the truly great cities of the future. In a technically advanced world transcending the malevolent hostilities of the age of nationalism, and with the Russian imperial colossus opening up to the industrial revolution, Warsaw evidently occupied a key nodal location between Europe and Asia. As a *Weltmetropole* and vital hub of intercontinental exchange, with a population set to exceed a dozen million by the dawning of the New Millennium, Warsaw, he declared, would surpass in size and importance Moscow, Berlin, Vienna and even Paris [10].

In spite of restrictions imposed by the tsarist military on its spatial growth, the city was already developing in precisely such a direction. From the early 1860s, the vast Russian market had been opened to imported goods from the truncated central-western provinces of pre-partition Poland (referred to after the Napoleonic Wars as the Congress Kingdom). Conceived in counter-reaction to the abortive uprisings of 1830-31 and 1863-4, the concept of 'organic work' was widely supported by Polish reformers and acculturating Jewish entrepreneurs. Social justice and international reconciliation, it was claimed, would be achieved by means of technological progress, material improvement and education. Rejection of the Romantic insurrectionary tradition, with its irrational notions of Polish national messianism, was part of an altogether wider movement to emancipate Russia through modernisation [11]. As elsewhere, industrialisation was hugely accelerated by the coming of the railways. At Warsaw the wide-gauge system unique to Russia linked up with standard-width lines leading to Vienna, the Prusso-German Baltic

Coast and also, albeit indirectly, Berlin. While no other city of Central-Eastern Europe could rival the its economic potential, in a century dominated by international conflict the strategic importance of such a crossroads and focal point was to bring catastrophic results.

**Table 1: Comparative Demographic Change in Fifteen Major Urban Agglomerations***

| A | B | C | D | E | F |
|---|---|---|---|---|---|
| urban agglomeration | 'million city' in or since: | population 1939-41 | Population in 2005* | proportion of state populace | rank in Europe |
| **Rome** | 100AD, 1921 | 1,400,000 | 3,800,000 | 6.6% | 10 |
| **London**\*\* | 1801 | 8,615,050 | 12,300,000 (18,542,746) | 20.7% (31.7%) | 2 (1) |
| **Paris** | 1836*** | 4,800,000 | 11,331,000 | 19.0% | 3 |
| **Vienna** | 1860s | 1,771,000 | 2,320,000 | 28.3% | 22 |
| **Berlin** | 1870s | 4,339,000 | 4,200,000 | 5.1% | 9 |
| **St. Petersburg** | 1890s | 3,015,000 | 5,881,000 | 3.9% | 5 |
| **Moscow** | 1901 | 4,536,000 | 13,200,000 | 8.9% | 1 (2) |
| **Constantinople** | 1910 | 794,000 | 11,000,000 | 16.5% | 4 |
| **WARSAW** | 1913**** 1925,1951 | 1,307,000 | 2,200,000 | 5.7% | 25 |
| **CAIRO** | 1927 | 1,750,000 | 16,000,000 | 23.0% | (1)***** |
| **Madrid** | 1920s | 1,300,000 | 5,150,000 | 12.9% | 6 |
| **Budapest** | 1930 | 1,165,000 | 2,591,000 | 25.7% | 18 |
| **Bucharest** | 1941 | c.950,000 | 2,200,000 | 9.8% | 24 |
| **Athens** | post-1945 | c.600,000 | 3,600,000 | 29.7% | 12 |
| **Alexandria** | post-1952 | c.600,000 | 5,000,000 | 7.2% | (5)***** |

\*      from various statistical sources, incl. rounded estimations, esp. for 1939-41 and varying definitions of metropolitan and urbanised areas extending beyond the city limits in 2005
\*\*     Greater London area for 1801 (bracketted figure for the 'Greater Metropolitan Area' is based on the 2001 national census and this author's definition of its functional area)
\*\*\*    within the current *Boulevard Periphérique*
\*\*\*\*   including the suburban periphery of the Greater Warsaw urban area, set up in 1911-16
\*\*\*\*\* Cairo & Alexandria are ranked among the cities of Africa

Far from solving the issues afflicting the first city of a stateless country, the potent mixture of *laissez-faire* capitalism with Positivist pseudo-philosophy, confounded by vacilations between reformist and reactionary policies in St. Petersburg aggravated an already antagonistic state of affairs. Accelerated, and in large measure unregulated, industrialisation combined with intensifying property speculation led to extreme social polarisation. Furthermore, tsarist coercive policies aimed specifically at confining Jewish habitation to a 'Pale of Settlement' further exacerbated ethnic tensions, especially in the bigger cities. Apart from being the fulcrum of the highly vexed Polish Question, Warsaw became home to the largest Jewish population in the Old World. Known disparagingly as 'Litvaks', a very significant proportion of the city's Jewry did not originate from Central Poland but the eastern territories of pre-Partition Poland (i.e. today's Ukraine, Belarus, Western Russia and Latvia as well as Lithuania). In response to the vicious and widespread pogroms that heralded the reactionary reign of tsar Alexander III (1881-94),

'Lithuanian' Jews in their hundreds of thousands emigrated to what the russifying bureaucrats of St. Petersburg called the Vistula Provinces. Since 'the Jews' were already regarded in certain 'patriotic' circles and political groupings as undermining the country's cultural and ethnic identity, anti-Semitism unavoidably became a corner stone of Polish nationalism. Be that as it may, the intricate history of Jewish life and labour in Warsaw – and particularly in Praga – draws its origins from the Middle Ages [16].

Throughout much of the second half of the 19th and first years of the 20th centuries Warsaw was in a state of constant flux. The failings of industrialisation had rapidly come to light as the brutally exploitive aspects of 'unfettered capitalism', practised in a land under colonial rule and the official corruption encouraged by that kind of overlordship, made their impact on urban fabric and society alike. The detrimental effects of unrestricted urban accretion, already observed in other major continental cities, thus also shaped the social geography of Warsaw [8]. All in all, at the start of the 20th century Warsaw was one of the most dynamically growing, but by the same measure one of the most potentially explosive, cities in the Russian Empire. It was also home to cosmopolitan-minded propagators of humanity's ethical, moral and philosophical development, as well as scientific innovation. Thus, deeply rent by social conflict, ethnic tensions and political ferment though it was, Warsaw was also emerging as a centre for mutual human understanding and inter-cultural reconciliation on a world scale [7].

In the year 2004, with a population and market exceeding that of the other nine acceding states combined, Poland was accepted as a full member into the European Union. Despite a much enhanced political status as the capital city of a sovereign country, in contrast to that of ninety years before, Warsaw just scraped in at the bottom of the list of 25 most populous urban agglomerations among the expanded economic community's 25 member states. The rudimentary statistics recorded in the table above clearly reflect the disruptions inflicted on Poland's tragically awesome first city since 1914.

## PRAGA, INNER-URBAN PARADIGM OF A METROPOLITAN PARADOX

Urban civilisation in the low-lying plains extending from middle-eastern Germany through much of central Poland into the Pripet marshlands of southern Belarus and northern Ukraine would have begun to evolve around five times more recently than in the lower Nile valley. The impact of the River Vistula, as a natural barrier no less than a communication route, on Warsaw's spatial plan bears comparison with the way the Nile shaped the urban layout of today's Greater Cairo. Partly because the courses of both rivers were liable to erratic change, the earlier corresponding stages of concentrated human inhabitation in the areas occupied by the present-day Polish and Egyptian capitals featured a succession of settlements in various locations. If the focus of urban life in post-antiquity Cairo shifted from one side of the Nile to the other, archaeological evidence in the Warsaw area suggests that settlement was initially more advanced on the eastern rather than the western side of the Vistula. The low-lying right- (i.e. east-) bank fortified palisade of Bródno and market townships of Kamion, Targowe Małe and Targowe Wielkie are known to have existed centuries before the merchants' town that was founded as late as 1300. The privileged status of this rationally laid-out *Kolonialstadt* is clearly indicated by the fact that Praga and the neighbouring township of Skaryszew were granted municipal charters over three centuries later than Warsaw's mediaeval 'Old Town' (marked 'Stare Miasto' in map I).

What amounts to a conflict in urban culture and identity draws its origins in the deep sense of entrenchment that would have existed among the socially distinct and economically well-organised burgher population of pre-modern Warsaw in relation to the potentially unruly populace of the surrounding region. The string of market settlements organically developing on the opposite side of the Vistula that came to be known by the single name of Praga played a significant and mutually beneficial role in the province of

Mazovia. The retrogressive imposition of a 'manorial' economy, controlled by polonised magnate clans and semi-moribund nobility (*szlachta*), undermining monarchical authority but above all urban power and influence [19], explains the Poles' failure to play an actively formative role in modern European history. The mounting political disasters of the 17th and 18th centuries sealed the country's extraordinary fate. On the one hand, Poland became a battle zone between peninsular Europe's expansion into the East and periodic invasions from the Euro-Asian hinterland – typically interpreted as threatening to annihilate 'Western' (European) civilisation for ever. On the other hand, in an age of growing international understanding nurtured by discovery, empirical observation and technological innovation, the territories of the partitioned *Respublica* of Poland-Lithuania lay at a vital watershed between East and West. The cultural as well as social, economic and political fusion of Orient and Occident, in which the so-called Polish lands might serve as a major crossroads, was confidently expected to transcend the colonial exploitation and petty nationalisms of the 19th century.
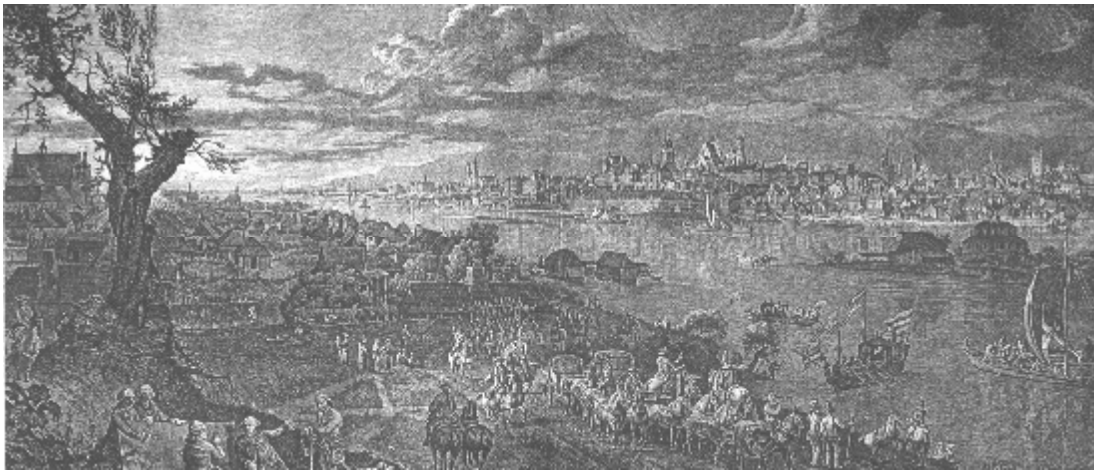


**Fig. 1a. Warsaw Seen From the Eastern Vistula Bank before the Polish Partitions**



**Fig. 1b. Panoramic Skyline of Central Warsaw, Summer 2005** (Phot.: P. Jamski, IS PAN)

The stark contrast between the Vistula's 'wild', unregulated eastern shoreline and the reinforced concrete embankment of its western riverfront is a symbolic reflexion of how Praga's urban history followed quite a different course to that of metropolitan Warsaw. Designated only recently the status of an ecological reservation, the naturally stabilising accumulation beyond the flood dyke is thus likely to remain a permanent feature. The skyline of central Warsaw embraces a profusion of reconstructed merchant-patrician houses, churches and palaces, which are seen as belonging very much to the Western-European architectural heritage. These buildings, dwarfed since the 1950s by the

Stalinist 'Palace of Culture and Science', which is now besieged by the tower blocks of a belated and diminutive American-style 'CBD', may be 'admired' from a vantage point uncannily reminiscent in its rusticity of a *veduta* from 1767 by the Venetian urban landscape painter, Bernardo Bellotto-Canaletto (figs. 1a, 1b).  At the same time the dense vegetation of this natural reserve at the very heart of the built-up area conceals almost entirely from view the East-bank districts.

Already sacked by a succession of invading armies from the mid-17th century, Praga was devastated and its inhabitants slaughtered at the close of the Kościuszko Uprising (1794) in order to intimidate the Main City into submission. At the express orders of Napoleon Bonaparte, most of what remained was cleared to make way for a citadel and maidan (1807-11). However, there are two significant points in Warsaw's history when circumstances took an unexpected turn in Praga's favour. The earlier reversal of fortunes occurred in the mid-1800s.  Newly regulated, then partly by default and partly through military intervention, the East-bank became a terminus for the St. Petersburg, Moscow and Danzig/Koenigsberg railways. Suspicions roused among the Polish middle classes that a 'russified' city on the river's eastern side might overawe the predominantly Roman-Catholic West Bank were further intensified by the investing of non-Polish capital to plan and build this 'new' Praga. In accordance, nevertheless, with practices long predating the Partitions, urbanisation was initiated by entrepreneurs and real-estate investors intent on securing social advance by adopting Polish language, customs and even religion. Praga rapidly grew from a group of ruinous hamlets containing barely 5000 inhabitants into a fan-like network of districts with a population by 1913 of 90,000. Just as tsarist army strategists were turning Warsaw at a key moment in its urban aggrandisement into a grotesquely oversized military fortress, Praga received the double blessing of a rational street plan and ample incorporation (1889). Until the Greater Warsaw metropolitan area, established from 1911 and crowned by the suburban incorporation of 1916, the right-bank districts, while accounting for just 10% of the population, covered one third of the otherwise minimally extended area under municipal administration (i.e. 945 out of 3275ha, including military terrain) [5]. On the other hand, regardless of the fortuitous conditions for property investment and industrial location, Praga's provincial and shtetl-like character tended merely to confirm many Poles in their conviction that it was a 'foreign and obnoxious … husk' [21] that compromised the 'European character' of Warsaw.

The second and far more dramatic twist of historical fate occurred in September 1944, when the East-Bank districts were 'liberated' from Nazi occupation at the height of the calamitous Warsaw Uprising. The built-up area of Praga – if certainly not its residents – was largely unaffected by the Ghetto Uprising of April-May 1943 and climactic confrontation of August-October 1944. As Varsovians were slaughtered in their tens of thousands and insurgents waged a quite hopeless battle with the vindictively resolute Nazi war machine, life for most surviving *Prażanie* was already returning to some kind of norm. Never had the two halves of the same metropolis been rendered so far apart by such overwhelming circumstances imposed from outside. Praga's confused and highly problematical modern history is impossible to understand without objectivised consideration of such vaguely defined factors which shaped its urban development. While the nonetheless limited benefits secured on the East bank were to the manifest detriment of West-bank Warsaw, the overriding determinant took the form of Russian-imperial dominance from the mid-19th and Russo-Soviet 'victory' over the Third Reich in the mid-20th centuries (figs. 2a, 2b). Only where they are perceived in juxtaposition with the Main City of Warsaw, with its quite distinct role of chief metropolitan centre of successive carnations of the Polish State, can Praga's contrasting urban-architectural and social-cultural qualities be fully appreciated and, moreover, comprehensive-ly analysed. Finding no trace of her past on the left bank, an Israeli writer's mother, revisiting

**Fig. 2a. Russian Orthodox (1860s) and Soviet Liberation Monument (1945);**
**Fig. 2b. Pachulski tenements and site of the Nowa Praga bazaar.** Author's photos, 1986

Warsaw in 1996 for the first time since she emigrated in the early 1930s, could discover that on Praga's Stalowa St. not only the house she once lived in and courtyard but even the staircase have remained unchanged [18]. But how can that kind of 'living past' be maintained in the present?

## FROM URBAN ATTRITION TOWARD 'REVITALISATION'

Any appraisal of the current state of affairs in Praga, with an aim to assessing its prospects for the future, must begin with a precise definition of what its name signifies in purely spatial terms. In the wake of the urban attrition under the four regimes of the People's Republic – prolonged well into the 1990s – that neither removed nor replaced altogether the prewar urban fabric, such fundamental topography relies very heavily on historical perspective. The administrative 'reform' of 1951, secured by architect-planners with full approbation from the Polish Workers' Party inner ranks, involved a vast incorporation (from 11,485 to 41,173 ha),  was to prove an unmitigated disaster for the city. The short-lived 'mid-town' right-bank district (*Praga Śródmieście*) was divided between the borough councils of Praga North and South which took on the responsibility of administering the entire eastern half of Warsaw. Covering 16,484 ha and subject to further enlargements into the 1980s, these two boroughs now extended some 30km along the Vistula. The historically-based perception of Praga had thus been as good as nullified. Demarcating in the mid-1990s an inner-central urban area (*Centrum*) did restore the Praga districts to the political map of the contemporary Polish capital, and yet this amalgamation of inner-urban boroughs embraces the cores of both sides of the river. The 'centre' of Warsaw has thus been expanded to envelope, and assimilate, not just the left-bank inner-urban districts of Mokotów, Ochota, Wola and Żoliborz but also Praga North and South. Defining what is meant by the name 'Praga' has never been a priority for these dual local borough councils, which must in any case comply with directives issued by Warsaw City Hall (*Ratusz*). The simple fact remains that the greatest harm to the city has been caused by the very body that is responsible for its administration, and equally the well-being of its citizens. The rudimentary question of territorial extent and internal administrative divisions (not even to mention urban-political status in relation to left-bank Warsaw) comprises a vital prior condition to urban regeneration and (alongside the much trumpeted politics of 'revitalisation') any solidly grounded policy of rehabilitating Praga socially.

Viewed on the contemporary map of Warsaw, in the author's opinion the districts of Praga ought to be broadly distinguished on the basis of a three-way territorial division between:

(1) those areas once comprising the mediaeval and early-modern settlements of Praga, Skaryszew and Golędzinów nearest the Vistula (i.e. Stara [Old] Praga, with Warsaw Zoo);

(2) neighbourhoods of mixed residential and industrial development laid out and built up from the 1860s down to 1914 and 1939 (Nowa Praga, the Szmulowizna and Kamionek);

(3) the postwar housing estates or piecemeal raising of state-allocated apartment blocks; i.e. the second, more recent 'Nowa' Praga (refer to map 1 overleaf).

Even while no architectural monument of mediaeval Praga (a chain of almost wholly wooden townships) has come down to modern times, the high road that formed the backbone of the pre-modern street network still bears a name that alludes to the origins of organised human settlement on this side of the river. Targowa (i.e. Market Street) is a living archaeological testimony to the market theory of urban genesis. A more intriguing example is the enduring, in spite of its absence from most 19th-century maps and directories, of Ratuszowa (Town Hall) Street, which recalls the separate municipal status of Praga (divided between bishop and magnate 'owners'). This retention of names from vestiges of the pre-industrial urban street plan proves how a sense of localised identity has persisted, and with it a *genius loci* that is indubitably *praskie*; i.e. of Praga, rather than of Warsaw (*warszawskie*) [cf.:2].

To encounter the true heart of Praga and what survives of its legendary folklore, it is necessary to move away from Targowa Street and visit the celebrated, but no less infamous Różycki Bazaar which has been threatened with closure for decades. Even now most (left-bank) Varsovians would never dare to actually walk from one end of Brzeska (Brest Litovsk) Street to the other; let alone wander the streets stretching to the north and east of the Russian Orthodox Church as far as the railway embankment that once marked the city limits.

The discerning of a 'new' Praga was associated with districts laid out beyond the tollgates and incorporated before 1914. Recalling its founder, Ksawery Konopacki, the earliest and most compactly built-up of these districts was known popularly as the *Konopacczyzna*. United with the adjacent *Kurakowszczyzna* (named after Joachim Kurakowski), 'Konopacki-land' formed part of the earlier, pre-first-world-war Nowa Praga. Wedged between the tracks and sidings of the Vilna and Eastern railway stations, Szmulki (from *Szmulowizna*), derived its named from an 18th-century Jewish entrepreneur, Szmul Jakubowicz Zbytkauer, who was granted the then still pastoral lands from the last Polish monarch. Although it lies beyond the East-West railway, and so outside Praga-North borough, Kamionek is more closely related historically with Praga than the *Konopacczyzna-Kurakowszczyzna* or *Szmulowizna*. Recalling the mediaeval village of Kamion (destroyed in the mid-1600s), this district has been amalgamated with the neighbouring inner suburb of Grochów, which, alongside Saska Kępa and Gocław, forms part of Praga South – also embraced by the 'Centrum' super-borough.

Deterioration of the urban fabric must be dated back to 1915, when a significant proportion of Praga's Russian and Jewish residents evacuated the city, and thus their homes – most never to return – before the advancing German *Wehrmacht*. While the inter-war years represent a specific sub-epoch all of their own, this diminishing of urban community, and the running down of building stock it caused, was to continue right down to the moment of writing. The abandoning of flats and whole properties reached its nadir with the mass expulsions in 1941 and 1942 of the East-bank districts' Jewish inhabitants (broadly estimated at 35%-45% of the population). Whole streets stood deserted; but not for long, since the houses once belonging to and resided in by the victims of Nazi Germany's Final Solution were allocated to, or illegally taken over by, others. Much in accordance with the 'this-isn't-ours' mentality (i.e. in anticipation that someone would

claim the property back), these often migratory residents tended to treat their new homes as nothing more than temporary shelter. The lack of interest, both at the official level as well as from the tenants' point of view, in maintaining what generally were soundly constructed buildings proved the one overriding factor in Praga's gradual demise after the war. In October 1945 property within the municipal boundaries was nationalised and placed accordingly under the direct administration of the state capital's municipal authorities. Official complicity in the running down of Praga's older domestic architecture, including water, electrical, gas and other installations, echoed the widespread redundancy that preceded clearance of tenement housing in Warsaw city centre – a policy originating in the late 1940s and continued to the present moment, with disastrous effects for nurturing any sense of urban community that had outlived the Second World War [25].

While in central left-bank Warsaw architectural, following on from social, transformation was a foretold conclusion, wholesale redevelopment in the right-bank inner districts was constantly deferred. Initially required to accommodate the tide of new inhabitants flocking in the later 1940s and 1950s to a devastated city at the frenzied height of state-controlled 'reconstruction', the prewar housing stock of Praga was condemned to gradual elimination, which proceeded, in less and less coordinated steps, during the 1960s and 1970s. Tenants were either rehoused or moved out under their own initiative from poorly maintained houses allowed to fall into ruin. Wooden buildings were removed altogether, their sites having on the whole remained empty to the present day. By the 1980s, run-down medium-sized town and multi-apartment tenement houses were being abandoned; in particular their outbuildings. In the meantime, the suburban districts of Targówek, Bródno and Pelcowizna were redeveloped as soulless multi-storey housing estates. These formerly wooden suburbs, laid out in the immediate vicinity of the Russian Citadel esplanade (whence the tsarist ban until 1911 on brick or stone buildings, including the former Praga railway station), were thus absorbed into the greater urban agglomeration. Add to these high-density residential areas the less compactly built, lower-middle-class quarters of Grochów and interwar 'villadom' of Saska Kępa, and it is plain to see that – following on from the state-municipal 'plans' drawn up in the 1920s to forge a homogenised urban organism – the East-bank inner districts of Praga have been enveloped by an inner-suburban ring which was fully assimilated into the urban and social-occupational infrastructure of the all-encompassing greater metropolitan body [22].

Pockets of apartment blocks and rationally laid-out housing ensembles raised in close proximity to – or even planted metaphorically within – the decaying built-form of the inner right-bank districts offer some insight into the urban order and aesthetics the central party technocracy had in store for Praga at various stages in the rise, decline and corruption of state-directed town planning. The names in themselves bear witness to the aggressive plans for the entire area that otherwise advanced little beyond the drawing board: Praga I (protracted inter-war avantgarde, 1945-8), Praga II ('socialist realist', 1948/9-56); Praga II and Praga III (reinstated modernism, increasingly mass-produced to tackle the housing shortage, 1956-mid-1960s); 'Szmulowizna' (prefabricated high-density housing blocks of monumental proportions, mid-1960s and 1970s); Białostocka ('human scale', but standardised, 1980s).

One of the earliest overt signs that substantial changes (typically delayed in comparison to left-bank Warsaw) were in store for Praga after the political and supposed socio-economic watershed of 1989-1991 was the enormous interest shown in the late 1990s by businessmen at the cutting edge of a combination of the so-called information revolution, culture industries and symbolic economy. While, at the initiative of what looked like a new kind of district borough and city council functionary, artists were encouraged to rent studio space and accommodation at subsidised or minimal rent below those in standard left-bank properties, at least two major cultural centres have established themselves in adapted factories [27a, 27f]. Closely scrutinised by security guards and accessible exclusively by gated entrances, both of these institutions are isolated from their urban

and social surroundings. Another art centre was planned on the other side of the North-South Praga divide, on Mińska (Minsk) Street, but

**Map I: Praga, Vestigial Urban Fabric Pre-Dating 1914/1939 and Post-War Development**
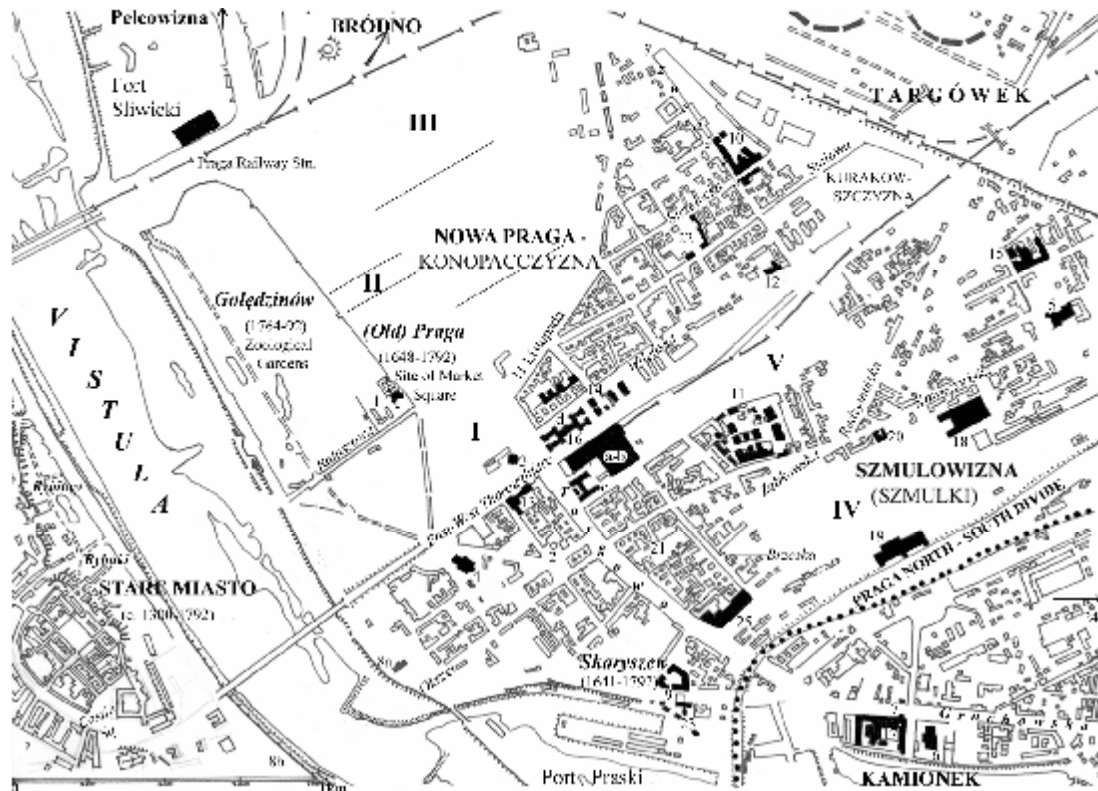


KEY: 1. Our Lady of Loretto RC Church (1640-44, adjoining non-extant Bernardine church and monastery); 2. Site of Jewish Synagogue (c. 1835); 3. St. Mary Magdalen Russian Orthodox Church (1867-9); 4. RC Parish Church of Archangel Michael and St. Florian (1888-1901, rebuilt 1947-72); 5. Basilica of the Sacred Heart of Jesus (1907-14, 1920-23); 6. Our Lady Victorious RC Church (1929-30: site of mediaeval Kamion parish church); 7. Grochów tollgates (1818-23); 8a-8b. River customs houses (1824-5, 1832-5); 9. Fire Station (c. 1878); 10. Schicht factory and workers' housing complex (1896-); 11. Municipal Spirits Distillation Plant (1897-1900); 12. Peasants' Workhouse (1904-5); 13. ex-all-male grammar (later: King Ladislaus IV high) school (1904-7); 14. Artists' colony and 'alternative' gallery complex in ex-Wróblewski furniture depot (built successively 1885-1910); 15. Trzciny cultural and business centre in former early-C20 factory complex; 16a-d. Vilna Station terminus, 'Carrefour' hypermarket, Polish State Railway (PKP) HQ & workers' housing complex (1925-30); 17. Wedel Chocolate Factory (ext. 1927-9); 18. Tram depot (c. 1930); 19. Eastern Railway Station (1964-9); 20. Brother Albert Social Welfare Centre (1980-3); 21. Różycki Bazaar; 22. Site of Nowa Praga Bazaar; 23. Vietnamese Cultural Centre; 24. Higher School of Social Psychology (SWPS).; 25. 'Millennium' centre of commerce and finance
**Housing estates**: **I**. PRAGA I (1948-52); **II**. PRAGA II phase 1 (1950-56); **III**. PRAGA II, phase 2 and PRAGA III (1959-1967); **IV**. SZMULOWIZNA (from 1968); **V**. BIAŁOSTOCKA (1984 onwards)

for the time being the main sign of urban change in Kamionek is the setting up, inside the gutted remains of an ex-factory, of the private Higher School of Social Psychology [27e].

The attracting of creatively-minded people to 'raw space' in rundown parts of cities has innumerable precedents in the West. Apart from the emotional appeal of old and generally authentic built surroundings, and the attraction (potentially fatal) of genuine as opposed to *ersatz* urban folklore, the incentives are inevitably orientated to profit-gain. Media attention was drawn to Praga by the adapting of its street profiles (Mała, Konopacka and Stalowa) as backdrops to films portraying Warsaw, and especially the Jewish Ghetto,

under Nazi occupation [26]. While at least two fringe theatres are now based in Praga, a crop of art galleries has opened on the premises or in the vicinity of the artists' colony set up in cooperation with the Warsaw Academy of Fine Arts, in an impressive complex of monumental red-brick warehouses on Inżynierska Street [27b]. The pattern so cogently portrayed by Sharon Zukin of entire areas of Lower Manhattan regentrified to house the marketing of culture has repeated itself in selected industrial buildings and mixed-residential tenements of Praga [27c]. The imitating or passive adoption of Western models is arguably as old as the Polish State, but it remains unclear to what extent the virulent form of post-industrial capitalism that transformed beyond all recognition the functional and social structures of selected parts of 'downtown' New York like Greenwich Village is reproducing itself some three decades later in Praga [24].

## URBAN EMPIRICISM: NOTES FROM A BELEAGURED SETTLEMENT

It is no coincidence that the first international conference devoted to urban revitalisation, organised by the 'Biuro of Promotion' for Warsaw Municipal Council in September 2004, was staged in the popularly-called Trzciny Factory visual arts and business centre. Alongside town councillors from numerous Western European cities, this unprecedented event was attended by specially invited EU bureaucrats, the 'reps' of private companies (including architectural and urban-planning offices), corporations and various non-governmental organisations. The very evident motivation behind this official function was Praga's impending urban rehabilitation – to which end, in the context of Poland's imminent accession to the European Union, Warsaw City Hall confidently expected lavish funds from Brussels. The typical procedure practised in these and related events, staged in what serve as hubs of inner-urban regeneration, involves virtually every 'guest' attendant arriving either by taxi or his/her own car in order to avoid any immediate contact with the actual neighbourhood.

Of telling significance to Praga's ongoing transformation in the New Millennium is the response to the aforementioned and similar developments from the local populace. Public events may attract the interest of individual figures, some of the artists claim to be at one with their surroundings, and private initiative is tolerated where it brings tangible benefits to the residents, but the huge majority of *Prażanie* avoid contact with semi or fully institutionalised bodies they intuitively feel are alien to themselves and their own.

Their instincts may well be strong and self-preserving, but just who the *Prażanie* actually are is an extremely confused issue that, lying at the very core of the area's multilayered past, provokes bitter dispute among the residents of today's Praga. As of 30th September 2003 the population of Praga North stood at 74,304. Since it records only registered inhabitants, and a significant proportion of the populace is not registered as living here, this figure is no more than a vague approximation of the actual state of affairs. Nationalised in 1945, or raised by the state as communal housing, the vast proportion of densely, on the whole, populated residential property is still administered by the local borough authorities. In the absence of claimants to pre-war property, the responsibility for maintaining the older housing stock, which, in varying degrees of dilapidation, accommodates anything up to one third of the district's population, remains a burden the borough council has no alternative but to bear.

In light of the prevailing economic climate, a strictly controlled annual budget and the growing proportion of tenants in arrears with their rent, the central municipal and local borough councils are eager to promote privatisation. Rising numbers of first-time buyers have taken advantage of flat prices which, until recently, were considerably lower than in most parts of Warsaw. In those tenement houses and individual apartment blocks where owner- and council tenants have managed to reach a common consensus, housing cooperatives have come into being which, among other things, pool resources for renovation, and also lobby the council on any variety of local matters. Praga remains a frayed, in many places tattered, patchwork of individual, and in numerous cases isolated,

houses and tenement or apartment blocks better or less suited to the realities of today. The carcasses of buildings in a state of terminal decline are unlikely to stand much longer. Not exactly as yet communities, the varied examples of domestic architecture from the pre-1914 as well as inter-war and post-war eras have the potential to function as autonomous units within the all-embracing East-bank inner-urban microcosm. It is in this direction that the main hope would seem to rest, if the area's unique identity and character is not doomed to extinction or, worse still, neo-urban parody.

No definitive social study of Praga has ever been carried out; partly, no doubt, because the usual kind of research institutes responsible for such investigations – like Warsaw University's Institute of Sociology – will not send students or employees into an area with such a notorious reputation. Inquiries made by individual analysts are usually limited or over-selective. Now that the borough has ceased employing resident caretakers (an institution inherited from the 19th century 'axed' by recent 'cuts'), the conducting of a comprehensive housing census has quite probably been rendered all but out of the question.

The non-historical and anti-functional drawing of the administrative borders undermines coordinated policy-making. Excluding the area behind the post-war Praga Station (misguidedly defined as Golędzinów) what is evident at the time of writing (January, 2006) is the spontaneous reaffirmation of the historical four-way division, as defined by the two bisecting railway lines and Targowa Street, between Kamionek (in Praga South), the Szmulowizna, Nowa Praga and 'Old' Praga districts. With the future of Kamionek firmly tied to that of Grochów, and the area west of Targowa with the Port Praski fast becoming an assimilation zone for 'Downtown' Warsaw, the essence of artisans' and working-class Praga is focused on the Szmulowizna and Nowa Praga. The former area, defined by Ząbkowska, Radzymińska and Kawęczyńska streets, is now to be revitalised. Initiated as recently as November 2005 by the central municipal council on the left bank, this extensive programme is supported by EU funds as part of a so-called 'Integrated Operational Programme for Regional Development'. Preceded by the façadal 'restoration' of tenement and townhouses on what is claimed to be 'The most beautiful street of pre-war Warsaw' [27g], this 'next stage' involves the (permanent?) evacuating of tenants from properties requiring 'extensive renovation'. Forming part of a series of ongoing 'projects', the actual 'restoration' will be executed by 'non-governmental organisations appointed by way of a competition'. Revitalising Praga is in this case defined as: 'a process embracing spatial, economic and social alterations undertaken in degraded urban areas or post-industrial terrain … to improve the inhabitants' quality of life'. At the same time, 'under the supervision of the conservator in cooperation with social guardians of historical monuments', the plan envisages 'galleries, new shops, service points and pubs [shall] come into being in the renovated buildings' [27d].

The so-called 'Bermuda Triangle', bounded by the Vilna and former circular railway lines and 11 Listopada (i.e. [1918] Independence Day) Street, is not to be the object of any allegedly coordinated strategies of revitalisation, regentrification or (social) rehabilitation. Having set up its headquarters in a formerly derelict, two-floor tenement on Strzelecka Street, the private company, known as 'Holding Wars', responsible for surveying selected street blocks fell out of favour with the powers that be in the City Hall and ceased all activity in the area from early 2005. It is unclear what is to happen to the cartographic and documentary materials. It was revealed that in the most densely inhabited tenements (nick-named 'Pekings' by Warsaw's working classes) an average of 20% of the residents should have long since been evicted and a further 20% issued with eviction orders for not paying their rent [17]. No such procedure has been followed, because of fears among councillors that forced displacement on such a scale would cause more problems than advantages – hence 'residents' have remained where they are. Very much in accordance with the *Zeitgeist* of today, the underlying rationale is that people should find a solution to what is inevitably perceived as their own (and nobody else's) predicament. Ranging from families trapped in the vicious cycle of poverty through *Prażanie* finding their own way in brave 'new' times to ambitious 'urbanites' who have only recently moved in, the social

spectrum is certainly a broad, but also a somewhat grotesque, one. The situation remains undefined and conditions in some street blocks continue to deteriorate, while in April 2006 the chief councillor (or 'burgermeister') was removed from office in grossly compromising circumstances. While the justice system may leave a great deal to be desired, history at least will judge to what extent Warsaw and Praga alike have been administered ,in 'a free and democratic Poland',  by hypocrites and criminals.

Apart from teenagers lapsing into drug addiction or alcoholism, the long-term unemployed who resort to petty crime or work for mafia syndicates are broadly termed *żule*. This word, meaning swindler and rogue, derived from the Russian *zhulik* (polonised to *żulik*), is applied to anyone seen to be living on the edge of social norms or who drops out of 'society' altogether. For much of the long-term resident populace the 'new times' have proved ever harsher ones. Apart from factory redundancies and closures, small-scale manufacturers, craftsmen and traders face unequal competition from 'hi-tech' mass production and imports, as well as new businesses locating from outside the area, including international chain hypermarkets on the site of ex-industrial terrain. Most often it is those who consider themselves to be respectable citizens, paying their own way and observing conventional codes of conduct, that most earnestly wish to see the backs of neighbours whom they regard as renegades. Much as in the countryside, however, deep-seated animosities (all the more heightened by difficulties of a purely material kind) may be linked to a whole variety of ulterior motives. The atmosphere reigning in many tenement blocks and courtyards is consequently one of mutual distrust and entrenchment, further intensified by the prejudice and intolerance for human distress that comes out of feeling threatened both by 'those at the top' and 'those at the bottom'.



**Fig. 3: 'THE BETTER TOMORROW CAME YESTERDAY': Stalowa St. graffiti, Sept., 2004**

The people who stayed put, and for whom central Warsaw was as remote as Praga remains to this day for most left-bank Varsovians, tended to be small shopkeepers or artisans, retail traders and factory workers. In adapting to whatever economic and political forces are shaping the city at a given time, the upwardly mobile classes tend also to be the first to move out. But now it is Praga that is attracting the 'bright (and usually young) things', while – very much like the *true* London Cockney – the crafty, quick-witted *Prażan/in/-ka* with his-her strongly Eastern Slavonic lilt, Russian-influenced slang and

grim sense of humour appears to be on the verge of extinction. On the other hand, localised initiatives, originating 'from below' among newly arrived and local residents 'born-and-bred' (rather than 'on high' by legislative bodies based in borough or municipal offices, as well as profit-motivated business), have created a ferment that could not be experienced anywhere else in the city. As far as nurturing a genuine and enduring sense of civil identity is concerned, the ideal solution to Praga's social question and deteriorating pre-war housing stock might well be autonomous communities responsible for the upkeep and maintenance of their jointly possessed homes.

In the meantime, the social and economic changes under way in Praga have begun to make their impact on the built landscape. It should be underlined that the value of the inner East-bank districts' architectural heritage lies not in individual buildings, of which a mere handful predate the year 1860, but in the comparative completeness of what (in spite of extensive piecemeal demolition since the 1960s) has come down to the present. With large-scale public-state building projects now a thing of the past, and most private investors more interested in building from scratch, new development has tended to consist of individual designs adapted to the preexisting urban fabric. One of the most active participants in this 'infill' construction has been the Society of Social Building (TBS). Set up with credit provided by the State Housing Foundation to raise blocks of flats, which are leased by people unable to buy their own homes, the TBS is allocated land that private developers, where granted the rights to build, must purchase at standard market prices. Even if their scale is in keeping with their immediate surroundings, the architectural design of most TBS blocks – featuring vulgar interpretations of post- or epigone modernism, finished in multi-pastel colours with exterior details that crudely allude to *fin-de-siècle* tenement houses – is hopelessly inadequate. Unfortunately, much the same must be said about the growing proportion of private property development; especially in the vicinity of 11 Listopada St. Far from letting the forces of 'free' market enterprise in (or out), to protect the area's aesthetic qualities a general ban should have been upheld on new building until existing structures had been restored and their architectural merits fully appreciated by designers and prospective developers alike. The dilemma of what kind of architecture may be meritorious in today's urban environment is very much a universal one. In Warsaw the evident bias is for a raw, functional kind of updated, so-called 'grand-urban' modernism, with echoes of neo-Classical or Baroque styles drawn from certain traditions and shockingly selective perceptions of the past. The preferences of too many currently practising architects and their frequently nouveau-riche clients is totally out of tune with Praga's later-19th- and early-20th-century urban-architectural landscape.

The future of Praga's architectural heritage depends in part on the work of people employed at the regional conservator's office. Their dedicated research in preparing inventories of domestic, sacral and industrial buildings has led to the registering of some of the more authentic and inimitable testimonies from the past as protected monuments. This generally spontaneous initiative among young specialists, making up for decades of official inertia, may well tip the precarious odds in favour of saving whole tracts of 'historical' Praga from demolition. Most houses predating 1914 contain floors constructed entirely of wood, rather than iron or reinforced concrete, which means they would require conservation or even replacement before a thorough renovation, or adaptation into offices, were possible. Eager at most to retain outer walls and construct new premises within a pre-existing building's gutted shell (the standard procedure in Britain or the US), the majority of private developers regard investment in such property to be economically viable only if planning permission is given to rip virtually the entire edifice down, retaining forlorn vestiges of what otherwise amounts to a wholly new development. In this context the perfidious implications become crystal clear behind the weighing up in certain bureaucratic and corporate circles of Praga's future architectural profile in terms of two superficially opposing extremes: (1) extensive demolition to make way for a new, contemporary 'district' to suit the scale and aesthetics of a 'great metropolis'; and (2) adapting the 'historic' architecture, effectively turning Praga into a Skansen museum that would function as 'an attractive tourist offer' (literal translation) [27d].

A sign of how far attempts might be taken to develop the area's potential as a tourist attraction is whether the synagogue, the burnt-out ruins of which were demolished in the 1960s, shall be rebuilt. The answer to the question: 'For whom when no Jewish community here even survives?(!)' would naturally be: 'for the development of the district's tourist potential'. And in this context the Praga Synagogue would function as a 'museum' (much, ironically, as Soviet commissars turned Roman Catholic churches in the western provinces of the Ukraine and Belarus into museums of aetheism). The most appropriate word in this instance is *simulacrum*; but this could well be the (final) direction Western civilisation has gone in since the turn of the 1970s [3]. The point has been argued very succinctly that people can be tourists as much in their own city as when they travel abroad [20].

If the nature of the current epoch is such that a landscape built up for exchange and production must function principally as an environment of consumption, then Praga might well be destined to 'settle down' and become another more or less stereotypical part of Warsaw's post-war, neo-capitalist (post-communist), and even post-nationalist ('neo-Euro'), incarnation. If this is the case, then Praga faces a death as total as that emanating from the lifeless, post-architectural complex of apartment blocks, posing as monumental tenement houses on Ząbkowska beyond Brzeska St., which were raised to ring in the New Millennium.

## CONCLUSIONS: PRAGA AS AN INDEPENDENT URBAN VARIABLE

Having functioned for most of its history outside the jurisdiction of a city that was itself constantly subjected to disruption from internal as well as external forces, Praga and its residents have long been the victims of technocrats and government agents. Throughout most of the 1800s, occupying Prussian, Russian and even French administrations may be held directly responsible for what happened on both sides of the Vistula. However, for almost the entire 20th century the legislators were Polish. While having their own conceptions as to the way Praga should look and function, these supposedly homegrown decision-makers showed little, if indeed any, concern for the built environment and social conditions as they actually existed. The overriding objective concerning the so-called Right-Bank City Centre was that it become a fully absorbed part of the state capital (*stolica*). The blatant official prejudice that lay behind the urban schemes devised by the leaders and architect-technocrats of 'People's' Poland – as well as their procrastination when visions of that brave-new world miscarried – may be understood as a latter-day expression of deep-seated social and cultural antagonisms with roots long predating the partition era and yet earlier.

Instead of emerging as a society based on mutual inclusion and respect, humanity was plunged into a series of wars and revolutions that left Europe in particular an altogether more impoverished part of the world [cf.: 15]. Rather than becoming a centre of social and cultural integration, Warsaw reached its apogee as a collision point of irreconcilability that ended in its own localised Armageddon. It is obvious enough that the Vistula proved the making of this city, but the same river – still occasionally defined as a border between Europe and Asia – also dictated the evolution of two distinctive urban bodies. Rather than developing in mutually beneficial symbiosis, Warsaw and Praga were fated to encapsulate the geopolitical divide so brutally reimposed from 1914 between (peninsular) 'Europe' and (continental) 'Eurasia'. While Warsaw functioned as the capital city of a Latin-Christian representative reincarnate of Western-European civilisation, its culturally hybrid and provincial twin settlement on the opposite bank was treated as the antithesis of this would-be Polish Athens, Rome and Paris. As a factory town and railway junction of wooden and low white-washed 'country-town' houses, juxtaposed with modernist multi-apartment tenement blocks, Praga might easily have lain anywhere between two hundred and six thousand kilometres East of Warsaw. Its masonry-built synagogue (non-extant), onion-domed Russian Orthodox church and monumental red-

brick neo-Gothic RC 'cathedral' certainly share as much in common with the architecture of Brest Litovsk, Białystok, Baranovichi or even distant Irkutsk as a 'Central-European' town. It is lamentable that such a remarkable conjunction should be regarded as a liability and even a humiliation. The resultant urban-cultural anomoly lies at the crux both of Praga's gradual demise and the threat the current free-market system poses to the beleaguered remnants of what always has been a highly distinctive and in very large part an independent urban variable.

Bearing a name that by the 1960s was synonymous with criminality, Praga degenerated into a medley of socially marginalised neighbourhoods. As soon proved evident, the breakdown in social order issuing out of the traumatic events of the first half of the 20th century was aggravated enormously by state-municipal endeavours to amalgamate the area within the greater metropolitan body, known to planning circles as 'Functional Warsaw'. As official policies failed to produce the desired results, Praga, more than any other part of the city, contradicted the preordained aesthetics, images and social conventions that the capital city of a model socialist, and nation, state should 'demonstrate' to the outside world. Its status in relation to the left-bank city thus sank to similar depths of misfortune and degradation as during calamitous episodes in the past (1655-8, 1794-1811, 1831). Then again, being largely excluded from the urban-destructive no less than main urban-creative processes that made today's Warsaw what it is, the vestiges of Praga's architecture, and what survived of social customs passed down from one generation of *Prażanie* to another, comprise the final tangible link with a past that 'historians' have portrayed selectively or ignored altogether. Profounder appreciation of the specific qualities of human habitation on the eastern Vistula bank is the crucial 'missing link' to historical analysis of the modern Polish capital.

It has been argued that Praga holds the key to comprehending Warsaw's violently fluctuating potentialities in history. As a city founded, on the invitation of regional feudal lords, by settlers from the Holy Roman Empire, that later served as a royal seat and ultimately capital city of the Polish state, Warsaw was shaped to a very considerable extent by external forces. Once it is understood that the way of life and architecture unfolding on the Praga side of the Vistula was more closely related to localised forces, then the constantly abortive endeavours by the ruling elite based on the river's western scarp to control and ingest all vernacular forms of urban culture and identity may be reexamined from quite another perspective. Notions of subjugating the East-bank to the West-bank city would appear to contradict the essence of the commonly shared senses of community and identity that made Praga what it was in the past and have come down, albeit as a beleaguered and pauperised residue, to the present day. In spite of being rendered subservient to the manorial economy and society, being made victims of virtual urban erasure before facing rational planning under 'Home Rule' followed by half-hearted policies of russification in the second part of the 19th century, the residents of the East-bank settlements evolved a specific sense of identity of their own which endured and outlasted all; even the prolonged deprivations and indolence of the People's Republic.

This brief and generalised appraisal makes no pretence to examine in any great detail the social, economic as well as political and cultural mechanisms currently at work in the inner-urban areas of 'Right-bank Warsaw' (*Warszawa Prawobrzeżna*). For a number of very plain reasons, in-depth analysis of this kind is impossible. Muddied by fraudulent activities in various areas of 'public life', but also confounded by the inherent inconsistencies of 'free-market economics', the precise nature of these mechanisms remains undefined. Rather, this text has been an attempt to place the prospects as they currently present themselves for the people and architecture of Praga in relation to its ambiguous, seriously misinterpreted, past. The only enduring solution to the paradoxical relationship between Warsaw and Praga is a symbiotic one; between what in practice should (like Cairo and Giza) be autonomously functioning twin cities. Unfortunately for Praga and the *Prażanie*, in the latest, and bravest, of all new eras to come out of the Middle Ages; i.e. of rejuvenated and allegedly free-market enterprise, the overriding

tendency is still confrontation. The urban body centred on the West bank still consumes any spontaneously evolving urban forms in its immediate vicinity.

In his erudite summary of the 'radical contradiction' of 'metropolitan civilization', Lewis Mumford juxtaposed the city's 'nature as a mothering and life-promoting environment' with its growing tendency to mutate into 'a power-trapping utility'. Designed by 'royal agents' and, 'gathering the dispersed energies of little communities' into a 'mighty reservoir', the capital city proceeded to violently release its pent-up energies 'in destructive assaults against other cities' – on a scale that would become international and, ultimately, global [14]. Placed in the context of the new-age metropolitan civilisation that Warsaw represents today, the left-bank 'CBD' is the core of a reinvigorated accumulation of capital and political power, while Praga has remained until very recently its impoverished urban sister. The tsarist authorities once toyed with the concept of a competing 'reservoir' to confront the 'Main City', but this demonic vision proved a fallacy every bit as absurd as the 'socialist' city that was supposed to rise out of the ruins of the pre-war, 'capitalist' city. Praga took on the shape and architectural profile of a provincial town with an urban life and built form typical of that in the Eastern borderlands of pre-partition Poland – as well as certain, primarily multi-cultural cities in the Russian interior. The essential uniqueness of what remains in the here and now of that urban microcosm may be all that is protecting Praga from being transmuted into a constituent part of yet one more largely dehumanised agglomeration. Then again, being labelled 'historical' may lead to the area's commoditisation as a new-age simulation, as devoid of life as a 'Funland' theme park.

In the current circumstances of 'global economy', having for some time been in the course of gathering their resources in the reclaimed Main City [23], the (hyper?) modern-age agents are no longer merely poised to strike but are already in the process of claiming prized parts of Praga as their own. Much as governmental and non-governmental agencies alike have devoted considerable lip service, glosy brochures and 'www' sites to questions of civic duty and civil life, the underlying ethos since 1989 has been to make money, not build society.

As long as the city continues to harbour its one intrinsic component with the latent capacity both to make and destroy the culture it nurtures, but also to rebuild its physical structure and so reinvigorate urban life and, in the final outcome, identity, there must always be hope. That component is people, of which there is no lack in Praga at the current moment. It has been said that the role Praga plays in the left-bank city's life has always provided a way of assessing the overall condition of Warsaw. If this maxim is true, and historic process would seem to confirm its accuracy, then never has Praga been more important to Warsaw than in the current age. If an urban renaissance is to come from anywhere in the twin cities on the River Vistula, then it shall have to come not from the West- but the East-bank city.



**Fig. 4: Panorama of Praga from the Nowa Praga housing estate.** Phot.: P. Antonov, 2005

## REFERENCES

1. Aasaar Al-Belaad w Akhbaar Al-Zebaad, ('Secrets of Lands and News of the Peoples'), ed. Al emaam al Zaalem Zakareyya bn Mohammad bn Mahmoud Al-Qazwiini, nd., Beirut.
2. Praga, the Right Side of Warsaw, ed. Harasimowicz-Grodecka, H. (2006), Holding Wars
3. Baudrillard, J. (1981), Simulacres et Simulation, Paris.
4. Castells, M. (1996-8), The Information Age: Economy, Society, Cutlure, vols. I-III, Oxford.
5. Chrościcki, J., Rottermund, A. (1978), Atlas of Warsaw's Architecture, (esp. pp. 8-48); cf.: Leśniakowska, M. (1999), Architektura w Warszawie; Eng. trans. (2006) in preparation.
6. Dickenson, R.E. (1951), The West European City, London, pp. 211-22 ('Warsaw').
7. 'Dr Esperanto' (1887), Język międzynarodowy, Warszawa  (real name: Zamenhof, L.L.; cf.: An attempt towards an international language [1889], New York, trans. H. Phillips Jr.).
8. European Association of Urban Historians, Stockholm 2006 (P. Martyn, 'The Contesting of Urban Space in Warsaw…'); www.historia.su.se/urbanhistory/eauh, main session 10.
9. ISMARMED (2005), International Seminar on Management of the Shared Mediterranean Heritage UNESCO in cooperation with L'Institut de Recherche pour le Développement (IRI) and Cairo University (Theme III: P. Martyn:, 'Praga: on the Brink of Urban Renovation or Oblivion? The mounting drama of Warsaw's inner East-Bank districts').
10. Karabell, Z. (2003), Parting the Desert. The creating of the Suez Canal, New York (cf.: Bonnet, G.E. (1951) Ferdinand de Lesseps, Paris; Beatty, C.R. (1956) De Lesseps of Suez, the man and his times, London-New York.
11. Leslie. R.F. (1983), [in:] The History of Poland since 1863, Cambridge 1983 (2nd ed.).
12. LIFE IN THE URBAN LANDSCAPE, Swedish Research Council, Chalmers University of Technology, Ministry of Sustainable Development, etc. (P. Martyn, 'Praga: Historical perspective in relation to … "Regeneration"…'); www.life in the urban landscape, F.
13. Martyn, P. (2001), Brave New-Old Capital City: Questions relating to the rebuilding and remodelling of Warsaw's architectural profile from the late-1940s…', Światowid., vol. VIII; idem. (2003), 'Seeking to Place One City … in its own context', BHS, R.LXV, nr 3-4.
14. Mumford, L. (1961), The City in History, London-New York, pp. 636-7.
15. Orwell, G. (1949), Nineteen Eighty-Four, Penguin ed. (1954), pp. 192ff ('War is Peace').
16. Polin (1988), A Journal of Polish-Jewish Studies, vol. 3, on Warsaw Jewry, Oxford.
17. Rewitalizacja (2004);  www.um.warszawa.pl/v_syrenka/wydarzenia/konferencja/english)
18. Ronen, S. (2001), In Pursuit of the Void (The 2000 Aleksander and Alicja Hertz Annual Memorial Lecture), Cracow, pp. 53-60 ('Where do I come from?').
19. Samsonowicz, H., [in:] A Republic of nobles: studies in Polish history to 1864, ed. J.K. Fedorowicz (1982), co-eds. Bogucka, M., Samsonowicz, H., Cambridge-New York.
20. Sudjic, D. (1992), The One Hundred Mile City, London (chapter 14).
21. Szwankowski, E. (1970), „Praga w latach 1814-1880", [in:] Dzieje Pragi, Warszawa.
22. The Polish Avant Garde: Architecture, Town Planning (1981), exhib. cat., Wrocław.
23. Warsaw, Past, Present, Future, exhib. cat. (1997), Warsaw City Hall, etc.
24. Zukin, S. (1982), Loft Living: Culture and capital in urban change; idem. (1995), The Cultures of Cities, New York.

### Cinematographic
25. Pekin, Złota 83 (2003), dir. E. Borzęcka (with very effective Eng. subtitles).
26. The Pianist (2002), dir. R. Polanski, after memoirs of Szpilmann, W. (1999),1st pub. Los Angeles (Eng. trans.); (2000), Pol. original, Kraków.

### **W**-orld **W**-ide **W**-eb
27a. www.fabrykatrzciny.pl; 27b. www.inzynierska.pl; 27c. www.Nizio.com; 27d. www.praga-pn.waw.pl („rewitalizacja"); 27e. www.swps.edu.pl; 27f. www. monopolwarszawski.pl; 27g. www.zabkowska.waw.pl; 27h. www.skladbutelek.pl; 27i. www.wikipedia/'Poland'/.

# INTEGRATION OF SERVICES AT THE METROPOLITAN LEVEL;
## A Case Study of City District Government, Lahore – Pakistan

**Ijaz Ahmad**
*Assistant Professor, Department of City and Regional Planning*
*University of Engineering and Technology, Lahore-Pakistan (e-mail: ijaz47@wol.net.pk)*

**Ihsan Ullah Bajwa**
*Professor, Department of City and Regional Planning*
*University of Engineering and Technology, Lahore-Pakistan*

## ABSTRACT

In World, most of the developing countries are experiencing a high population growth rate.  As a result the population of these countries is increasing at a much faster rate than ever before.  This rapid increase in population has radically boosted the urbanization phenomena in small towns as well as big cities.  Resultantly, the towns are being converted to cities, then metropolitan cities and those metropolitan cities into mega cities.  This rapid population increase exerts huge pressure on the already available basic services.  These pressures then force the line agencies to take remedial measures in form of an efficient provision of basic services to residents of these cities.  The services provided can best be utilized if planning is done on wide area basis.  Likewise the quality of services can be increased if the line agencies keep an eye on the population growth trends.  This paper highlight services provision mechanism at the metropolitan level.

**Key Words:** Urbanization, Metropolitan Cities, Service Delivery Mechanism

## INTRODUCTION

Man as the only culture-building animal on the globe not only adapts to environment but also creates environment to which to adapt.  The metropolitan area is man's more complex cultural construct, which on the one hand is an eye opener example of his achievements, and on the other the matrix of serious and pressing problems.  The emergence of a metropolitan area is a modern phenomenon dependent on the technology and the economic, social and political organization identified mostly as a consequence of industrial revolution.  One can say that the metropolitan area is not only the consequence of such developments but also is a determinant of further change.  Urbanism has profoundly affected the social order, thereby, producing increased demand for changes in the political order.  Thus many contemporary problems in the metropolitan area are symptomatic of the continuing strains arising from our traditional political order.

## THE RESEARCH QUESTIONS

In the last three decades there has been a shift in the demography of most Asian countries. Most large cities in Asia account for a significant proportion of their country's urban population. More than one-half of Thailand's urban population resides in Bangkok, one-third of the urban population of the Republic of Korea, Bangladesh and the Philippines reside in Seoul, Dhaka and Metro Manila, respectively.  Jakarta, Karachi, Istanbul and Tehran have almost 20 per cent of their nation's urban population. Most of Asia's largest cities grew at 3 per cent per annum in the

period 1970-1990, but population growth in mega-urban agglomerations is still probably underestimated.   Natural increase and rural to urban migration as major factors have contributed to the increase in population living in urban centers [1].

Public policies of a group of individual local units do not add up to a public policy capable of controlling the destinies of the metropolitan area.  Service problems can effectively be solved through political integration [2].

Service delivery system efficiencies particularly in developing countries are decreasing due to many reasons.  Unstable *political set up* seem to be one of the core factor in this regard.  The varied nature of causes for shortage of poor service delivery system poses challenge to the local units, which are called upon to render such services.   It seems that our concerned authorities are not privy to the concept of integration of services.   In the face of radically changed requirements of metropolitan areas, the crucial question, therefore, ***is whether the political order is able to cope with the growth requirements and socio-cultural exigencies of urbanization***.  Our urban complexes are now so closely linked economically and socially because of the daily human movements and activities that a problem of one town is actually a spill over from an adjacent jurisdiction.  Pollution, for example, cannot be efficiently constrained within the confines of one local jurisdiction since pollutants are carried away by air or water beyond the boundaries of that political unit.   Because of the interdependency of urban communities, there becomes a need for an integrative or cooperative action among local government units comprising the metropolitan area.  Certain services are administered more economically and planned more rationally when handled on an area-wide basis.   In the backdrop of above-mentioned facts, two crucial questions need faithful answers:

   a.  Whether to integrate certain services or not?
   b.  What specific services require an area-wide authority & on what criteria shall the change or need for such area-wide authority be determined?
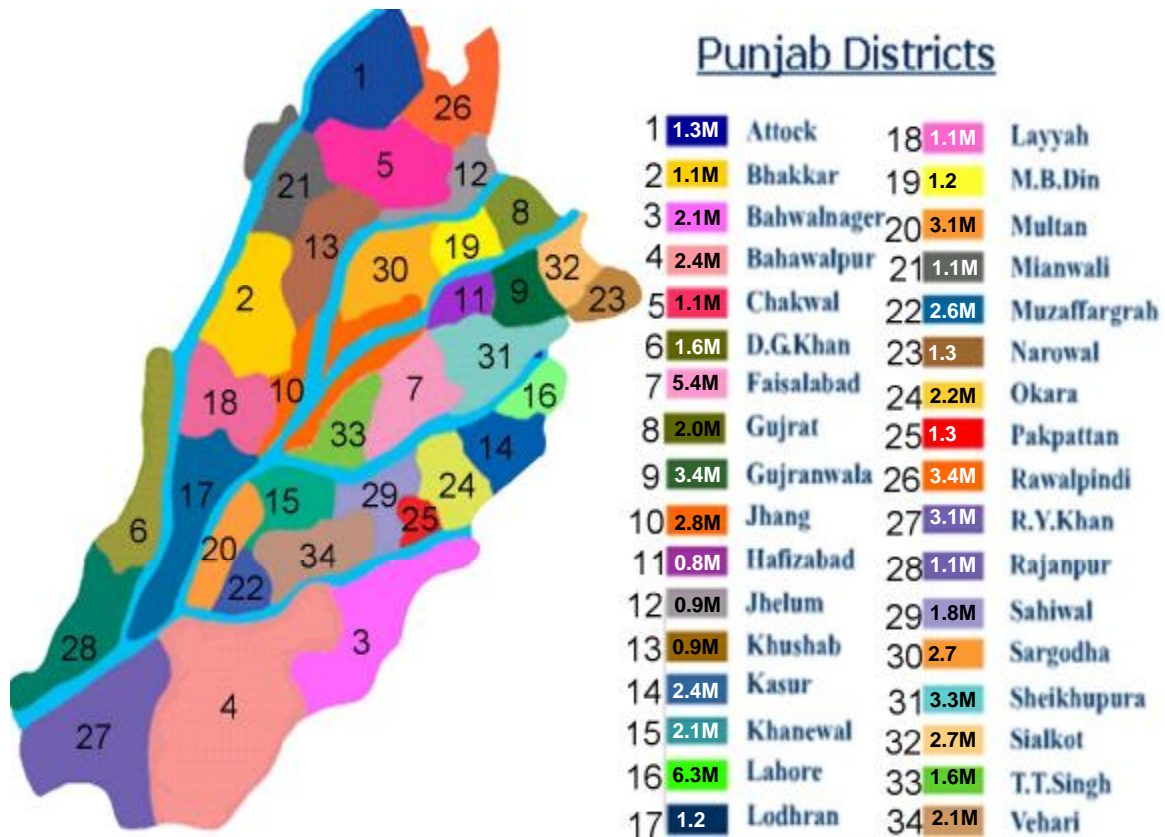

## OBJECTIVES OF RESEARCH

The research has the following main objectives:

   i.   To explore services provided by the City District Government, Lahore
   ii.  To find out bases for integration of services in the Lahore Metropolitan Area


## LAHORE; THE CASE STUDY AREA

Lahore, the second biggest city (by population) of Pakistan is a provincial headquarter of the thickly populous province of Punjab (name of one province of Pakistan).  Over the past ten years, Lahore has grown at least more than twice to become an impressive **Metropolitan Area** housing more than 06 millions inhabitants.  Metropolitan Lahore today assumes hegemony over the other metropolitan urban areas of the country.  It is among one of the main center of the country's political, administrative, commercial, transportation, religious, recreational and educational activities.  For this reason, Lahore Metropolitan Area (LMA) represents the center of progress and excitement, release from the monotony and confining pressures of rural life and opportunities that will come one's way either through luck or effort.  Therefore, it is not surprising that LMA invites a large agglomeration of people of variegated interests, diverse backgrounds and occupations.  LMA is considered as the center of national political life.  For instance, issues that affect the politics of LMA are often brought into sharper focus and consequently attract national attention.  Political leadership in LMA may sometimes even serve as a springboard for key national positions.  LMA as the foremost center of social and cultural activities offers a variety of entertainment places, shopping centers and educational institutions that indeed attract a greater number of people from the rural communities.   In addition, there are commuters coming from the nearby districts of *Kasur*, *Okara*, *Gujranwala*, *Sheikhupura*, and alike (See map-1).  The mass media is similarly concentrated in the area.  Daily newspaper and weekly

## Punjab Districts

| | | | | | |
|---|---|---|---|---|---|
| 1 | 1.3M | Attock | 18 | 1.1M | Layyah |
| 2 | 1.1M | Bhakkar | 19 | 1.2 | M.B.Din |
| 3 | 2.1M | Bahwalnager | 20 | 3.1M | Multan |
| 4 | 2.4M | Bahawalpur | 21 | 1.1M | Mianwali |
| 5 | 1.1M | Chakwal | 22 | 2.6M | Muzaffargrah |
| 6 | 1.6M | D.G.Khan | 23 | 1.3 | Narowal |
| 7 | 5.4M | Faisalabad | 24 | 2.2M | Okara |
| 8 | 2.0M | Gujrat | 25 | 1.3 | Pakpattan |
| 9 | 3.4M | Gujranwala | 26 | 3.4M | Rawalpindi |
| 10 | 2.8M | Jhang | 27 | 3.1M | R.Y.Khan |
| 11 | 0.8M | Hafizabad | 28 | 1.1M | Rajanpur |
| 12 | 0.9M | Jhelum | 29 | 1.8M | Sahiwal |
| 13 | 0.9M | Khushab | 30 | 2.7 | Sargodha |
| 14 | 2.4M | Kasur | 31 | 3.3M | Sheikhupura |
| 15 | 2.1M | Khanewal | 32 | 2.7M | Sialkot |
| 16 | 6.3M | Lahore | 33 | 1.6M | T.T.Singh |
| 17 | 1.2 | Lodhran | 34 | 2.1M | Vehari |

**Map – 1: Location of City District Lahore (16) with reference to
Other Districts of Punjab Province**

**Note: Digits in Rectangles represent the population of
relevant District in Millions**

magazines with nation-wide circulation are printed here.  Since LMA is the hub of political, economic and social activities, it has become very attractive to migrants.

The population of Lahore in 1961 was 1,62,60,00, which raised to 2,58,80,00 in 1972.  The population increases at a growth rate of 4.54%.  This population growth trend continues and it becomes 3,54,50,00 in 1981 and it increases with annual growth rate of 3.70% from 1972-81. Presently, the population of Lahore is over 06 millions covering an area of 1776 square kilometers [3].  The results show a rapid increase in population, which occurs either by natural increase or migration.  However, the figures may have very little significance if we consider the fact that the population that Lahore lost could have been accommodated within the metropolitan area.

Aside from being the center of national political life, LMA is the trade and commercial center of national import.  In LMA, a variety of industries are operating.  In view of the existing industries there exist very good prospects for steel re-rolled flat/non flat products, brick making, food processing, electrical accessories and alike.  Major industrial zones are *Kot Lakhpat, Sundar, Kala Shah Kaku* (See map-2).  All major commercial banks have their central offices in the LMA. The dry port of Lahore handles the largest volume of the nation's exports and imports, while the airport in Cantt area serves the international flights coming into and out of the country.

The continuous rapid population growth and the increasing industrialization of LMA have given rise to multifarious urban requirements, which at the same time impose additional strain upon existing services and facilities.  Metropolitan problems continue to mount: *traffic congestion,*
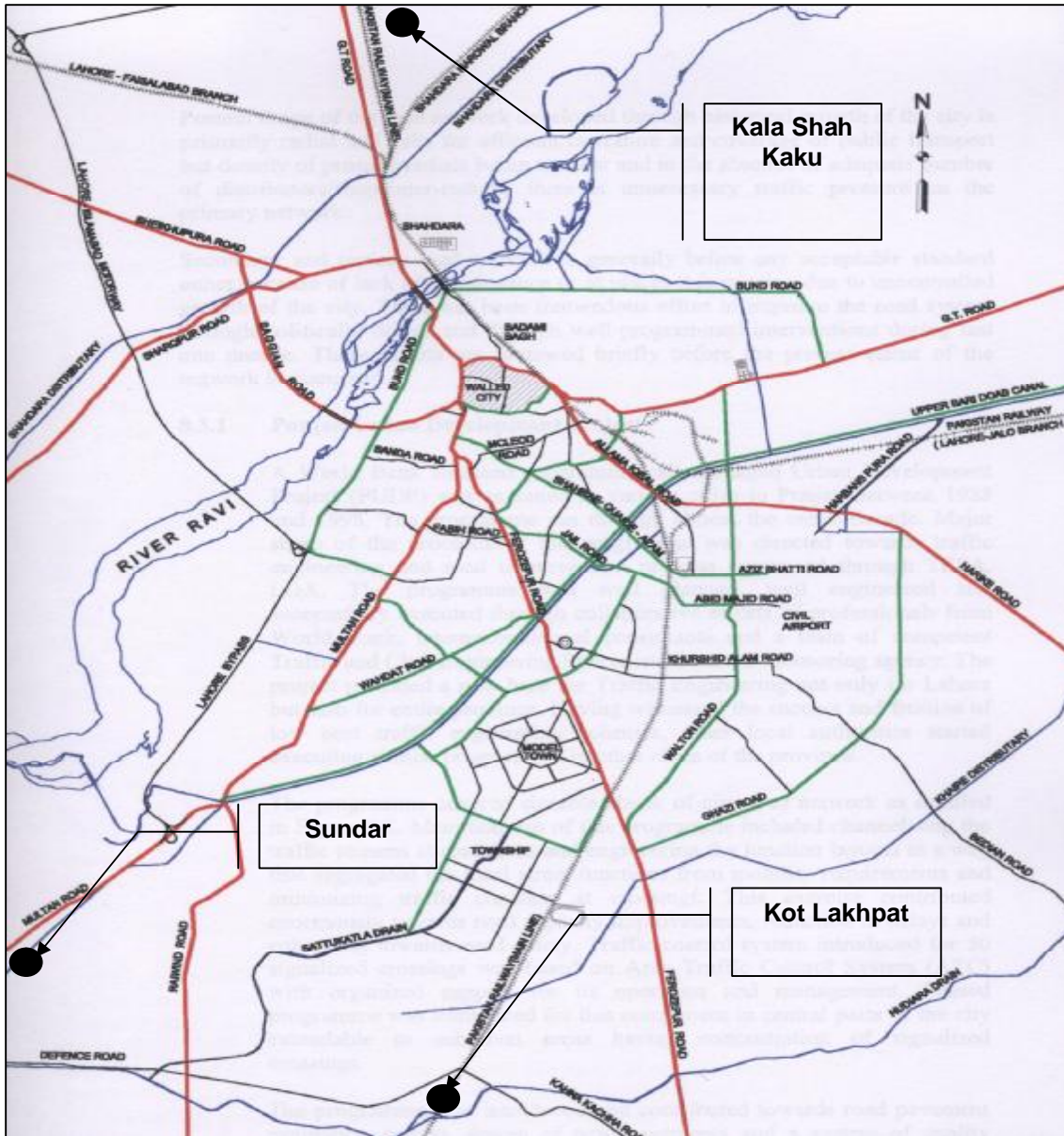
**Map – 2: Location of Industrial Estates in Lahore Metropolitan Area**

*rampant crimes and vices, spreading slums and lack of health and recreational facilities*.  The increasing number of people living in the metropolitan area has generated more demands for essential public services and facilities which are not adequately met.   For administrative purposes the LMA is divided into nine towns, vis-à-vis; *Shalimar*, *Aziz Bhatti*, *Daata Gunj Buksh*, *Ravi*, *Nishtar, Allama Iqbal, Wagha, Samanabad and Gulberg,* Towns (see map – 3).  These administrative towns are formulated under the newly evolved Local Government Ordinance 2001 and were assigned variety of functions to perform in their areas of jurisdiction.  Wide powers are given to these administrative towns as to monitor and streamline the development pace.  These are also made responsible to provide services and facilities to inhabitants of LMA. The functions included are in form of services rendered in the areas of Infrastructure Provision, Planning & Coordination, Finance, Revenue and alike.  Likewise at the Metropolitan Level other functions as Education, Health, Agriculture, etc. are included.  Under the new local government ordinance 2001, the City District Lahore is providing the following services:

**Works and Services;** Water Supply, Sewage Disposal, Collection and Disposal, Fire Control
**Education Service;** Elementary, Secondary, College
**Agriculture;** Agriculture, Livestock, Fisheries, Forestry, Farm water
**Community Development;** Labor, Social Welfare, NGO, Sports & Culture
**Enterprise & Development;** Investment Promotion, Medium Sized Enterprise & Industrial Estate Development
**Finance & Planning;** Planning, Development, Accounts
**Health;** Public Health, Population Welfare, Medical Care
**Information and Technology;** Information Technology Development, Information Technology Promotion & Data Base
**Law;** Legal matters
**Literacy;** Basic Education Enhancement Service
**Public Transport;** Roads and other Transportation related Services
**Revenue;** Land Revenue & Estate, Excise and Taxation
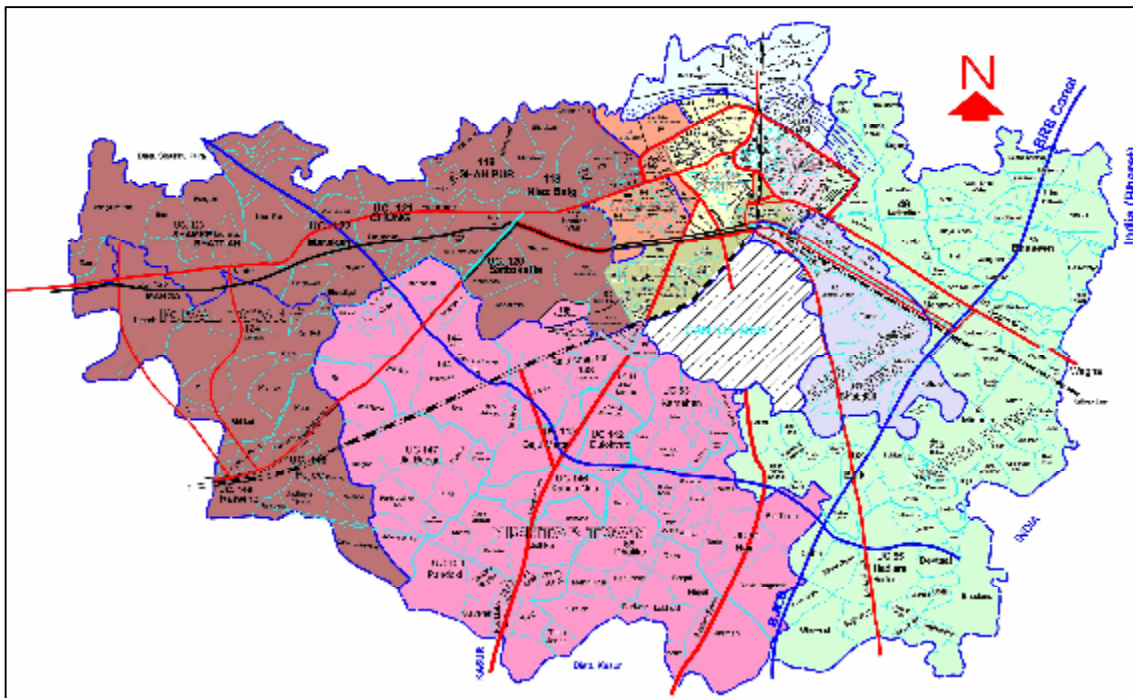


**Map – 3: Division of Lahore Metropolitan Area into Towns**

In LMA, some town administrations are not able to adequately provide all the services due to financial constraint; richer towns, however, are not undergoing this difficulty. It was pointed out earlier that a fragmented system of administering services creates problem in raising the standard of such services. It is the reason for the lack of uniformity in the quality of services available in different communities that comprise the metropolitan area. Moreover, the system breeds competition among the political units precluding thereby the possibility of a cooperative venture wherein the units undertake jointly certain vital projects. Integrated transport system, improved water distribution and sewage disposal systems are core matters of concern for local governments since these affect greatly the quality of life in the metropolitan area.

## BASES FOR INTEGRATION

In determining which services require an area-wide authority, we shall be guided by the economic, administrative and political criteria. The economic criterion includes the following considerations:

**Benefit Area;** The scope of government agencies jurisdiction is extensive to enable the benefits of a service to be consumed primarily within the jurisdiction.  The benefit from the service and the cost of failing in its adequate provision is minimum of spill-over into other jurisdiction.  "Spill-over" here refers to social benefits and social costs being broadly diffused beyond the community as against consumption service benefits narrowly confined to individuals.  In LMA, the towns are given freedom to prepare and execute development plans.  Sometimes, these towns face severe difficulties in executing projects either due to shortage of finance or lack of trained manpower, political unwillingness and other factors of such kind.

**Economy of Scale;** The unit of government is an area large enough to permit realization of the economies of scale.  In case of Lahore it is meant for the nine towns with varying sizes performing their functions in the jurisdiction of Metropolitan Area.  "Economy of Scale" is the tendency for unit costs of output to decline with increased output resulting from the application of assembly line methods, greater efficiency of centralized overhead functions such as purchasing and greater flexibility in coping with the problem of discontinuities in capital capacity.

The administrative criterion include the following:

**Geographic Adequacy;** The geographical boundary to carry on the function is adequate for effective performance.  It is desirable to preserve neighborhood and small community area for the boundaries of governmental functions.  At the same time, it is necessary to follow natural boundaries or expand the geographical coverage.  In case of Lahore, the towns are assigned specific area to perform certain functions.  But due to overlapping in geographical boundaries sometimes conflicts occur for provision of services.

**Legal and Administrative Ability;** The unit of government performing the function should be equipped with the resources like sufficient legal authority, adequate structure and administrative personnel, civic leadership and proper financial base.  In LMA, although there exist a legal service at the city district level but due to lack of coordination among different town administrations, desired results could so far not achieved.  In LMA, the divided towns are lacking in this sector.  The result sometimes appears in form of poor service delivery system.

**Comprehensiveness of Governmental Unit;** The local government unit is responsible for lot of functions.  A broad and comprehensive scope for a level of government is important because services are interdependent.  And when a government controls sufficient services, it can balance present needs and assign priorities as well as plan for the future.  In LMA, town administration sometimes face severe shortage in trained manpower, which results incompleteness of development works started by the town administrations.

The last two items are of political nature & forms a separate category:

**Controllability and Accessibility;** The performance of functions by a unit of government should remain controllable by and accessible to its residents.  Some structural and procedural features include election, distribution of power, initiative and referendum, recourse to court and grievance procedures.  This component is very strong and part and parcel of the new system.  Very strong political system exist at the Metropolitan Area and its lower levels, vis-à-vis; *Tehsil* (sub district) and union council levels.  These political persons play a crucial role in decision-making.

**Citizen participation;** For effective integration of services, active citizen participation is a pre requisite.  Functions should be assigned to that level of government, which maximizes citizen participation.  The idea of bringing the citizen closer to the government is significant in view of increasing citizens' demand for services with accompanying increase in cost of performance, changes in methods of administering functions and agglomerations of population in metropolitan areas.  In LMA, this is now mandatory to include people in decision-making and the provision of services without consultation of people cannot be started.

## CONCLUSIONS

Following main conclusions are drawn from the study:

The installation of water supply and sewage disposal facilities certainly require area-wide planning and management if one has to apply the "economy of scale" principle. Besides, the water mains and the sewage disposal system can be laid out in a manner that they can influence urban development toward desired metropolitan objectives. Presently in Lahore Metropolitan Area, WASA (Water and Sanitation Agency) provides water and sewerage services to the people. This agency has to tap other sources to cope successfully with the increasing demand due to population growth and industrial development.

In view of the metropolitan character of the "benefit-area", the desirability of providing a higher standard of education and the advantages, which can be derived from the "economy of scale", it is more beneficial for a school system to be supported by a large population and tax base. This suggests that the educational system (elementary and secondary) must be integrated at the metropolitan level in order that costs can be minimized and the uniformity of standard can be achieved. Location of elementary and secondary schools can also be properly planned in relation to residential areas.

Regarding recreational facilities in LMA, district, neighborhood parks and playfields may be owned and administered by the individual towns in the metropolitan area for reasons of "local control" and "accessibility". However, the metropolitan authority can provide regional parks, which may attract users all over the area.

The three main categories of roads in LMA are: national, provincial and city or town. The national government through the National Highway Authority takes care of the national highways while the province is charged with the responsibility of constructing and maintaining provincial roads. Each city or town undertakes road projects (within its jurisdiction) classified under the third category. From the above arrangement, it is possible to reorganize the system of road classification by introducing the category of "metropolitan highways". The local units can continue to improve and maintain local access roads together with the sidewalks within their boundaries while the metropolitan highways consisting of collectors and arterials may be the concern of a metropolitan authority. The national government may retain its responsibility over national highways, which directly connect the metropolitan area to the districts. Another aspect to be considered in relation to the road network is the planning of coordinated metropolitan transport system. The transport system is an integral part of the highway development program of the metropolitan area. A metropolitan transport authority with adequate powers and resources can, perhaps, design a more efficient bus and private vehicle movement, traffic signaling and parking facilities to avoid traffic congestion and accidents. It can make studies and prepare plans for an integrated and modernized transport system.

## REFERENCES

1. United Nations Center for Human Settlements (HABITAT) Community Development Programme for Asia (1997), Partnership for Local Action, Bangkok, Thailand
2. Stephens, G. R. (1961), Metropolitan Reorganization: A Comparison of Six Cases, Michigan
3. Punjab Development Statistics (1987), Bureau of Statistics, Government of the Punjab, Lahore

**Additional Readings**

1. Abid, S. A. and Haider, S. A. (2001), "The Punjab Local Government Ordinance (XIII of 2001); A Compendium of Laws Punjab Local Government", Kausar Law Publishers, Muttaqi Printer, 1 Turner Road, Behind High Court, Lahore

2. District Census Reports (1998), Population Census Organization, Statistics Division, Government of Pakistan, Islamabad, December 2000

3. Weber, K. E., et. al. (1986), Rural Development Planning in Pakistan, Course Handbook and Survey Report, AIT, Bangkok, Thailand

4. The SBNP Tehsil Municipal Administration (Model) Rules of Business 2001, National Reconstruction Bureau, Islamabad, Pakistan

5. The SBNP Tehsil Local Government Ordinance 2001, National Reconstruction Bureau, Islamabad, Pakistan


**Web Links**

1.  http://www.lahore.gov.pk/, City Government, Lahore-Pakistan, accessed on 10.04.2006

2.  http://www.nrb.gov.pk/, National Reconstruction Bureau, Islamabad-Pakistan, accessed on 20.01.2006

3.  http://www.lda.gop.pk, Lahore Development Authority, Lahore-Pakistan, accessed on 20.03.2006


**Key Informant Interviews**

1.  Interviews with the Officials of City District Government, Lahore-Pakistan
2.  Interviews with the Officials of Lahore Development Authority, Lahore-Pakistan
3.  Interviews with Officials of Punjab Housing and Town Planning Agency, Lahore


## ACKNOWLEDGEMENTS

# EFFECT OF TEMPERATURE AS A SHOCK LOAD ON AEROBIC BIOMASS ACTIVITY FOR COMPLEX WASTEWATER

**M.H. Mostafa**

*Assisstant Professor, Sanitary &Environmental Engineering Department ,National Center for Housing & Building Research, Dokki, Giza, Egypt.*

**A. H. Mostafa**

*Lecture, Sanitary &Environmental Engineering Department ,National Center for   Housing & Building Research, Dokki, Giza, Egypt.*

**S.M. Ahmed**

*Assisstant Lecture , Sanitary &Environmental Engineering Department ,National Center for Housing & Building Research, Dokki, Giza, Egypt.*

## ABSTRACT

This research focuses on the effect of temperature changes on the activity of aerobic biomass in the mixture  of industrial& domestic wastewater.

The study depends on the present returned activated sludge (RAS) in Zenien Wastewater Treatment Plant as the inoculated sludge for treatment of mixtures of  70%domestic sewage and  30% raw industrial wastewater in batch identical reactors provided with the DO level (2-2.5 $mgO_2$/l), MLVSS (1.5gVSS/l), and wastewater volume (60 L) at the different temperature ranges from (20 $^0$C- 55 $^0$C ) .

The experiments were determined by measuring the concentrations of Chemical Oxygen Demand (COD), Biological Oxygen Demand ($BOD_5$), and total suspended solids (TSS) .

The research aimed also to investigate the optimum range of temperature that can be sustained by the aerobic bacteria in biological method to improve the removal biological activity.

The research ensures that the mixture of domestic and industrial wastewater enable the bacterial microbial group to resist shock loads and this was represented in the sustainability  of high temperature which reached to $45^0$C and in addition at this temperature range the sludge achieved maximum  retention time in the reactor with good activity and maximum yielding coefficient.

**Key Words:** Wastewater, Industrial Wastewater, Aerobic Biomass Activity, Temperature.

## INTRODUCTION

Activated sludge is a commonly used biological treatment process employed in the removal of colloidal and soluble organic matter present in wastewater. Although, the traditional role of municipal treatment plants was to remove soluble and colloidal organic matter, metals which are also frequently present in the municipal sewage due to industrial wastewaters admitted to the sewerage(3). Metals may originate from industries such as metal finishing, hydrometallurgical refining, battery manufacturing, etc. (5)

The research aimed to investigate the effect of temperature changes on the improve of the removal biological activity of the aerobic bacteria for complex wastewater. (6)

A great environmental change was occurred in the last decade which reflected on great temperature changes in air and subsequently changes in water (15-35) °C. Also, temperature shock load may be resulted from combined domestic and industrial wastewater contains wastes of high temperature exceeding the regulation limits of domestic wastewater (35°C).

One of the most important factors affecting microbial growth is temperature. It has been observed that bacteria grow quite slowly at low temperatures but increase their rate of reaction as the temperature increases. It has been generally stated that the rate of microbial growth doubles with every $10^oC$ increase in temperature up to the limiting temperature (9).

The growth reactions are normal chemical reaction which follow definite patterns as showen in fig (1). The two patterns which are interposed with microorganisms are the increased rate of reaction with increased temperature and denaturation of specific proteins at definite temperatures. (2)
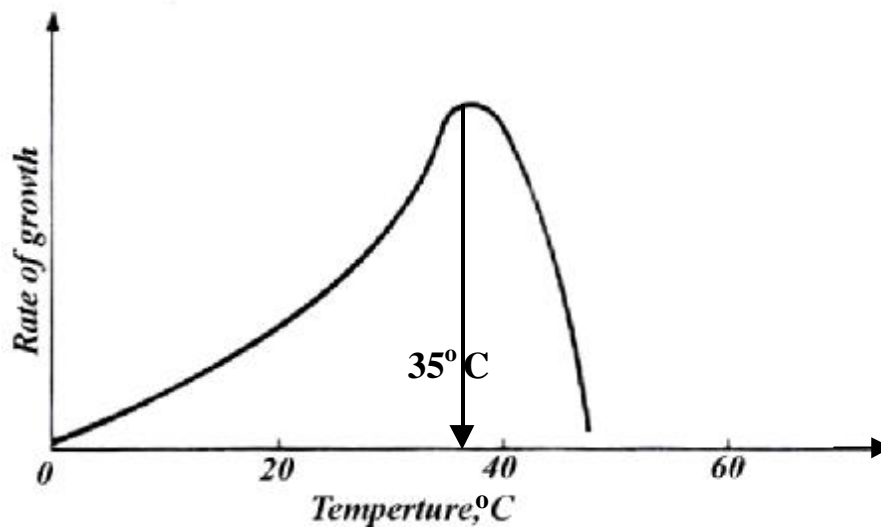


**Fig.1: Typical Bacterial Temperature Effect Curve**

There are some microorganisms, which can live at high temperature where most microorganisms die off. It has been found that these heat-tolerant microorganisms have proteins, which resist denaturation at the lower temperatures. At high temperature the heat resistant proteins are denatured and even the heat-tolerant microorganisms soon die off. The microorganisms which grow best at the elevated temperature range between 55 and $65^oC$ are called thermophilic microorganisms. The majority of microorganisms which grow best at the lower temperatures are called mesophilic microorganisms. The optimum temperature for the mesophilic bacteria is around $35^oC$, they die at $40\ ^oC$ to $45^oC$. Most microorganisms can't grow in low temperatures since the water which makes up 80 percent of the cell freezes and prevents further reaction. Some few microorganisms with a minimum of water have the ability of withstanding temperature slightly below freezing and are known as psychophysics microorganisms. The rate of growth and metabolic reactions of the psychophysics microorganisms are very slow.

## Cell Growth

In batch culture systems, the rate of growth of bacterial cells can be defined by the following relationship (6).

$$rg = \frac{dx}{dt}$$

Where $rg =$ rate of bacterial growth, mass / unit volume. time

$\frac{dx}{dt}$ = increase of concentration of micro organism, mass / unit volume. time

## Cell Growth and Substrate Utilization

In both batch- and continuous-growth culture systems, a portion of the substrate is converted to new cells and a portion is oxidized to inorganic and organic end products. Because the quantity

of new cells produced has been observed to be reproducible for a given substrate, the following relationship has been developed between the rate of substrate utilization and the rate of growth.

$$r_g = -Yr_{su}$$

Where $r_g =$ rate of bacterial growth, mass/unit volume. time $= \dfrac{\Delta X}{q}$

Y=maximum yield coefficient, mg/mg (defined as the ratio of the mass of cells formed to the mass of substrate consumed, measured during any finite period of logarithmic growth).
$r_{su}$=substrate utilization rate, mass/unit volume. time.
Also, in batch Reactor, sludge age Ɵc = hydraulic retention time ( Ɵ ) .
On the basis, of laboratory studies, it has been concluded that yield depends on (a) the oxidation state of the carbon source and nutrient elements, (b) the degree of polymerization of the substrate, (c) pathways of metabolism, (d) the growth rate, and (e) various physical parameters of cultivation (7,8).

**Effects of Endogenous Metabolism**
In bacterial systems used for wastewater treatment, the distribution of cell ages is such that not all the cells in the system are in the log-growth phase. Consequently, the expression for the rate of growth must be corrected to account for the energy required for cell maintenance. Other factors, such as death and predation, must also be considered. Usually, these factors are lumped together, and it is assumed that the decrease in cell mass caused by them is proportional to the concentration of organisms present. This decrease is often identified as the endogenous decay. The endogenous decay term can be formulated as follows:
$r_d$ (endogenous decay) = - $k_d$X
Where $k_d$ = endogenous decay coefficient, time-1
X = concentration of cells, mass/unit volume
And as a result:

$$rg = Yr_{su} - k_d X$$

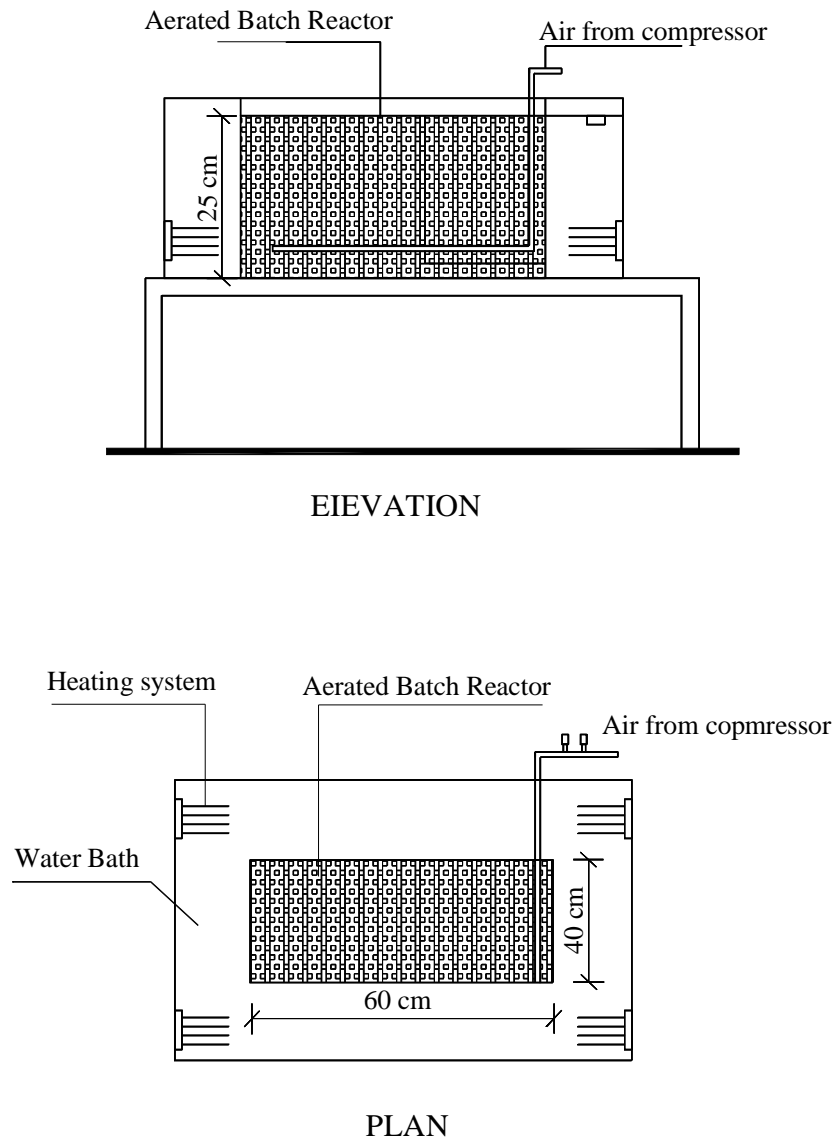And as a result:

$$\frac{\Delta X}{q} = Y\frac{So-S}{q} - k_d X$$

$$\frac{\Delta X}{q\,X} = Y\frac{So-S}{q\,X} - k_d$$

## MATERIALS & METHODS

**Batch Reactor System**: The present experimental work has bean conducted in a batch aerated reactor system shown in figure (2).
The working volume of the reactor was = 60 lit with dimensions, 60cm×40×25cm this reactor was surrounded with water bath, using heater to heat the water bath and reach the required temperature for each run inside the reactor.
The reactor was provided with a compressor to generate a diffused air inside the reactor. The DO was maintained in a range between 2-2.5 mg/l, using online ox -meter.

Aerated Batch Reactor

Air from compressor

25 cm

EIEVATION

Heating system

Aerated Batch Reactor

Air from copmressor

Water Bath

40 cm

60 cm

PLAN

**Fig. 2: The Batch Aeration Reactor Unit Running for The Experimental Work**

**Seed Sludge:** The aerobic sludge was the returned activated sludge collected from the sump of return activated sludge pumping station at ZWWTP. The concentration of seed sludge was 2.2 g SS per liter of MLVSS=1500 mg/l inside the reactor working volume. The concentration of the MLSS of Zenien returned sludge was 8.5 g/L while the concentration of its volatile suspended solids (VSS) was 6 g/L.

**Experimental Set-Up:**

The study was conducted at Zenien wastewater treatment plant. The following physical and chemical analysis was performed according to the Standard Methods: Chemical Oxygen Demand (COD), Biological Oxygen Demand (BOD),Total suspended solids (TSS), Temperature and MLVSS.

The study was conducted by running aeration process on typical batch reactor incubated with concentration of seed sludge (1.5gVSS/L) and filled with volume of wastewater (60 L).

The wastewater in the reactor contained a mixture of industrial and domestic sewage (30% industrial + 70% domestic) and this ratio was the optimum ratio reached by Sherien Mohamed ( 2004 ) effect of industrial wastewater on the activity of aerobic sludge**(12).**
The dissolved oxygen (DO) concentration was maintained at the level of (2-2.5) mg/L for the reactor.

**Source of Industrial Wastewater & Domestic Sewage**: Composite Samples with total volume of one liter were collected during 24 hors / day. These samples were settled in imhoff cone for 1 hour. The following physical and chemical analysis was performed according to the standard methods: COD, $BOD_5$, TSS, MLVSS and DO.
The experimental program was divided into three groups as shown in table (1).

**Table 1: Experimental Program**

| Group No. / Parameter | Group (1) | | | Group (2) | | Group (3) | |
|---|---|---|---|---|---|---|---|
| | Run No.1 | Run No.2 | Run No.3 | Run No.1 | Run No.2 | Run No.1 | Run No.2 |
| Temperature Ranges | $20\text{-}25^o$ | $25\text{-}30^o$ | $30\text{-}35^o$ | $35\text{-}40^o$ | $40\text{-}45^o$ | $45\text{-}50^o$ | $50\text{-}55^o$ |
| Time lasted (days) | 6 | 7 | 8 | 9 | 10 | 11 | 12 |
| Started Time | December 2004 | | | | | | |
| Finished time | February 2005 | | | | | | |

Group No. (1):
It was carried out for 3 runs under operating conditions:

DO = 2-2.5 mg/l, MLVSS = 1500 mg/l, temperature ranges 20-35$^o$ c which represents the normal wastewater temperatures.

Group No. (2):
It was carried out for 2 runs under operating conditions:

DO = 2-2.5 mg/l, MLVSS = 1500 mg/l, temperature ranges 35-45$^o$ c which represents high wastewater temperatures.

Group No. (3):
It was carried out for 2 runs under operating conditions:

DO = 2-2.5 mg/l, MLVSS = 1500 mg/l, temperature ranges 45-55$^o$ c which represents very high wastewater temperatures.

## RESULTS & DISCUSSIONS

-The results for Group No. (1), Runs No. (1, 2, 3) which represents temperature ranges (20-25$^o$), (25-30$^o$), (30-35$^o$) are shown in tables No. (2, 3, 4) and Figs. No. (4,5,6).
-The results for Group No. (2), Runs No. (1,2) which represents temperature ranges (35-40$^o$) , (40-45$^o$) are shown  in tables No. (5,6) and Figs. No. (7,8).
-The results for Group No. (3), Runs No. (1,2) which represents temperature ranges (45-50$^o$) , (50-55$^o$) are shown  in tables No. (7,8) and Figs. No. (9,10).

The data in table (9) are used in determining the kinetic coefficients ($y$,$k_d$) as  shown in fig. (3) and as explained before .

$$rg = \frac{\Delta X}{q\,X}, \; r_{su} = \frac{So - S}{q}$$

$$\frac{\Delta X}{q\,X} = y\,\frac{So - S}{q\,X} - k_d$$
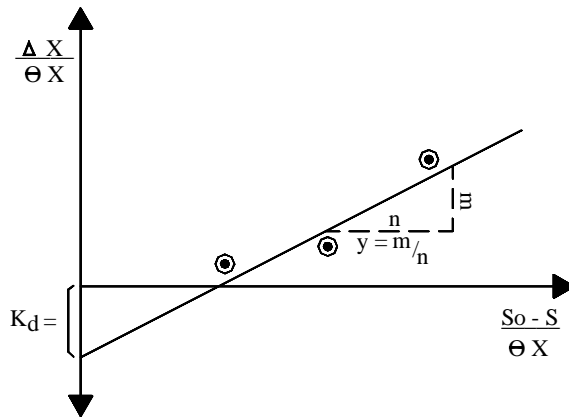


**Fig.3 : Determing Kinetic Coefficient (y,K$_d$) for the Different Temperature Ranges**

By drawing this relationship which is represented by a line , where X. axis represents

S0-S/ $q$ X and y-axis represents $\dfrac{\Delta X}{q\,X}$ for $q$ = 4,5 and the value of the run end, the inclination

of this line represents the value of y (Yielding coefficient ) and the value of intersection of this line with y axis re presents (k$_d$).

The values of y and k$_d$ are shown in table (10).

**Table2:  Gruoup 1 Run No.(1) - (20 - 25)$^o$C**

| Day | Temp $^0$C | TSS | η% | COD | η% | BOD | η% | MLVSS |
|---|---|---|---|---|---|---|---|---|
| | | mg / L | | mg / L | | mg / L | | mg / L |
| 1 | 20.2 | 953.5 | 0 | 771 | 4 | 275.3 | 0 | N.D |
| 2 | 20.9 | 901 | 5.5 | 717.5 | 6.9 | 256.2 | 6.9 | N.D |
| 3 | 21.3 | 809 | 15.1 | 681 | 11.6 | 243.2 | 11.6 | N.D |
| 4 | 21.9 | 701 | 26.4 | 601 | 16.2 | 214.6 | 16.2 | N.D |
| 5 | 22.8 | 481 | 49.5 | 392 | 42.4 | 140 | 42.4 | 1527 |
| 6 | 23.7 | 476 | 50.1 | 385 | 50.1 | 137.5 | 50.1 | 1528 |
| Average Value | 24.8 | 720 | 24 | 591 | 22 | 211 | 21 | |
| Max. Value | 22.2 | 954 | 50 | 771 | 50 | 275 | 50 | |
| Min. Value | 24.8 | 476 | 0 | 385 | 4 | 138 | 0 | |

**Table3: Group 1 Run no.(2) - (25 - 30)$^o$C**

| Day | Temp $^0$C | TSS mg / L | η% | COD mg / L | η% | BOD mg / L | η% | MLVSS mg / L |
|---|---|---|---|---|---|---|---|---|
| 1 | 25.2 | 950 | 3.5 | 770 | 4.7 | 308 | 0 | N.D |
| 2 | 26.9 | 900 | 5.2 | 621 | 19.3 | 248.4 | 19.3 | N.D |
| 3 | 27.3 | 814 | 14.3 | 514 | 33.2 | 205.6 | 33.2 | N.D |
| 4 | 27.9 | 620 | 34.7 | 400 | 48.1 | 160 | 35.5 | 1570 |
| 5 | 28.8 | 480 | 49.4 | 350 | 54.5 | 140 | 54.5 | 1575 |
| 6 | 29.7 | 390 | 58.9 | 319 | 58.5 | 127.6 | 58.5 | N.D |
| 7 | 30 | 380 | 60 | 308 | 60 | 123.2 | 60 | 1565 |
| Average Value | **25.3** | **648** | **32** | **469** | **40** | **188** | **37** | |
| Max. Value | **30** | **950** | **60** | **770** | **60** | **308** | **60** | |
| Min. Value | **25.2** | **380** | **4** | **308** | **5** | **123** | **0** | |

**Table4:Group 1  Run No.(3)  - (30 - 35)$^o$C**

| Day | Temp $^0$C | TSS mg / L | η% | COD mg / L | η% | BOD mg / L | η% | MLVSS mg / L |
|---|---|---|---|---|---|---|---|---|
| 1 | 30.2 | 959 | 0 | 770 | 0 | 275 | 0 | N.D |
| 2 | 30.7 | 710 | 25.9 | 695 | 9.7 | 248.2 | 9.74 | N.D |
| 3 | 31.6 | 600 | 37.4 | 511 | 33.6 | 182.5 | 33.6 | N.D |
| 4 | 32.1 | 436 | 54.5 | 420 | 45.4 | 150 | 45.4 | 1585 |
| 5 | 32.7 | 320 | 66.6 | 290 | 62.3 | 103.5 | 62.3 | 1628 |
| 6 | 33.6 | 300 | 68.7 | 260 | 66.2 | 92.8 | 66.2 | N.D |
| 7 | 34.0 | 282 | 70.5 | 230 | 70.1 | 82.1 | 70.1 | N.D |
| 8 | 34.7 | 278 | 71. | 223 | 71.0 | 79.6 | 71.0 | 1600 |
| Average Value | **32.5** | **486** | **49** | **425** | **45** | **152** | **45** | |
| Max. Value | **34.7** | **959** | **71** | **770** | **71** | **275** | **71** | |
| Min. Value | **30.2** | **278** | **0** | **223** | **0** | **80** | **0** | |

**Table5: Group 2  Run No.(1) - (35 - 40)Oc**

| Day | Temp $^0$C | TSS mg / L | η% | COD mg / L | η% | BOD mg / L | η% | MLVSS |
|---|---|---|---|---|---|---|---|---|
| 1 | 35.2 | 955 | 0 | 760 | 0 | 253.3 | 0 | N.D |
| 2 | 35.7 | 711 | 25.5 | 600 | 21.1 | 200 | 21.1 | N.D |
| 3 | 36.6 | 600 | 37.1 | 500 | 34.2 | 166.6 | 34.2 | N.D |
| 4 | 37.1 | 410 | 57.1 | 390 | 48.6 | 130 | 48.6 | 1615 |
| 5 | 37.7 | 300 | 68.5 | 311 | 59.1 | 103.6 | 59.1 | 1638 |
| 6 | 38.0 | 285 | 70.1 | 290 | 61.8 | 96.6 | 61.8 | N.D |
| 7 | 38.3 | 269 | 71.8 | 225 | 70.3 | 75 | 70.3 | N.D |
| 8 | 38.6 | 263 | 72.4 | 215 | 71.7 | 71.6 | 71.7 | N.D |
| 9 | 39.0 | 260 | 72.7 | 209 | 72.5 | 69.6 | 72.5 | 1615 |
| Average Value | 37.4 | 450 | 53 | 389 | 49 | 130 | 49 | |
| Max. Value | 39.0 | 955 | 73 | 760 | 73 | 253 | 73 | |
| Min. Value | 35.2 | 260 | 0 | 209 | 0 | 70 | 0 | |

**Table6: Group 2 Run No.(2) - (40 - 45)oC**

| Day | Temp $^0$C | TSS mg / L | η% | COD mg / L | η% | BOD mg / L | η% | MLVSS |
|---|---|---|---|---|---|---|---|---|
| 1 | 40.3 | 955 | 0 | 760 | 0 | 304 | 0 | N.D |
| 2 | 40.9 | 718 | 24.8 | 590 | 22.3 | 236 | 22.3 | N.D |
| 3 | 41.8 | 590 | 38.2 | 430 | 43.4 | 172 | 43.4 | N.D |
| 4 | 42.3 | 400 | 58.1 | 315 | 58.5 | 126 | 58.5 | 1688 |
| 5 | 42.9 | 330 | 65.4 | 229 | 69.8 | 91.6 | 69.8 | 1720 |
| 6 | 43.0 | 290 | 69.6 | 211 | 72.2 | 84.4 | 72.2 | N.D |
| 7 | 43.3 | 255 | 73.2 | 190 | 75 | 76 | 75 | N.D |
| 8 | 43.9 | 235 | 75.3 | 188 | 75.2 | 75.2 | 75.2 | N.D |
| 9 | 44.2 | 230 | 75.9 | 186 | 75.5 | 74.4 | 75.5 | N.D |
| 10 | 44.7 | 229 | 76.1 | 182 | 76.1 | 72.8 | 76.1 | 1655 |
| Average Value | 42.7 | 423 | 56 | 328 | 57 | 131 | 57 | |
| Max. Value | 44.7 | 955 | 76 | 760 | 76 | 304 | 76 | |
| Min. Value | 40.3 | 229 | 0 | 182 | 0 | 73 | 0 | |

### Table7: Group 3 Run No.(1) - (45 - 50)°C

| Day | Temp °C | TSS mg / L | η% | COD mg / L | η% | BOD mg / L | η% | MLVSS |
|---|---|---|---|---|---|---|---|---|
| 1 | 45.3 | 960 | 0 | 760 | 0 | 304 | 0 | N.D |
| 2 | 45.9 | 601 | 37.4 | 520 | 31.5 | 208 | 31.5 | N.D |
| 3 | 46.2 | 550 | 42.7 | 490 | 35.5 | 196 | 35.5 | N.D |
| 4 | 46.9 | 490 | 48.9 | 411 | 45.9 | 164.4 | 45.9 | 1538 |
| 5 | 47.1 | 400 | 58.3 | 360 | 52.6 | 144 | 52.6 | 1539 |
| 6 | 47.9 | 330 | 65.6 | 320 | 57.8 | 128 | 57.8 | N.D |
| 7 | 48.3 | 300 | 68.7 | 296 | 61.1 | 118.4 | 61.1 | N.D |
| 8 | 48.6 | 280 | 70.8 | 250 | 67.1 | 100 | 67.1 | N.D |
| 9 | 48.9 | 268 | 72.1 | 220 | 71.1 | 88 | 71.1 | N.D |
| 10 | 49.0 | 265 | 72.3 | 211 | 72.1 | 84.4 | 72.2 | N.D |
| 11 | 49.6 | 260 | 72.9 | 205 | 73. | 82 | 73.1 | 1490 |
| Average Value | 47.6 | 428 | 55 | 368 | 52 | 147 | 52 | |
| Max. Value | 49.6 | 960 | 73 | 760 | 73 | 304 | 73 | |
| Min. Value | 45.3 | 260 | 0 | 205 | 0 | 82 | 0 | |

### Table8: Group 3 Run No.(2) - (50- 55)°C

| Day | Temp °C | TSS mg / L | η% | COD mg / L | η% | BOD mg / L | η% | MLVSS |
|---|---|---|---|---|---|---|---|---|
| 1 | 50.3 | 966 | 0 | 761 | 0 | 306 | 0 | N.D |
| 2 | 50.9 | 600 | 37.4 | 526 | 31.5 | 206 | 31.5 | N.D |
| 3 | 51.2 | 552 | 42.7 | 493 | 35.5 | 196 | 35.5 | N.D |
| 4 | 51.9 | 496 | 48.9 | 416 | 45.9 | 164.9 | 45.9 | 1538 |
| 5 | 52.1 | 405 | 58.3 | 366 | 52.6 | 149 | 52.6 | 1539 |
| 6 | 52.9 | 331 | 65.6 | 322 | 57.8 | 129 | 57.8 | N.D |
| 7 | 53.3 | 302 | 68.7 | 293 | 61.1 | 118.9 | 61.1 | N.D |
| 8 | 53.6 | 289 | 70.8 | 256 | 67.1 | 108 | 67.1 | N.D |
| 9 | 53.9 | 265 | 72.1 | 223 | 71.1 | 89 | 71.1 | N.D |
| 10 | 54.0 | 266 | 72.3 | 213 | 72.1 | 84.5 | 72.2 | N.D |
| 11 | 55.6 | 269 | 72.9 | 203 | 73. | 83 | 73.1 | 1490 |
| Average Value | 53.6 | 426 | 55 | 366 | 52 | 148 | 52 | |
| Max. Value | 55.6 | 966 | 73 | 766 | 73 | 309 | 73 | |
| Min. Value | 50.3 | 266 | 0 | 206 | 0 | 83 | 0 | |

**Table 9: Bacterial Growth and Substrate Utilization Rate for $q$ = 4,5 and the Value for the End of Each Run**

| Group No. | Group (1) | | | Group (2) | | Group (3) | |
|---|---|---|---|---|---|---|---|
| | Run No1 20-25 $^0$C | Run No2 25-30 $^0$C | Run No3 30-35 $^0$C | Run No1 35-40 $^0$C | Run No2 40-45 $^0$C | Run No1 45-50 $^0$C | Run No2 50-55 $^0$C |
| $q$ = $q$c = 4 | | | | | | | |
| $\Delta$ X | N.D | 70 | 85 | 115 | 188 | 110 | 38 |
| $\Delta$ X/$q$ X | N.D | 0.012 | 0.014 | 0.019 | 0.03 | 0.018 | 0.006 |
| So-S | 170 | 370 | 350 | 370 | 445 | 349 | 270 |
| So-S/$q$ X | 0.028 | 0.062 | 0.058 | 0.06 | 0.074 | 0.058 | 0.045 |
| $q$ = $q$c = 5 | | | | | | | |
| $\Delta$ X | 47 | 75 | 128 | 138 | 220 | 118.5 | 39 |
| So-S | 379 | 420 | 480 | 449 | 531 | 400 | 320 |
| So-S/$q$ X | 0.05 | 0.056 | 0.064 | 0.06 | 0.071 | 0.053 | 0.043 |
| $\Delta$ X/$q$ X | 0.006 | 0.01 | 0.017 | 0.018 | 0.029 | 0.016 | 0.005 |
| $q$ =End of each run | 6 | 7 | 8 | 9 | 10 | 11 | 12 |
| $\Delta$ X | 28 | 65 | 100 | 115 | 155 | 85 | - 10 |
| $\Delta$ X/$q$ X | 0.003 | 0.006 | 0.008 | 0.0085 | 0.01 | 0.005 | $\approx$ 0 |
| So-S | 386 | 462 | 547 | 551 | 578 | 555 | 539 |
| So-S/$q$ X | 0.043 | 0.044 | 0.046 | 0.041 | 0.038 | 0.034 | 0.03 |
| X for the all runs | 1500 mg/l | | | | | | |

**Table 10: Values of Kinetic Coefficients (y,$k_d$) for the Different Temperature Ranges**

| Group No. | Group (1) | | | Group (2) | | Group (3) | |
|---|---|---|---|---|---|---|---|
| Kinetic coefficients | Run No1 Temp $(20-25^o)$ | Run No2 Temp $(25-30^o)$ | Run No3 Temp $(30-35^o)$ | Run No1 Temp $(35-40^o)$ | Run No2 Temp $(40-45^o)$ | Run No1 Temp $(45-50^o)$ | Run No2 Temp $(50-55^o)$ |
| y | 0.4 | 0.43 | 0.47 | 0.52 | 0.59 | 0.50 | 0.25 |
| $k_d$ | 0.014 | 0.014 | 0.013 | 0.013 | 0.0125 | 0.013 | 0.03 |

**From group No( 1) it can be noted the following:**
* The removal efficiency of TSS was increased by increasing water temperature and this is due to increasing of the yielding biomass for achieving more adhesion among the bacterial cells and as a result TSS removal efficiencies was increased.
* The removal efficiency of COD and BOD$_5$ were increased by increasing the water temperature and this is due to increasing of the bacterial sludge activities which is represented in the increase of yielding coefficient values as the temperature increased.

**From group No. (2) , (shock load effect), it can be noted the following:**
* The removal efficiency of TSS was increased by increasing water temperature achieving maximum removal efficiency = 76% at temperature range (40-45)$^o$ as maximum cell bacterial growth was achieved at this Temperature range.
* The removal efficiency of COD and BOD$_5$ were increased by increasing water temperature and achieved maximum removal efficiencies = 75,76% respectively at temperature range (40-45)$^o$.

**From group No (3) it can be noted the following:**

* The removal efficiency of TSS was decreases by increasing water temperature achieving removal efficiency = 71% at temperature range (45-55) $^o$.
* The removal efficiency of COD and BOD5 were decreased also by increasing water temperature achieving maximum removal efficiency = 73% at temperature range (45-55$^o$).

* It was obvious that the activity decrease due to dieing the non spore former bacteria and the spore formar bacteria began to resist the high temperature, It has been found that these heat-tolerant microorganisms have proteins, which resist denaturation at the lower temperatures. And at high temperatures, the heat resistant proteins are denatured and even the heat-tolerant microorganisms soon die off.
* The yielding coefficient increased with increasing temperature changes with maximum value = 0.59 at temperature range (40-45)$^o$ and decrease smoothly at temperature range (45-50)$^o$ and then decreased deeply at temperature range (50-55)$^o$ where it reached a value =0.25.
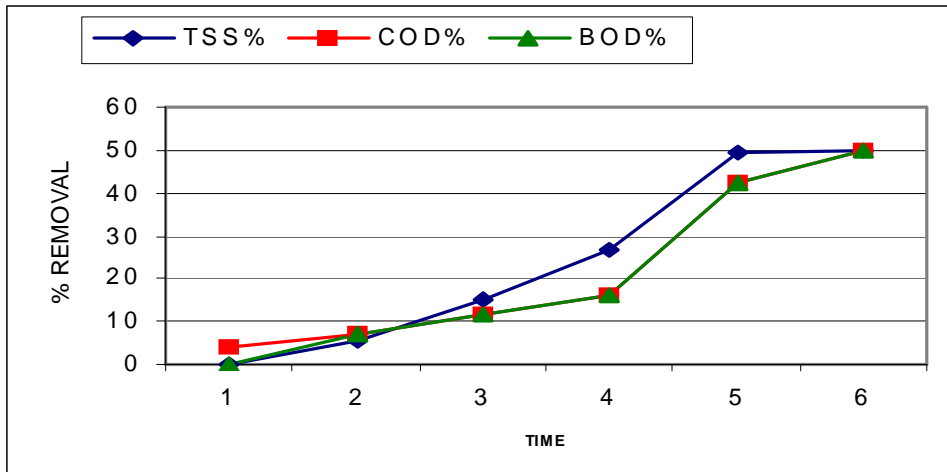


**Fig.4: TSS, COD Removal Efficiencies for Group No. (1) - Run No. (1)**
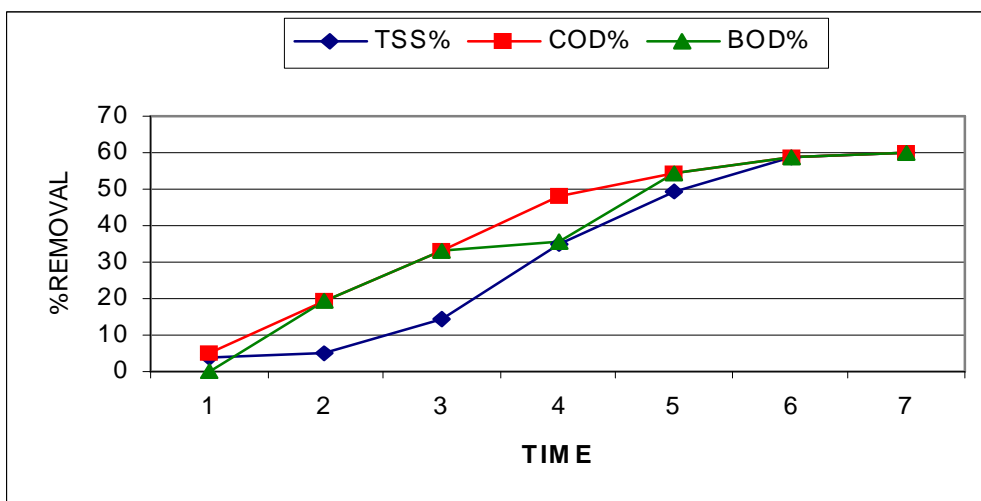


**Fig. 5: TSS, BOD5, COD Removal Efficiencies for Group No. (1) - Run No. (2)**
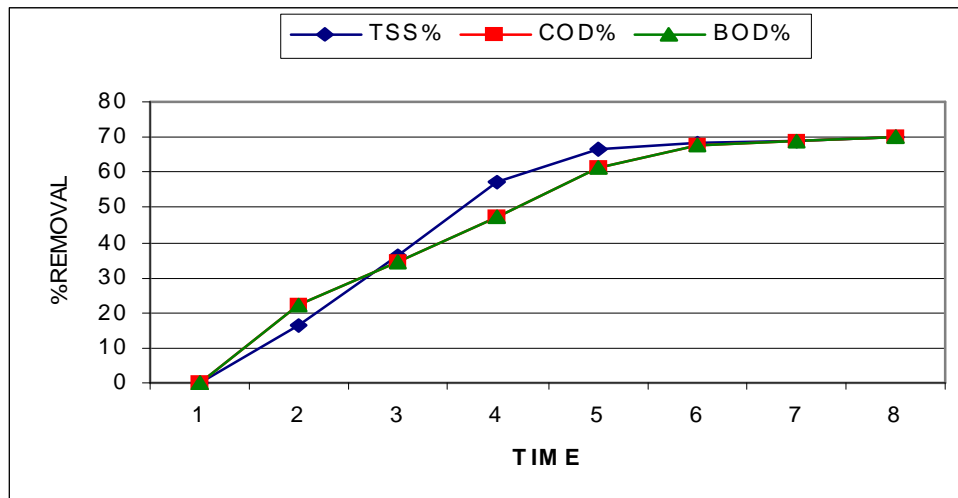
**Fig. 6: TSS, BOD5, COD Removal Efficiencies for Group No. (1) - Run No. (3)**
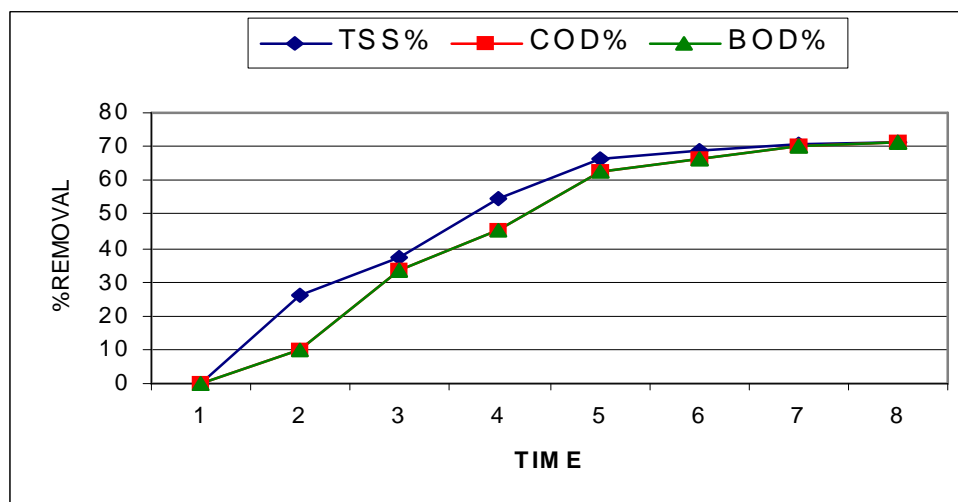


**Fig. 7: TSS, BOD5, COD Removal Efficiencies for Group No. (2) - Run No.( 1)**
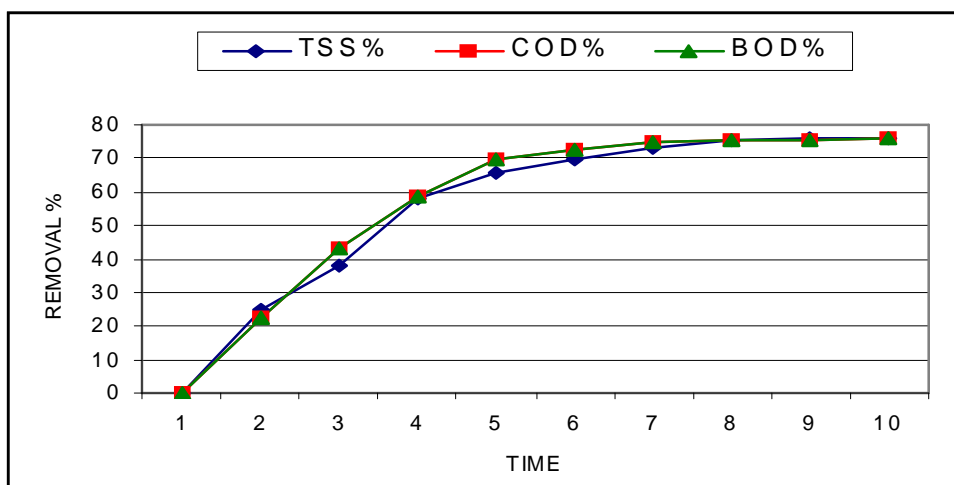


**Fig. 8: TSS, BOD5, COD Removal Efficiencies for Group No. (2) - Run No. (2)**
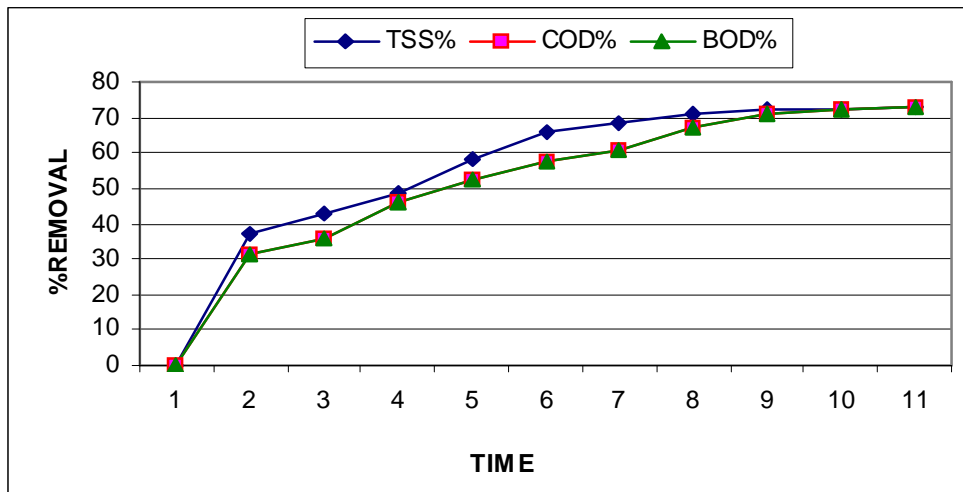
**Fig. 9: TSS, BOD5, COD Removal Efficiencies for Group No.( 3) - Run No. (1)**
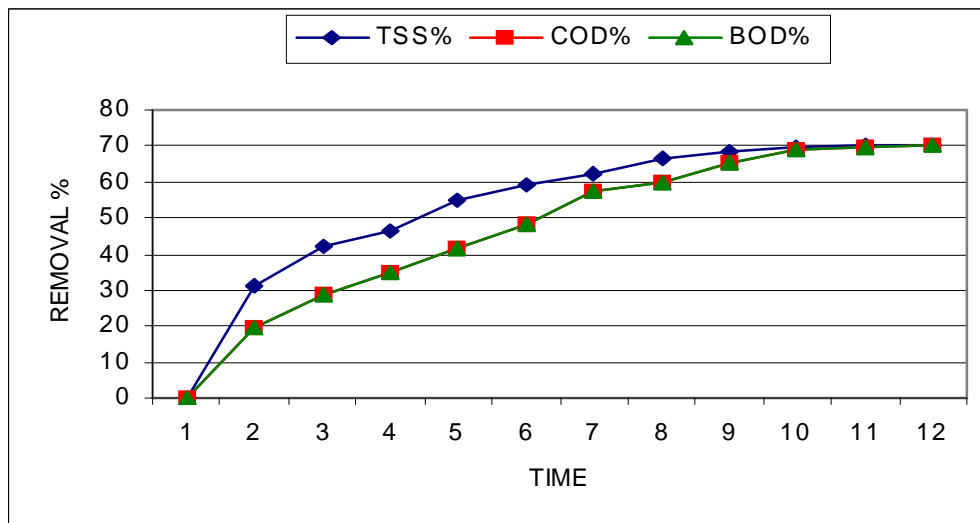


**Fig. 10: TSS, BOD5, COD Removal Efficiencies for Group No. (3) - Run No. (2)**

## CONCLUSIONS

In conclusion, the most important findings in this study can summarized as follows:

1. The removal efficiencies of TSS, COD,BOD were increased by increasing water temperature and this is due to increasing the bacterial activity.

2. The optimum removal efficiencies for  TSS, COD,BOD occurred at 70% domestic+30% industrial at temperature range 40-45$^o$C because this ratio gave the microbial group addition characteristic and resistance to bacterial cell to resist the shock load which reached it's maximum activity and maximum bacterial growth rate at (40-45$^o$C) insisted of 35 $^o$C in conventional activated sludge .

3. The removal ratio for COD,BOD and TSS increases  until reach temperature range (40-45)$^0$C which enable the biological treatment of mixture domestic and industrial wastewater to be preferably applied in hot climate countries .

4.TSS, COD and BOD removal values increase with the increasing of temperature changes till reach (40-45)C$^˙$  range, and this is due to the increasing of the reaction rate of the

microorganisms enzymes and forming new cells which was represented in increasing the value of MLVSS , yielding coefficient with the increasing of temperature changes causing hurrying up the rate of the organic matter degradation and as a result, the biological removal increases, and after the range (40-45) $^{o}$C, TSS and COD,BOD removal values begin to decrease with increasing the temperature and this is due to the denaturation of the protein fraction of the enzymes, resulting in the destruction of the enzymes and this increases the dissolved organic matters which decrease the percent of TSS and COD removals.

**5.**As temperature increase, the SRT also increased until reached 11 day with temperature range 40-45$^{o}$ compared with the original case temperature range (20-25$^{o}$) where is constant the max removal occurred after 6 day so the heating increase the SRT of bacteria.

## REFERENCES

1. Abia AA, Horsfall M Jnr, Didio (2003). The use of chemically modified and unmodified cassava waste for the removal of Cd, Cu and Zn ions from aqueous solution. Bioresource Technol. (in press).
2. A.Hassan , 2002, " Effect of temperature changes on biological treatment by activated sludge process without using primary settling". Ms.c. Thesis, Faculty of Engineering, Cairo University.
3. Blanco AB, Sanz B, Lama MJ, Serra JL (1999). Biosorption of heavy metals to immobilized Phormidium laminosum biomass. J.Biotechnol. 69: 227-240.
4. B. BOHNKE, B. DIERING AND S. AN W. ZUCKUT,1997, "AB Process Removes Organic and Nutrients". Water Environmental & Technology, Rediscovering Natural System. March.
5. B.BOHNKE, Ausgable 1992, "The Adsorption – Bio-Oxidation Treatment (AB-Process)". Das AB-Verfahren zur biologischen Abswasserreinigung, S. 4-5.
6. Gray, N.F.,1990, Activated Sludge Process. Theory and Practice OXFORD University Press, Newyork.
7. Metcalf&Eddy edition 3 (wastewater treatment technology).
8. Marck Silin . (1994)bilogical wastewater treatment technology .
9. Mofa AS (1995). Plants proving their worth in toxic metal cleanup.Science 269: 302-305.
10. Standard methods for the examination of Water and Wastewater.APHA, AWWA, WPCF, Washington, DC, 1992.
11. Singleton I. (1994) Microbial metabolism of xenobiotics: Fundamental and applied research. J.chem.Tech.Biotechnol.59, 9-23.
12. Sherien Mohamed ( 2004 ) effect of industrial wastewater on the activity of aerobic sludge . Ms.C. Thesis, Faculty of Engineering Ain Shams University .

## List of Abbreviation:

| | |
|---|---|
| DO | Dissolved oxygen |
| MLVSS | Mixed liquor volatile Suspended Solids |
| Y | Yielding coefficient |
| $R_g$ | Cell growth |
| $r_{su}$ | Substrate utilization |
| $K_d$ | Decay rate |
| $BOD_5$ | Biochemical oxygen demand |
| COD | Chemical oxygen demand |
| TSS | Total Suspended Solids |

| | |
|---|---|
| So | Concentration of Initial COD |
| S | Concentration of COD at any time |
| $q$ | Hydraulic retention time = sludge retention time ($q_c$) |
| X | Concentration of Initial ML VSS |
| $\Delta X$ | Increase of Concentration of Initial ML VSS |
| η | Removal efficiency |

# ON THE MODELING OF FLOW REGIMES AND THERMAL PATTERNS INTERACTIONS IN COMPLEX APPLICATIONS

**Essam E. KHALIL**

*Cairo University - Faculty of Engineering*
*Email:     khalile1@asme.org*

## ABSTRACT

The recent advances in numerical methods and the vast development of computers had directed the designers to better development and modifications to airflow pattern and heat transfer in complex geometries such as combustion chambers, aluminum reductions cells and air conditioned operating theatres. The Present work fosters mathematical modeling techniques to primarily predict what happens in three-dimensional complex geometries and presents a summary of its status quo. Applications include, among others, combustion chambers, aero engines in terms of flow regimes and interactions .It also includes predictions of flow and heat transfer in Aluminum reduction pots where the pot is full with the molten metal and electrolyte in the anodes- cathode void. Magnetic field and forces would result in molten metal movement, stirring and consequently possible re-oxidation of aluminum at anode surfaces causing low productivity. The flow in air-conditioned operating theatres is also addressed in this paper. The present work is generally devoted to demonstrate the effect of design and operational parameters on performance of such systems.

The governing equations of mass, momentum, species and energy are commonly expressed in a general finite difference form to be solved with the aid of SIMPLE Algorithm. The results are obtained in this work with the aid of the three-dimensional program; applied to axe symmetrical and three-dimensional complex geometries. The present numerical grid comprises, typically, 80 x 60 x 30-grid mesh of total 144000-grid node covering the volume in the X, R or Y and Z coordinates directions. The numerical residual in the governing equations are typically less than 0.001 %.

The obtained results include velocity vectors, turbulence intensities, temperatures and wall heat fluxes. Flow regimes and heat transfer were found to be strongly dependent on turbulent shear, mixing, blockages, wall conditions and inlet conditions. Examples of large industrial furnaces, reduction cells and operating theatres are shown and are in good agreement with available measurements in the open literature .One may conclude that flow patterns, turbulence and heat transfer in complex geometries are strongly affected by the inlet and boundary conditions; both micro and macro mixing levels are influential. The present modeling capabilities can adequately predict the local flow pattern and turbulence kinetic energy levels in complex geometries

**Keywords:** Thermal Modeling, Thermal & Flow Interaction, Flow Regimes in Complex Applications

## INTRODUCTION

The Present mathematical approach solves numerically flow regimes interaction and turbulence characteristics. The governing equations of mass, momentum and energy are commonly expressed in a preset form. The source terms in the equations represent pressure gradients, viscous action and chemical reactions in these equations. The governing equations are to be solved in the finite difference mode at discretized grid nodes mapping the furnace. The physical and chemical characteristics of the air and fuels are obtained from tabulated data in the literature. The flow regimes and heat transfer plays an important role in the efficiency and utilization of energy. Khalil [1, 2 & 3] reported these to be strongly dependent on turbulent shear

behavior, mixing, chemical kinetics, wall conditions and geometry of burners. Fluid flow and turbulent characteristics in turbulent combustion chambers play an important role in the thermal balance and performance of the combustor.   The fluid flow, recirculation patterns and turbulence enhance mixing between different layers in the chamber. The second example is to analyze carefully the flow pattern in the combustion chamber and to relate the flow to mixing and heat transfer.   As seen above, the flow   regime is complex and of three- dimensional nature. Previous work to model the chambers flow field was reported in the open literature by Khalil [1], Gupta et al [4], etc.  Due to nature of the flow in the combustor and the steep velocity gradients, turbulent shear stress are generated and coupled with flow velocities will impose additional production of turbulence aiding mass and momentum exchange. With the advance of computational techniques it is now possible to numerically simulate three-dimensional flows.

The recent advances in numerical methods and the vast development of computers had directed the designers to better development and modifications to Aluminum Reduction Cell design. Extensive efforts are exerted to reduce the energy requirements to produce aluminum by reduction of its ore in prebaked cells.   The 150 k A Soderberg Reduction cell considered in the present work is one of the end-to-end pot line cells at EGYPTALUM, Nage Hammady, Egypt, Khalil [5].  Mathematical modeling is concerned primarily with what happens in the metal pad and bath. The pot is full with the molten metal and electrolyte in the anodes- cathode void. Magnetic field and forces due to electric currents flowing between the anode and cathode would result in molten metal stirring and consequently possible re-oxidation of aluminum at anode surfaces. Such action would be a loss of energy and aluminum, typically represented by low current efficiency.  Cells with higher current efficiencies have better yield and the status quo for current efficiencies is of order of 94%.

The source terms in the governing equations represent the pressure gradients, viscous action, magnetic forces etc. in the momentum equations. Fx, Fy and Fz are obtained from the electromagnetic modeling procedure. In Aluminum reduction cells, the flow regimes and heat transfer play an important role in the current efficiency and utilization of cell. The behavior was found by Khalil [5] , to be strongly dependent on turbulent shear , mixing, ledge formation , wall lining thickness and composition as well as bus bar arrangements and physical-chemical properties of cell constituents .  The present work demonstrates the capabilities of predicting Flow behavior in  an End-To-End Cell with  144000-grid node mapping  the cell cavity  volume in the X , Y and Z coordinates directions, Khalil et al [6] .The numerical residual in the governing equations is typically less than 0.001 %.

Air conditioning implies the conditioning of airflow and heat transfer characteristics, temperatures, humidity, and dust level inside an enclosed space. The conditions to be maintained are dictated by the function of the conditioned space; therefore air conditioning embraces more than cooling or heating. Comfort air conditioning is defined as "the process of treating air to control simultaneously its temperature, humidity, cleanliness, and distribution to meet the comfort requirements of the occupants of the conditioned space.", ASHRAE [7]. Air conditioning therefore includes the regulation of velocity, thermal radiation, quality of air, and removal of foreign particles and vapors, Chow [8]. Thermal comfort is generally associated with a neutral body thermal sensation, Berglund [9], which in turn depends on thermal balance, metabolism and clothing. It is imperative that all attempts should be focused on assuring the satisfaction of the required balance of rate of water loss from human body and surrounding air. Air movement in a room, therefore, becomes of vital importance to comfort, Khalil [10]. The healthcare requirements in residential applications differ basically from those applied to medical applications.

## NUMERICAL METHOD

### Mathematical Formulation

Three time averaged velocity components in X, Y, and Z coordinate directions were obtained by solving the finite difference form of the governing equations using a "SIMPLE Numerical Algorithm" [Semi Implicit Method for Pressure Linked Equation] described earlier in the work [11-12]. The turbulence characteristics were represented by a modified $k - \varepsilon$ model to account

for normal and shear stresses and near-wall functions. Fluid properties such as densities, viscosity and thermal conductivity were obtained from references. The present work made use of the computer Package, which is developed, by Khalil [5, 10]. The program solves the differential equations governing the transport of mass, three momentum components and energy in three-dimensional configurations. The equations are typically expressed as:

$$div\left(\rho V \Phi - \Gamma_{\Phi,\text{eff}} \cdot grad\, \Phi\right) = S_{\Phi} \tag{1}$$

Where:

$\rho$ = Air density, kg/m3        $\Phi$ = Dependent variable.

V = Velocity vector         $\Gamma_{\Phi,\text{ eff}}$ = Effective diffusion coefficient.

$S_{\Phi}$ = Source term of $\Phi$.

The effective diffusion coefficient and source term for the differential equations are listed in Table 1. The CFD model uses approximations in calculating the turbulence quantities, such as isotropic turbulence and the Boussinesq eddy viscosity concept.

Table 1. Values of $\Phi$, $\Gamma_{\Phi,\text{eff}}$, and $S_{\Phi}$ for Partial Differential Equations

| | $\Phi$ | $\Gamma_{\Phi,\text{eff}}$ | $S_{\Phi}$ |
|---|---|---|---|
| Continuity | 1 | 0 | 0 |
| X-momentum | U | $\mu$ | $-\partial P/\partial x + \rho g_x$ |
| Y-momentum | V | $\mu$ | $-\partial P/\partial y + \rho g_y$ |
| Z-momentum | W | $\mu$ | $-\partial P/\partial z + \rho g_z + \rho g \beta \Delta t$ |
| H-energy equation | H | $\mu / \sigma_H$ | $S_H$ |
| Fuel-equation | Fu | $\mu / \sigma_{Fu}$ | $S_{Fu}$ |
| k-equation | k | $\mu / \sigma_k$ | $G - \rho \varepsilon$ |
| $\varepsilon$-equation | $\varepsilon$ | $\mu / \sigma_\varepsilon$ | $C_1 \varepsilon G / k - C_2 \rho \varepsilon^2 / k$ |
| $\mu = \mu_{lam} + \mu_t$     $C_1 = 1.44$, $C_2 = 1.92$, $C_\mu = 0.09$    $\sigma_H = \sigma_{Fu} = 0.9$,    $\sigma_k = 1.0$,   $\sigma_\varepsilon = 1.3$ ||||
| $\mu_t = \rho C_\mu k^2 / \varepsilon$ <br> $G = \mu\,[2\{(\partial U/\partial x)^2 + (\partial V/\partial y)^2 + (\partial W/\partial z)^2\} + (\partial U/\partial y + \partial V/\partial x)^2 + (\partial V/\partial z + \partial W/\partial y)^2 + (\partial U/\partial z + \partial W/\partial x)^2]$ ||||

**Boundary Conditions**

The solution of the governing equations can be realized through the specifications of appropriate boundary conditions. The values of velocity, temperature, kinetic energy, and its dissipation rate should be specified at all boundaries.

External Walls: A non-slip condition at all solid walls is applied to the velocities. The logarithmic law or wall function has been used as Launder and Spalding [12], for the near wall boundary layer.

Air Inlets: At inlets the air velocity was assumed to be have a uniform distribution; inlet values of the temperature were assumed to have a constant value and a uniform distribution. The kinetic energy and its dissipation are estimated as follow.

$k_{in} = 3\,(0.5\,(I_{in}\,U_{in})^2)$, where $I_{in}$ = Intensity of disturbance at air inlet.

$\varepsilon_{in} = C_\mu\,(k_{in})1.5 / I_e$, where $I_e$ = Dissipation length at air inlet.

Initial Guessed Values: All velocity components were set as zeros initially, and temperatures were assumed to be equal to the steady state value of the comfort condition. The kinetic energy and its dissipation are estimated as follow.

$k_{initial} = 11E^{-5}$, $\varepsilon initial = C_\mu\,(k_{in})^{1.5} / c\,d$, where c = constant, and d = distance to nearest side wall.

**Numerical Procedure**

The Computer Program was used to solve the time-independent (steady state) conservation equations together with the standard k-ε model as Launder and Spalding [12], and the corresponding boundary conditions. The numerical solution grid divided the surgical operating theatre into a discretized computational cells (80 x 60 x 30 grid nodes) using the modified hyperbolic equation as in equation 2. The discrete finite difference equations were solved with the SIMPLE algorithm as in Spalding & Patankar [11]. The solution convergence criteria used at each iteration ensured the total normalized residuals were less than 0.1% for flow, 1% for k and ε, and 0.1 for energy.

$$X_k = L_{k-1} + 0.5\,L_i\,[1 + \frac{Sinh(\alpha_i\,(I/n_i - 0.5))/Cosh(\beta\,\alpha_i\,(I/n_i - 0.5))}{Sinh(\alpha_i\,/\,2)/Cosh(\beta\,\alpha_i\,/\,2)}] \tag{2}$$

The staggered grid arrangement and computational procedure are shown in figures 1and 2.
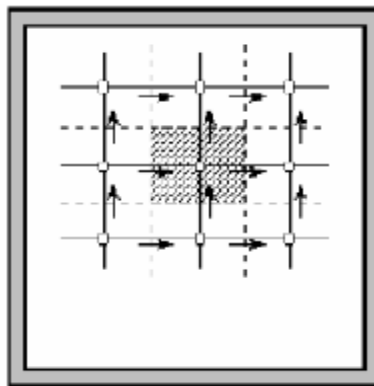


**Fig. 1: Staggered Grid Arrangement**
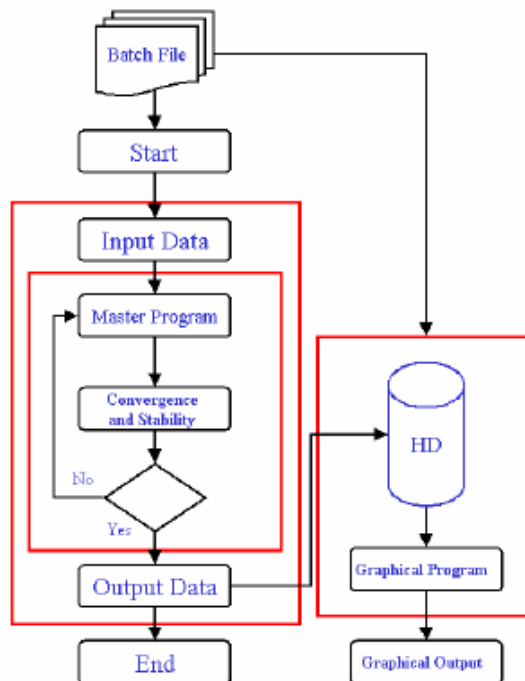


**Fig. 2: General Flowchart**

## COMPUTATIONAL RESULTS

Previous comparisons between measured and predicted flow pattern, turbulence characteristics, and heat transfer were reported earlier in the open literature utilizing the present computational capabilities , reference should be made to these for further details and assessments. A summary of the main assessment is expressed here as follows. The present predictions of flow and turbulence characteristics are in general qualitative agreement with the corresponding experiments and numerical simulations, Khalil [10]. The trends are in adequate agreement for engineering purposes. Nevertheless discrepancies exist and particularly in the vicinity of recirculation zone boundaries. More discrepancies can also be viewed in situation with heated flows than those of ventilation or cooling. Stratified flows and buoyancy effects may not be adequately predicted with the present simple form of the two equation turbulence models.

### Industrial Furnaces

The present geometrical configuration represents the flow situations in the furnace of the IFRF data published by Bartelds et al  [13] .The furnace configurations were of 2x2x6 m firing natural gas at a firing rate of 2.96 MW with excess air of 4% relating to flame 29. The measured and predicted heat flux distributions along the furnace walls are shown in Figure 3. Two-dimensional predictions of Khalil  [1]  are shown by the dashed curve while the present three-dimensional predictions are shown by the solid curve using the new grid generation technique. Both measured and predicted distributions are in relatively good agreement considering the experimental error and modeling assumptions. General qualitative agreement was observed at different locations in the vicinity of the burner wall in both the X-Z plane as well as the X-Y plane.  Velocity profiles in the X-Y, X-Z and X-Y planes were automatically obtained from the three-dimensional solution algorithm. These indicated that the vertical velocity component W is responsible, to some extent, for merging and macro mixing of combustion air . The component gradient $\partial W/\partial Z$ as well as $\partial W/\partial Y$ and $\partial W/\partial X$ will influence the mean flow shear and turbulence generation.
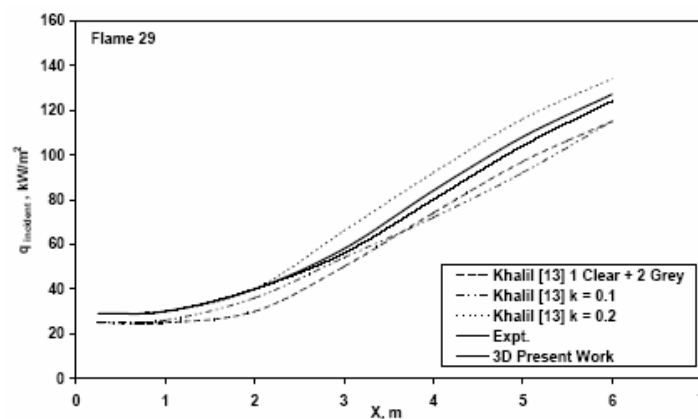


**Fig. 3: Incident Radiant Flux Distribution along Furnace of Reference**

### Aluminum Reduction Cells

The present work made use of an orthogonal Cartesian grid mesh that maps the flow domain. A grid of 80 X 60 X 30 are used. The present section describes the numerical results obtained with the aid of the program developed to predict the aluminum reduction cell behavior under various geometrical and operating conditions. Newly operated cells show different behavior than that with formed ledge. For these cells, cell current, and magnetic forces distributions in three dimensions were prepared by the experts of electro-magnetic and presented in tabulated forms as $F_x$, $F_y$ and $F_z$. The grid utilized in this work was 80 x 60 x 30 grid nodes in the X, Y and Z directions. Numerical computations were obtained for convergence criteria of residuals less than $10^{-3}$, typically $10^{-6}$ as percentage error in satisfying conservation equations.
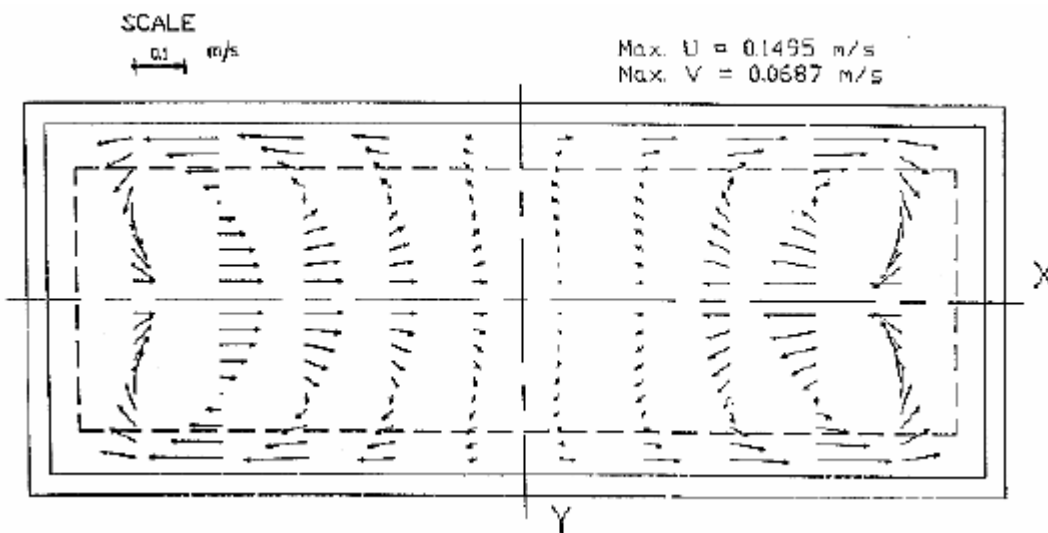
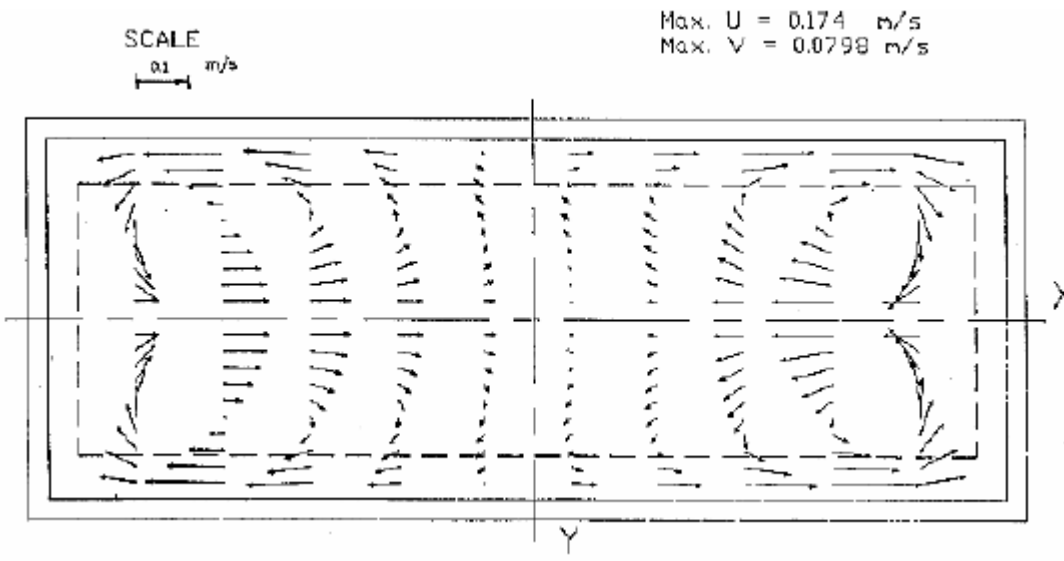**Fig. 4: Vector Velocity Plot (xy plane) at Mid Electrolyte Z= 0.27 m from Cell Cavity Bottom**



**Fig. 5: Vector Velocity Plot (xy plane) at Mid Aluminum Z= 0.12 m from Cell Cavity Bottom**
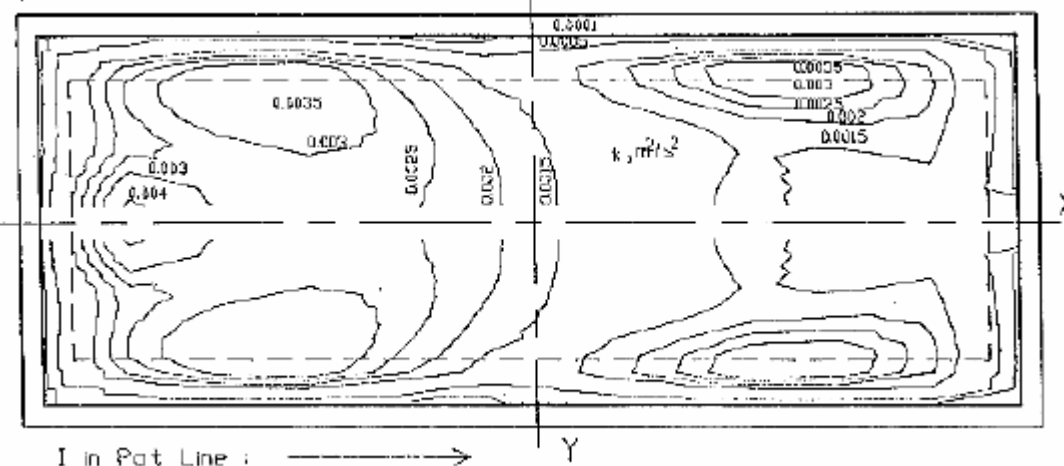


**Fig. 6: Kinetic Energy of Turbulence (xy plane) at Z= 0.12 m**

Figures 4 and 5 represent the mean time averaged velocity vectors in the horizontal X-Y planes at Z=0.12 and 0.27 m respectively. These locations represent mid aluminum plane and middle of electrolyte. Figure 6 shows the kinetic energy of turbulence contours for working cell with ledge (conventional cell) at plane 0.12 m from cathode bottom.  The corresponding X-Y plane vector plot for Silicon Carbide cells showed higher maximum absolute resultant velocities as indicated in Figures display the velocities for cell with and without ledge. Generally the flow pattern is similar in nature but differs in details. The component gradient $\partial W/\partial Z$ as well as $\partial W/\partial Y$ and

$\partial W/\partial X$ will influence the mean flow shear and turbulence generation. Variation of W velocity in Z direction was more influential from dimensional order of magnitude analysis; as $\Delta Z$ is relatively smaller than $\Delta X$ and $\Delta Y$.

### 3.3 Surgical Operating Theatre Configuration

A typical operating theatre configuration is shown in figure 7 is for a room that represents actual surgical operating theatre and including the operating table.
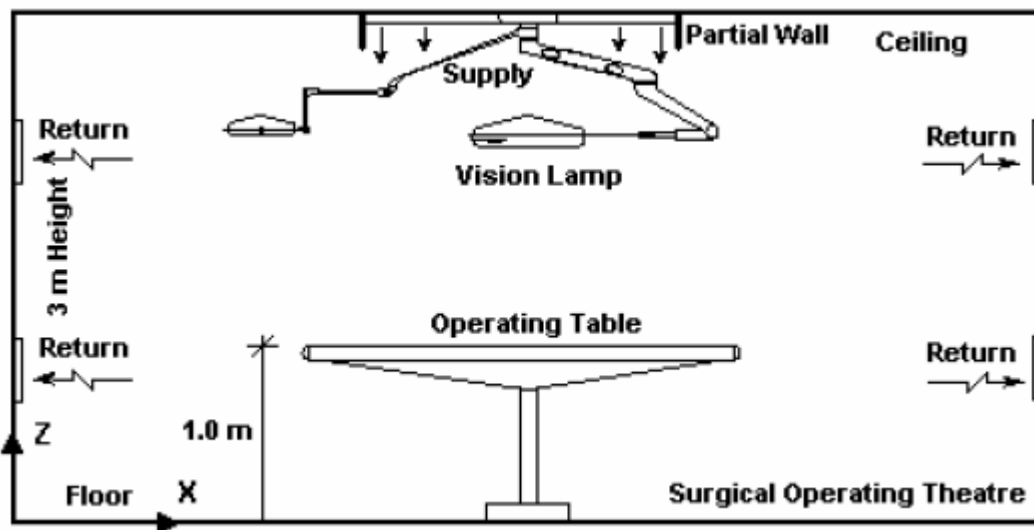


**Fig. 7: Schematic Sketch of the Surgical Operating Theatre (Elevation View).**

The room dimensions are 6.0 m length (L), 5.0 m width (w), and 3.0 m height (H). The operating table has a length of 2.0 m and a width of 1.0 m, and is located at 1.0 m high as shown in figure 7. Ceiling Square Perforated Supply air grilles were located at the center of the room with total dimensions 1.8 m x 1.8 m (9 modules of 0.6 m x 0.6 m with absolute filter banks). The partial walls dropped 200 mm from ceiling. The exhaust ports were located on the left and right walls, see figure 1. The return port dimensions are 0.6 m x 1.8 m. the lower outlet center point is located at 0.7 m from the floor. The higher return port center point located at 1.7 m from the floor Kameel [14]and Henkes [15],.

According to HTM 2025, the down flow of supply air should cover a minimum projected area of 2.8 m by 2.8 m. The boundary of the supply air diffuser should be provided with either partial or full wall rim. A fixed partial wall that terminates at 2 m above the finished floor level (FFL) was introduced. The discharge velocity at the diffuser is a crucial factor to ensure that sufficient air reaches the operating table plane. HTM quotes this as 0.38 m/s as a minimum. The following flow cases were investigated;

*Case 1:* This was based on a discharge velocity of 0.287 m/s, the velocity of the lower exhaust ports is 0.15 m/s, and the velocity of the higher exhaust ports is 0.29 m/s.  In this the Operating Table and partial walls were not considered.

*Case 2*: This was based on a discharge velocity of 0.287 m/s, the velocity of the lower exhaust ports is 0.15 m/s, and the velocity of the higher exhaust ports is 0.29 m/s.  This case was performed for a model room with no partial partition wall.

*Case 3:* This was based on a discharge velocity of 0.287 m/s, the velocity of the lower exhaust ports is 0.15 m/s, and the velocity of the higher exhaust ports is 0.29 m/s.  This case was performed for a model room with partial partition wall.

*Case 4:* This was based on a discharge velocity of 0.287 m/s, the velocity of the lower exhaust ports is 0.15 m/s, and the velocity of the higher exhaust ports is 0.29 m/s.  This case was performed for a model room with rotated Operating Table and presence of partial wall . For all cases the inlet temperature is 286 $^{o}$K and the room temperature is 296 $^{o}$K.

The following figures show the airflow and temperature distributions for the four cases under investigation. Figure 8 shows the predicted velocity contours (W component) in X-Z plane at Y=2.5 m (case 1); the velocity in the vicinity of the operating area was predicted as 0.05 m/s. From the figure, the air velocity in the operating plane varied from 0.01 m/s to 0.05 m/s, compared to a velocity of about 0.2 m/s. Such difference may be regarded to be due to the high extract velocity values and poor distribution of the exhaust ports. Chow et al., [8] performed their simulations and the presence of the long partial walls, which directed the airflow streams as a laminar flow.

 Figure 9 shows the prediction of velocity contours (W component) in Y-Z plane at X=3.0 m (case 1). The figure represents the downward of the airflow in the all width of the room. The figure demonstrates the effect of the supply diffuser size to the width of the operating room, this ratio guarantees the efficiency of air distribution along the room width. From figures 8 and 9, one can visualize the airflow action along the empty operating room, considering the reverse flow and downward flow positions. The presence of the four exhaust ports in the side-walls decrease the regions of the recirculating flow, and directs the flow downward.

The other walls in the plane X-Z do not contain any exhaust ports and the flow was directed naturally downward. The flow in the figures 8 and 9 appear more symmetrical in X-Z plane than the corresponding Y-Z plane. The flow under the edges of the air supply outlet demonstrated more penetration downward that was due to the flow induction from the stagnant area. Figure 10 represents the prediction of turbulent kinetic energy in X-Z plane at Y=2.5 m (case 1); it also shows the distribution of the turbulent kinetic energy to be concentrated in the vicinity of the air supply outlet.
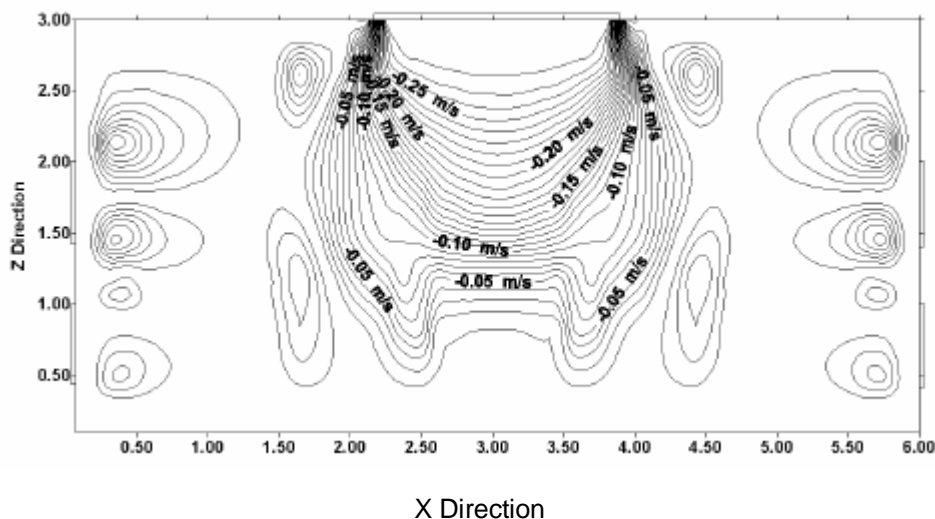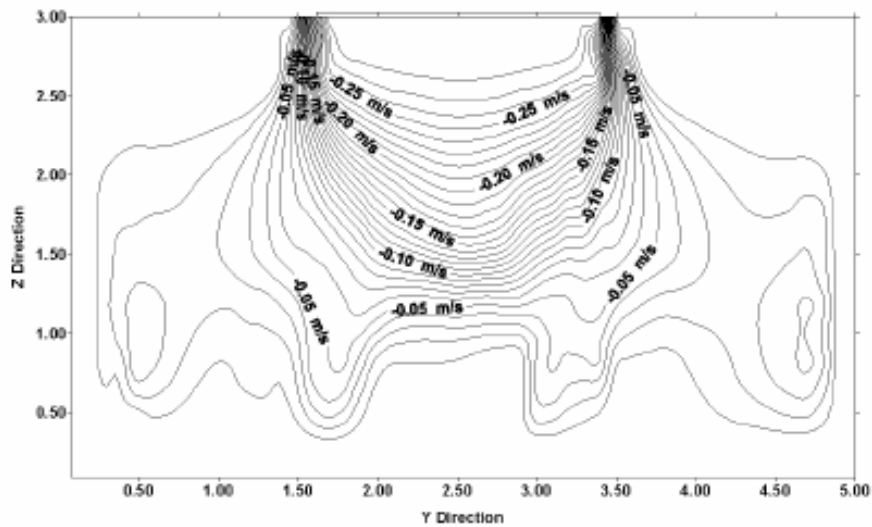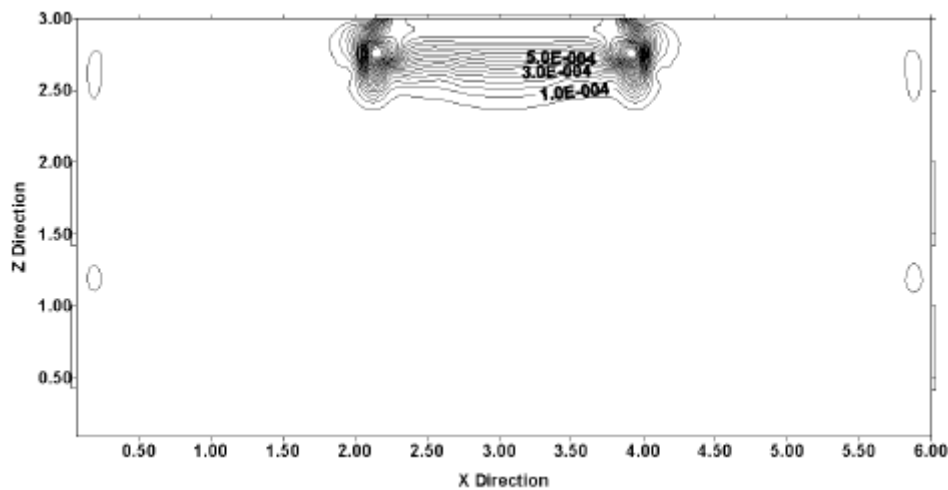


X Direction

**Fig. 8: Prediction of Velocity Contours (W component) in X-Z plane at Y=2.5 m, Case1**

**Fig. 9: Prediction of Velocity Contours (W component) in Y-Z plane at X=3.0 m, Case 1**



**Fig. 10: Prediction of Turbulent Kinetic Energy Contours in X-Z plane at Y=2.5 m, Case 1**

The whole domain indicated very low turbulence. The turbulence kinetic energy (k) has a value equal to 1E-4 $m^2/s^2$ at 0.5 m under the air supply outlet. The turbulence kinetic energy near the air exhaust ports had lower values.
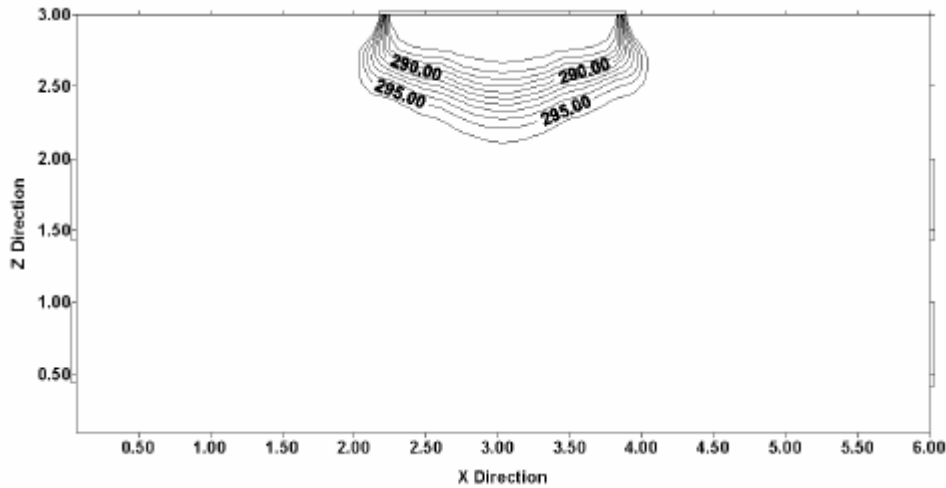
Figure 11 shows the prediction of temperature in X-Z plane at Y=2.5 m (case 1); the heat gradients were concentrated at 1.0 m under the air supplies diffusers.

From the figure 11, one can observe the whole domain to be maintained at the temperature 296 $^{o}$K. Steep temperature gradients were concentrated in the same region of high turbulent kinetic energy. One can observe that the laminar flow produced in that simulation leads to maintain the domain at the same temperature.

The higher values of the turbulent kinetic energy were concentrated at the edge of boundary area, influenced by the turbulent flow in the edge of the air supply outlet. Those higher values were influenced by the airflow penetration, as indicated in the figures 8 and 9.

The turbulent characteristics were also investigated and presented in the operating area in that simulation that didn't contain the operating table, to visualize the effect of the presence of operating table. From the figure 12 one can access the influence of the air supply outlet and its size and position in the ceiling. Finally the simulation of the vacant room can lead the designer

of the HVAC systems to put a preliminary design of the air supply outlets and exhaust ports in the surgical operating theatre.
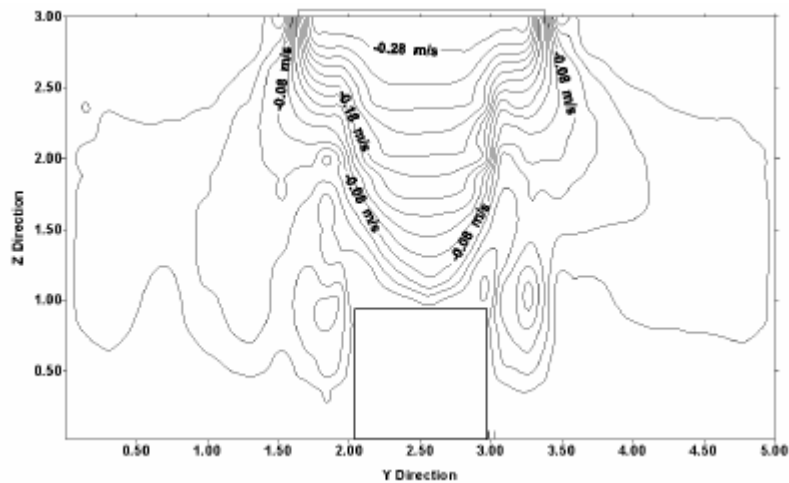


**Fig. 11: Prediction of Temperature Contours in X-Z plane at Y=2.5 m, Case 1**

For (case 2), figure 12 shows the prediction of velocity contours (W component) in X-Z plane at Y=2.5 m (case 2). The velocity in the vicinity of the operating area was predicted as 0.02 m/s, in comparison to a velocity of about 0.05 m/s found in case 1. This difference is attributed due to the presence of the operating table in the model of case 2. The presence of the operating table downstream of the flow direction leads to create eddies over the operating table as shown in the figure 12. This figure shows the interaction between the supply and extract flow in the upper zone in the room near to the air exhaust ports. The figure display the downward flow around the operating table, which created a semi-shield of the flow around the operating table, and resulted in creating more eddies over the table.

Figure 13 shows the prediction of velocity contours (W component) in Y-Z plane at X=3.0 m (case 2). The figure shows the large eddies, which were produced over the operating table surface. The figure shows the influence of the operating table's edges on the airflow stream in the vicinity of the air supply outlet. A recirculation zone appeared near the operating table as shown in the figure 13. This reverse flow was produced due to the bluff-body shape of the operating table. The flow in the lateral Y direction was asymmetrical in shape. Figure 13 shows the large size eddies that were formed over the operating table surface. The two figures 12 and 13 show the eddies formed near the operating table edges.
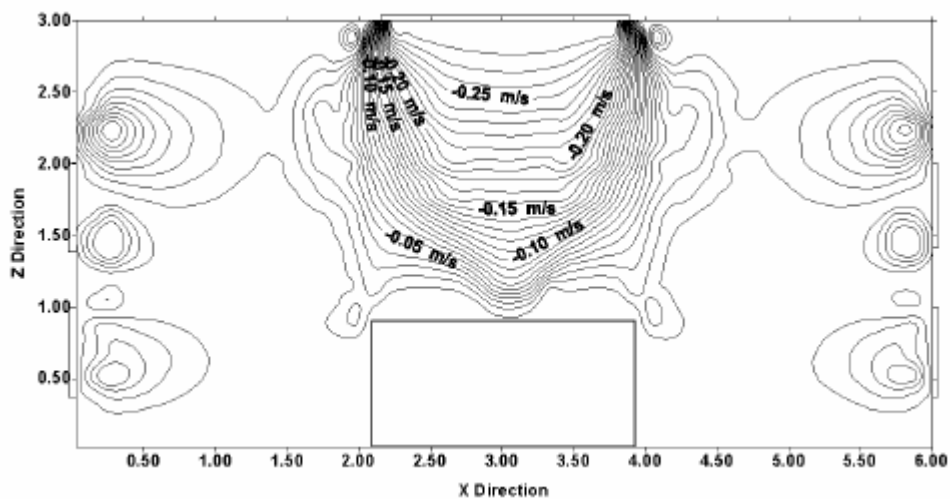


**Fig. 12: Prediction of Velocity Contours (W component) in X-Z plane
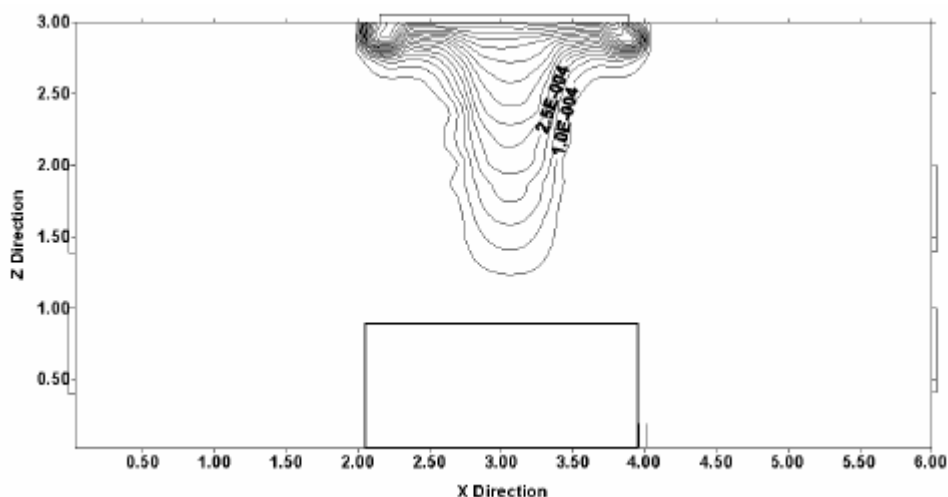at Y=2.5 m, Case 2**

**Fig. 13: Prediction of Velocity Contours (W component) in Y-Z plane at X=3.0 m, Case 2**

Figure 14 represents the prediction of turbulent kinetic energy in X-Z plane at Y=2.5 m (case 2);it shows the distribution of the turbulent kinetic energy that indicated significant values down to level Z=1.25 m. The turbulence distributions represent the direct effect of the operating table on the discharged flow. The turbulence kinetic energy (k) has a value equal to 1E-4 $m^2/s^2$ at 2.0 m downstream the air supply diffusers. The turbulence kinetic energy near the air exhaust ports had low values. The figure shows also the highest turbulence level to be near the edges of the air supplying diffusers.

Figure 15 represents the prediction of temperature in X-Z plane at Y=2.5 m (case 2). In that case 2, the temperature distribution indicated weaker gradient change as compared to that of case 1. The figure indicated the influence of the turbulent flow distribution on the temperature distribution.

The turbulent kinetic energy distribution was symmetrical in the X direction but not in the Y direction. That asymmetrical distribution was due to numerical round off error that may be accumulated near the edge of the table, especially near the corners of the operating table.

From figures 12-14, the simulation of the operating table in the room can guide the designer of the HVAC systems to propose better design of the air supply outlets and exhaust ports in the surgical operating theatre.
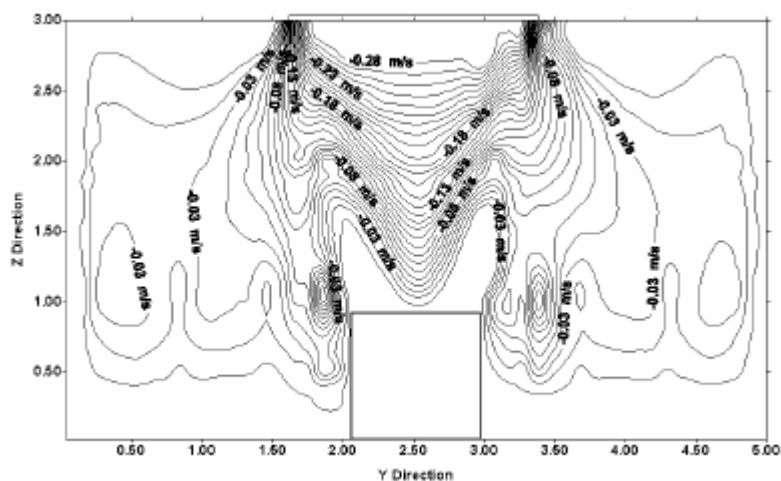


**Fig. 14: Prediction of Turbulent Kinetic Energy Contours in X-Z plane at Y=2.5 m, Case 2**
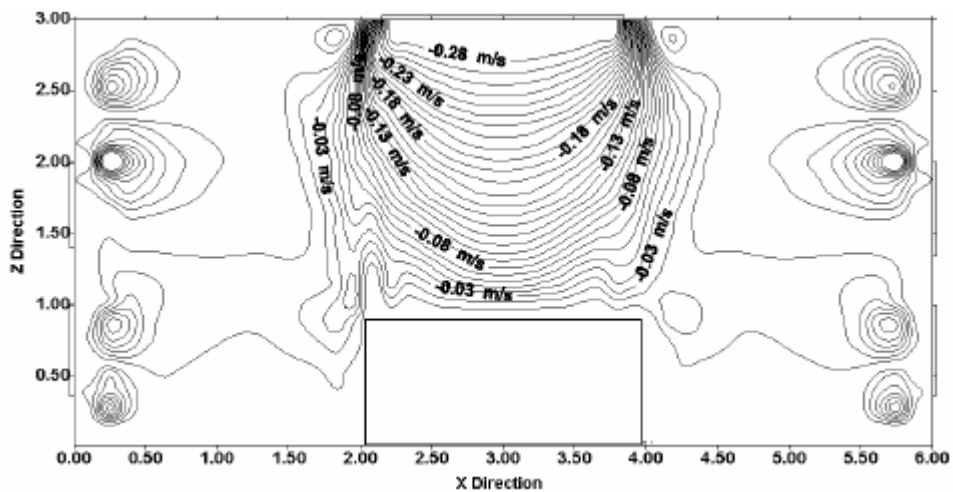
**Fig. 15: Prediction of Velocity Contours (W component) in X-Z plane at Y=2.5 m, Case 3**

For third simulation case, figure 15 indicated the prediction of velocity contours (W component) in X-Z plane at Y=2.5 m (case 3). The velocities in the vicinity of the operating area were predicted as 0.02 m/s. The figure shows the interaction between the supply and extract flow at lower level in the room near to the air exhaust ports. The figure represents that the downward flow around the operating table, resulted in airflow shield around the operating table, which was persistent due to the interaction between the downward stream and the lower extract flow. The interaction between downward stream and lower extract flow increased due to the presence of the partial walls, which at the same time, decreased the interaction between the supply flow and higher extract flow. Eddies' formation over the operating table was decreased relative to the second simulation due to the presence of partial walls. Figure 16 shows the prediction of velocity contours (W component) in Y-Z plane at X=3.0 m (case 3). The figure shows the large eddies, which were produced over the operating table surface. The figure shows the influence of the operating table's edges on the airflow stream in the vicinity of the air supply outlet. The presence of the partial walls didn't improve the flow distribution completely over the operating table. The downward flow penetrated the region around the operating table in the lateral direction. The partial walls affected partly the flow behavior improvement in the operating area that was due to the using short partial walls. When reviewed with the results of Chow et al. [8], and Kameel and Khalil [19], one can realize the effect of the partial wall length on the flow improvement on the operating area.



**Fig. 16: Prediction of velocity contours (W component) in Y-Z plane at X=3.0 m, Case 3**
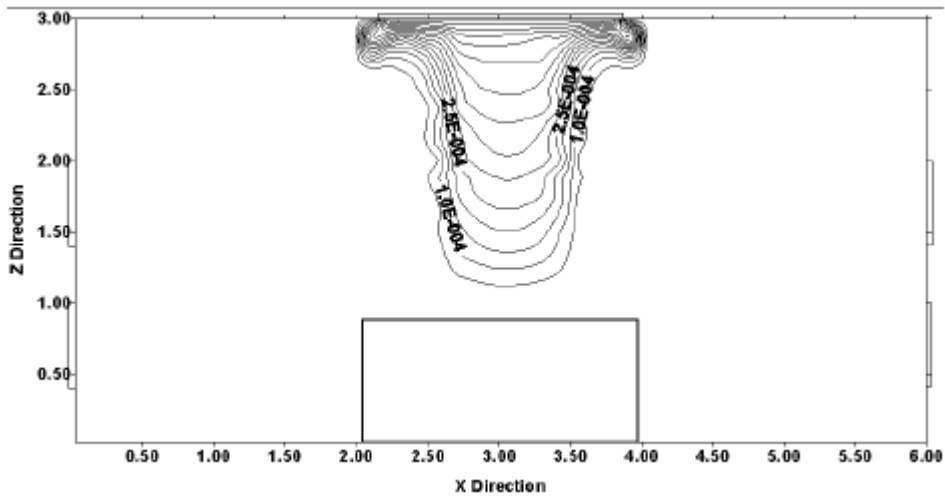
**Fig. 17: Prediction of turbulent kinetic energy contours in X-Z plane at Y=2.5 m, Case 3**

Figure 17 represents the prediction of turbulent kinetic energy in X-Z plane at Y=2.5 m (case 3). The prediction of the turbulent kinetic energy in this case doesn't differ trend-wise from the previous simulation. This is due to the slight difference in the flow action in the two cases.

Figure 18 represents the prediction of temperature in X-Z plane at Y=2.5 m (case 3). The influence of partial walls had a great effect on the temperature distribution. The temperature gradient reaches the level of the surgery team.  The figure represents the effect of partial wall on the air temperature in the vicinity of the supply outlet. The supply temperature distribution penetrated persisting downstream the supply outlet.

From the second and third simulation, one can conclude that the effect of the partial walls is rather limited on flow improvement. The partial walls can increase the forward flow and decrease the reverse flow, then the concept of the completely downward flow, can be implemented using the partial walls. The presence of the partial walls decreases  the airflow short circuits with the higher exhaust ports and increases the flow movement toward floor to remove by the lower exhaust ports.
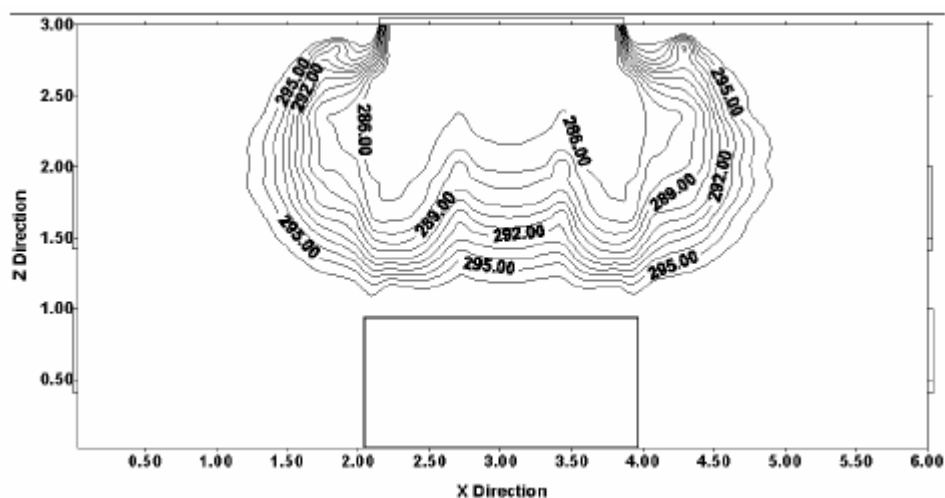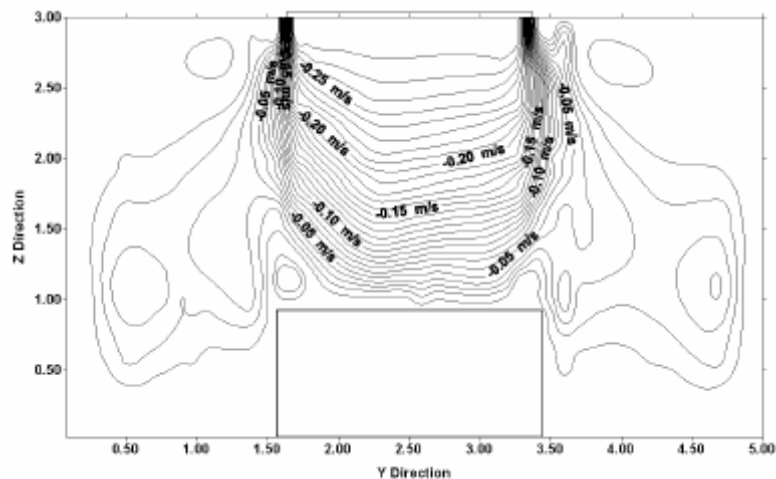


**Fig. 18: Prediction of Temperature Contours in X-Z plane at Y=2.5 m, Case 3**
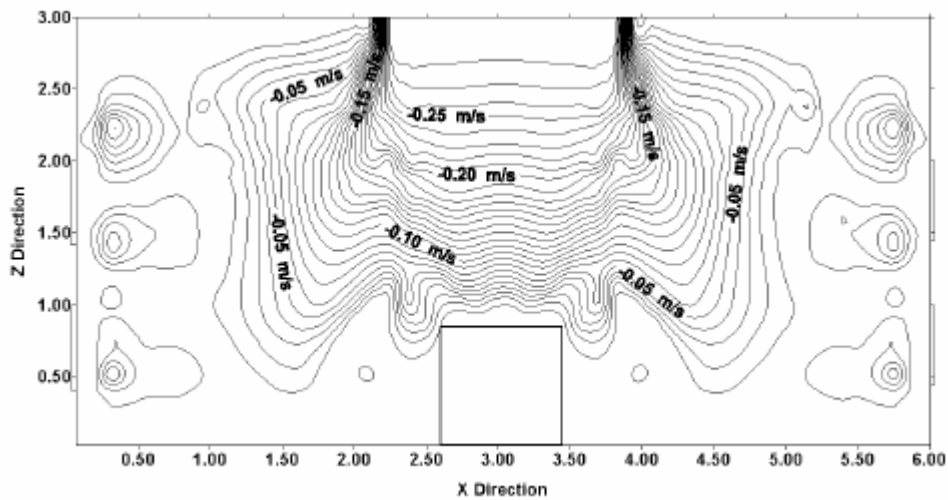
**Fig. 19: Prediction of Velocity Contours (W component) in X-Z plane at Y=2.5 m, Case 4**

Figure 19 shows the prediction of velocity contours (W component) in X-Z plane at Y=2.5 m (case 4). This case was predicted under the presence of the partial walls, and the rotated operating table at right angle. The airflow became fully downward in the operating theatre. The flow formed an envelope around the operating table as shown in figure 19. The interaction between the discharged flow and extracted flow at higher or lower levels decreased to minimum. This occurred due to the presence of partial walls, which decreased the higher short circuit and the rotated operating table shares in the increase of the downward flow. The flow velocity over the table was found closely to range from 0.02 to 0.05 m/s. Eddies formation decreased relative to the previous simulation cases, due to the effect of table rotation in the operating room.

Figure 20 shows the prediction of velocity contours (W component) in Y-Z plane at X=3.0 m (case 4). The flow in that lateral direction was improved especially in the operating area. The two figures 19 and 20 represented the effect of the furniture location on the airflow stream. It is not advisable that designers ignore the presence of furniture or even their location. One can conclude that the optimum design should consider obstacles, furniture, and operating equipment during design.



**Fig. 20: Prediction of Velocity Contours (W component) in Y-Z plane at X=3.0 m, Case 4**
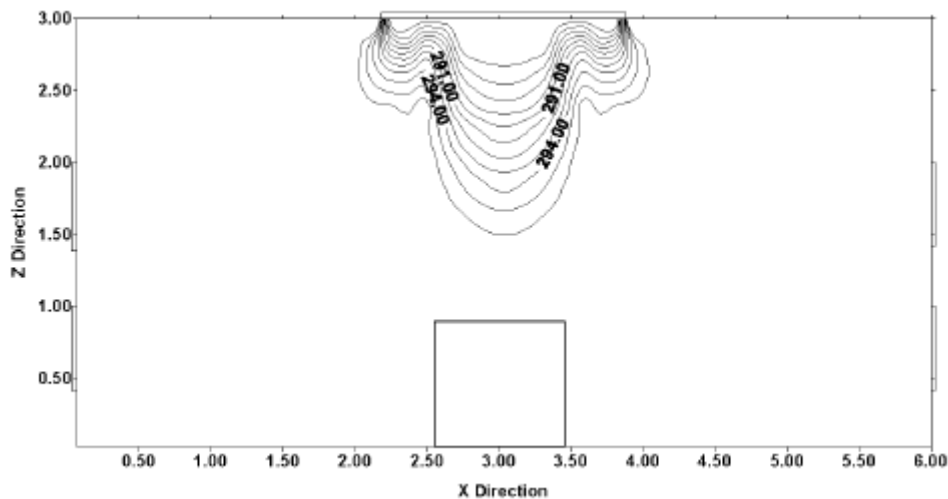
**Fig. 21: Prediction of Temperature Contours in X-Z plane at Y=2.5 m, Case 4**

Figure 21 represents the prediction of temperature in X-Z plane at Y=2.5 m (case 4). The influence of table orientation was pronounced on the temperature distribution.  The figure demonstrates the uniformity of the temperature outside the jet domain; the temperature distribution was similar to one in the simulation of case 2.

The effect of the table orientation was clearly observed on the flow characteristics. The flow in the inner domain of the operating table was unaffected.

## DISCUSSIONS

From previous results, one can access the merits of such air supply outlet and the exhaust ports arrangement in the surgical operating theatre. Previous researches on HVAC systems in the surgical operating theatres recommended the downward flow as optimum for the air distribution in that sensitive places, [16-23]**.** Some other studies for air distribution recommended that the direction of airflow is critical. For example, in isolation rooms, the direction of airflow should be away from the Health Care Worker (HCW) and towards the patient. On the other hand, in operating rooms, airflow should be directed away from the patient and towards the HCW.

The designers of the HVAC systems should consider the importance of the air distribution; the positioning of air supply outlets, air exhaust ports, and partial walls may be useful to maintain the air environment in the surgical operating theatre.

The higher exhaust ports were recommended to decrease the airflow direction towards the patient. This appeared strongly in the prediction of the airflow pattern over the operating table. The higher exhaust prevented the high level of turbulence in the airflow direction near the operating table.

The partial walls were so effective in directing of the airflow to get the most benefit of the cooled air. The presence of the partial wall has a positive influence on the airflow distribution, it also has a great effect on eddies formation in the operating area over the operating table surface. The height of the partial walls is an important factor in the effectiveness of the partial walls on the airflow.

The presence of the operating table in the operating area influenced the air distribution. The simulation of the vacant room may be useful only in the predicting velocities but that simulation doesn't predict accurate distribution of airflow turbulence over the operating table. Meaningful predictions of the flow characteristics over the operating table surface enhance the knowledge of the flow action near the operating area. The turbulence level over the operating area was affected by the presence of operating table itself, the position of the air supply outlet, the

distribution of the exhaust ports, and the discharge and extract velocities. The orientation of the operating table has a pronounced effect on the air characteristics in the operating area. The higher exhaust ports enhance the air actions near the edges of the operating table, which decreases partially the penetration of the airflow of the supply outlet.

The turbulence distribution over the operating table surface exhibited similar trends, and indicated higher values on the edge of the table and the lower values in the middle. Such distribution was expected because the presence of the bluff bodies (operating table) downstream the jet flows. The effect of partial walls on the turbulence distribution was limited. From the simulation cases it was found that the presence of temperature difference (room/supply) has no great influence on the airflow pattern.

## CONCLUSIONS

The 3DHVAC tool was so useful in the prediction of air behavior in multi cases of the room configurations. More experimental investigation about the airflow characteristics in the vicinity of air supply outlets, exhaust ports, and operating area are needed. Those details will enhance our understanding of the airflow conditions near the boundaries. The HVAC system has a great influence in the controlling of the health requirement in the surgical operating theatres. The production of a proper air distribution in the operating suites and its direction to the right positions will aid in the decreasing of the infections.

The effect of the furniture distribution on the airflow stream is strongly indicated. Designers should not ignore the furniture presence and/or even its distribution. One may conclude that the optimum design should take all these considerations during the design, (obstacles, furniture, and operating devices). The present work showed the importance of exhaust ports location in the operating room and indicated the particular importance of the high-level air extract. The size of air supply outlet and its location was found to be important.

Well-designed HVAC systems serving health care facilities with properly balanced air distribution is probably one of the most important factors in the IAQ problem. All guidelines mentioned earlier should include ventilation rates, pressure relationships, temperature, humidity, outdoor air quality, and filtration requirements. However, air distribution, shape and locations of air outlets and intakes, and the furniture distribution were also found to be very important.

## Acknowledgement

## References

1.  Khalil E.E. , (1977) Flow, Combustion & Heat Transfer in Axisymmetric Furnaces, (1977) PhD.Thesis , London Univ.
2.  Khalil E.E. (1980) On the Modeling of Reaction Rates in Turbulent Premixed Confined Flames, AIAA –80-0015.
3.  Khalil E.E. (1986) Numerical Calculations of Turbulent Reaction Rates in Combustors ASME 86-WA/HT-37.
4.  Gupta A.K. and Lilley ,D.G. (1985) Flow field Modeling and Diagnostics. Abacus Press , 1$^{st}$ Edition
5.  Khalil,E.E. (1988) Mathematical Modelling of Aluminum Reduction Cells, EC1, Proc.ICES88, Chapter 52.
6.  Khalil E.E., Spalding D.B. and Whitelaw, J.H. (1975) The Calculation of Local Flow Properties in Two-Dimensional Furnaces, int., Heat & Mass Transfer, Vol.18, pp775.
7.  ASHRAE Fundamentals Handbook (SI), 1999, ASHRAE, USA
8.  Chow, T. T., Ward, S., Liu, J. P., and Chan, F. C. K., 2000, Airflow in hospital operating theatre: the Hong Kong experience, Healthy Buildings, Finland.
9.  Berglund, L. G., 1998, Comfort and Humidity, ASHRAE Journal, Page. 35-41, 1998.
10. Khalil, E. E., 2000, Computer aided design for comfort in healthy air conditioned spaces, Proceedings of Healthy Buildings 2000, Finland, Vol. 2, Page 461-466.

11. Spalding, D.B. and Patankar, S.V. (1974) A Calculation Procedure for Heat, Mass and Momentum Transfer in Three Dimensional Parabolic Flows. Int.J.Heat & Mass Transfer, Vol.15, pp1787.

12. Launder B.E. & Spalding D.B. (1974) The Numerical Computation of Turbulent Flows, Comput. Methods Appl.Mech.,pp269-275.

13. Bartelds, H, Lewis, T.M.Michelfelder, S.and Pai, B.R. (1973) Prediction of Radiant Heat Flux Distribution in Furnaces and Its Experimental Testing,IFRF Doc.G02/a/23.

14. Kameel, R., 2003, Computer aided design of flow regimes in air-conditioned operating theatres, Ph.D. Thesis, Cairo University, Egypt.

15. Henkes .R.W.M, (1990) Natural Convection Boundary Layers, PhD.Thesis, Delft University, Netherlands.

16. Kameel, R. and Khalil, E.E. (2002) Generation of the Grid Nodes Distribution Using Modified Hyperbolic Equations, AIAA-2002-0656

17. Kameel, R., and Khalil, E. E., 2000, Computer aided design of flow regimes in air-conditioned Spaces, Proc. ESDA2000 ASME 5 th Biennial Conference on Engineering Systems Design & Analysis, Montreaux 2000.

18 .Kameel, R., and Khalil, E. E., 2001, Numerical computations of the fluid flow and heat transfer in air-conditioned spaces, NHTC2001-20084, 35th National Heat Transfer Conference, Anaheim, California.

19. Kameel, R., and Khalil, E. E., 2001, Air quality appraisal in air-conditioned spaces: numerical analyses, Proc.4th IAQVEC Conference, Changsha, China, Page 287-297.

20. Kameel, R., and Khalil, E. E., 20041, Effect of Swirl on Flame Characteristics in Furnaces, $2^{nd}$ IECEC, Rhode Island, AIAA-2004-5539, 15-19 August 2004..

21. Khalil, E. E., 2005, HVAC For Operating Theatres and Intensive Care Units: Comfort, Air quality and Energy Utilization, ASHRAE/COMFEX, India, January 2005, pp102-117.

22. Khalil, E. E., 2004, Energy Efficient HVAC Design Applications in Hospitals, $2^{nd}$ IECEC, Rhode Island, AIAA-2004-5591, 15-19 August 2004.

23. Huzzain,O and Khalil, E.E. (2005) On the Modelling of Airflow Regimes in Surgical Operating Rooms $43^{rd}$ Aerospace Sciences Meeting & Exhibit, Reno, Nevada, AIAA-2005-753, 10-13 January 2005.